

TALLINN UNIVERSITY OF TECHNOLOGY  
DOCTORAL THESIS  
36/2018

**Interplay between Creatine Kinase  
and Adenylate Kinase Networks  
in Health and Disease**

ALEKSANDR KLEPININ



NATIONAL INSTITUTE OF CHEMICAL PHYSICS AND BIOPHYSICS  
Laboratory of Bioenergetics  
TALLINN UNIVERSITY OF TECHNOLOGY  
Department of Chemistry and Biotechnology

This dissertation was accepted for the defence of the degree 25/05/2018

**Supervisor:** Tuuli Käämbre, PhD,  
Laboratory of Bioenergetics, National Institute of  
Chemical Physics and Biophysics, Tallinn, Estonia

**Co-supervisor:** Anu Planken, PhD,  
Department of Oncology North-Estonian Medical  
Centre, Tallinn, Estonia

**Opponents:** Emirhan Nemetlu, PhD,  
Hacettepe University, Faculty of Pharmacy, Department  
of Analytical Chemistry Sihhiye, Ankara, 06100, Turkey

Professor Allen Kaasik, PhD,  
University of Tartu, Institute of Biomedicine and  
Translational Medicine, Estonia

**Defence of the thesis:** 20/06/2018, Tallinn

**Declaration:**

Hereby I declare that this doctoral thesis, my original investigation and achievement, submitted for the doctoral degree at Tallinn University of Technology, has not been previously submitted for doctoral or equivalent academic degree.

Aleksandr Klepinin

---



Copyright: Aleksandr Klepinin, 2018  
ISSN 2585-6898 (publication)  
ISBN 978-9949-83-283-5 (publication)  
ISSN 2585-6901 (PDF)  
ISBN 978-9949-83-284-2 (PDF)

TALLINNA TEHNIKAÜLIKOOL  
DOKTORITÖÖ  
36/2018

**Kreatiinkinaasi ja adenülaatkinaasi  
energiaülekanne võrgustike vaheline  
koosmõju normis ja patoloogias**

ALEKSANDR KLEPININ



# Contents

<b>LIST OF PUBLICATIONS .....</b>	<b>7</b>
<b>AUTHOR'S CONTRIBUTION TO THE PUBLICATIONS.....</b>	<b>8</b>
<b>ABBREVIATIONS .....</b>	<b>9</b>
<b>1. PHOSPHOTRANSFER NETWORKS AND THEIR COUPLING WITH OXPHOS .....</b>	<b>13</b>
1.1 REGULATION OF MITOCHONDRIAL OXIDATIVE PHOSPHORYLATION.....	13
1.2 BASIC PRINCIPLE OF FUNCTIONAL COUPLING MECHANISM BETWEEN PHOSPHOTRANSFER ENZYMES AND OXPHOS.....	14
1.3 GLYCOLYTIC NETWORK – HEXOKINASE.....	17
1.4 CREATINE KINASE NETWORK.....	17
1.5 ADENYLATE KINASE NETWORK .....	18
1.5.1 <i>Adenylate kinase and AMP signaling</i> .....	19
<b>2. ENERGY METABOLISM OF HUMAN CANCERS .....</b>	<b>22</b>
2.1 LARGE INTESTINE HISTOLOGY AND COLON TISSUE ENERGY METABOLISM REARRANGEMENT DURING COLORECTAL CANCER MALIGNANT TRANSFORMATION .....	22
2.2 BREAST TUMORS ENERGY METABOLISM DEPENDENTS ON BREAST CANCER MOLECULAR SUBTYPES .....	24
2.3 PHOSPHOTRANSFER NETWORK IN NEUROBLASTOMA AND HOW MODULATES TROPHIC FACTOR MOLECULE NEUROBLASTOMA ENERGY METABOLISM .....	25
<b>3. CANCER MODELS.....</b>	<b>26</b>
3.1 OXPHOS VERSUS GLYCOLYSIS IN CANCER.....	26
3.2 MITOCHONDRIAL INTERACTOSOME .....	26
3.3 WARBURG-PEDERSEN MODEL IS A LINK BETWEEN OXPHOS AND GLYCOLYTIC PATHWAY IN CANCER .....	29
<b>AIM OF THE STUDY.....</b>	<b>30</b>
<b>MATERIALS AND METHODS .....</b>	<b>31</b>
<b>4. MATERIALS .....</b>	<b>31</b>
4.1 HUMAN POST-OPERATIVE SAMPLES .....	31
4.2 ANIMALS .....	31
4.3 CELL CULTURES .....	31
4.4 CHEMICALS .....	32
<b>5. METHODS .....</b>	<b>32</b>
5.1 ISOLATION OF RAT CARDIOMYOCYTES AND LIVER MITOCHONDRIA .....	32
5.2 PREPARATION OF SKINNED TUMOR AND RAT HEART FIBERS.....	32
5.3 DETERMINATION OF CELL GROWTH .....	33

5.4	MITOCHONDRIAL RESPIRATION IN PERMEABILIZED TISSUE SAMPLES, CELLS AND ISOLATED MITOCHONDRIA .....	33
5.5	ANALYSIS OF FUNCTIONAL COUPLING BETWEEN OXPHOS AND MITOCHONDRIAL CREATINE KINASE .....	33
5.6	EXPERIMENTAL MODEL TO ESTIMATE THE PRESENCE OF ADENYLATE KINASE 1 AND 2 .....	33
5.7	CONFOCAL MICROSCOPY IMAGING .....	36
5.8	ASSESSMENT OF ENZYMATIC ACTIVITY .....	36
5.9	RNA ISOLATION AND QUANTITATIVE RT-PCR .....	37
5.10	DATA ANALYSIS .....	37
	<b>RESULTS .....</b>	<b>38</b>
	<b>6. CHARACTERIZATION OF THE MITOCHONDRIAL RESPIRATION AND MITOCHONDRIA COMMUNICATION WITH PHOSPHOTRANSFER NETWORK IN CANCER .....</b>	<b>38</b>
6.1	LOCALIZATION OF MITOCHONDRIA AND MITOCHONDRIA INTERACTION WITH GLYCOLYTIC PATHWAY IN NEUROBLASTOMA AND COLORECTAL CANCER (ARTICLE I, II AND III) .....	38
6.1.1	<i>Quality test</i> .....	40
6.1.2	<i>ADP dependent respiration and mitochondria interaction with glycolytic pathway – aerobic glycolysis</i> .....	41
6.2	INTERPLAY BETWEEN CREATINE KINASE AND ADENYLATE KINASE IN N2A CELLS AND COLORECTAL CANCER (ARTICLE I, II) .....	45
6.3	SEMI-QUANTITATIVE RESPIROMETRY METHOD TO QUANTIFY AK1 AND AK2 DISTRIBUTION IN HEALTH AND DISEASE .....	47
6.3.1	<i>Application of respirometry method to estimate changes in AK network during malignant transformation of Breast and Colorectal cancer</i> .....	47
6.3.2	<i>Mitochondrial respiration in rat liver is controlled by adenylate kinase 2</i> ...	49
6.3.3	<i>AK1 and AK2 distribution in normal and cancer cells</i> .....	51
6.3.4	<i>Application of respirometry method to research mitochondrial outer membrane permeability for AMP</i> .....	54
	<b>DISCUSSION .....</b>	<b>58</b>
	<b>CONCLUSION .....</b>	<b>63</b>
	<b>ACKNOWLEDGEMENTS .....</b>	<b>74</b>
	<b>ABSTRACT .....</b>	<b>75</b>
	<b>LÜHIKOKKUVÕTE .....</b>	<b>76</b>
	<b>APPENDIX .....</b>	<b>77</b>
	<b>CURRICULUM VITAE .....</b>	<b>134</b>
	<b>ELULOOKIRJELDUS .....</b>	<b>136</b>

## List of publications

**I. Aleksandr Klepinin**, Lyudmila Ounpuu, Rita Guzun, Vladimir Chekulayev, Natalja Timohhina, Kersti Tepp, Igor Shevchuk, Uwe Schlattner, Tuuli Kaambre. (2016) Simple oxygraphic analysis for the presence of adenylate kinase 1 and 2 in normal and tumor cells. *Journal of Bioenergetics and Biomembranes*, 48 (5), 531–548.

**II. Kaldma, Andrus; Klepinin, Aleksandr;** Chekulayev, Vladimir; Mado, Kati; Shevchuk, Igor; Timohhina, Natalja; Tepp, Kersti; Kandashvili, Manana; Varikmaa, Minna; Koit, Andre; Planken, Margus; Heck, Karoliina; Truu, Laura; Planken, Anu; Valvere, Vahur; Rebane, Egle; Kaambre, Tuuli. (2014). An in situ study of bioenergetic properties of human colorectal cancer: The regulation of mitochondrial respiration and distribution of flux control among the components of ATP synthasome. *The International Journal of Biochemistry & Cell Biology*, 55, 171–186.

**III. Klepinin, Aleksandr;** Chekulayev, Vladimir; Timohhina, Natalja; Shevchuk, Igor; Tepp, Kersti; Kaldma, Andrus; Koit, Andre; Saks, Valdur; Kaambre, Tuuli (2014). Comparative analysis of some aspects of mitochondrial metabolism in differentiated and undifferentiated neuroblastoma cells. *Journal of Bioenergetics and Biomembranes*, 46(1), 17–31.

## **Author's Contribution to the Publications**

I – Author participated in preparing the study design and all oxygraphic protocols to research adenylate kinase network. Additionally, carried out oxygraphic measurements, cell culturing, human sample preparation and mitochondria isolation and also participated in data analysis and had a leading role in writing the paper.

II – Author together with colleagues, processed human samples, participated in protocol design to research phosphotransfer network, conducted oxygraphic studies, and participated in manuscript writing and data analysis.

III – Author participated in preparing the study design to research phosphotransfer network. Additionally, carried out oxygraphic measurement, cell culturing as well as participated in data analysis and had a leading role in writing the paper.



## Abbreviations

AChE	acetylcholinesterase
ADP	adenosine di phosphate
AK	adenylate kinase
AMPD	AMP deaminase
AMPK	AMP-activated protein kinase
ANT	adenine nucleotide translocase
AP5A	diadenosine pentaphosphate
ATP	Adenosine triphosphate
CAT	carboxyatractyloside
CK	creatine kinase
CK-BB	brain type creatine kinase
CK-MM	muscle type creatine kinase
CM	cardiomyocytes
cN	5'-nucleotidase
Cr	creatine
CSC	cancer stem cells
Ct	threshold cycles
cyt c	cytochrome-c
DMEM	Dulbecco's modified Eagles medium
dN2a	differentiated N2a
ER	estrogen
ETS	electron transport system
G-6-P	glucose-6-phosphate
G6PDH	glucose-6-phosphate dehydrogenase
HBC	human breast cancer
HCC	human colorectal cancer
HER2	epidermal growth factor receptor 2
HK	hexokinase
I <sub>AK</sub>	adenylate kinase index
K <sub>m</sub>	apparent Michaelis-Menten constant
LDHA	lactate dehydrogenase A
LKB1	tumor suppressor kinase LKB1
MI	Mitochondrial Interactosome
MIM	mitochondrial inner membrane
MOM	mitochondrial outer membrane
MtCK	mitochondrial creatine kinase
N2a	Neuro-2A
NADH	nicotinamide adenine dinucleotide
NB	neuroblastoma
NEM	Nethylmaleimide
OXPHOS	mitochondrial oxidative phosphorylation
PCr	phosphocreatine
PEP	phosphoenol pyruvate
PET	positronemission tomography
Pi	inorganic phosphate

PK	pyruvate kinase
PR	progesterone
RA	retinoic acid
RCI	respiratory control index
RT-PCR	real-time reverse transcriptase polymerase chain reaction
SEM	error of the mean
sMtCK	sarcomeric mitochondrial creatine kinase
SNS	sympathetic nervous system
uMtCK	ubiquitous mitochondrial creatine kinase
uN2a	undifferentiated N2a
$V_0$	basal respiration
VDAC	voltage dependent anion channel
$V_{max}$	maximal mitochondria respiration rate

## Introduction

Cancer is the second leading cause of death after cardiovascular diseases globally. In 2015 8.8 million deaths (nearly 1 in 6 deaths) were caused by cancer (WHO 2018). It has been predicted that by 2030 new cancer cases will grow from 14.1 to 21.7 million mostly due to aging of the population (ACS 2015). Colorectal cancer is the third most common cancer in men and second in women. For women breast cancer is the leading cancer diagnosis and for men it is lung cancer (ACS 2015). Aside from the older generation, cancer also affects children as well. In 2012, around 163 000 new cancer cases were diagnosed among children 0-14 years of age, with leukemia being the most common form of cancer (ACS 2015) in this age group. In infants (0-5 years old) 30 % of all cancer cases is caused by neuroblastoma (NB) (Kaatsch 2010).

In Estonia, the annual number of new colorectal cancer cases has increased from 614 in 1995–1999, to 885 in 2010–2014 (Innos, Reima et al. 2018). The breast cancer annual incident numbers have also increased from 676 in 1995-1999, to 785 in 2005-2009 (Baburin, Aareleid et al. 2016). For the childhood NB cancers in Estonia there are about 50 cases diagnosed each year (Kaatsch 2010). Despite the annual increase in the number of diagnosed cancer cases per year, the 5 year survival rate has risen from 38 % to 56 % in the case of rectal cancer, and 64.4 % to 75.9 % in the case of breast cancer (Baburin, Aareleid et al. 2014; Innos, Reima et al. 2018). Increased survival rates among both cancer types may be associated with improved screening programs.

Recent studies have revealed some limitations in screening programs. Colonoscopy is the main method to detect both colorectal cancer and adenomatous polyps. Some evidence has been published demonstrating that colonoscopy can prevent death from left-sided colorectal cancer, but such benefit for right sided colorectal cancer has not been observed (Baxter, Goldwasser et al. 2009). Moreover, it has been found that screening can lead to overdiagnosis, which is harmful for patients because it influences their life (Marmot, Altman et al. 2013). Therefore, to solve the limitations of screening, it is necessary to discover novel cancer biomarkers. In 2011, Hanahan and Weinberg proposed that cells energy metabolism could be a new therapeutic target for cancer treatment (Hanahan and Weinberg 2011).

Otto Warburg was the first researcher who proposed that cancer is a metabolic disease (Warburg 1956). According to his assumption cancer cells use predominantly the glycolytic pathway since cancer cells have malfunctioning mitochondria. This hypothesis remained the main dogma for cancer for a long period of time. Recent contradicting studies have however revealed that mitochondria of cancer cells are functional, and even in some malignant cells increased rate of mitochondrial respiration compared to normal cells has been observed (Jose, Bellance et al. 2011; Moreno-Sanchez, Marin-Hernandez et al. 2014).

In the present work, the cell permeabilization technique together with the oxygraphic method was applied to investigate cancer energy metabolism. This technique enables to examine mitochondrial function in both isolated cells and tissues. Moreover, it is also beneficial over similar methods. Use of the permeabilization techniques allows studying mitochondrial respiration without isolation of mitochondria and thereby avoids artefacts linked to the mitochondrial isolation procedure. Furthermore, this method can permit all interaction between mitochondria and the surrounding organelles.

The current study experiments were performed on NB cell line Neuro-2a cells, and on post-operative samples from human breast cancer (HBC) and colorectal cancer (HCC) tissues. In this thesis we examined the role of mitochondria in cancer formation, as well as how mitochondrial communication *via* phosphotransfer network with surrounding organelles during cancer formation is altered.

## Review of literature

### 1. Phosphotransfer networks and their coupling with OXPHOS

#### 1.1 Regulation of mitochondrial oxidative phosphorylation

Adenosine triphosphate (ATP) is the universal energy currency molecule of living cells. It supports various energy-consuming pathways in cells, like the biosynthesis of proteins and nucleotides, muscle contraction and cell motility, metabolic transport through cell membrane and nerve conduction. Aerobic organisms synthesize ATP mainly by two ways: by glycolysis in the cytosol and by mitochondrial oxidative respiration (OXPHOS). ATP production *via* glycolysis vs. OXPHOS depends on the type of cells, growth state and the cell microenvironment. In normal condition around 70% of total ATP in cells is supplied by OXPHOS, where in heart cells the ATP production *via* mitochondrial respiration is reached up to 90% (Mootha, Arai et al. 1997; Zheng 2012).

Structurally, mitochondria are organelles which contain two distinct membranes: the mitochondrial outer membrane (MOM) and the mitochondrial inner membrane (MIM). The MOM is smooth and moderately selective but the MIM, in turn, is protein rich, highly selective and can form protuberances into the mitochondrial matrix known as cristae. On MIM also the machinery of OXPHOS are located, which consist of four electron transport system (ETS) complexes: (I) NADH-coenzyme Q reductase, (II) succinate-coenzyme Q reductase, (III) coenzyme Q-cytochrome c reductase, and (IV) cytochrome c oxidase (Figure 1).

The main principle of OXPHOS is proton transport across MIM against the proton gradient, which is coupled with thermodynamically favorable reactions. Mitochondrial respiration in general contains three reactions coupled with each other: firstly, electrons from respiratory substrate are transferred during MIM to terminal acceptor oxygen as a result of thermodynamical reaction, the free energy release which is used to accord next reaction. Secondly, protons from the mitochondrial matrix side are transported against the proton gradient to the external side of the MIM through all ETS complexes (except Complex II) to create proton electrochemical potential (Figure 1). Finally, from the mitochondrial intramembrane space protons are returned through  $F_1F_0$ ATP synthase back to the mitochondrial matrix, and the chemical energy formatted by proton gradient, is coupled with ATP synthesis (de Oliveira, Amoedo et al. 2012).

Chance and Williams proposed their theory based on experiments with isolated mitochondria. They showed that OXPHOS was regulated by ADP through the negative feedback mechanism (Chance and Williams 1955). Three decades later Kadenbach postulated that control over mitochondrial respiration occurred through complex IV allosterical regulation by nucleotides (Kadenbach 1986). Later, Napiwotzki and Kadenbach demonstrated that neither ADP nor ATP concentration, but only cellular ATP/ADP ratio regulated mitochondrial complex IV activity and OXPHOS (Napiwotzki and Kadenbach 1998). To avoid the inhibition effect of nucleotides on OXPHOS, the molecules of ATP do not diffuse in cells, but its energy-rich phosphoryl group is transferred by more efficient enzymatic pathway *via* sequent rapid equilibrating phosphotransfer reaction chain (Zeleznikar, Dzeja et al. 1995).

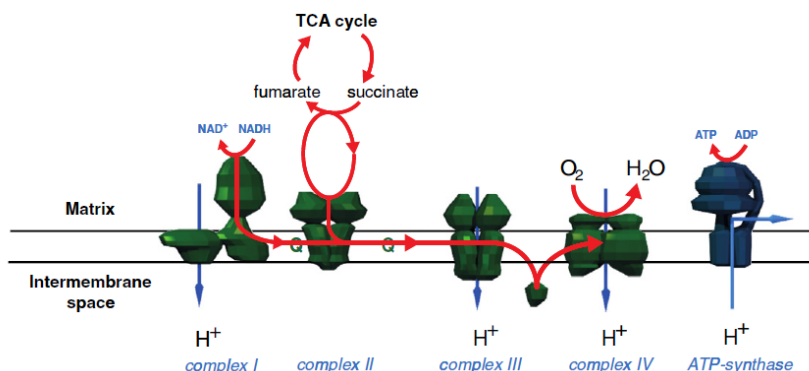


**Figure 1.** Mitochondrial respiration chain. Proton transport through mitochondrial respiration complexes I, III and IV is coupled with electron transport within mitochondria inner membrane. From (Zielinski, Smith et al. 2016) with permission

## 1.2 Basic principle of functional coupling mechanism between phosphotransfer enzymes and OXPHOS

Precise communication between ATP consumption and ATP production sites is fundamental to the bioenergetics of living organism. There are two competitive theories how nucleotides move within the cell. First, nucleotides diffuse between energy production and consumption sites. This process is not kinetically and thermodynamically efficient since it requires a significant concentration gradient. There is also the alternative vector ligand conduction theory, whereby nucleotides do not diffuse, but are divided into intra- and extramitochondrial pools (macrocompartments), which interact *via* MIM located adenine nucleotide translocase (ANT). Within those compartments nucleotide levels remain unchanged, even if increased energy flux is observed. The reason of this phenomenon is functional coupling *via* energy transfer networks between cell compartments (Saks, Khuchua et al. 1994; Zeleznikar, Dzeja et al. 1995).

Between ATP consumption and ATP production processes, the energy flux is regulated *via* phosphotransfer networks where adenosine di phosphate (ADP) plays important roles in feedback signaling of the cell (Dzeja and Terzic 1998; Saks, Kuznetsov et al. 2004). If the cell energy requirements are increased, then the OXPHOS rate rises at the same time with increase of ATPases activity. To keep ATPases active near energy-consuming sites, the phosphotransfer network enzymes maintain high ATP-ADP turnover rate. Moreover, in order to avoid inactivation of ATPases the ATP hydrolyzation products like ADP, Pi (inorganic phosphate), and H<sup>+</sup> are removed (Dzeja, Redfield et al. 2000). At the same time it is also important to maintain ADP/ATP ratio in another microcompartament of mitochondria intermembrane space, where accumulation of ATP can lead to energetic communication disturbances between the mitochondrial and cytosolic compartments, due to locking of ANT (Mannella, Pfeiffer et al. 2001).

In cells the main phosphotransfer enzymes are adenylate kinase (AK), creatine kinase (CK) and glycolytic enzymes (Figure 2). According to the enzymatic ligand conduction theory, the phosphotransfer networks rapidly equilibrating reactions drive high-energy phosphoryl flux into two directions (Zeleznikar, Dzeja et al. 1995). On one end of the system, near ATPases, the reaction is shifted to the direction of ADP formation

and, on the other end, in mitochondrial microcompartments, through feedback signaling, ADP controls OXPHOS rate. In the mitochondrial microcompartment the mitochondrial creatine kinase (MtCK) or AK2 facilitates phosphotransfer reactions toward phosphocreatine (PCr) and ADP formation respectively (Gellerich 1992; Saks, Kuznetsov et al. 2004). Due to the functional coupling between mitochondrial enzymes (MtCK and AK2) with OXPHOS, increased ADP levels stimulate mitochondrial respiration *via* exchange of ATP/ADP through ANT. Next, the transport of nucleotides and PCr/creatine between mitochondrial and cytosolic compartment are conducted *via* cytosolic isoform CK or AK until energy fluxes reach the microcompartment of ATPase, where CK/AK propagate reactions towards ATP formation (Saks, Khuchua et al. 1994; Dzeja and Terzic 1998; Saks, Kuznetsov et al. 2004).

The main principle of the glycolytic phosphotransfer network is to deliver mitochondrial high-energy phosphoryls *via* Pi, nicotinamide adenine dinucleotide (NADH) and ADP (Figure 2). ATP produced *via* OXPHOS is used at the beginning of the glycolytic pathway to mediate glycolysis. Moreover, it has been found that glycolytic enzymes have an important role in maintaining ATP/ADP ratio near the ATPase compartment. Pyruvate kinase (PK) transfer phosphoryl group from phosphoenol pyruvate (PEP) to ADP, support the work of ATPases. Another glycolytic enzyme pair, glyceraldehydes 3-phosphate dehydrogenase and phosphoglycerate kinase, catalyze a rapidly equilibrating reaction transfer Pi, NADH and ADP between OXPHOS and ATPases (Dzeja and Terzic 1998; Dzeja and Terzic 2003).

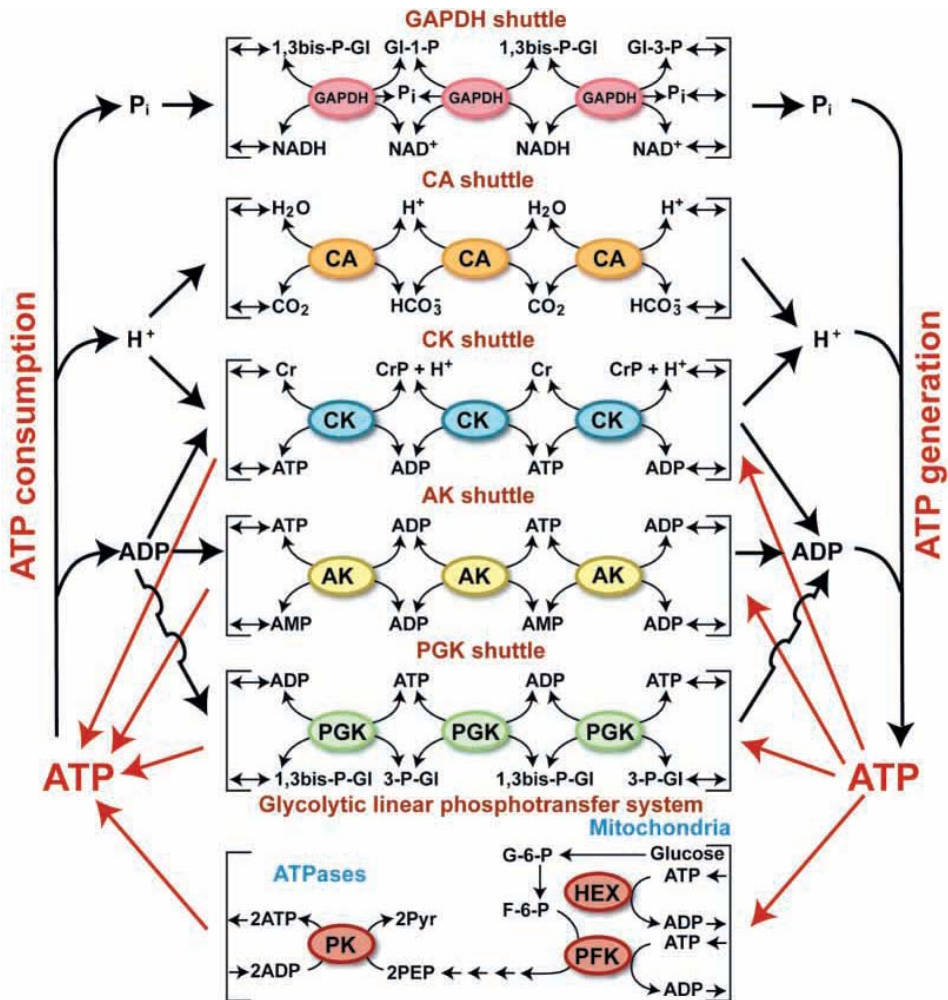


**Figure 2.** Integrated cellular energetic communication network between ATP consumption and ATP generation sites is facilitated by phosphotransfer system. To sustain efficient energy utilization and to avoid ATP hydrolyze products (ADP, H<sup>+</sup>, Pi) accumulation for this purpose cells use different parallel coupled near-equilibrating enzyme reactions. Energy transport from ATP consumption sites to ATP production sites are facilitated through creatine kinase (CK), adenylate kinase (AK), and the glycolytic system, which includes hexokinase (Hex), pyruvate kinase (PK) and 3-phosphoglycerate kinase (PGK) as well as glyceraldehydes 3-phosphate dehydrogenase (GPDH) shuttle and carbonic anhydrase (CA). Gl, glucose; PEP, phosphoenol pyruvate; Pyr, pyruvate; Cr, creatine; Pi, inorganic phosphate. Adapted with permission (Dzeja and Terzic 2003).



### 1.3 Glycolytic network – hexokinase

Four isoforms of hexokinase (HK), named as HK I, II, III and IV (more known as glucokinase), have been characterized in mammalian tissues. All these isoforms catalyze the first steps of glycolysis, where HK phosphorylate glucose and its product glucose-6-phosphate (G-6-P) may enter in the catabolic or anabolic pathways, depends on cellular physiological conditions. Wilson in 2003 proposed that anabolic and catabolic fate of glucose is regulated by cellular compartmentalization of HK isoforms (Wilson 2003).

HKI, is ubiquitously expressed in most tissues especially in brain and red blood cells, where glycolytic pathways play critical roles in energy production. In those tissues, HKI binds to voltage dependent anion channel (VDAC) located on MOM, where the HKI predominantly use ATP produced *via* OXPHOS. In contrast, HKII, is expressed only in insulin-sensitive tissues, such as the skeletal muscles, heart and adipose tissue. The HKII plays the dual metabolic function, which depends on its cellular localization: channeling G-6-P into the anabolic pathways, such as the pentose phosphate shunt, when present in the cytoplasm, and preferentially shuttling G-6-P into glycolysis and OXPHOS, when bound to mitochondria. HKIII is expressed in many tissues like the liver, brain, lung, spleen and kidney, in which it has a perinuclear location (Wilson 2003). In contrast to previous HK isoforms (I-III), HK IV has low glucose affinity and G-6-P does not inhibit its activity. Altogether, these properties are required for HK IV to monitor blood glucose concentrations in liver and pancreatic  $\beta$  cells, where glycogen synthesis and glycolytic pathways are controlled by the level of G-6-P (Postic, Shiota et al. 2001).

The main difference between major members of HK (I and II), and HKIII and HK IV, is the presence or absence of specific hydrophobic N-terminal sequence. It has been found that N-terminal tail on HKI and HKII facilitates the binding with VDAC, resulting in decreased G-6-P product inhibition action (Wilson 2003). There are also extracellular signals transduced by Akt (also known as protein B), which increase HK binding on MOM *via* its phosphorylation. Moreover, Akt activation and binding of HK on VDAC can protect against apoptosis induction (Majewski, Nogueira et al. 2004).

### 1.4 Creatine kinase network

CK is a guanidine kinase that catalyzes the reversible reaction transferring of a high-energy phosphate from ATP to specific energy carrier creatine (Cr), as a result generating ADP, PCr and protons. In vertebrates CK is encoded by four genes, and CK enzymes are divided according to their localization into mitochondrial (MtCK) and cytosolic isoforms. The cytosolic subtype is formed by both homodimer CK-BB (B-brain type) and CK-MM (M-muscle type) or monomers are organized into heterodimer CK-MB (Wallimann, Wyss et al. 1992).

The CK gene is expressed in a tissue specific manner. Ubiquitous mitochondrial creatine kinase (uMtCK) is expressed in many tissues, especially in brain. By contrast, sarcomeric mitochondrial creatine kinase (sMtCK) is exclusively expressed in muscle tissue, like heart and skeletal muscle, but not in smooth muscle, where instead of sMtCK the uMtCK is expressed (Wallimann, Wyss et al. 1992; Ishida, Riesinger et al. 1994). Octamer is the active form for MtCK, and through dynamics transformation between dimer and octamer form can be regulated its activity. In addition, it has been found that in neurons, smooth muscle and intestinal epithelial cells the uMtCK exclusively is co-

expressed with CK-BB, and in muscle cells sMtCK is co-expressed with CK-MM (Jockers-Wretou, Giebel et al. 1977; Haas and Strauss 1990; Wallimann and Hemmer 1994).

The CK is predominantly expressed in high energy demand tissues like muscles and brain. In different muscle types it has been found that the content of PCr was in proportion to CK expression levels, which altogether depends on their physiological requirements. For example, the fast twitching skeletal muscles have a large intracellular pool of PCr and a high level of CK in the cytosolic compartment. In such muscle types, the CK has 'energy buffer' functions, where cytosolic subtype of CK-MM regenerates ATP from PCr when the energy requirements are growing rapidly, because in glycolytic muscle the supply of energy by the mitochondria is insufficient. By contrast, in slow twitching muscles the CK possess 'special energy buffer' functions, which link between mitochondrial ATP production and ATP utilization site by PCr/Cr shuttle. Moreover, since the reaction of CK towards ATP production is utilized by both ADP and  $H^+$ , therefore the CK functional coupling with ATP consuming sites avoids the acidification of cytoplasm during fast ATP hydrolysis (Wallimann, Wyss et al. 1992). In addition, CK network can interplay with the glycolytic pathway, since PCr hydrolysis is a major source of  $P_i$  for activation of glycogenolysis and glycolysis (Wallimann, Wyss et al. 1992). Previous studies have shown that in NB, breast and ovarian cancer cells the CK-BB is overexpressed (Ishiguro, Kato et al. 1990; Zarghami, Giai et al. 1996; Li, Chen et al. 2013). For ovarian cancer there is evidence that CK-BB levels correlate with increased glycolytic metabolism (Li, Chen et al. 2013). Moreover, recent studies have shown that MtCK is downregulated in some human cancers (Patra, Bera et al. 2008; Amamoto, Uchiumi et al. 2016), but little is known about MtCK role in cancer formation. Experiments on CK knockout mice have indicated that the absence of the CK network can be partly compensated by other phosphotransfer enzymes, such as AK and the glycolytic networks (Dzeja, Terzic et al. 2004).

## 1.5 Adenylate kinase network

AK is an evolutionally conserved enzyme, which catalyzes reversible transfer of a  $\gamma$ -phosphoryl group from ATP to AMP, as a result releasing 2 molecules of ADP. The unique properties of AK lie on its ability to deliver not only  $\gamma$ - but also  $\beta$ -phosphoryl groups of ATP, thereby doubling the ATP energetic potential. To monitor intracellular ATP/ADP level the AK distributes practically all along the cell (Dzeja and Terzic 2009).

In mammals, nine different isoform of AK have been cloned (AK1-AK9) (Panayiotou, Solaroli et al. 2014). High variability of AK isoforms are associated with their distinct intracellular distribution and also different tissue specific expression patterns. Such mode of AK localization and expression is not occasional, but it is designed to support specific cellular processes from muscle contraction, to neuronal electrical cavity, from cell motility until mitochondrial communication with ATP consumption sites. In tissues with high energy demand like the brain, heart and skeletal muscles, the AK1 is the main isoform which usually is localized in the cytosol. AK2 is expressed in mitochondria rich tissues such as the liver, kidney and the heart, where it is located in the mitochondrial intermembrane space. Both isoforms catalyze the reverse reaction: during muscle contraction the AK1, in cytosolic compartment, produces ATP to support ATPase activity, and adenosine mono phosphate (AMP) serves as the feedback signal to synchronize ATP production and consumption rate. Even if small amounts of AMP reach to the

mitochondria, then AK2 immediately is converted from AMP to ADP, which is later channeled into mitochondrial matrix (Dzeja and Terzic 2009).

In the mitochondrial matrix, two AK isoforms the AK3 and AK4 are located. Despite their similar localizations and high structural homology, they show different catalytical activities. AK3 is ubiquitous GTP: AMP phosphotransferase is linked with the Krebs cycle to catalyze GTP converting to GDP (Noma, Fujisawa et al. 2001). The AK4 is expressed in brain, kidney, liver and heart tissues (Miyoshi, Akazawa et al. 2009). Although, AK4 is less active than AK3, the AK4 retains nucleotide binding capability. In cells AK4 is overexpressed under stress conditions. In cancer cells the AK4 overexpression can protect cells from H<sub>2</sub>O<sub>2</sub> induced cell death *via* its interaction with ANT (Liu, Strom et al. 2009).

The existence of additional AK1 gene product AK1 $\beta$ , has been reported (Collavin, Lazarevic et al. 1999). The AK1 $\beta$  protein differs from AK1 by two aspects. Firstly, the AK1 $\beta$  has extra 18 amino acids at its N-terminus and myristoylation of this tail facilitates the AK1 $\beta$  binding with the cell membrane. The second aspect is related to the fact that only the AK1 $\beta$  expression is under the control of the p53 transcription factor. In this context, in cancers where p53 is mutated or absent, the AK1 $\beta$  downregulation is induced during cancer formation (Vasseur, Malicet et al. 2005). Co-expression of AK1 with AK1 $\beta$  has been reported in brain neurons. The main role of AK1 $\beta$  is to mediate cell membrane propagation, by interaction with ATP-sensitive potassium channel in neurons (Janssen, Kuiper et al. 2004).

### 1.5.1 Adenylate kinase and AMP signaling

Growing evidence has shown that AK plays a significant role in monitoring of cellular energy metabolism (Dzeja, Zeleznikar et al. 1998; Dzeja and Terzic 2003; Noma 2005). In cells, oxidative stress and ischemia are the main AK pathway activators. Due to the unique property of the AK catalytical reaction, small changes in ATP and ADP levels lead to drastic increase of intracellular AMP concentrations. Raised AMP levels indicate a signal of compromised energy status of the cell. There are two AMP signaling pathways. Firstly, AMP can allosterically activate glycolytic and glycogenolytic pathway enzymes 6-phosphofruktokinase (Ramaiah, Hathaway et al. 1964) and glycogen phosphorylase (Klinov and Kurganov 1994) (Figure 3). The second pathway is indirect where by in cells the AMP signal activates metabolic sensors and effectors, such as the ATP-sensitive potassium channel or AMP-activated protein kinase (AMPK). Both regulate energy balance by phosphorylation target proteins (Dzeja and Terzic 1998; Dzeja and Terzic 2009).

AMPK is a heterotrimeric complex which consists of a catalytic subunit  $\alpha$  and two regulatory subunits  $\beta$  and  $\gamma$ . The AMPK activity is regulated by two ways: allosteric activation by AMP and phosphorylation of  $\alpha$  subunit (Thr172). The major Thr172 kinase is the tumor suppressor kinase LKB1 (Liver kinase B1), for which the AMPK phosphorylation action is AMP dependent (Hawley, Boudeau et al. 2003; Woods, Johnstone et al. 2003; Shaw, Kosmatka et al. 2004). Many cells display an alternative pathway such as calmodulin-dependent protein kinase kinase- $\beta$ , which activity is regulated by intracellular Ca<sup>2+</sup> (Hawley, Pan et al. 2005; Hurley, Anderson et al. 2005; Woods, Dickerson et al. 2005). AMPK has a central role in monitoring of the cellular energy state. Once activated by metabolic stress, the AMPK switches the metabolic processes from anabolic (main ATP consumers) to catabolic (main ATP generators)

pathways to restore normal intracellular ATP level. To stop this process, the AMPK action is needed to dephosphorylate Thr172 by serine/threonine phosphatase (Figure 3). However, there are evidences that dephosphorylation efficiency is dependent on intracellular level of AMP (Gowans, Hawley et al. 2013).

When the stress situation has ended, there are two pathways in order to remove the AMP signal: enzymatic and catabolic reactions (Figure 3). Efficient enzymatic elimination of cytosolic AMP is catalyzed by AK2. Due to AK2 high affinity (low  $K_m$ ) for AMP ( $\leq 10 \mu\text{M}$ ), almost all AMP which reaches the mitochondria is immediately converted to ADP, as a result AK2 can decrease cytosolic AMP levels (Dzeja and Terzic 2009). Moreover, alternatively AMP can be removed by the catabolic pathway which is facilitated by AMP deaminase (AMPD) or 5'-nucleotidase (cN) (Figure 3). AMPD catalyzes AMP deamination to inosine monophosphate and it plays an important role in the purine nucleotide cycle. There is evidence that chemical inhibition of AMPD, or AMPD gene deletion, can activate AMPK (Plaideau, Lai et al. 2014). The cN catalyzes AMP dephosphorylation to adenosine. The cN can also regulate AMPK activation. Silencing of cN-I activates AMPK (Kulkarni, Karlsson et al. 2011) and the overexpression of this gene decreases AMPK activity (Plaideau, Liu et al. 2012).

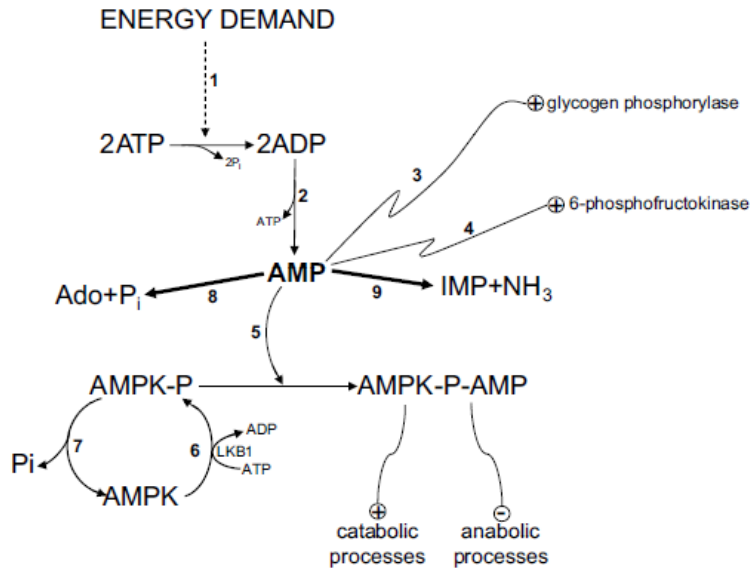


**Figure 3.** Adenylate kinase and AMP signaling network. During raised energy demand (1) intracellular ADP rapidly increase. In stress situation AK pathway (2) is activated, which leads to increased AMP. Biding of AMP allosterically activates glycogen phosphorylase (3) and 6-phosphofructokinase (4) or facilitates AMPK activation (5) via its phosphorylation by LKB1 (6). The phosphorylated AMPK (AMPK-P) inhibits cell anabolic processes at the same time activates catabolic processes. The AMPK-P dephosphorylation (7) by serine/threonine phosphatase stops AMPK action. Finally, when stress situation has ended, AMP signal is removed by cN (8) or AMPD (9) to modulate the cell energetic metabolism. AK, adenylate kinase; AMPK, AMP-activated protein kinase; cN, 5'-nucleotidase; AMPD, AMP deaminase; LKB1, Liver kinase B1. Adapted with permission (Ipata and Balestri 2013).

## 2. Energy metabolism of human cancers

### 2.1 Large intestine histology and colon tissue energy metabolism rearrangement during colorectal cancer malignant transformation

The large intestine is 1.5 meters in length and around 6-7 centimeters in diameter, with the narrowest part being about 2.5 centimeters. The Large intestine can be separated into two parts: the colon and the rectum. The colon starts from the ascending colon which is connected with the small intestine *via* the cecum and colon, ending at the sigmoid colon. The rectum is only 10 to 12 centimeters in length and it ends at the anal canal. The main function of the large intestine is waste movement from small intestine towards the anal canal. During waste movement along the large intestine, water and electrolytes are absorbed at the same time the waste material is concentrated, and finally it is formed into feces. At the end of the large intestine in the section of the rectum, the feces are stored until they are removed out of the body through the anal canal (Michael H. Ross 2010).

The Large intestine consists of four layers: starting from the *mucosa*, the *submucosa*, the muscle layer (*muscularis mucosa* and *muscularis propria*) and the *serosa* (Figure 4). The mucosa is lined with columnar epithelial cells (goblet cells) which are organized into crypts (Michael H. Ross 2010). The colonic epithelial cells have high regenerative and proliferative rates, because they are directly in contact with the aggressive environment, such as the pathogens, chemicals and toxins. The mucosal cells are generated from stem cells at the base of the crypt. During cellular migration towards the top of the crypts, the colon cells become more mature, and after three to five day they go into apoptosis. The *Lamina propria*, which supports the epithelia, contains numerous connective tissue cells, elastin collagen fibers and also immune cells, such as plasma cells, mast cells, macrophages, eosinophils and lymphocytes (Michael H. Ross 2010).

The *muscularis mucosa* is a thin smooth muscle with separate *mucosa* from the *submucosa* (Figure 4). The *submucosa* is a fibrous connecting tissue layer, which is made up of fibroblasts, mast cells, blood and lymphatic vessels. The *muscularis propria* surrounds the submucosa and it is composed of two smooth muscle layers (Michael H. Ross 2010): an inner circular coat and an outer longitudinal coat (Figure 4). Although smooth muscles have less mitochondria and the contraction is slower than in skeletal muscle and heart, they are able to contract for a long period of time without fatigue, like slow twitch muscle can (Park, Gifford et al. 2014). Thus, colon two muscle layers can move towards each other perpendicularly to form the basis of peristalsis.

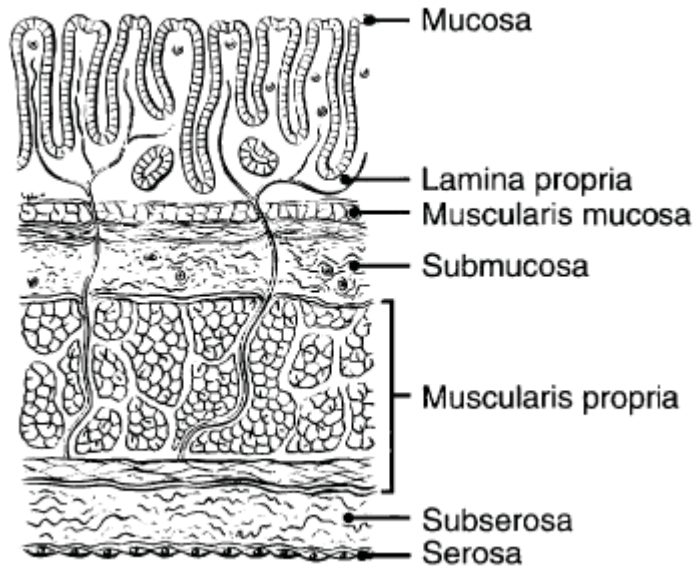


**Figure 4.** Cross section of colon tissue wall. The colon tissue contains four layers: mucosa, submucosa, smooth muscle coat (*muscularis mucosa* and *muscularis propria*) and serosa. From (Frederic L. Greene 2002) with permission.

The mucosa cells express cytosolic CK-BB together with uMtCK (Glover, Bowers et al. 2013). Although the *muscularis mucosa* and *muscularis propria* are both muscle tissues instead of that colon smooth muscles expressed more ubiquitous CK types CK-BB and uMtCK (Jockers-Wretou, Giebel et al. 1977; Ishida, Riesinger et al. 1994). There are evidences that the CK network plays an important role in cellular bioenergetics in both colon epithelia and smooth muscles (Takeuchi, Fujita et al. 1995; Glover, Bowers et al. 2013). In mucosal cells the CK-BB not only facilitates PCr/Cr cellular circulation but it also has an important role in cell-cell adhesion. Indeed, CK-BB overexpression increases colon cancer cell adhesion (Glover, Bowers et al. 2013). Moreover, CK-BB downregulation in colon cancer cells does not only decrease cell-cell adhesion, but also promotes epithelial-to-mesenchymal transition (EMT) (Mooney, Rajagopalan et al. 2011).

Impaired barrier function of the intestine, caused by bacteria (Amieva, Vogelmann et al. 2003), viral pathogens (Nava, Lopez et al. 2004) and pro-inflammatory cytokines (Utech, Ivanov et al. 2005), can lead to a leaky gut. Increased large intestine permeability is a predisposing factor to inflammatory bowel disease, such as Crohn's disease and ulcerative colitis (Michielan and D'Inca 2015). There is evidence that the chronic inflammation in the intestine can raise the risk of tumorigenesis (Gupta, Harpaz et al. 2007; Herrinton, Liu et al. 2012). It has been found that bowel inflammation, not only disrupts the mucosal barrier, but it also dysregulates the CK pathway. Namely, the studies in Crohn's disease and ulcerative colitis patients have demonstrated altered expression of CK-BB, as well as changes in CK-BB compartmentation, which lead to disruption of mucosal barrier properties (Glover, Bowers et al. 2013). This data highlights that there is a fundamental link between epithelial bioenergetics and mucosal barrier function. In addition, mitochondrial AK2 has an important role in activation of intestinal inflammation. It was found that AK2 knockout in colon mast cells, suppresses the

immune system activation (Kurashima, Amiya et al. 2012). However, the exact role of AK in colorectal cancer formation, and the interplay of AK network with CK, has remained unknown.

## **2.2 Breast tumors energy metabolism depends on breast cancer molecular subtypes**

For a long time, patient age, axillary lymph node status, tumor size as well as hormone receptor and human epidermal growth factor receptor 2 (HER2) status, and proliferation marker Ki67 expression levels, have been the major factors for categorization of patients into four main breast cancer subtypes (Dai, Li et al. 2015). The luminal tumors are both estrogen (ER) and progesterone (PR) receptor positive and HER2 negative. The luminal tumors can be further separated into Luminal A and Luminal B subtypes, according to the level of Ki67 expression. Luminal A has low and B has high levels of Ki67 expression. Both tumor types have quite a good prognostic outcome and they also respond well to hormone therapy. The other two breast cancer subtypes do not have ER and PR receptors, and they differ only by the presence (HER2 positive) or absence of HER2 (triple negative). Both, HER2 positive and triple negative type patients have a poor prognostic outcome. The drug trastuzumab is available to treat HER2 positive patients (Nagata, Lan et al. 2004). Unfortunately, regular drugs which are used to treat Luminal or HER2 breast cancer types are not efficient for triple negative breast cancer patients. Due to the absence of efficient drugs, the triple negative breast cancer patients follow an aggressive clinical course (Dai, Li et al. 2015). In 2011, Hanahan and Weinberg proposed that cells energy metabolism could be a new therapeutic target for cancer treatment (Hanahan and Weinberg 2011).

Our recent study has shown that malignant transformation is caused by rearrangement of energetic metabolism in breast cancer (Koitz, Shevchuk et al. 2017). Namely, increased OXPHOS respiration rate and raised mass of mitochondria were observed in breast cancer. Another research group has found that in breast cancer mitochondrial kinase uMtCK expression strongly correlates with tumor stage, and it is expressed preferentially in the ER negative breast cancer subtype (Cimino, Fuso et al. 2008). Overexpression of uMtCK in breast cancer enhanced tumor growth by protecting malignant cells against apoptosis, through stabilization of mitochondrial membrane potential, as well as deregulation of apoptosis pathway proteins (Qian, Li et al. 2012). The uMtCK co-expression partner CK-BB is also highly expressed in breast cancer (Zarghami, Gai et al. 1996). Nevertheless, no correlation has been seen between CK-BB levels and tumor stage, grade, size and histological subtypes (Zarghami, Gai et al. 1996).

There exists contradicting data about AK network isoenzyme expression patterns in breast cancer. On one hand, Kim and colleagues have postulated that AK2 is a negative regulator of tumor growth (Kim, Lee et al. 2014). They have shown that in breast cancer AK2 is downregulated. On the other hand, Speers and colleagues have found that AK2 is overexpressed in ER negative breast cancer (Speers, Tsimelzon et al. 2009). They proposed that AK2 should be a novel target for the treatment of ER negative breast cancer. Moreover, recently it has been found that AK6 is highly expressed in both breast and colorectal cancer, and AK6 expression correlates with a worse prognosis (Bai, Zhang et al. 2016; Ji, Yang et al. 2017). Nevertheless, AK role in cancer formation, and its functional coupling with OXPHOS in breast cancer and colorectal cancer, has remained unclear.



## 2.3 Phosphotransfer network in neuroblastoma and how modulates trophic factor molecule neuroblastoma energy metabolism

Neuroblastoma is a neuroendocrine tumor arising from any neuronal crest element of the sympathetic nervous system (SNS). NB usually developed from adrenal glands, but it can also start from neck, chest, abdomen or pelvis (Jiang, Stanke et al. 2011). The characteristic feature of tumors is quite high clinical heterogeneity. NB will undergo spontaneous regression (benign ganglioneurons) or it will show very slow progression (Brodeur 2018), but approximately in half of cases NB is very aggressive. This type of NB tumor has a high level of undifferentiated and poorly differentiated cells, which are characterized by high growth rates and strong inclination to metastasis (Schlitter, Dornenburg et al. 2012).

One possible treatment strategy of aggressive NB is to differentiate cancer cells towards normal neurons, in order to decrease the migration and proliferation potential of malignant cells. Retinoic acid (RA) is a trophic molecule which *in vitro* induces NB cell differentiation towards neuronal cells (Reynolds, Matthay et al. 2003). RA acts on cells through own nuclear retinoic acid receptors RAR or RXR, which belong to the steroid/thyroid hormone family of transcription factors (Lin, Lien et al. 2008). RA binding with RAR or RXR induces NB cells differentiation towards sympathetic neurons (Clagett-Dame, McNeill et al. 2006). It has been shown that RXR is not only located on cell nuclear, but also on mitochondrial membranes (Lin, Lien et al. 2008). RXR activation by RA does not change mitochondrial DNA content, but it increases mitochondrial reserve capacity. Indeed, the treatment of NB cells with RA increases mitochondrial respiration rate, but at the same time it does not change mitochondrial mass (Xun, Lee et al. 2012).

There is limited information about AK and CK networks in NB. In NB patient's, increased level of CK-BB in serum has been observed, which correlated with worse outcomes for patient's (Ishiguro, Kato et al. 1990). The study on mice models showed that the treatment of NB cells with cyclo-creatine (analog of creatine) decreased cancer cells growth (Miller, Evans et al. 1993). This data indicates that CK network could play a substantial role in NB cell growth. Nevertheless, there is no data about uMTCK expression and its functional coupling with OXPHOS in NB cells.

In NB cells both cytosolic AK1 and AK1 $\beta$  are expressed (de Bruin, Oerlemans et al. 2004). In dividing cells AK1, which is located in cell nucleus, is assembled with mitotic spindles to supply energy for cellular proliferation (Dzeja, Chung et al. 2011). However, absence or presence of AK1 or AK1 $\beta$  does not influence the NB cells proliferation rate (de Bruin, Oerlemans et al. 2004). In addition, overexpression of mitochondrial AK4 protects NB cells against H<sub>2</sub>O<sub>2</sub> induced cell death *via* the AK4 interaction with ANT (Liu, Strom et al. 2009). Nevertheless, the functional coupling of cytosolic AK1 and mitochondrial AK2 with OXPHOS in NB cells has never been researched.

### 3. Cancer models

#### 3.1 OXPHOS versus glycolysis in cancer

Malignant transformation and tumor progression depends on the bioenergetic status of the cell (Tan, Baty et al. 2014). Otto Warburg was the first researcher to propose that cancer is a metabolic disease (Warburg 1956). According to his assumption, tumor cells use predominantly the glycolytic pathway, even under normal O<sub>2</sub> exposure. This phenomenon is known as “the Warburg effect” or aerobic glycolysis (Pedersen 2007). There are several reasons why some cancers use the glycolytic pathway instead of OXPHOS. Firstly, although glycolysis is less efficient than OXPHOS (2 ATP/glucose versus 36 ATP/glucose) the ATP production *via* glycolysis is 100 times faster than by OXPHOS (Pfeiffer, Schuster et al. 2001). Moreover, aerobic glycolysis is able to produce enough ATP to maintain the high cellular ratio of ATP/ADP (Vander Heiden, Cantley et al. 2009). Secondly, the high glycolytic metabolism is a metabolic strategy which allows cancer cells to survive in stochastic or fluctuating tumor environments (Epstein, Xu et al. 2014). Malignant cells which are under normoxic conditions still produce high amount of lactate which is released into the extracellular space. An acidic microenvironment protects cancer cells against immune system infiltration into the tumor (Singer, Kastenberger et al. 2011), as well as extracellular acidification enhances the invasion and metastasis of cancer cells (Kato, Ozawa et al. 2007). Thirdly, hypoxia is often observed in cancer tissues, and in order to grow under hypoxic conditions, the cancer cells switch their metabolism to the aerobic glycolytic pathway (Fantin, St-Pierre et al. 2006).

Not all tumors intensely use glucose, but there is evidence that in cancer cells the mitochondria are functional and, in some tumors, increased OXPHOS rates have been observed (Jose, Bellance et al. 2011; Moreno-Sanchez, Marin-Hernandez et al. 2014; Koit, Shevchuk et al. 2017). Indeed, in cancer cells up to 64% from total ATP is produced *via* glycolysis, which means that OXPHOS has also an important role in ATP production (Zu and Guppy 2004). This assumption is also supported by several reports, which have shown that cancer cells use glutamine as energy fuel instead of glucose (Wise, DeBerardinis et al. 2008). Moreover, cancer cells also use the glycolysis and glutaminolysis pathways, to support fast tumor growth by macromolecules, such as nucleotides, lipids and amino acids (Lunt and Vander Heiden 2011). Altogether, cancer cells are forced to balance between glycolysis and OXPHOS, in order to maintain high proliferation rates to optimally meet the energy demands, and to keep fast response to changes in cellular metabolism, in order to survive within the fluctuating tumor environment.

#### 3.2 Mitochondrial Interactosome

Mitochondria are the main ATP suppliers in heart, skeletal muscle, smooth muscle and neurons, where mitochondrial respiration is controlled by mitochondrial porin (VDAC) permeability for ADP (Kuznetsov, Tiivel et al. 1996; Monge, Beraud et al. 2008; Koit, Shevchuk et al. 2017). The mitochondrial affinity for ADP can be described by apparent Michaelis-Menten constant (K<sub>m</sub>). For heart and skeletal muscle, the apparent K<sub>m</sub> for ADP ranges among 300-400 μM (Kuznetsov, Tiivel et al. 1996). As a result of the isolation of mitochondria from muscle tissue, the mitochondria lose interactions with surrounding

environment, which leads to disruption of diffusion barrier for ADP and therefore isolated mitochondria apparent  $K_m$  for ADP is dropped to 10-20  $\mu\text{M}$  (Monge, Beraud et al. 2008). In 2008, Rostovtseva showed that the MOM permeability for ADP was regulated by VDAC interaction with the cytoskeleton component tubulin (Rostovtseva, Sheldon et al. 2008).

The mathematical model of Vendelin *et al.* have indicated that in heart mitochondria, respiration is controlled by ANT, which functionally interacts with MtCK (Vendelin, Lemba et al. 2004). Due to functional coupling between ANT and MtCK, ATP is transmitted from ANT directly to MtCK, which results in acceleration of PCr production. Guzun with colleagues, demonstrated that in cardiomyocytes (CM), the VDAC permeability is only selectively limited for ATP and ADP but not for Cr or PCr (Guzun, Timohhina et al. 2009). Altogether, in cardiac cells PCr is the main energy carrier from mitochondria into cytoplasm, where interaction between tubulin and VDAC decreases the MOM permeability for nucleotides, which significantly enhances PCr production, due to functional coupling between ANT and MtCK. In order to support the high energy need of cardiac cells, the mitochondrial respiration is regulated by interaction of ANT-MtCK-VDAC-tubulin and ATP synthasome (Pedersen 2007) into a supercomplex, which is known as Mitochondrial Interactosome (MI) (Figure 5) (Timohhina, Guzun et al. 2009).

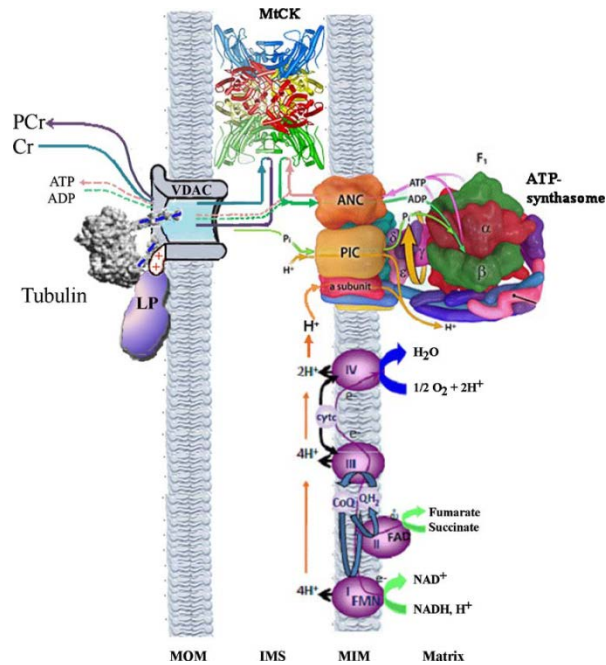


**Figure 5.** Mitochondrial Interactosome (MI) model. The MI in cardiac, oxidative skeletal muscle and brain cells is formed to control mitochondrial respiration regulation and energy flux. MI consisting of ATP synthasome (formed by ATP synthase, adenine nucleotide carrier (ANC) and inorganic phosphate carrier (PIC) as proposed by P. Pedersen (Pedersen 2007) and mitochondrial creatine kinase (MtCK), functionally coupled to ATP synthasome, and Voltage dependent anion channel (VDAC) with regulatory proteins (tubulin and linker protein (LP)). MOM, mitochondrial outer membrane; MIM, mitochondrial inner membrane; IMS, mitochondrial intermembrane space ((Timohhina, Guzun et al. 2009) with permission).

### 3.3 Warburg-Pedersen model is a link between OXPHOS and glycolytic pathway in cancer

During malignant transformations the composition and structure of MI may be radically reorganized (Eimre, Paju et al. 2008; Patra, Bera et al. 2008; Simamura, Shimada et al. 2008; Guzun, Karu-Varikmaa et al. 2011). In many glycolytic tumors HK1/2 are overexpressed (Shinohara, Yamamoto et al. 1994; Altenberg and Greulich 2004; Botzer, Maman et al. 2016). One of the key events in carcinogenesis is tubulin replacement on VDAC channel with HK (Guzun, Karu-Varikmaa et al. 2011). The HK binding on MOM causes the opening of VDAC channel (Majewski, Nogueira et al. 2004), which facilitates coupling between OXPHOS and glucose phosphorylation. As a result of such transformation, tumor cells switch their metabolism towards the aerobic glycolytic pathway. Tumor aerobic glycolysis mechanism is described by the Warburg-Pedersen model (Figure 6) (Pedersen 2007), where OXPHOS is linked with the glycolytic pathway *via* HK2 binding on VDAC, to support malignant cells with energy. The Warburg-Pedersen mechanism has also been applied in medicine. The imaging technique positron emission tomography (PET) technique uses the glucose analog fluorodeoxyglucose (Phelps 2000). In cancer patients PET is used to monitor the elevated HK reaction activity. Mainly, PET is used to diagnose human tumors and also to monitor their treatment.

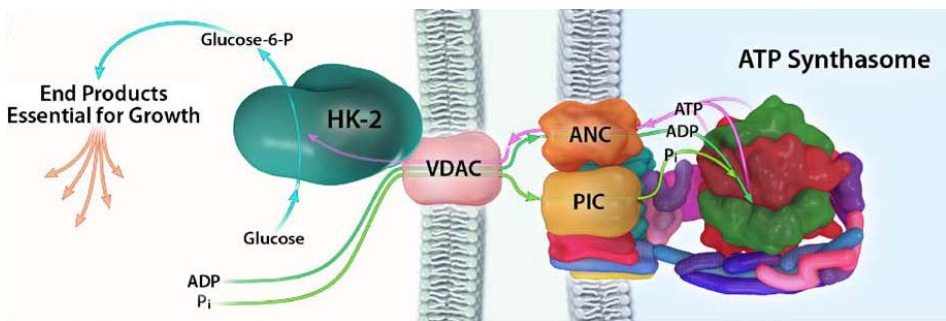


**Figure 6.** Warburg-Pedersen model. Warburg – Pedersen model described aerobic glycolytic mechanism in tumor cells where OXPHOS is regulated by hexokinase isoenzyme (HK-2) binding on voltage dependent anion channel (VDAC) which located on mitochondrial outer membrane. Glycolytic enzyme binding on VDAC increases HK-2 access to ATP which is produced by ATP synthasome. ATP synthasome is a complex which consists of ATP synthase, adenine nucleotide carrier (ANC) and inorganic phosphate carrier (PIC). From (Pedersen 2007) with permission.

## **Aim of the study**

The aims of the study were the following:

1. To perform kinetic analysis of the regulation of mitochondrial respiration in post-operative human samples and cancer cells.
2. To analyze the interplay of adenylate and creatine kinase networks in colorectal cancer and neuroblastoma cells.
3. To estimate the functional coupling between OXPHOS and the phosphotransfer network enzymes in permeabilized post-operative human samples and cancer cells.
4. To develop a semi-quantitative respirometry method, in order to quantify AK1 and AK2 distribution in health and disease.

## Materials and methods

### 4. Materials

#### 4.1 Human post-operative samples

Post-operative samples (0.1-0.5 g) were obtained from Oncology and Hematology Clinic at the North Estonian Medical Centre (Tallinn). Before every experiment all samples were checked by the North Estonian Medical Centre pathologist. For the current study only primary tumors, which had not received any radiation or chemotherapy, were used. For this thesis two distinct groups of patient cohorts were used: breast cancer group consisted of 10 patients and they varied from age 50-71, and the colorectal cancer group consisted of 29 patients and they varied from age 63-92. For colorectal and breast cancer, the normal tissue were cut out from 5 and 2 cm tumors, respectively. Control tissue for colorectal cancer consisted of colonocytes and smooth muscle cells, and breast cancer control tissue mainly contained fibroblast and adipocytes. 1 h after surgery samples were delivered to the Laboratory of Bioenergetics, where human samples were examined for not more than 3 h. All samples were transported in pre-cooled Mitomedium –B solution (0,5 mM EGTA, 3 mM MgCl<sub>2</sub>\*6H<sub>2</sub>O, 3 mM KH<sub>2</sub>PO<sub>4</sub>, 20 mM taurine, 20 mM HEPES, 110 mM sucrose, 0,5 mM DTT, 60 mM K-lactobionate, 5 mg/ml BSA and leupeptine). All investigations were approved by the Medical Research Ethics Committee (National Institute for Health Development, Tallinn) and were in accordance with Helsinki Declaration and Convention of the Council of Europe on Human Rights and Biomedicine.

#### 4.2 Animals

Adult (3-month-old) male Wistar rats weighing about 350 g were used in experiments. These animals were kept on a standard laboratory diet and given tap water *ad libitum*. Animal procedures were approved by the Estonian National Committee for Ethics in Animal Experimentation (Estonian Ministry of Agriculture).

#### 4.3 Cell cultures

Stock culture of Neuro-2A (N2a) cells was obtained from the American Type Culture Collection, Cat. No. CCL-131. The murine NB cells were grown as a loosely adhering monolayer in high glucose Dulbecco's modified Eagles medium (DMEM) with L-glutamine, supplemented with 10% FBS, 100 U/ml penicillin and 100 µg/ml streptomycin and 50 µg/ml gentamicin (complete growth medium). The cells were sub-cultured at 3 days intervals and had received no more than 20 cell culture passages. For neural differentiation of N2a cells to cholinergic neurons, cells were seeded at an initial density of  $2 \times 10^4$  cells/cm<sup>2</sup> and differentiation was induced by 10 µM RA in complete growth medium, for details see in (Blanco, Lopez Camelo et al. 2001).

The HL-1 murine cardiac sarcoma cell line was originally established by William Claycomb (Claycomb, Lanson et al. 1998) and was kindly provided to us by Dr. Andrey V. Kuznetsov (Innsbruck Medical University, Austria). HL-1 cells were grown in fibronectin–

gelatin (5 µg/ml/0.2%) coated T75 flasks containing Claycomb medium (Sigma-Aldrich), supplemented with 10% FBS, 100 U/ml penicillin, 100 µg/ml streptomycin, 50 µg/ml gentamicin, 2 mM L-glutamine, 0.1 mM norepinephrine, and 0.3 mM ascorbic acid. Both N2a and HL-1 cells were cultured at 37°C in humid air with 5 % of CO<sub>2</sub>.

## 4.4 Chemicals

Unless stated otherwise, all materials and reagents were purchased from Sigma-Aldrich Company (St. Louis USA). DMEM and phosphate buffered saline (PBS, Ca/Mg free) were obtained from Corning (USA) whereas heat-inactivated fetal bovine serum (FBS), accutase, penicillin-streptomycin solution (100×), gentamicin and 0.05% Trypsin-EDTA were purchased from Gibco Life Technologies (Grand Island, NY). Primary and secondary antibodies were obtained from Santa Cruz Biotechnology Inc. or Abcam PLC whereas mitochondrial specific fluorescence dye MitoTracker Red CMXRos was obtained from Molecular Probes. Trizol (Life Technologies), RNeasy Minikit (QIAGEN Sciences), cDNA Reverse Transcription Kit and TaqMan Gene Expression Master Mix for mRNA isolation and real-time reverse transcriptase polymerase chain reaction (RT-PCR) were purchased from Applied Biosynthesis.

## 5. Methods

### 5.1 Isolation of rat cardiomyocytes and liver mitochondria

Adult CM were isolated after perfusion of the rat heart with collagenase-A (1.0 mg/ml, Roche) exactly as described in our previous work (Saks, Belikova et al. 1991). The sarcolemma of cells was permeabilized by saponin treatment (25 µg/ml, for 5 min at 25 °C) directly in oxygraphic chambers (Tepp, Shevchuk et al. 2011).

Rat liver mitochondria were isolated by mild trypsin digestion (at 1 mg/ml for 10 minutes at 4°C) of the tissue homogenate, exactly as described previously (Saks, Chernousova et al. 1975). After differential centrifugation, the final mitochondrial pellet was suspended in isolation medium containing 1 mg/ml BSA to a mitochondrial protein concentration of 10–15 mg/ml, and this suspension was stored at 4 °C until use.

### 5.2 Preparation of skinned tumor and rat heart fibers

Skinned fibers from rat heart muscle and HCC and HBC were prepared according to methods described by Kuznetsov and coworkers (Kuznetsov, Veksler et al. 2008): tissue samples were dissected on ice into small (25-35 mg) fiber bundles and tissue cells plasma membranes were permeabilized in pre-cooled solution-A (20 mM imidazole, 20 mM taurine, 3 mM KH<sub>2</sub>PO<sub>4</sub>, 5.7 mM ATP, 15 mM PCr, 9.5 mM MgCl<sub>2</sub>\*6H<sub>2</sub>O, 49 mM KMES, 2.77 mM K<sub>2</sub>Ca EGTA, 7.23 mM EGTA, 1 µM leupeptine and 50 µg/ml saponin) for 30 minutes at 4°C. The permeabilized fibers were then washed three times for 5 minutes in pre-cooled Mitomedium-B solution (0.5 mM EGTA, 3 mM MgCl<sub>2</sub>\*6H<sub>2</sub>O, 3 mM KH<sub>2</sub>PO<sub>4</sub>, 20 mM taurine, 20 mM HEPES, 110 mM sucrose, 0.5 mM DTT 60 mM K-lactobionate and 5 mg/ml BSA, pH 7.1). After washing the samples were kept at 4 °C in Mitomedium-B until use.



### **5.3 Determination of cell growth**

The effect of RA on the rate of N2a cells growth (seeded in 96-well plates at a density of  $5 \times 10^3$  cells/well) was estimated by the use of MTT Cell Proliferation Assay Kit (ATCC® 30-1010 K) according to the manufacturer manual. The absorbance of samples at 570 nm (reference wavelength, 620 nm) was measured spectrophotometrically using a microplate reader (Multiscan Spectrum, Thermo Electron Corporation).

### **5.4 Mitochondrial respiration in permeabilized tissue samples, cells and isolated mitochondria**

Rates of O<sub>2</sub> consumption by the permeabilized, N2a, HL-1 tumor cells (at a density of 0.5– $1.0 \times 10^6$  cells/ml), CMs, HCC and HBC samples or isolated liver mitochondria were measured under magnetic stirring (300 rpm) at 25°C in 2-ml glass chambers of a two-channel titration-injection respirometer (Oxygraph-2 K, OROBOROS Instruments, Austria). Mitochondrial respiration was measured in medium-B supplemented with 5 mM glutamate, 2 mM malate and 10 mM succinate as respiratory substrates; solubility of oxygen was taken as 240 nmol/ml. For N2a cells, a final concentration of 40 µg/ml saponin was determined to yield maximal respiration response for exogenously added ADP, at the same time mitochondrial membrane remained intact. For HL-1 cells, 25 µg/ml digitonin was used as was found early on (Monge, Beraud et al. 2009). All respiration rates of tissue samples and cells were normalized per mg dry weight, million cells or mg protein respectively.

### **5.5 Analysis of functional coupling between OXPHOS and mitochondrial creatine kinase**

In the current study, the corresponding respirometry protocol (Guzun, Timohhina et al. 2009) was used to analyze functional coupling between OXPHOS and MtCK. Experiments were performed in Mitomedium-B in the presence of respiration substrate (glutamate, malate and succinate) with PEP 5 mM. Addition of MgATP (0.2 mM for HCC and colon tissue and 0.1 mM for N2a cells) activated OXPHOS due to increased circulation of ADP in mitochondrial compartment. Next, PK 10 U/ml addition (5 mM PEP was already present in solution) trapped the extramitochondrial ADP produced by cytoplasmic isoforms of creatine kinases (CK-MM or CK-BB) and MgATPase. Finally, addition of 10 mM Cr activated only MtCK dependent mitochondrial respiration.

### **5.6 Experimental model to estimate the presence of adenylate kinase 1 and 2**

The respirometry protocol for estimating the presence of AK1 and AK2 in permeabilized cells or tissues, was modified from Guzun *et al.* (Guzun, Timohhina et al. 2009) and Gruno *et al.* (Gruno, Peet et al. 2006). The principles of this study are illustrated by four schemes of increasing complexity (Figure 7): schemes A and B represent simple system where only AK2 is present (isolated liver mitochondria) and the reference system on schemes C and D are more complex where both AK1 and AK2 are present. Experiments were performed

in two types of conditions: in the presence of ADP trapping system after or before activation cytosolic (AK1) and mitochondrial (AK2) adenylate kinase isoform. PK, in the presence of PEP, traps extramitochondrial ADP produced by AK1 and MgATPase reactions and subsequently regenerates extramitochondrial ATP. In mitochondria, AK2 forms a micro-domain within the intermembrane space, where AK2 produces 2 molecules of ADP, which is re-imported into the matrix via ANT due to its functional coupling with AK2.

In permeabilized HCC, normal colon tissue and HBC, the total AK coupling with OXPHOS was expressed by adenylate kinase index ( $I_{AKtotal}$ ): [ $I_{AKtotal}=(V_{AMP}-V_{AP5A})/V_{AP5A}$ ], where  $V_{AMP}$  is a mitochondrial respiration rate in the presence of 2 mM AMP and  $V_{AP5A}$  is a remaining respiration rate after inhibition of the total AK by 0.2 mM diadenosine pentaphosphate (AP5A). AK coupling with OXPHOS was measured in the presence of 0.1 mM ATP.

The presence of cytosolic AK1 and mitochondrial AK2 in permeabilized tumor and normal cells was assayed semi-quantitatively by respirometry methods. These measurements were performed in medium-B in the presence or absence of PK-PEP ADP trapping system. The AK1 functional coupling with OXPHOS, linked with this isoenzyme activity, was characterized by the corresponding AK index ( $I_{AK1}$ ). The  $I_{AK1}$  was calculated according to the equation: [ $I_{AK1} = ((V_{AMP} - V_{PK}) / (V_{AMP} - V_{AP5A})) \times 100\%$ ], where  $V_{AMP}$ ,  $V_{PK}$  and  $V_{AP5A}$  are rates of  $O_2$  consumption that were measured after subsequent addition of 2 mM AMP, 10 U/ml PK and 0.2 mM AP5A, respectively. The AK2 functional coupling with OXPHOS was calculated as  $I_{AK2}=100\%-I_{AK1}$ .

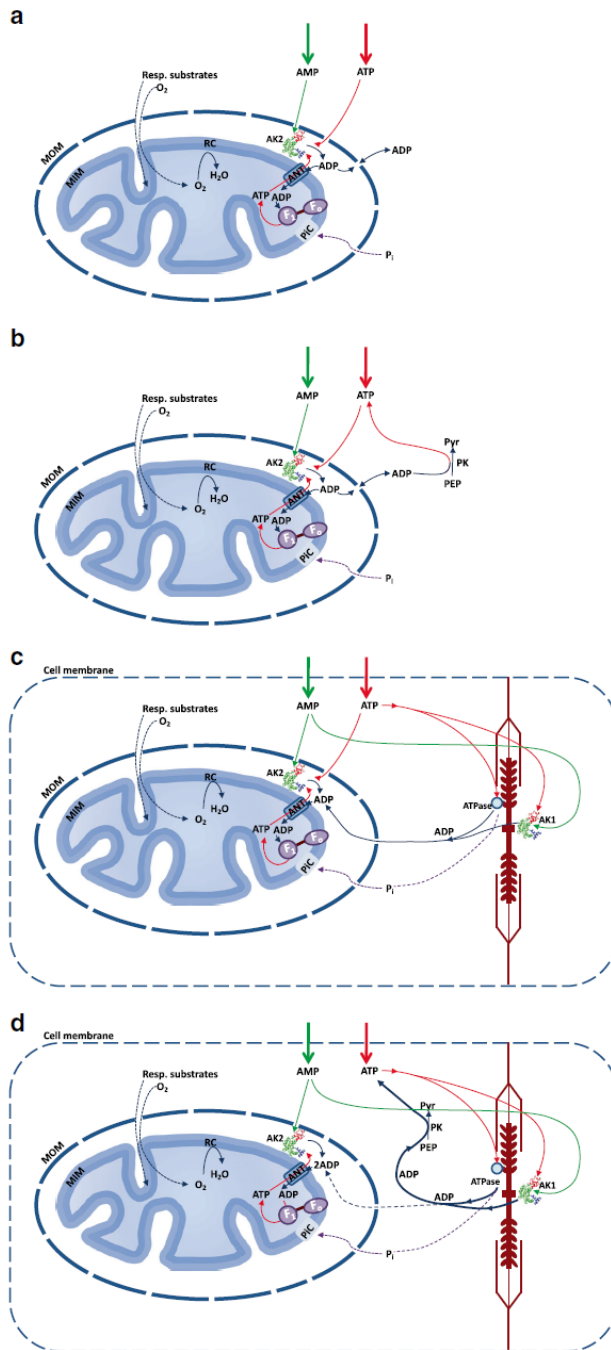


**Figure 7.** The principles of this study are illustrated by four schemes of increasing complexity: Schemes A and B represent isolated liver mitochondrion as a reference system. Schemes C and D illustrate permeabilized cells chosen as experimental study model. From (Klepinin, Ounpuu et al. 2016) with permission.

## 5.7 Confocal microscopy imaging

For immunohistochemistry, formalin fixed paraffin-embedded tissue sections from normal colon tissue and HCC were rinsed 4 times with xylene for 5 min and ethanol/xylene (1:1) for 5 minutes then the slide was rehydrated step-by-step by 100-50 % ethanol (100 %, 95 %, 70 % and 50 %). Finally, slides were treated with antigen retrieval buffer (100 mM tris buffer with 5 %, w/v urea, pH 9,5) at 98 °C for 15 min. Tissue samples were then blocked with 2 % BSA solution in PBS and kept overnight at 4 °C with primary antibodies. In order to quantify the mitochondrial mass in cancer and normal tissue, mitochondria were labeled by Tom20 antibody (SantaCruz Biotechnology, sc17764). The Tom20 fluorescence intensity was normalized against the total  $\beta$ -tubulin (Abcam®, ab6046) fluorescence. Samples were washed and incubated at room temperature for 2 hours with DyLight-488 goat anti-rabbit IgG (Abcam®, ab96899) or DyLight-549 goat anti-mouse IgG (Abcam®, ab96880) secondary antibodies.

The mitochondria in N2a cells were visualized by MitoTracker® Red CMXRos (Molecular Probes). The labeling procedure was carried out according to the manufacturer instructions. Before the labeling procedure, cells were fixed by 4% paraformaldehyde. In the current study, confocal images were collected by Olympus FV10i-W inverted laser scanning confocal microscope equipped with a 60× water immersion objective.

## 5.8 Assessment of enzymatic activity

All cells and tissue samples were frozen in liquid nitrogen and stored at -80 °C until use. HK activity was measured as the total glucose phosphorylating capacity of whole cell extracts, using a standard glucose-6-phosphate dehydrogenase (G6PDH)-coupled spectrophotometric assay (Robey, Raval et al. 2000). One milliunit (mU) of HK activity was calculated as the amount of enzyme activity required to phosphorylate 1 nmol of glucose in 1 min at 25 °C.

The CK activity was assessed spectrophotometrically at 25 °C in the direction of ATP formation in the presence of AP5A, 20 mM PCr and with 2 U/ml G6PDH and 2 U/ml HK as the coupled enzymes (Monge, Beraud et al. 2009). One mU of CK activity represents the formation of 1 nmole of ATP per minute at 25 °C.

The activity of acetylcholinesterase (AChE) in N2a cells was measured spectrophotometrically by applying the technique of Ellman et al. (Ellman, Courtney et al. 1961). One unit of AChE activity represents the hydrolysis of 1  $\mu$ mol of the acetylthiocholine per minute at 37 °C.

AK1 and AK2 activities were measured in whole cell or tissue extracts at 25°C by an enzyme-coupled spectrophotometric assay in the direction of ATP formation, essentially as described earlier by Dzeja et al. (Dzeja, Vitkevicius et al. 1999). The reaction mixture contained 20 mM HEPES (pH 7.5), 0.1 M KCl, 4 mM Mg-acetate, 1 mM EDTA, 20 mM glucose, 2 mM NADP<sup>+</sup>, 4.5 units/ml HK, and 2 units/ml G6PDH as the coupled enzymes. The reaction was initiated with 2 mM ADP.

AK1 is a thiol-containing enzyme that is inhibited by Nethylmaleimide (NEM), while AK2 is not (Khoo and Russell 1972). AK2 activity was determined as the activity remaining after the NEM treatment of cell/tissue extracts. For the NEM treatment, enzyme samples (in 20 mM MOPS-buffered solution with 0.2 M NaCl, pH 8.0) were

incubated in the presence of 1 mM NEM for 1 h at 25°C before assay. One unit of AK activity was defined as 1  $\mu$ mole of ATP produced per minute at 25 °C.

AMPD activity was measured spectrophotometrically in whole cell or tissue extract by an enzyme-coupled spectrophotometric assay in the direction of inositol monophosphate formation in the present of 50 mM HEPES (pH 7.1), 100 mM KCl, 1mM EDTA, 1mM DTT, 5 mM  $\alpha$ -ketoglutarate, 0.15 mM NADH, and 5 U of glutamate dehydrogenase containing 0.25 mg of extract protein, and the reaction was initiated by 10 mM AMP (Ashby and Frieden 1978). One unit of AMPD activity was defined as 1  $\mu$ mole of AMP deaminated to inosine monophosphate.

All enzyme activities were measured using Cary 100 Bio UV-visible spectrophotometer. The absorption at 340 nm was used for all enzyme activity assays except for AChE, which absorption was measured at 405 nm. Protein concentration of the used cell/tissue homogenates was determined by a Pierce BCA Protein Assay Kit according to the manufacturer recommendations using BSA as a standard.

## 5.9 RNA isolation and quantitative RT-PCR

HCC and normal colon tissue samples were frozen in liquid nitrogen and stored at -80 °C until RNA isolation. RNA from 29 human samples was isolated using Trizol (Life Technologies) solution, followed by purification using the RNeasy Mini Kit (QIAGEN Sciences) with DNase treatment. Extracted RNA was dissolved in RNase-free water, quality and concentration were measured using Nanodrop and RNA was stored at -80°C until cDNA synthesis.

For cDNA synthesis 2  $\mu$ g of total RNA was used. cDNA was synthesized using High Capacity cDNA Reverse Transcription Kit with RNase Inhibitor (Applied Biosystems). cDNA was used as a template for TaqMan<sup>®</sup> quantitative RT-PCR analysis in the Roche Light Cycler 480 system (Roche). TaqMan<sup>®</sup>Gene Expression Master Mix and FAM labeled TaqMan<sup>®</sup> (Applied Biosystems) gene assays were used to detect the mRNA expression level of the gene of interest and of actin as a reference gene. The used TaqMan<sup>®</sup> probes were the following: actin beta –Hs01060665 g1; hexokinase I – Hs00175976 m1; hexokinase II –Hs00606086 m1; creatine kinase, mitochondrial 1B – Hs00179727 m1; creatine kinase, mitochondrial 2 – Hs00176502 m1.

Threshold cycles (Ct) were automatically calculated by Light Cycler 480 software (Roche). Data were analyzed with the formula  $2^{-\Delta Ct}$  (Livak and Schmittgen 2001), normalized to the endogenous housekeeping gene actin beta.

## 5.10 Data analysis

Data in the text, tables and figures are presented as mean  $\pm$  standard error of the mean (SEM). Results were analyzed by Student's t -test. Values of p <0.05 were considered statistically significant. All data and statistics were calculated by using SigmaPlot 11 software (Systat Software, Inc). Apparent Km values for ADP and AMP were estimated by fitting experimental data to a non-linear regression (according to a Michaelis-Menten model) equation.

## Results

### 6. Characterization of the mitochondrial respiration and mitochondria communication with phosphotransfer network in cancer

#### 6.1 Localization of mitochondria and mitochondria interaction with glycolytic pathway in neuroblastoma and colorectal cancer (Article I, II and III)

In the presented work, N2a cells treated with RA were used as an *in vitro* model of normal neurons of the SNS. Indeed, the enzyme activity study (Table 1) confirmed that RA induced N2a differentiation (dN2a) towards SNS *via* increased neurons specific AChE activity. On the day after RA addition, a drastic morphological change in N2a cells can be observed (Figure 8). During RA treatment N2a cells go through several transformations: cell size increases several times and strong neurite outgrowth takes place in cells. RA not only influences the N2a cell morphology, but it also impacts mitochondrial localization (Figure 8). Although, in both cell types, mitochondria are predominantly localized around the cell nucleus, in dN2a cells a significant part of mitochondria are found in neurites (Figure 8 B, C). Moreover, RA significantly diminishes N2a cells proliferation rate (Figure 9). On the third day the proliferation rate decreases 1.5 times in RA treated cells compared to undifferentiated N2a (uN2a) cells.

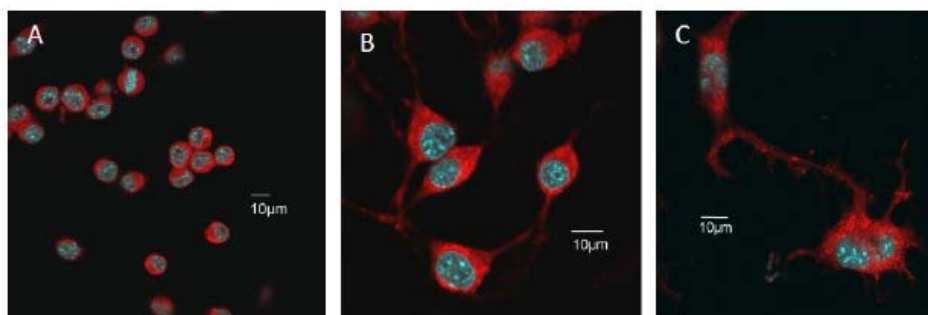


**Figure 8.** Confocal microscopy images of N2a cells with and without all *trans*-retinoic acid (RA) treatment. (A) -control cells, whereas (B) and (C) are N2a cells treated with 7  $\mu$ M RA for 5 days. During 5 days RA-treated N2a cells go through morphological transformation (B, C): increased cell body size as well as in cells take place strong neurite outgrowth. In RA-treated cells mitochondria (red fluorescence) not only located around the nucleus (blue fluorescence) like in N2a control cells (A) but also significant part can find in neurites (B, C). Mitochondria in the cells were stained with Mito Tracker Red CMXRos and cell nuclei with DAPI.

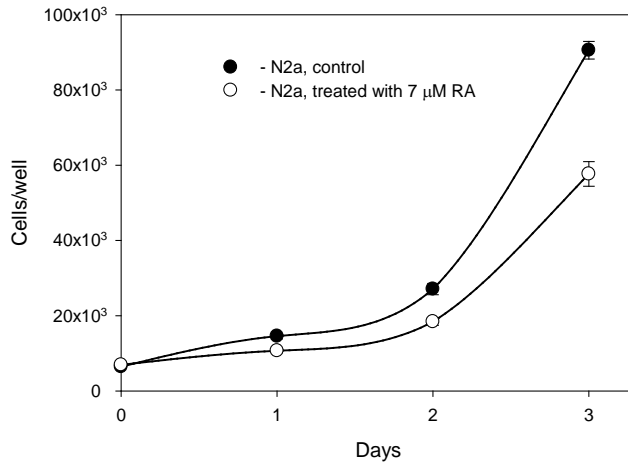


**Figure 9.** Effect of all-trans-retinoic acid (RA) on proliferation of N2a cells. Cell count was performed by MTT assay during 3-day cell culturing. RA-treated cells show decline trend in proliferation activity compare to control N2a cells. N=3 and Bars are SEM.

For HCC, changes in mitochondrial mass were quantified by confocal microscopy (Figure 10) to characterize main alterations in bioenergetic profiles caused by cancer formation. Figure 10A shows that the mitochondrial specific marker Tom20 distributed diffusely within both tumor and control tissue. Mitochondrial mass was quantified by normalization of Tom20 fluorescence signal against total tubulin fluorescence signal (Figure 10B). The current experiments revealed that malignant tissue possessed ~70% more mitochondrial mass than the surrounding healthy colon tissue.

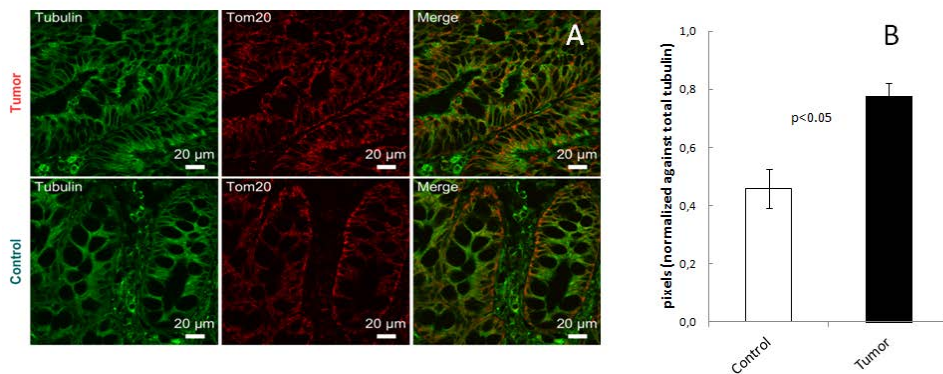


**Figure 10.** Immunohistochemistry quantification of the total mitochondrial mass in paraffin-embedded colorectal cancer and control colon tissue sections. (A) Confocal microscopy imaging of paraffin-embedded tissue section where mitochondria and tubulin were preloaded with anti-total  $\beta$  tubulin and anti-Tom20 antibodies. (B) Mitochondrial mass was quantified in healthy and colorectal tissue by normalization of Tom20 fluorescence signal intensity against total  $\beta$  tubulin fluorescence intensity. Bars are SEM, N=7,  $p < 0.05$ .

### 6.1.1 Quality test

Before every respirometric experiment, the intactness and quality of mitochondria (Kuznetsov, Veksler et al. 2008) in tissue samples or cancer cells were evaluated. If mitochondrial respiration parameters did not pass quality control, we discarded such tissues or cells in this work. In the current study, the technique of permeabilized cells, elaborated by Kuznetsov (Kuznetsov, Veksler et al. 2008), was used to measure respiratory activities of mitochondria. This method gives an opportunity to estimate mitochondrial respiration near physiological condition.

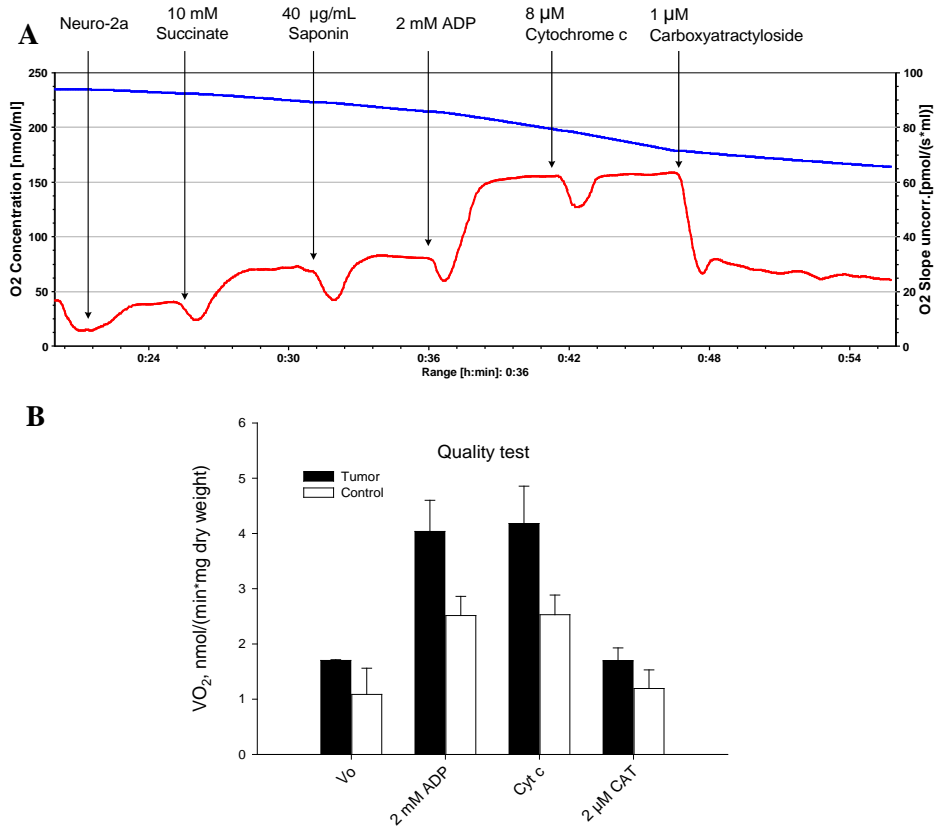


**Figure 11.** Quality test to control intactness of mitochondrial membranes in (A) permeabilized N2a cells, (B) human colorectal cancer and control colon tissues. (A) Original respirometry graph for N2a cells. Blue traces represent the O<sub>2</sub> concentration and red traces the respiration rates. (A) and (B) experiments were performed in medium-B with 5 mM glutamate, 2 mM malate, and 10 mM succinate as respiratory substrates. Respiration was activated by 2 mM ADP and intactness of mitochondrial membranes were controlled by cytochrome c (Cyt c) and carboxyatractyloside (CAT). (B) All respiratory substrates and inhibitors were added sequentially as indicated in the x-axis; bars are SEM, N=11.



Figure 11A represents quality test protocols for N2a cells. In the current study, the optimal saponin concentration (40  $\mu\text{g/ml}$ ) for N2a cells was found. To estimate mitochondrial quality the intactness of both mitochondrial membranes was controlled. Firstly, mitochondrial basal respiration rate ( $V_0$ ) in the presence of mitochondrial respiration substrates was monitored. Mitochondrial respiration was activated by 2 mM ADP as a result mitochondrial respiration reached nearly maximal level ( $V_{\text{max}}$ ). Next, MOM intactness was controlled. After addition of cytochrome-c (cyt c) (final concentration, 8  $\mu\text{M}$ ), mitochondrial respiration did not increase significantly (<10%) if the MOM was intact. Finally, carboxyatractyloside (CAT) (1  $\mu\text{M}$ ), an ANT inhibitor, blocked ATP/ADP turnover within mitochondria inner membrane as a result mitochondria respiration decreased to  $V_0$  level. CAT test showed that MIM was also intact. Same quality test protocol (Figure 11B) was made on post-operative permeabilized HCC and healthy colon tissues.

Next,  $V_0$  and  $V_{\text{max}}$  respiration rates were determined and compared between uN2a and dN2a (Table 2) and also between HCC and control colon tissue (Figure 11B). For uN2a and dN2a cells, no any significant differences were found in  $V_0$  ( $3.38 \pm 0.12$  versus  $4.07 \pm 0.46$ ) and in  $V_{\text{max}}$  ( $11.0 \pm 0.43$  versus  $12.05 \pm 1.06$ ). Moreover, changes in mitochondrial respiration rates during colorectal cancer formation were monitored (Figure 11B). For HCC, both mitochondrial respiration parameters were higher compared to control tissue, the  $V_0$  was ( $1.70 \pm 0.01$  versus  $1.09 \pm 0.47$ ) and  $V_{\text{max}}$  was ( $4.04 \pm 0.56$  versus  $2.51 \pm 0.35$ ). Finally, respiratory control index (RCI) values ( $V_0/V_{\text{max}}$ ) were calculated. For uN2a and dN2a cells RCI values were 3.28 and 3.13, respectively (Table 2). Although our studies showed that HCC had higher mitochondria mass (Figure 10) and mitochondrial respiration rate (Figure 11B) compared to control tissue, no differences between HCC and control colon tissue in RCI values was found (2.4 versus 2.32).

### **6.1.2 ADP dependent respiration and mitochondria interaction with glycolytic pathway – aerobic glycolysis**

According to the MI model (Figure 5) in healthy tissues, such as heart muscle and neurons, mitochondrial respiration is controlled by permeability of VDAC for ADP. Therefore, the kinetics of mitochondrial respiration by exogenously added ADP was studied in N2a cells and HCC and colon tissue. For uN2a cells, the apparent Michaelis-Menten constant ( $K_m$ ) value for ADP  $K_m(\text{ADP})$  was  $20.3 \pm 1.4 \mu\text{M}$  and during cell differentiation by RA the MOM permeability for ADP did not change ( $19.4 \pm 3.2 \mu\text{M}$ ). Same mitochondrial respiration kinetic analysis was done on post-operative samples. Current study revealed that mitochondrial affinity for ADP was low in colon tissue ( $K_m(\text{ADP})=260 \pm 55 \mu\text{M}$ ) and during malignant transformation the permeability of VDAC for exogenous ADP was increased ( $K_m(\text{ADP})=126 \pm 17 \mu\text{M}$ ).

**Table 1** Enzymatic activities of undifferentiated (uN2a), all-trans-retinoic acid differentiated (dN2a) N2a cells, colorectal cancer and healthy colon tissue.

Enzymes	uN2a cells, mean $\pm$ SEM, N = 5 <sup>a</sup>	dN2a cells, mean $\pm$ SEM, N = 5	Colorectal normal tissue mean $\pm$ SEM, N=11 <sup>b</sup>	Colorectal cancer mean $\pm$ SEM, N=11
Hexokinase	19.57 $\pm$ 1.86	32.15 $\pm$ 3.73*	244 $\pm$ 50	215 $\pm$ 40
Creatine kinase	7.59 $\pm$ 0.89	11.78 $\pm$ 0.59***	497 $\pm$ 142	204 $\pm$ 84*
Adenylate kinase	121.5 $\pm$ 9.4	151.1 $\pm$ 8.5*	257 $\pm$ 35	411 $\pm$ 43*
Acetylcholinesterase	2.52 $\pm$ 0.52	4.62 $\pm$ 0.27 **	-	-

<sup>a</sup> mU per 1 $\times$ 10<sup>6</sup> cells

<sup>b</sup> mU per mg protein

\* $p < 0.05$ , \*\* $p < 0.02$  and \*\*\* $p < 0.001$  show significant difference between cancer and control cells

Our previous work showed that during cancer formation  $\beta$ II tubulin on VDAC replaced with HK, and as a result of MI transformation, VDAC permeability for ADP increased (Guzun, Karu-Varikmaa et al. 2011). Therefore, the aerobic glycolysis pathway (Figure 6) was researched on N2a cells and post-operative tissue samples. Firstly, total HK activity and HKI and HKII expression levels were estimated. The HK activity of uN2a cells was 19.57  $\pm$  1.86 and its activity was increased 1.5 times (32.15  $\pm$  3.73) during N2a cells differentiation with RA (Table 1). Moreover, HK activity was measured in HCC and colon tissue. Although, the current study did not reveal any difference in HK activity between HCC and colon tissue (Table 1), a slight decrease in HK II expression was observed during cancer formation (Figure 12).

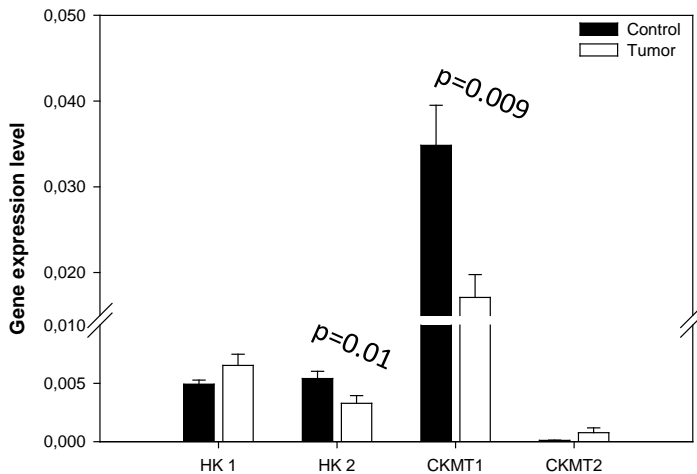


**Figure 12.** Expression profile of creatine kinase and hexokinase isoform in human colorectal cancer and normal colon tissue. mRNA levels were assayed by real-time reverse transcriptase polymerase chain reaction. On y-axis is break 0,01-0,015 and bars are SEM, N = 2). HK-1 and HK-2 are hexokinase-1 and -2; CKMT1 and CKMT2 are ubiquitous and sarcomeric mitochondrial creatine kinase, respectively.

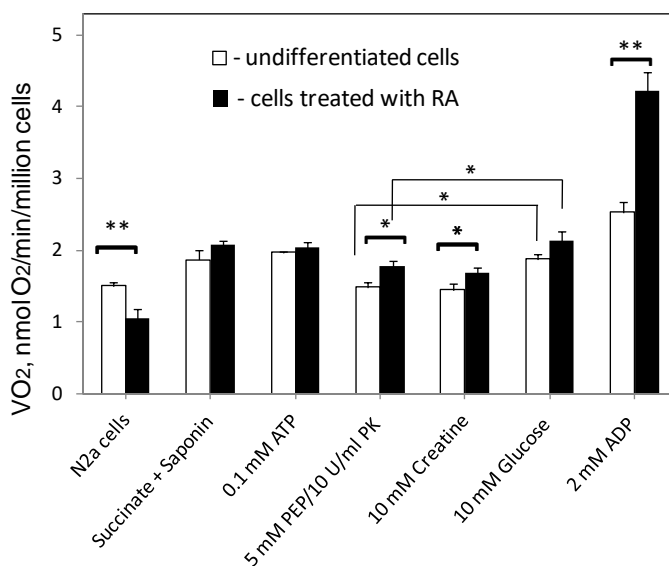


**Figure 13.** Effects of exogenously added creatine and glucose on the rate of oxygen consumption by permeabilized RA-treated N2a cells and undifferentiated N2a cells. The creatine (10 mM) and glucose (10 mM) mediated mitochondrial respiration were estimated in the presence of pyruvate kinase/phosphoenolpyruvate ADP trapping system and exogenously added 0.1 mM MgATP. Finally, 2 mM ADP was added to maximally activate mitochondrial respiration. Bars are SEM; N=5; \* and \*\* indicate a statistical significant difference between the mean values;  $p < 0.05$  and  $p < 0.01$ , respectively.

According to the Warburg-Pedersen model (Figure 6), the mitochondrial-associated HK coupling with OXPHOS, was investigated in NB cells and post-operative samples (Figure 13, 14). The N2a cells respiratory study was performed in the presence of PK-PEP system. Figure 13 shows that addition of glucose (10 mM) stimulated mitochondrial respiration in both cell lines. Next, we estimated percentage of aerobic glycolysis (glucose dependent) from ADP stimulated mitochondria respiration. We found that the mitochondrial-associated HK coupling with OXPHOS was higher in uN2a than dN2a (aerobic glycolysis ~40% and ~5%, respectively). Same protocol was used to estimate HK coupling with OXPHOS in HCC and colon tissue. In these experiments PK-PEP system was not used. Respiratory study showed (Figure 13A) that in HCC glucose stimulated more mitochondrial respiration than in colon tissue samples was observed. If the percentage of aerobic glycolysis from ADP stimulated mitochondrial respiration is compared, then HCC aerobic glycolysis formed 30-35 % from total OXPHOS whereas in colon tissue aerobic glycolysis pathway formed from total mitochondria mediated ATP production less than 10 %.

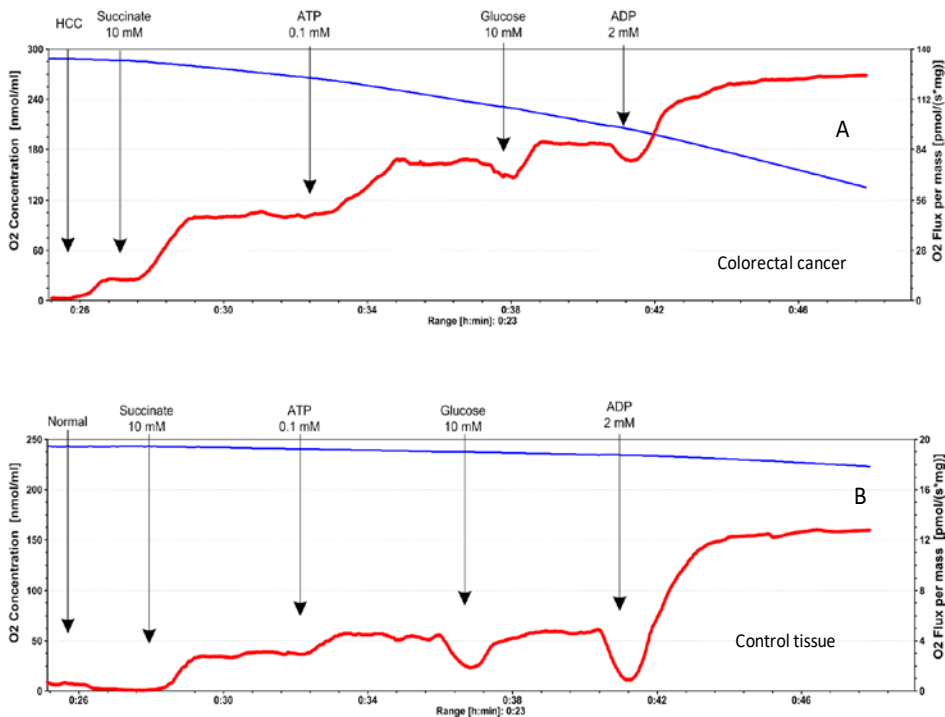


**Figure 14.** Oxygraphic protocol to estimate mitochondrial-associated HK coupling with OXPHOS in permeabilized colorectal cancer (A) and control colon tissues (B). The addition of 10 mM glucose in the presence of 0.1 mM Mg-ATP caused a stimulatory effect on mitochondrial respiration in different manner: (A) significant increase OXPHOS rate in the tumor and slight increase in the normal tissue. Finally, 2 mM ADP was added to nearly maximally activate mitochondrial respiration. Blue line – O<sub>2</sub> concentration, red – rates of O<sub>2</sub> consumption.

## **6.2 Interplay between creatine kinase and adenylate kinase in N2a cells and colorectal cancer (Article I, II)**

According to the MI model (Figure 5) MtCK plays an important role in the regulation of mitochondrial respiration in heart muscle and neurons. There are evidences that in some cancers MI is rearranged due to downregulation of MtCK (Eimre, Paju et al. 2008; Patra, Bera et al. 2008; Amamoto, Uchiumi et al. 2016). Therefore, in N2a cells and HCC the role of MtCK in cancer formation was investigated. Firstly, enzyme activity study was performed. Table 1 data show that the total CK activity in N2a cells is 40% lower than in normal neurons (dN2a). Similar result was found for HCC. During colon cancer formation CK activity decreased around 60% (Table 1).

Next, MtCK expression and its functional coupling with OXPHOS were examined. The respirometry method was performed in the presence of PK-PEP system to study functional coupling between MtCK and OXPHOS. Figure 13 shows that addition of Cr does not increase mitochondrial respiration in both uN2a and dN2a cells. The same protocol was used for HCC and normal colon tissue (Figure 15). In colon tissue increased OXPHOS rate was observed after addition of Cr. The 60 % of Cr mediated respiration in colon tissue was formed from ADP-dependent respiration. In contrast to normal tissue, Cr-stimulated mitochondrial respiration in HCC was not observed. The quantitative RT-PCR study (Figure 12) showed that absence of functional coupling between MtCK and mitochondria in HCC was due to downregulation of CKMT1 gene (uMtCK).

Previous CK knockout mice study has demonstrated plasticity of phosphotransfer networks: in heart muscle absence of MtCK can be compensated by AK phosphotransfer network. Our current study demonstrated that both uN2a and dN2a possessed high AK activity and during RA-treatment AK activity was increased only slightly (Table 1). Moreover, in contrast to CK network, around 40 % higher AK activity observed in HCC compared to normal colon tissue (Table 1). To research AK function in cancer formation and to estimate distribution of AK1 and AK2 in health and malignant cells in this thesis a new respirometry method was developed.

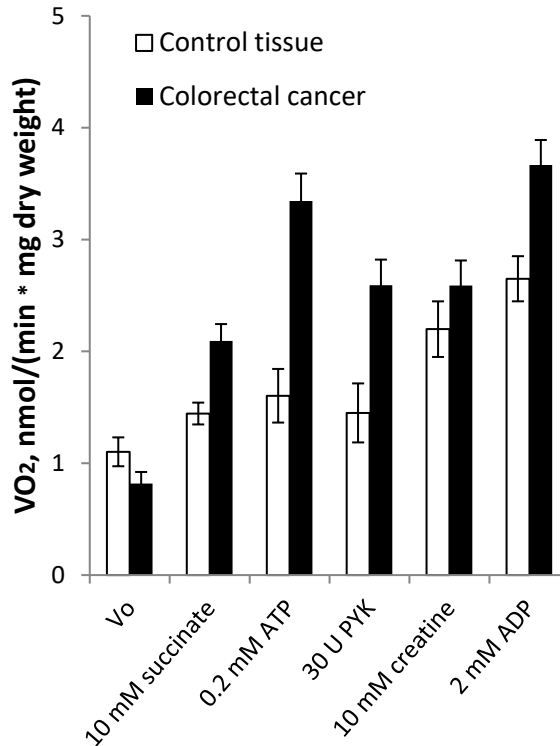


**Figure 15.** Creatine dependent respiration in Colorectal cancer and control normal tissue which mediated by mitochondrial creatine kinase (MtCK) coupling with OXPHOS. Experiment was performed in medium B in the presence of mitochondrial respiration substrate succinate 10 mM, malate 2 mM and glutamate 5 mM. Addition of 0.2 mM MgATP increased circulation of ADP in mitochondria and cytosol due to activation of MgATPases reaction. To remove extramitochondrial ADP pyruvate kinase (PYK) 30U with phosphoenol pyruvate 5 mM was used. In this condition Cr stimulate mitochondrial respiration via activation of MtCK. Finally, addition of 2 mM ADP mitochondrial respiration was reached to near maximal level. Bars are SEM, N=8.

## 6.3 Semi-quantitative respirometry method to quantify AK1 and AK2 distribution in health and disease

### 6.3.1 Application of respirometry method to estimate changes in AK network during malignant transformation of Breast and Colorectal cancer

To estimate AK coupling with OXPHOS in post-operative HBC and HCC samples the corresponding protocol (Figure 16) was applied. In permeabilized HCC sample addition of 0.1 mM ATP slightly raised ADP circulation between mitochondria and ATPases (Scheme 1 C) as a result mitochondrial respiration increased (Figure 16). Next, addition of 2 mM AMP activated both AK1 (cytosolic) and AK2 (mitochondrial) which led to significant increase of OXPHOS rate (~40 %). AMP-dependent respiration was inhibited by AK specific inhibitor AP5A (0.2 mM). The intactness of both mitochondrial membranes was controlled by cyt c (8 $\mu$ M) and CAT (1 $\mu$ M). The same protocol was performed with control colon tissue and breast tissue.

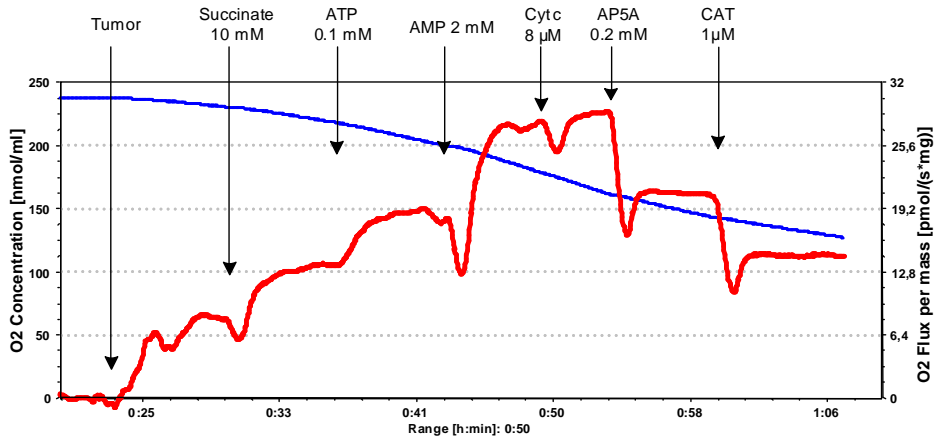


**Figure 16.** Represented oxygenography tracing to estimate adenylate kinase coupling with OXPHOS in post-operative sample. Experiment was performed in Mitomedium-B in the presence of mitochondria respiration substrate succinate 10 mM, glutamate 5 mM and malate 2 mM. AMP dependent respiration was activated with 2 mM AMP in the presence of 0.1 mM ATP. To confirm AK coupled respiration an AK specific inhibitor AP5A 0.2 mM was used. Moreover, intactness of mitochondrial outer membrane was confirmed by Cytochrome c (Cyt c) (8 $\mu$ M) as well as mitochondrial inner membrane intactness was confirmed by carboxyatractyloside (CAT) (1 $\mu$ M). From (Chekulayev, Mado et al. 2015) with permission.

To estimate functional coupling of AK with OXPHOS,  $I_{AKtotal}$  was calculated (see Material and Methods). For healthy colon tissue,  $I_{AKtotal}$  was  $0.28 \pm 0.04$  and during colorectal malignant transformation AK activated respiration increased 1.5 times ( $I_{AKtotal} = 0.51 \pm 0.02$ ) (Figure 17). For normal breast tissue, no any mitochondrial response for mitochondrial respiration substrates and different nucleotide was observed. Therefore, only total AK activity between normal breast tissue and HBC was compared. Table 3 shows that during breast cancer formation the total AK activity increased ~6 times whereas AK1 remain as main AK isoform. In addition, for HBC  $I_{AKtotal}$  was also calculated ( $0.37 \pm 0.06$ ) (Figure 17). If compare HCB result with HCC data, then in HBC  $I_{AKtotal}$  is 1.35 times lower than HCC. These respirometry data correlate well with total AK activity in HBC, normal colon tissue and HCC tissue (Figure 17).

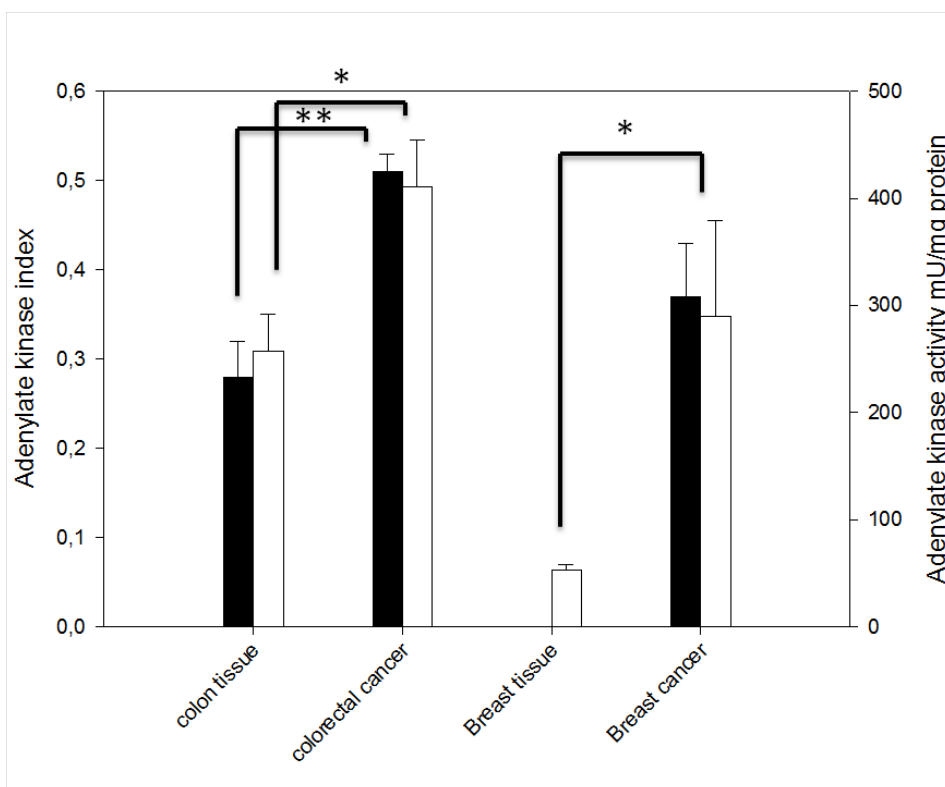


**Figure 17.** Assessment of adenylate kinase (AK) functional coupling with OXPHOS in normal colon tissue, breast and colorectal cancer expressed by adenylate kinase index. The Adenylate kinase index value for all tissue samples was compared with their total AK activity. Black bars indicate AK coupling strength with OXPHOS expressed by Adenylate kinase index. White bars indicate AK activity. Bars are SEM, N=6-11; \* and \*\* indicate a statistical significant difference between the mean values;  $p < 0.05$  and  $p < 0.001$ , respectively.



### 6.3.2 Mitochondrial respiration in rat liver is controlled by adenylate kinase 2

The main isoform of adenylate kinase in a rat liver is AK2 (Noma 2005). Figure 18 represents original protocol to study AK2 coupling with OXPHOS on isolated mitochondria. The mitochondrial respiration was activated by 2 mM AMP in the presence of 0.1 mM ATP, as a result, OXPHOS rate was increased ~8 times. Due to AK2 functional coupling with OXPHOS two molecules of ADP, produced *via* AK2 reaction, directly transfer through ANT into the mitochondria matrix (Figure 7A). Moreover, cyt c and CAT test were performed on isolated liver mitochondria to control mitochondrial inner and outer membrane intactness (Figure 18A). Next, AMP dependent respiration was measured in the presence of PK-PEP system (Figure 18B) under same condition as in Figure 18A with an exception: 2 mM ATP was used instead of 0.1 mM ATP. Under such condition 80 % of ADP, produced *via* AK2 reaction, was trapped by PK due to the high permeability of VDAC for adenine nucleotides (Figure 7B). In the presence of PK-PEP system AMP dependent respiration was not exceeded more than 20 % of the maximal respiration (Figure 18B). Figure 18B represents which part of ADP (AK2-generated) reached to mitochondrial space due to AK2 coupling with OXPHOS. The AK2 coupling with OXPHOS was confirmed by AP5A which inhibited AMP-dependent respiration back to the initial level. Moreover, ADP dependent respiration was also measured in isolated liver mitochondria. It was found that the same level of maximal respiration was obtained with ADP and AMP (Table 2).

**Table 2.** Rates of basal ( $V_o$ ), ADP ( $V_{ADP}$ )- and AMP ( $V_{AMP}$ )-activated respiration, respiratory control index (RCI) and apparent  $K_m$  (AMP) values for human breast cancer tissue, isolated rat liver mitochondria and cardiomyocytes (CMs) as well as some tumor cells of different histological type.

Cells and tissues	$V_o^{(a)}$ mean $\pm$ SEM	$V_{ADP}^{(b)}$ mean $\pm$ SEM	RCI <sup>(b)</sup> , ADP	$V_{AMP}^{(c)}$ mean $\pm$ SEM	$K_m$ (AMP) mean $\pm$ SEM
Mitochondria	4.75 $\pm$ 0.44	42.4 $\pm$ 4.06	8.88 $\pm$ 0.72	41.5 $\pm$ 6.3	23.5 $\pm$ 6.9
Rat CM(s)	7.5 $\pm$ 1.6 <sup>(d)</sup>	84.5 $\pm$ 13.9 <sup>(d)</sup>	11.2 $\pm$ 4.2 <sup>(d)</sup>	88.1 $\pm$ 2.7	369 $\pm$ 88
HL-1 cells	1.91 $\pm$ 0.8	9.12 $\pm$ 2.3	4.51 $\pm$ 0.63	2.9 $\pm$ 0.2	67 $\pm$ 9.3
uN2a cells	3.38 $\pm$ 0.12	11.0 $\pm$ 0.43	3.28 $\pm$ 0.05	7.2 $\pm$ 0.40	92 $\pm$ 14
dN2a cells	4.07 $\pm$ 0.46	12.05 $\pm$ 1.06	3.13 $\pm$ 0.16	6.8 $\pm$ 0.5	207 $\pm$ 24
Breast cancer	0.56 $\pm$ 0.04 <sup>(f)</sup>	1.09 $\pm$ 0.04 <sup>(g)</sup> (range, 0.10-2.02) <sup>(f)</sup>	1.95 $\pm$ 0.21	0.72 $\pm$ 0.07 <sup>(g)</sup> (range, 0.59-1.03)	-
Breast control tissue	0.02 $\pm$ 0.01 <sup>(f)</sup>	-	-	-	-

**Notes:** <sup>(a)</sup>rates of O<sub>2</sub> consumption are expressed in nmol O<sub>2</sub>/min per mg protein; <sup>(b)</sup> $V_{ADP}$  and RCI values were measured in the presence of 2 mM ADP; <sup>(c)</sup> these values were obtained in the presence of 2 mM AMP; <sup>(d)</sup>from (Timohhina, Guzun et al. 2009); <sup>(f)</sup>from (Kaambre, Chekulayev et al. 2012); <sup>(g)</sup> rates of respiration in nmol O<sub>2</sub>/min per mg dry weight of the tissue.

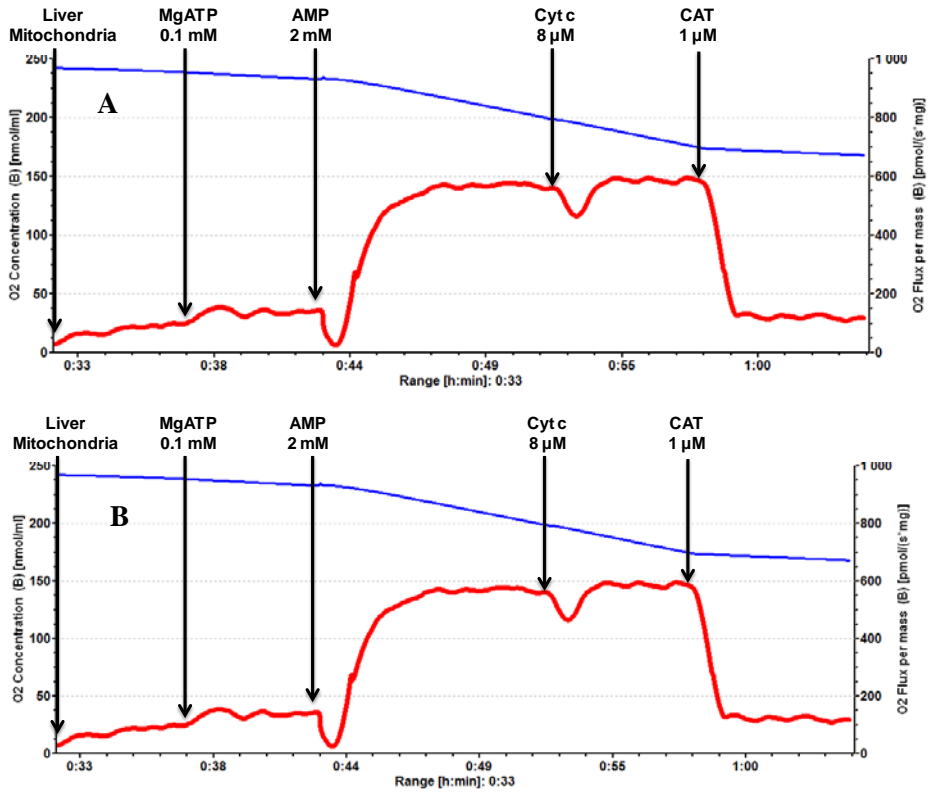


**Figure 18.** Oxygraphic analysis of the functional coupling between AK2 and OXPHOS (A) in the absent and (B) in the presence of PK-PEP system in isolated liver mitochondria. Experiment was performed in Mitomedium-B in the presence of mitochondria respiration glutamate 5 mM and malate 2 mM and PEP 5mM (A) The Mitochondrial respiration was activated by 2 mM AMP in the presence of 0.1 mM ATP as a result OXPHOS rate increased 8 times. The intactness of mitochondrial membrane was controlled by cytochrome c and carboxyatractyloside (CAT) test. (B) Addition of 2mM ATP to isolate mitochondria activated ATPases as a result OXPHOS rate increased due to raised ADP circulation in mitochondria. Then most of ADP was trapped by PK-PEP system. Moreover, PK-PEP system trapped also ADP which released via AK2 catalyzed reaction and therefore after addition of 2 mM AMP the OXPHOS rate did not exceeded more than 20 % of the maximal rate (A). The presence of AK2 activity was confirmed by addition of 0.2 mM diadenosine pentaphosphate (AP5A). Blue line – O<sub>2</sub> concentration, red – rates of O<sub>2</sub> consumption. PK- pyruvate kinase; PEP- phosphoenol pyruvate.

### 6.3.3 AK1 and AK2 distribution in normal and cancer cells

We hypothesized that the sensitivity of the proposed respirometry method could be applied at the cellular level to measure the distribution of AK1 and AK2 in normal and cancer cells. The method based on vector ligand conduction model (Figure 2) where precise communication between ATP consumption and ATP production site is provided by phosphotransfer network. For this purpose, a broad panel of normal and cancer cells with known and unknown AK network enzymes expression profile cells were studied.

Firstly, respiratory analysis was performed on known AK network enzymes expression profile cells (Tanabe, Yamada et al. 1993; Eimre, Paju et al. 2008): rat heart CM(s) and in HL-1 tumor cells of the cardiac origin. For CM and HL-1 cells basic respiration parameters were determined:  $V_0$  and maximal AMP- and ADP-activated respiration ( $V_{AMP}$ ,  $V_{ADP}$ ), as well as RCI (Table 2). Among the studied cells, adult rat CM(s) were characterized by the highest  $V_{ADP}$  and RCI values. It is important to emphasize that in cardiomyocytes  $V_{ADP}$  was at a similar level as  $V_{AMP}$ . Although HL-1 cardiac sarcoma cells have relatively high rates of mitochondrial respiration, their  $V_{ADP}$  values were nearly 10 times lower as compared to normal CM(s). Moreover, HL-1 cells had also diminished  $V_{AMP}$  compare to  $V_{ADP}$ . These data (Table 2) indicate that AK expression may be decreased in HL-1 cells as compare to CM. Nevertheless, it is not clear how exactly the AK profile changes in cardiac sarcoma cells. This question can be addressed to the respiratory protocol illustrated in Figure 7C and 7D where PK-PEP system is used.

In permeabilized CM and HL-1 cells, the addition of AMP and ATP activated both AK1 and AK2 (Figure 7C), as a result,  $O_2$  consumption was significantly increased ( $V_{AMP}$ ) (Figure 19). Subsequent addition of PK to the assay systems (Figure 7D) decreased the rates of  $O_2$  consumption ( $V_{PK}$ ) (Figure 19), since the added PK removes efficiently extra-mitochondrially generated ADP which is generated by AK1 and MgATPases (Figure 7D), as well as intra-mitochondrially generated ADP which not coupled to respiration and escaping from mitochondria. 10 IU of PK was sufficient to trap all ADP available in the bulk phase of the cytoplasm. Residual respiration is associated with AK2 fully coupled with OXPHOS. Remain AMP-dependent respiration was inhibited back to  $V_0$  by AP5A (Figure 19). According to the respirometry protocol (Figure 19) for CM and HL-1 cells, AK indexes ( $I_{AK1}$  and  $I_{AK2}$ ) were calculated (Figure 20A and see also Material and Methods). The  $I_{AK1}$  and  $I_{AK2}$  expressed distribution of AK1 and AK2 in cells. The respirometric analysis was compared with standard AK assay data (Table 3). Both, respirometry method and AK activity assay, demonstrated that AK1 is predominantly expressed in CM, whereas HL-1 cardiac tumor cells have decreased  $V_{AMP}$ , which is associated with downregulation of AK1 (Figure 20A and Table 3). Figure 20A and Table 3 also revealed that heart muscle carcinogenesis shifts AK profile from AK1 to AK2.

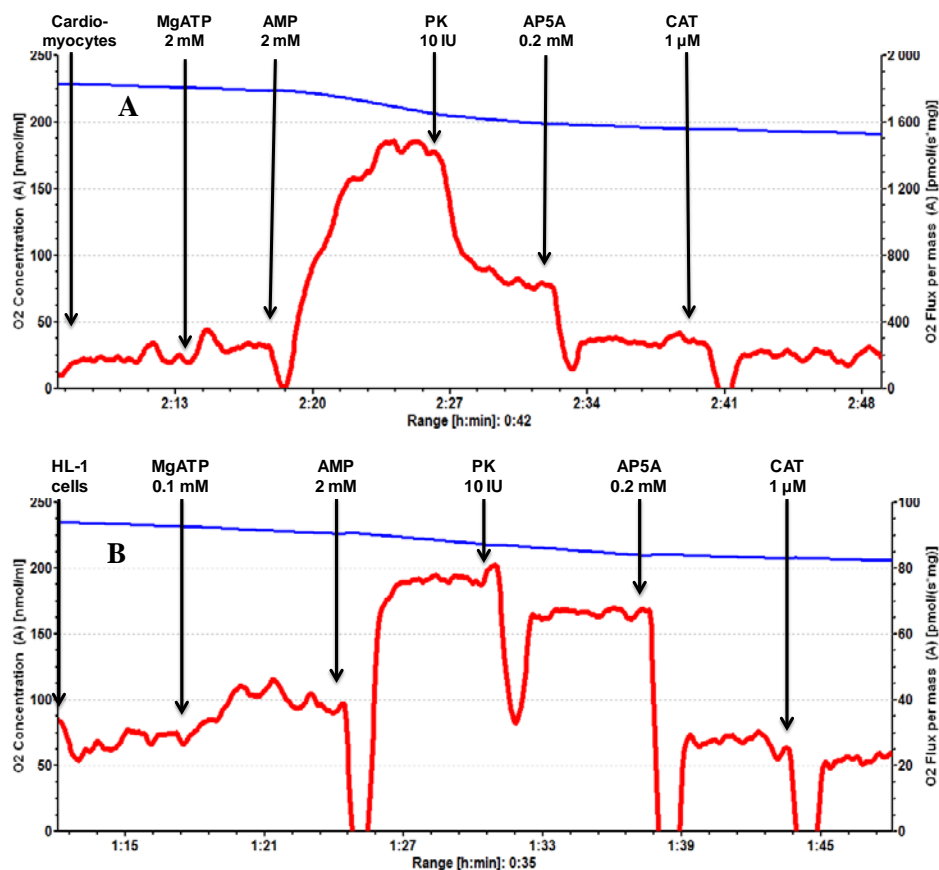


**Figure 19.** Analytical protocol to semi-quantify AK1 and AK2 distribution in permeabilized rat cardiomyocytes (A) and (B) HL-1 tumor cells. The protocol based on these isoenzymes coupling with OXPHOS. Experiment was performed in Mitomedium-B in the presence of mitochondria respiration succinate 10mM (for CM succinate was not used) glutamate 5 mM and malate 2 mM and PEP 5mM. Addition of AMP in the presence of ATP increases mitochondrial respiration due to activation of AK1 and AK2. Subsequent addition of pyruvate kinase (PK) decreases O<sub>2</sub> consumption since PK removes efficiently extra-mitochondrially generated ADP from AK1 and MgATPases. Remaining respiration is associated with AK2 coupling with OXPHOS. The functional coupling between AK2 and mitochondrial respiration was confirmed by addition of diadenosine pentaphosphate (AP5A) which decreased respiration back to the basal respiration. Finally, carboxyatractyloside (CAT) was added in order to control mitochondrial inner membrane intactness. Blue line – O<sub>2</sub> concentration, red – rates of O<sub>2</sub> consumption.

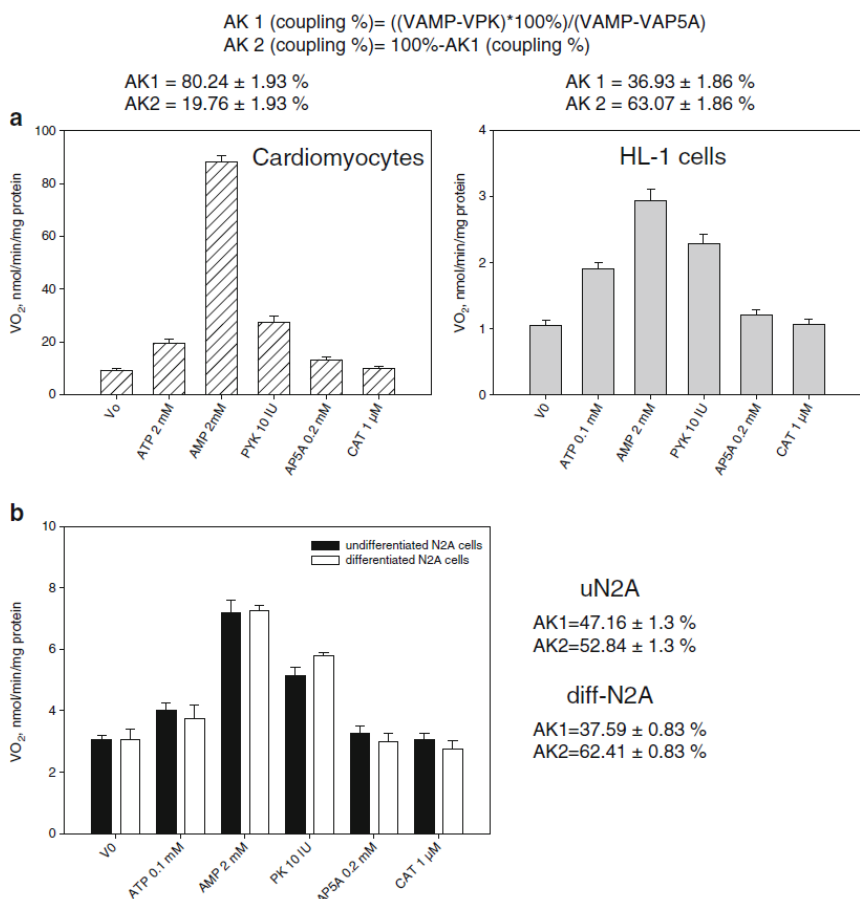


**Figure 20.** Application of a pyruvate kinase (PK)–phosphoenolpyruvate (PEP) protocol for determination of the presence of cytosolic (AK1) and mitochondrial (AK2) isoforms in one sample: (a) rat cardiomyocytes and HL-1 cardiac sarcoma cells; (b) undifferentiated and retinoic acid differentiated N2a cells (uN2a and dN2a, respectively). The presence of AK1 and AK2 in studied material can be quantified as the adenylate kinase index ( $I_{AK}$ ) which reflects AK1 and AK2 distribution in normal and cancer cells; the value of  $I_{AK}$  for AK1 and AK2 can be calculated as indicated in the corresponding section of “Materials and methods”. On these charts, bars are SEM, N=5

The same protocol (Figure19) was applied to examine effect of RA on AK isoenzymes distribution during N2a cells differentiation towards neuron cells (dN2a). The respirometry study and AK activity assay demonstrated that RA had no effect on the profile of AK1 and coupled AK2 activities in these NB cell (Figure 20B). Nevertheless, slight diminishing in the total AK activity during NB cell differentiation was observed (Table 3).

**Table 3.** The activity of adenylate kinase (AK) in human breast cancer tissue, adult rat cardiomyocytes (CMs), and some tumor cells of different histological type along with corresponding adenylate kinase indexes ( $I_{AK}$ ).

Cells and tissues	Total activity, mU/mg protein*	AK1, mU/mg protein	AK2, mU/mg protein	$I_{AK1}$ , %	$I_{AK2}$ , %
Rat CM(s)	2493 ± 113; N = 5	2394 ± 102 (96%**)	99 ± 18 (4%**)	80	20
HL-1 cells	311 ± 10; N = 5	174 ± 9 (56%)	137 ± 2 (44%)	37	63
uN2a cells	245 ± 12; N = 5	136 ± 9 (56%)	109 ± 8 (44%)	53	47
dN2a cells	172 ± 15; N = 5	81 ± 10 (47%)	91 ± 8 (53%)	39	61
Breast cancer	290 ± 89; N = 6	208 ± 64 (69%)	82 ± 15 (31%)	-	-
Non-tumor tissue	53 ± 5; N = 6	42 ± 4 (80%)	11 ± 2 (20%)	-	-

**Notes:** \*all data presented in the Table 2 are mean values ± SEM from at least 5 independent experiments; \*\* % from the total AK activity; uN2a and dN2a are undifferentiated and retinoic acid differentiated N2a cells, respectively; CM- cardiomyocytes.

#### 6.3.4 Application of respirometry method to research mitochondrial outer membrane permeability for AMP

In a previous study, Gellerich *et al.* (Gellerich 1992) showed that PEP-PK could be used to examine the affinity of mitochondria for exogenously added AMP. However, the roles of AK2 in the regulation of OXPHOS and MOM permeability for AMP have remained unclear. Therefore, we applied the PK-PEP respirometry protocol (Figure 21) to determine mitochondrial affinity for AMP. The method is based on AK2 coupling with OXPHOS.

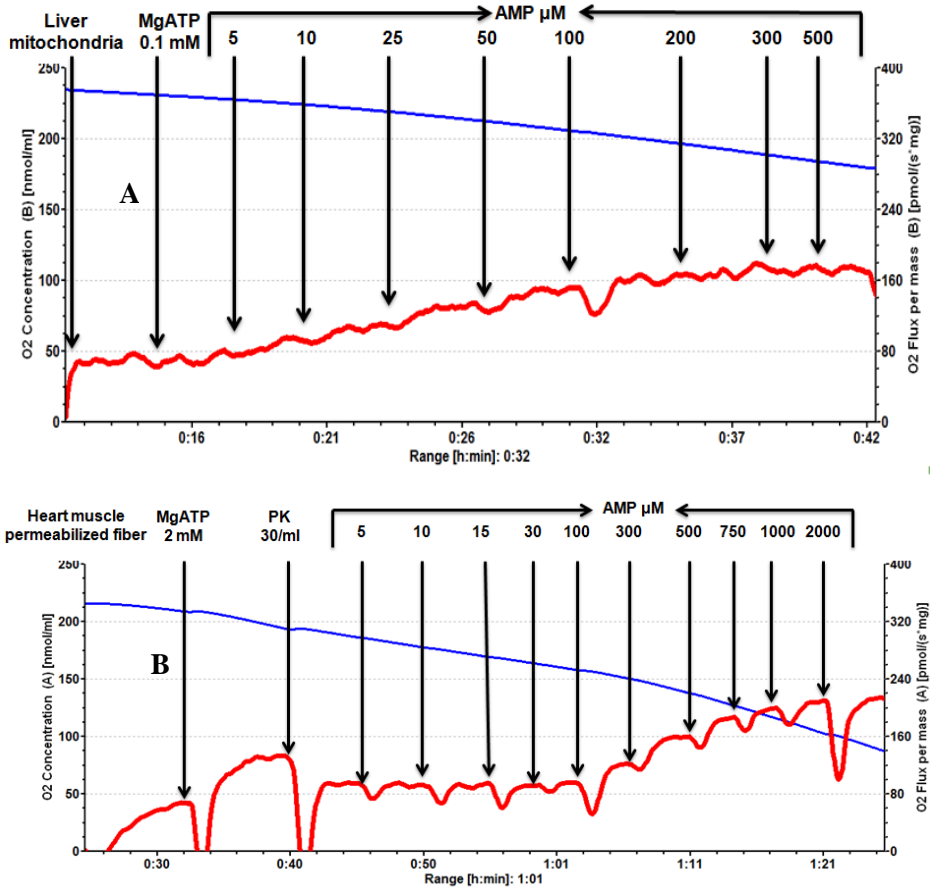


**Figure 21.** Repirometry protocol to determinate apparent  $K_m(\text{AMP})$  value (A) for rat liver mitochondria and (B) for rat heart muscle fiber. Samples were incubated in Medium B in the presence of mitochondria respiration substarte 2 mM malate and 5 mM glutamate as well as PK-PEP system and 0.1 mM ATP (for rat heart fiber 2 mM ATP), the rates of O<sub>2</sub> consumption were recorded after a step-wise addition of AMP. Blue line – O<sub>2</sub> concentration, red – rates of O<sub>2</sub> consumption. PK- pyruvate kinase; PEP- phosphoenol pyruvate. -

Respirometry study showed that isolated liver mitochondria had high affinity for AMP ( $K_m$  for AMP was  $23.5 \pm 6.9 \mu\text{M}$ ). This value is close to the affinity of isolated AK2 enzyme for AMP ( $K_m \leq 10 \mu\text{M}$ ) (Dzeja and Terzic 2009). However, in permeabilized adult rat heart muscle fibers and tumor cells,  $K_m$  (AMP) values were significantly higher and seem to depend on their proliferation and differentiation status. Non-proliferating highly-differentiated adult rat heart muscle have the highest  $K_m$  value ( $369 \pm 88 \mu\text{M}$ ) (Figure 22B) for exogenously-added AMP, whereas the  $K_m$  values found for rapidly-proliferating HL-1 cardiac sarcoma and NB cells were at least 4 times lower (Figure 22B and C). At the same time RA not only decreased proliferation rate in N2a cells, but also decreased MOM permeability for AMP (Figure 9 and 22C).

In resting muscle, cellular AMP concentration is  $\sim 10 \mu\text{M}$ , while during muscle contraction AMP concentration increases up to  $100 \mu\text{M}$  (Plaideau, Lai et al. 2014). Since our data for heart muscle and dN2a cells suggest an apparent  $K_m(\text{AMP})$  that is several times higher than the physiological AMP concentration, we became interested in reactions that could compete for the AMP substrate, such as AMPD (Figure 3). On the contrary to apparent  $K_m(\text{AMP})$  (Figure 22), the total AMPD activity was found 2.5 times higher in tumor HL-1 and uN2a cells compared to normal CM and dN2a cells (Table 4).

**Table 4.** The activity of AMP deaminase (AMPD) in differentiated neuron and adult rat cardiomyocytes (CM) cells and appropriate cancer cells.

**Notes:** \* $P < 0.001$  vs Rat CM(s), \*\* $P < 0.001$  vs dN2a cells; uN2a and dN2a are undifferentiated and retinoic acid differentiated N2a cells, respectively; CM-cardiomyocytes.

Enzyme activities, mU(s)/mg protein	HL-1 cells mean $\pm$ SEM, N=3	Rat CM(s) mean $\pm$ SEM, N=3	uN2a cells mean $\pm$ SEM, N=3	dN2a cells mean $\pm$ SEM, N=3
<b>AMPD</b>	40.1 $\pm$ 2.6 *	16.4 $\pm$ 0.4	36.0 $\pm$ 1.7 **	15.1 $\pm$ 1.3



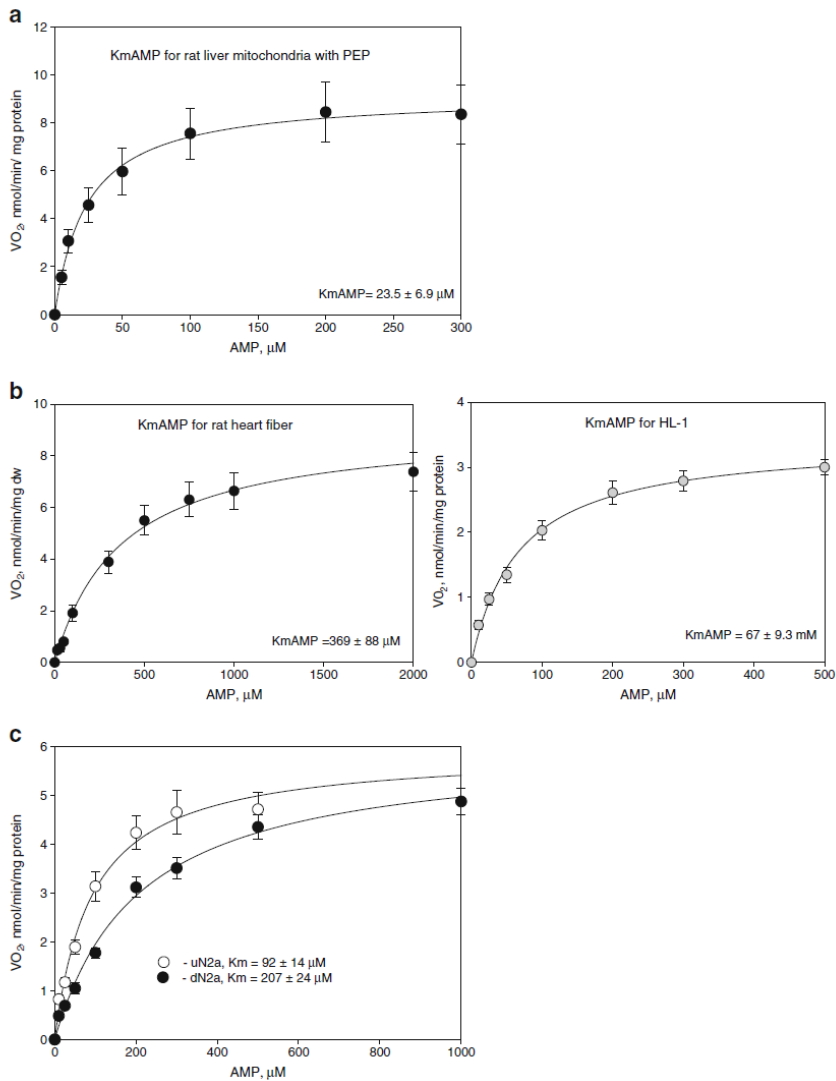


**Figure 22.** Kinetic analysis of regulation of the AMP-activated respiration in (A) isolated rat liver mitochondria, (B) for skinned rat heart myocytes and HL-1 cardiac tumor cells as well as (C) for undifferentiated or retinoic acid differentiated murine neuroblastoma cells; uN2a and dN2a, respectively. The corresponding apparent Michaelis-Menten constant (Km) values for exogenously-added AMP were determined. These measurements were performed in the presence of a PEP-PK system, bars are SEM, N=5. PK- pyruvate kinase; PEP- phosphoenol pyruvate.

## Discussion

In our studies, RA-treated N2a cells served as an *in vitro* model of normal neural cells. In N2a cells several morphological and metabolic changes were observed during NB cell differentiation towards SNS neurons. As a result, strong neurite outgrowth and cell hypertrophy in cells take place. In dN2a cells mitochondria are not only located in neuronal body, but also a significant part of mitochondria are located in neurites. The current study, and a study by Blanco *et al.* (Blanco, Lopez Camelo *et al.* 2001), found that RA causes cellular arrest in N2a cells. Moreover, RA also induced increase of AChE activity in N2a cells. Similar effects of RA on the activity of AChE in N2a cells have also been observed in other laboratories (Sato, Matsuda *et al.* 2002). Altogether, the dN2a cells are more similar to cholinergic neurons, based on their morphological and biochemical parameters

According to the literature, human high-risk NB is considered a highly glycolytic tumor (Feichtinger, Zimmermann *et al.* 2010; Levy, Zage *et al.* 2012). Nevertheless, the current study showed that considerable ATP amount is produced *via* OXPHOS in N2a cells. There is evidence that in metastatic NB cells HK2 is overexpressed (Botzer, Maman *et al.* 2016). Therefore, in the N2a cells, HK2 coupling with OXPHOS according to Warburg-Pedersen model (Pedersen 2007), was studied. Although, in uN2a cells the total HK activity was found to be 40 % lower than in dN2a, the aerobic glycolysis was higher in cancer cells. Altogether, our study supports the view that NB cells mainly produce ATP *via* aerobic glycolysis. Increased aerobic glycolysis in N2a cells may be associated with the fact that most HK2 is bound with VDAC, where OXPHOS supports their high glycolytic rate. Opel *et al.* (Opel, Poremba *et al.* 2007) have indicated that activation of Akt correlates with poor prognosis in primary neuroblastoma *in vivo* and with apoptosis resistance *in vitro*. It was shown that HK-2 phosphorylation with Akt increased HK binding with VDAC, which contributed to cancer cell resistance to apoptosis (Majewski, Nogueira *et al.* 2004).

The cytosolic CK-BB was found overexpressed in several tumors (Zarghami, Yu *et al.* 1995). The CK-BB is the main CK isoform in human NB, where serum CK-BB levels have been proposed to be the prognostic markers (Ishiguro, Kato *et al.* 1990). Our study showed that RA elevated CK activity in N2a cells might be associated with raised CKB expression. Similar results have been published by Wilson *et al.* (Wilson, Shen *et al.* 1997), where they demonstrated that NB had low CK-BB expression, compared to rat brain neurons or cultured primary astrocytes. The current oxygraphic experiments showed that in both uN2a and dN2a the uMtCK might be absent or not active. A further study is needed to confirm this assumption.

According to the literature, cell metabolism shifts from OXPHOS to aerobic glycolysis during HCC malignant transformation (Donohoe, Collins *et al.* 2012). For colon tissue the main energy and carbon source are short-fatty acids (butyrate, propionic acid), however tumors utilize glucose and glutamine, as the main provider of energy and carbon for the biosynthetic processes (Zhdanov, Waters *et al.* 2014). In the current study we have found that mitochondria have important roles in HCC formation. Tumor cells have higher OXPHOS rate, which is associated with increased mitochondrial mass, compared to normal tissue. In our previous article, the OXPHOS rate was proposed, as a prognostic parameter for HCC patients (Koit, Shevchuk *et al.* 2017). Elevated mitochondrial mass in tumor cells may be related to cancer cell adaptation to the

microenvironment, as well as for supporting cancer cell high glycolytic rate. Although the current work did not find any difference in HK activity, the aerobic glycolysis was higher in HCC compare to normal colon tissue. There is evidence that in colorectal cancer akt/mTOR pathway plays a critical role in cancer cell resistance to apoptosis (Ponnurangam, Standing et al. 2013). Akt facilitates HK binding on VDAC by phosphorylation of HK (Majewski, Nogueira et al. 2004). The HK binding on VDAC on one hand protects cancer cells against apoptosis, and on the other hand this complex formation supports cancer cell high glycolytic rate. Further study is needed to find which HK isoform binds on VDAC in HCC.

The CK network plays one of the key roles in production of PCr and maintaining the energy homeostasis, not only in muscle cells, but also in normal colonocytes (Kitzenberg, Colgan et al. 2016). Our studies showed that during colon carcinogenesis total CK activity was strongly decreased, which was associated with downregulation of uMtCK in HCC. Furthermore, we found a correlation between uMtCK expression levels and Cr-stimulated respiration: high expression level with high Cr-stimulated respiration in colon tissue and diminished expression level and absence of Cr-stimulated respiration in HCC. Similar correlation between sMtCK level and its functional coupling with OXPHOS was also observed in slow and fast twitch muscle (Varikmaa, Bagur et al. 2014). Furthermore, it was suggested that the downregulation of CK-BB in HCC cells may play an important role in the tumor progression (Mooney, Rajagopalan et al. 2011). Interestingly, in HCC unusual localization of CK-BB was found. The CK-BB is usually located in the cytosol, but during cancer formation it moves to the nucleus. Recently, Loo *et al.* (Loo, Scherl et al. 2015) demonstrated on mouse models, that extracellular CK-BB can promote HCC cells to metastasize towards the liver.

Differences in regulation of VDAC permeability for ADP between normal colon tissue and HCC, as well N2a cells and synaptosome (Monge, Beraud et al. 2008), may be related to the presence of MI key enzyme MtCK in normal colon tissue and brain neurons, and absence of this enzyme in HCC and N2a cells. Our previous studies and the current study have shown that in colorectal cancer, NB cells and cardiac sarcoma cells (Eimre, Paju et al. 2008) the apparent  $K_m$  of ADP is much lower compared to the normal tissue due to absence of MtCK. Study on MtCK knockout mice confirms this assumption. It was found that knockout of MtCK in heart muscle increased permeability of MOM for ADP 2.5 times (Kaasik, Veksler et al. 2001). Furthermore, there is evidence that in some cancers, like breast cancer (Qian, Li et al. 2012), liver cancer (Uranbileg, Enooku et al. 2014) and gastric cancer MtCK are overexpressed. In breast cancer and gastric cancer overexpression of MI key component MtCK, which also functionally coupled with OXPHOS correlates with decreased permeability of VDAC for ADP (Gruno, Peet et al. 2006; Kaambre, Chekulayev et al. 2012). Furthermore, in gastric cancer, addition of Cr affected mitochondrial affinity for ADP, similarly to cardiac and skeletal muscles, as well as brain neurons, was observed (Gruno, Peet et al. 2006; Monge, Beraud et al. 2008; Varikmaa, Bagur et al. 2014).

In the present study, we showed that in NB cells and HCC the MtCK were downregulated. Dzeja *et al.* have demonstrated that the phosphotransfer network is highly flexible and the absence of the CK network can be compensated by the AK network (Dzeja, Terzic et al. 2004). Therefore, the semi-quantitative respirometric method was developed, to estimate distribution of AK1/AK2 in permeabilized mammalian cells or tissues. The method is based on measurements of AMP-stimulated respiration rates catalyzed by AK delivering ADP to OXPHOS, where cytosolic ADP is trapped by the PK-PEP

system. AK2 and AK1 dependent respiration can be distinguished due to AK2 being strongly coupled and AK1 being less coupled with mitochondrial respiration. The main advantage of this method is its capacity to estimate the relative ratio of AK1 and AK2 activities in one sample without extraction of cellular protein(s). Furthermore, in presence of the PK-PEP system, the method can determine permeability of MOM for exogenous AMP. However, the method is not able to distinct AK1 and AK2 dependent respiration in cells with poor mitochondrial respiration ( $RCI < 2.5$ ).

Our current work and a previous study (Kaambre, Chekulayev et al. 2012) showed that post-operative samples have low mitochondrial respiration ( $RCI < 2.5$ ). Therefore, for those cases only total AK mediated respiration was measured (without PK-PEP system). Nice correlation between AK stimulated rate and total AK activity was found for HCC and HCB, as well as normal colon. We also demonstrated that elevated AK activity in HBC was associated with increased levels of both AK isoforms AK1 and AK2. A recent study has shown that the AK2 expression level is dependent on the ER receptor status in breast cancer. Namely, the AK2 is overexpressed in ER-receptor negative breast cancer, such as the highly aggressive triple-negative breast cancer (Speers, Tsimelzon et al. 2009). In our previous study weak coupling between MtCK and OXPHOS was observed in HBC (Kaambre, Chekulayev et al. 2012). Recently, a similar study has been performed on gastric cancer where it has been found that in HBC both phosphotransfer CK and AK networks are active in this tumor type (Gruno, Peet et al. 2006). Thus, according to the bioenergetic profile, the HBC looks more like gastric cancer than HCC.

AK1 is predominantly expressed in cells and organs with a high energy consumption, but with low proliferation rates (such as CM(s) and mature neural cells), while AK2 expression is rather pronounced in rapidly proliferating cells (Tanabe, Yamada et al. 1993). Indeed, our current study showed that fully-differentiated CM(s) had high activity of AK1 and minor levels of AK2, whereas in poorly-differentiated rapidly proliferating neuroblastoma cells (N2a line) and in cardiac sarcoma cells HL-1 cells, the main AK isoform was AK2. Furthermore, proteomics studies have also revealed the up-regulation of AK2 in human prostate (Lam, Yuan et al. 2010), pancreatic cancer cells (Liu, Zhang et al. 2010) and embryonal carcinoma cells (Ounpuu, Klepinin et al. 2017). In several tumors the AK2 up-regulation may be associated with the loss of mitochondrial creatine kinase (Eimre, Paju et al. 2008; Patra, Bera et al. 2008; Kaldma, Klepinin et al. 2014; Ounpuu, Klepinin et al. 2017). Although, this would suggest that AK2 should be a target for antitumor therapy, literature data on its association with tumor progression has remained contradictory. There is evidence that AK2 may be rather a negative regulator of tumor growth. AK2 interacts with nuclear dual-specificity phosphatase 26 and this protein complex dephosphorylates fas-associated protein with death domain resulting in suppression of cell growth (Kim, Lee et al. 2014).

During the last decade a new cancer treatment target has been proposed for cancer stem cells (CSC). The CSC share self-renewal properties with normal stem cells (Shackleton 2010). Under normal circumstances AK2 can promote cell proliferation, and full AK2 deletion (AK2<sup>-/-</sup>) in mice is embryonically lethal (Zhang, Nemutlu et al. 2010). Comparative analysis between embryonic stem cells and embryonal carcinoma cells have demonstrated that AK2 is up regulated in CSC (Ounpuu, Klepinin et al. 2017). Moreover, a cell surface oncoproteomic study revealed that overexpression of AK2 in murine teratoma cells, induced their inclination to metastasize (Roesli, Borgia et al. 2009). Our study showed that N2a cells have high AK2 levels, which may be related to the fact that NB cells have numerous CSC (Ross and Spengler 2007). Up-regulation of AK pathway has

also been observed in breast and colon CSC (Lamb, Bonuccelli et al. 2015; Ji, Yang et al. 2017). Therefore, AK2 and other AK isoforms could be the new cancer therapy targets in order to eliminate CSC.

In the current work we demonstrated that the AK pathway was up-regulated in HCC and HCB. This may be associated with increased AK6 (known as Human coilin-interacting nuclear ATPase protein) expression in those malignant cells (Bai, Zhang et al. 2016; Ji, Yang et al. 2017). It has found that AK6 is highly expressed in cancer and correlates with patients' worse outcomes (Bai, Zhang et al. 2016). Interestingly, in normal cells AK6 is located in nucleus where it participates in rRNA processing but during colon and breast tissue malignant transformation, part of AK6 enzyme is moved into cytosol (Bai, Zhang et al. 2016; Ji, Yang et al. 2017). Inhibition of AK6 leads to disruption of malignant cells inclination to metastasize, reduction of cellular tumorigenesis, while CSC lose their self-renewal properties and suppression of mRNA translation occurs (Bai, Zhang et al. 2016; Ji, Yang et al. 2017). Furthermore, in colon CSC, the Warburg effect is promoted by regulation of lactate dehydrogenase A (LDHA) activity, where its activity depends on posttranslational modification. AK6 can directly bind with LDHA and facilitate the glycolytic pathway *via* phosphorylation of LDHA C-terminal at 10 tyrosine (Ji, Yang et al. 2017). Interestingly, AK2 can also support high aerobic glycolysis in cancer. Namely, in hepatomas mitochondrial HK uses predominantly ATP, which is provided by AK2 (Nelson and Kabir 1985). Altogether, AK2 and AK6 are potent modulators, which can remodel cellular metabolism during malignant transformation.

The loss of AMPK activation is proposed to promote the development of malignancy, therefore AMPK behaves as a tumor suppressor (Liang and Mills 2013). Retrospective analysis has revealed that AMPK expression and activation status correlate with patients' prognosis (Cheng, Shuai et al. 2016). In the main upstream activator LKB1 gene was found mutated in several cancer (Zhao and Xu 2014). There is an allosteric pathway to activate AMPK. In stressful situations the AK pathway is activated and as a result intracellular AMP levels are rapidly elevated, which allosterically activates AMPK. In normal cells AK with AMPK together regulate cell AMP signaling response. It has been found that the well-known anti-diabetic drug metformin, can prevent cancer formation (Kasznicki, Sliwiska et al. 2014). Hardie *et al* have proposed that metformin acts through the AMP-AK-AMPK signaling pathway (Hardie 2013). According to the current study data, we hypothesize the mechanism by which poorly differentiated cancer cells can prevent AMPK activation: *via* up-regulation of AK2 and mitochondria high affinity for AMP. Due to AK2 high affinity for AMP and unique cellular localization (Dzeja and Terzic 2009)(a bottleneck between cytosol and mitochondria matrix compartment) most of the AMP which reaches the mitochondrial intermembrane space, is immediately converted to ADP. Moreover, we found that poorly differentiated cancer cells have increased mitochondrial affinity for AMP, and together with AK2 overexpression, they can prevent tumor suppressing action of AMPK. Further studies will be required to identify the underlying molecular mechanisms of the AK-AMP-AMPK signaling pathway in cancer.

The AMPD is an alternative pathway to diminish intracellular AMP signaling. The highest expression of AMPD was found in muscle where the main isoform was AMPD1. Other tissues have much lower activity of AMPD. AMPD2 is predominant in non-muscle tissues, and AMPD3 is found in erythrocytes (Plaideau, Liu et al. 2012). Plaideau *et al.* showed pharmacological inhibition of AMPD or AMPD1 deletion in muscle increased nucleotide level especially AMP (Plaideau, Lai et al. 2014). Our work suggested that in cardiac sarcoma cells AMPD activity was 6 times higher than previously reported for

mouse heart muscle (Rybakowska, Slominska et al. 2014). Similarly, the NB cells had 2.4 times higher AMPD activity than the RA-treated N2a cells. There is evidence that inhibition or downregulation of AMPD in normal cells leads to activation of the AMPK pathway (Plaideau, Lai et al. 2014). Moreover, an *in vitro* study on muscle cells demonstrated that metformin can activate AMPK via inhibition of AMPD (Ouyang, Parakhia et al. 2011). Nevertheless, the role of AMPD in malignant cell AMP signaling has remained unclear.

## Conclusion

1. The current study demonstrated that both NB and HCC were not pure glycolytic tumors. Both tumor types have functional mitochondria, but HCC possess even higher mitochondrial mass and mitochondrial oxygen consumption rate than adjacent healthy colon tissue. Nevertheless, in those malignant cells, considerable ATP amount is produced *via* aerobic glycolysis, where mitochondria support cancer cells high glycolytic rate. Moreover, malignant transformation also caused rearrangement of mitochondrial permeability for adenine nucleotides.
2. It was shown that the PCr/Cr shuttle plays an important role in colon tissue energetic homeostasis, but decreased PCr/Cr circulation occurred during colorectal cancer formation. Furthermore, the malignant transformation caused the bioenergetic shift from CK to the AK pathway. In NB cells the CK network has a minor role in cell energy homeostasis. Instead of CK in neuroblastoma cells, mitochondrial energy is transferred to cytosolic compartment *via* AK network, where the mitochondrial main kinase is AK2.
3. In this study a simple oxygraphic method was developed to evaluate semi-quantitative level AK1 and AK2 distribution in mammalian tissues and cultured cells. This method is rapid and enables to estimate AK1/AK2 in one sample. Moreover, the method is able to determinate changes in mitochondrial permeability for AMP in health and disease. The study also revealed that the method is not useful for samples which have poor mitochondrial respiration ( $RCI < 2.5$ ).
4. The oxygraphic method is sensitive enough to study the AK network also on tumor biopsies. This work revealed that the AK pathway was up-regulated in HCC, but also in HBC samples.
5. The mitochondrial kinase AK2 is expressed predominantly in poorly differentiated cells with high proliferative index. In addition, we also found strong differences between highly-differentiated and tumor cells in the affinity of their mitochondrial respiration for exogenous AMP.
6. Finally, we hypothesized that poorly differentiated cancer cells can avoid AK-AMP-AMPK signaling pathway activation *via* up-regulation of AK2 and changes of mitochondrial affinity for AMP.

## Reference

- ACS (2015). Global Cancer Facts and Figures 3 rd Edition. Atlanta, American Cancer Society.
- Altenberg, B. and K. O. Greulich (2004). "Genes of glycolysis are ubiquitously overexpressed in 24 cancer classes." Genomics 84(6): 1014-1020.
- Amamoto, R., T. Uchiumi, et al. (2016). "The Expression of Ubiquitous Mitochondrial Creatine Kinase Is Downregulated as Prostate Cancer Progression." J Cancer 7(1): 50-59.
- Amieva, M. R., R. Vogelmann, et al. (2003). "Disruption of the epithelial apical-junctional complex by Helicobacter pylori CagA." Science 300(5624): 1430-1434.
- Ashby, B. and C. Frieden (1978). "Adenylate deaminase. Kinetic and binding studies on the rabbit muscle enzyme." J Biol Chem 253(24): 8728-8735.
- Baburin, A., T. Aareleid, et al. (2014). "Time trends in population-based breast cancer survival in Estonia: analysis by age and stage." Acta Oncol 53(2): 226-234.
- Baburin, A., T. Aareleid, et al. (2016). "Recent changes in breast cancer incidence and mortality in Estonia: Transition to the west." Acta Oncol 55(6): 728-733.
- Bai, D., J. Zhang, et al. (2016). "The ATPase hCINAP regulates 18S rRNA processing and is essential for embryogenesis and tumour growth." Nat Commun 7: 12310.
- Baxter, N. N., M. A. Goldwasser, et al. (2009). "Association of colonoscopy and death from colorectal cancer." Ann Intern Med 150(1): 1-8.
- Blanco, V., J. Lopez Camelo, et al. (2001). "Growth inhibition, morphological differentiation and stimulation of survival in neuronal cell type (Neuro-2a) treated with trophic molecules." Cell Biol Int 25(9): 909-917.
- Botzer, L. E., S. Maman, et al. (2016). "Hexokinase 2 is a determinant of neuroblastoma metastasis." Br J Cancer 114(7): 759-766.
- Brodeur, G. M. (2018). "Spontaneous regression of neuroblastoma." Cell Tissue Res.
- Chance, B. and G. R. Williams (1955). "Respiratory enzymes in oxidative phosphorylation. I. Kinetics of oxygen utilization." J Biol Chem 217(1): 383-393.
- Chekulayev, V., K. Mado, et al. (2015). "Metabolic remodeling in human colorectal cancer and surrounding tissues: alterations in regulation of mitochondrial respiration and metabolic fluxes." Biochem Biophys Res 4: 111-125.
- Cheng, J., X. Shuai, et al. (2016). "Prognostic significance of AMPK in human malignancies: A meta-analysis." Oncotarget 7(46): 75739-75748.
- Cimino, D., L. Fusco, et al. (2008). "Identification of new genes associated with breast cancer progression by gene expression analysis of predefined sets of neoplastic tissues." Int J Cancer 123(6): 1327-1338.
- Claggett-Dame, M., E. M. McNeill, et al. (2006). "Role of all-trans retinoic acid in neurite outgrowth and axonal elongation." J Neurobiol 66(7): 739-756.
- Claycomb, W. C., N. A. Lanson, Jr., et al. (1998). "HL-1 cells: a cardiac muscle cell line that contracts and retains phenotypic characteristics of the adult cardiomyocyte." Proc Natl Acad Sci U S A 95(6): 2979-2984.
- Collavin, L., D. Lazarevic, et al. (1999). "wt p53 dependent expression of a membrane-associated isoform of adenylate kinase." Oncogene 18(43): 5879-5888.
- Dai, X., T. Li, et al. (2015). "Breast cancer intrinsic subtype classification, clinical use and future trends." Am J Cancer Res 5(10): 2929-2943.



- de Bruin, W., F. Oerlemans, et al. (2004). "Adenylate kinase I does not affect cellular growth characteristics under normal and metabolic stress conditions." Exp Cell Res 297(1): 97-107.
- de Oliveira, M. F., N. D. Amoedo, et al. (2012). "Energy and redox homeostasis in tumor cells." Int J Cell Biol 2012: 593838.
- Donohoe, D. R., L. B. Collins, et al. (2012). "The Warburg effect dictates the mechanism of butyrate-mediated histone acetylation and cell proliferation." Mol Cell 48(4): 612-626.
- Dzeja, P. and A. Terzic (2009). "Adenylate kinase and AMP signaling networks: metabolic monitoring, signal communication and body energy sensing." Int J Mol Sci 10(4): 1729-1772.
- Dzeja, P. P., S. Chung, et al. (2011). "Developmental enhancement of adenylate kinase-AMPK metabolic signaling axis supports stem cell cardiac differentiation." PLoS One 6(4): e19300.
- Dzeja, P. P., M. M. Redfield, et al. (2000). "Failing energetics in failing hearts." Curr Cardiol Rep 2(3): 212-217.
- Dzeja, P. P., R. J. Zeleznikar, et al. (1998). "Adenylate kinase: kinetic behavior in intact cells indicates it is integral to multiple cellular processes." Mol Cell Biochem 184(1-2): 169-182.
- Dzeja, P. P. and A. Terzic (1998). "Phosphotransfer reactions in the regulation of ATP-sensitive K<sup>+</sup> channels." FASEB J 12(7): 523-529.
- Dzeja, P. P. and A. Terzic (2003). "Phosphotransfer networks and cellular energetics." J Exp Biol 206(Pt 12): 2039-2047.
- Dzeja, P. P., A. Terzic, et al. (2004). "Phosphotransfer dynamics in skeletal muscle from creatine kinase gene-deleted mice." Mol Cell Biochem 256-257(1-2): 13-27.
- Dzeja, P. P., K. T. Vitkevicius, et al. (1999). "Adenylate kinase-catalyzed phosphotransfer in the myocardium : increased contribution in heart failure." Circ Res 84(10): 1137-1143.
- Eimre, M., K. Paju, et al. (2008). "Distinct organization of energy metabolism in HL-1 cardiac cell line and cardiomyocytes." Biochim Biophys Acta 1777(6): 514-524.
- Ellman, G. L., K. D. Courtney, et al. (1961). "A new and rapid colorimetric determination of acetylcholinesterase activity." Biochem Pharmacol 7: 88-95.
- Epstein, T., L. Xu, et al. (2014). "Separation of metabolic supply and demand: aerobic glycolysis as a normal physiological response to fluctuating energetic demands in the membrane." Cancer Metab 2: 7.
- Fantin, V. R., J. St-Pierre, et al. (2006). "Attenuation of LDH-A expression uncovers a link between glycolysis, mitochondrial physiology, and tumor maintenance." Cancer Cell 9(6): 425-434.
- Feichtinger, R. G., F. Zimmermann, et al. (2010). "Low aerobic mitochondrial energy metabolism in poorly- or undifferentiated neuroblastoma." BMC Cancer 10: 149.
- Frederic L. Greene, D. L. P., Irvin D. Fleming, April G. Fritz, Charles M. Balch, Daniel G. Haller, Monica Morrow, Ed. (2002). AJCC Cancer Staging Manual. Springer.
- Gellerich, F. N. (1992). "The role of adenylate kinase in dynamic compartmentation of adenine nucleotides in the mitochondrial intermembrane space." FEBS Lett 297(1-2): 55-58.

- Glover, L. E., B. E. Bowers, et al. (2013). "Control of creatine metabolism by HIF is an endogenous mechanism of barrier regulation in colitis." Proc Natl Acad Sci U S A 110(49): 19820-19825.
- Gowans, G. J., S. A. Hawley, et al. (2013). "AMP is a true physiological regulator of AMP-activated protein kinase by both allosteric activation and enhancing net phosphorylation." Cell Metab 18(4): 556-566.
- Gruno, M., N. Peet, et al. (2006). "Oxidative phosphorylation and its coupling to mitochondrial creatine and adenylate kinases in human gastric mucosa." Am J Physiol Regul Integr Comp Physiol 291(4): R936-946.
- Gupta, R. B., N. Harpaz, et al. (2007). "Histologic inflammation is a risk factor for progression to colorectal neoplasia in ulcerative colitis: a cohort study." Gastroenterology 133(4): 1099-1105; quiz 1340-1091.
- Guzun, R., M. Karu-Varikmaa, et al. (2011). "Mitochondria-cytoskeleton interaction: distribution of beta-tubulins in cardiomyocytes and HL-1 cells." Biochim Biophys Acta 1807(4): 458-469.
- Guzun, R., N. Timohhina, et al. (2009). "Regulation of respiration controlled by mitochondrial creatine kinase in permeabilized cardiac cells in situ. Importance of system level properties." Biochim Biophys Acta 1787(9): 1089-1105.
- Haas, R. C. and A. W. Strauss (1990). "Separate nuclear genes encode sarcomere-specific and ubiquitous human mitochondrial creatine kinase isoenzymes." J Biol Chem 265(12): 6921-6927.
- Hanahan, D. and R. A. Weinberg (2011). "Hallmarks of cancer: the next generation." Cell 144(5): 646-674.
- Hardie, D. G. (2013). "Metformin-acting through cyclic AMP as well as AMP?" Cell Metab 17(3): 313-314.
- Hawley, S. A., J. Boudeau, et al. (2003). "Complexes between the LKB1 tumor suppressor, STRAD alpha/beta and MO25 alpha/beta are upstream kinases in the AMP-activated protein kinase cascade." J Biol 2(4): 28.
- Hawley, S. A., D. A. Pan, et al. (2005). "Calmodulin-dependent protein kinase kinase-beta is an alternative upstream kinase for AMP-activated protein kinase." Cell Metab 2(1): 9-19.
- Herrinton, L. J., L. Liu, et al. (2012). "Incidence and mortality of colorectal adenocarcinoma in persons with inflammatory bowel disease from 1998 to 2010." Gastroenterology 143(2): 382-389.
- Hurley, R. L., K. A. Anderson, et al. (2005). "The Ca<sup>2+</sup>/calmodulin-dependent protein kinase kinases are AMP-activated protein kinase kinases." J Biol Chem 280(32): 29060-29066.
- Innos, K., H. Reima, et al. (2018). "Subsite- and stage-specific colorectal cancer trends in Estonia prior to implementation of screening." Cancer Epidemiol 52: 112-119.
- Ipata, P. L. and F. Balestri (2013). "The functional logic of cytosolic 5'-nucleotidases." Curr Med Chem 20(34): 4205-4216.
- Ishida, Y., I. Riesinger, et al. (1994). "Compartmentation of ATP synthesis and utilization in smooth muscle: roles of aerobic glycolysis and creatine kinase." Mol Cell Biochem 133-134: 39-50.
- Ishiguro, Y., K. Kato, et al. (1990). "The diagnostic and prognostic value of pretreatment serum creatine kinase BB levels in patients with neuroblastoma." Cancer 65(9): 2014-2019.

- Janssen, E., J. Kuiper, et al. (2004). "Two structurally distinct and spatially compartmentalized adenylate kinases are expressed from the AK1 gene in mouse brain." Mol Cell Biochem 256-257(1-2): 59-72.
- Ji, Y., C. Yang, et al. (2017). "Adenylate kinase hCINAP determines self-renewal of colorectal cancer stem cells by facilitating LDHA phosphorylation." Nat Commun 8: 15308.
- Jiang, M., J. Stanke, et al. (2011). "The connections between neural crest development and neuroblastoma." Curr Top Dev Biol 94: 77-127.
- Jockers-Wretou, E., W. Giebel, et al. (1977). "[Immunohistochemical localization of creatinkinase isoenzymes in human tissue (author's transl)]." Histochemistry 54(1): 83-95.
- Jose, C., N. Bellance, et al. (2011). "Choosing between glycolysis and oxidative phosphorylation: a tumor's dilemma?" Biochim Biophys Acta 1807(6): 552-561.
- Kaambre, T., V. Chekulayev, et al. (2012). "Metabolic control analysis of cellular respiration in situ in intraoperative samples of human breast cancer." J Bioenerg Biomembr 44(5): 539-558.
- Kaasik, A., V. Veksler, et al. (2001). "Energetic crosstalk between organelles: architectural integration of energy production and utilization." Circ Res 89(2): 153-159.
- Kaatsch, P. (2010). "Epidemiology of childhood cancer." Cancer Treat Rev 36(4): 277-285.
- Kadenbach, B. (1986). "Regulation of respiration and ATP synthesis in higher organisms: hypothesis." J Bioenerg Biomembr 18(1): 39-54.
- Kaldma, A., A. Klepinin, et al. (2014). "An in situ study of bioenergetic properties of human colorectal cancer: the regulation of mitochondrial respiration and distribution of flux control among the components of ATP synthasome." Int J Biochem Cell Biol 55: 171-186.
- Kasznicki, J., A. Sliwinska, et al. (2014). "Metformin in cancer prevention and therapy." Ann Transl Med 2(6): 57.
- Kato, Y., S. Ozawa, et al. (2007). "Acidic extracellular pH increases calcium influx-triggered phospholipase D activity along with acidic sphingomyelinase activation to induce matrix metalloproteinase-9 expression in mouse metastatic melanoma." FEBS J 274(12): 3171-3183.
- Khoo, J. C. and P. J. Russell (1972). "Isoenzymes of adenylate kinase in human tissue." Biochim Biophys Acta 268(1): 98-101.
- Kim, H., H. J. Lee, et al. (2014). "The DUSP26 phosphatase activator adenylate kinase 2 regulates FADD phosphorylation and cell growth." Nat Commun 5: 3351.
- Kitzenberg, D., S. P. Colgan, et al. (2016). "Creatine kinase in ischemic and inflammatory disorders." Clin Transl Med 5(1): 31.
- Klepinin, A., L. Ounpuu, et al. (2016). "Simple oxygraphic analysis for the presence of adenylate kinase 1 and 2 in normal and tumor cells." J Bioenerg Biomembr 48(5): 531-548.
- Klinov, S. V. and B. I. Kurganov (1994). "Kinetic mechanism of activation of muscle glycogen phosphorylase b by adenosine 5'-monophosphate." Arch Biochem Biophys 312(1): 14-21.
- Koit, A., I. Shevchuk, et al. (2017). "Mitochondrial Respiration in Human Colorectal and Breast Cancer Clinical Material Is Regulated Differently." Oxid Med Cell Longev 2017: 1372640.

- Kulkarni, S. S., H. K. Karlsson, et al. (2011). "Suppression of 5'-nucleotidase enzymes promotes AMP-activated protein kinase (AMPK) phosphorylation and metabolism in human and mouse skeletal muscle." J Biol Chem 286(40): 34567-34574.
- Kurashima, Y., T. Amiya, et al. (2012). "Extracellular ATP mediates mast cell-dependent intestinal inflammation through P2X7 purinoceptors." Nat Commun 3: 1034.
- Kuznetsov, A. V., T. Tiivel, et al. (1996). "Striking differences between the kinetics of regulation of respiration by ADP in slow-twitch and fast-twitch muscles in vivo." Eur J Biochem 241(3): 909-915.
- Kuznetsov, A. V., V. Veksler, et al. (2008). "Analysis of mitochondrial function in situ in permeabilized muscle fibers, tissues and cells." Nat Protoc 3(6): 965-976.
- Lam, Y. W., Y. Yuan, et al. (2010). "Comprehensive identification and modified-site mapping of S-nitrosylated targets in prostate epithelial cells." PLoS One 5(2): e9075.
- Lamb, R., G. Bonuccelli, et al. (2015). "Mitochondrial mass, a new metabolic biomarker for stem-like cancer cells: Understanding WNT/FGF-driven anabolic signaling." Oncotarget 6(31): 30453-30471.
- Levy, A. G., P. E. Zage, et al. (2012). "The combination of the novel glycolysis inhibitor 3-BrOP and rapamycin is effective against neuroblastoma." Invest New Drugs 30(1): 191-199.
- Li, X. H., X. J. Chen, et al. (2013). "Knockdown of creatine kinase B inhibits ovarian cancer progression by decreasing glycolysis." Int J Biochem Cell Biol 45(5): 979-986.
- Liang, J. and G. B. Mills (2013). "AMPK: a contextual oncogene or tumor suppressor?" Cancer Res 73(10): 2929-2935.
- Lin, Y. W., L. M. Lien, et al. (2008). "9-cis retinoic acid induces retinoid X receptor localized to the mitochondria for mediation of mitochondrial transcription." Biochem Biophys Res Commun 377(2): 351-354.
- Liu, R., A. L. Strom, et al. (2009). "Enzymatically inactive adenylate kinase 4 interacts with mitochondrial ADP/ATP translocase." Int J Biochem Cell Biol 41(6): 1371-1380.
- Liu, X., M. Zhang, et al. (2010). "Membrane proteomic analysis of pancreatic cancer cells." J Biomed Sci 17: 74.
- Livak, K. J. and T. D. Schmittgen (2001). "Analysis of relative gene expression data using real-time quantitative PCR and the 2(-Delta Delta C(T)) Method." Methods 25(4): 402-408.
- Loo, J. M., A. Scherl, et al. (2015). "Extracellular metabolic energetics can promote cancer progression." Cell 160(3): 393-406.
- Lunt, S. Y. and M. G. Vander Heiden (2011). "Aerobic glycolysis: meeting the metabolic requirements of cell proliferation." Annu Rev Cell Dev Biol 27: 441-464.
- Majewski, N., V. Nogueira, et al. (2004). "Hexokinase-mitochondria interaction mediated by Akt is required to inhibit apoptosis in the presence or absence of Bax and Bak." Mol Cell 16(5): 819-830.
- Mannella, C. A., D. R. Pfeiffer, et al. (2001). "Topology of the mitochondrial inner membrane: dynamics and bioenergetic implications." IUBMB Life 52(3-5): 93-100.
- Marmot, M. G., D. G. Altman, et al. (2013). "The benefits and harms of breast cancer screening: an independent review." Br J Cancer 108(11): 2205-2240.

- Michael H. Ross, W. P. (2010). Histology: A Text and Atlas, with Correlated Cell and Molecular Biology, Lippincott Williams & Wilkins.
- Michielan, A. and R. D'Inca (2015). "Intestinal Permeability in Inflammatory Bowel Disease: Pathogenesis, Clinical Evaluation, and Therapy of Leaky Gut." Mediators Inflamm 2015: 628157.
- Miller, E. E., A. E. Evans, et al. (1993). "Inhibition of rate of tumor growth by creatine and cyclocreatine." Proc Natl Acad Sci U S A 90(8): 3304-3308.
- Miyoshi, K., Y. Akazawa, et al. (2009). "Localization of adenylate kinase 4 in mouse tissues." Acta Histochem Cytochem 42(2): 55-64.
- Monge, C., N. Beraud, et al. (2008). "Regulation of respiration in brain mitochondria and synaptosomes: restrictions of ADP diffusion in situ, roles of tubulin, and mitochondrial creatine kinase." Mol Cell Biochem 318(1-2): 147-165.
- Monge, C., N. Beraud, et al. (2009). "Comparative analysis of the bioenergetics of adult cardiomyocytes and nonbeating HL-1 cells: respiratory chain activities, glycolytic enzyme profiles, and metabolic fluxes." Can J Physiol Pharmacol 87(4): 318-326.
- Mooney, S. M., K. Rajagopalan, et al. (2011). "Creatine kinase brain overexpression protects colorectal cells from various metabolic and non-metabolic stresses." J Cell Biochem 112(4): 1066-1075.
- Mootha, V. K., A. E. Arai, et al. (1997). "Maximum oxidative phosphorylation capacity of the mammalian heart." Am J Physiol 272(2 Pt 2): H769-775.
- Moreno-Sanchez, R., A. Marin-Hernandez, et al. (2014). "Who controls the ATP supply in cancer cells? Biochemistry lessons to understand cancer energy metabolism." Int J Biochem Cell Biol 50: 10-23.
- Nagata, Y., K. H. Lan, et al. (2004). "PTEN activation contributes to tumor inhibition by trastuzumab, and loss of PTEN predicts trastuzumab resistance in patients." Cancer Cell 6(2): 117-127.
- Napiwotzki, J. and B. Kadenbach (1998). "Extramitochondrial ATP/ADP-ratios regulate cytochrome c oxidase activity via binding to the cytosolic domain of subunit IV." Biol Chem 379(3): 335-339.
- Nava, P., S. Lopez, et al. (2004). "The rotavirus surface protein VP8 modulates the gate and fence function of tight junctions in epithelial cells." J Cell Sci 117(Pt 23): 5509-5519.
- Nelson, B. D. and F. Kabir (1985). "Adenylate kinase is a source of ATP for tumor mitochondrial hexokinase." Biochim Biophys Acta 841(2): 195-200.
- Noma, T. (2005). "Dynamics of nucleotide metabolism as a supporter of life phenomena." J Med Invest 52(3-4): 127-136.
- Noma, T., K. Fujisawa, et al. (2001). "Structure and expression of human mitochondrial adenylate kinase targeted to the mitochondrial matrix." Biochem J 358(Pt 1): 225-232.
- Opel, D., C. Poremba, et al. (2007). "Activation of Akt predicts poor outcome in neuroblastoma." Cancer Res 67(2): 735-745.
- Ounpuu, L., A. Klepinin, et al. (2017). "2102Ep embryonal carcinoma cells have compromised respiration and shifted bioenergetic profile distinct from H9 human embryonic stem cells." Biochim Biophys Acta 1861(8): 2146-2154.
- Ouyang, J., R. A. Parakhia, et al. (2011). "Metformin activates AMP kinase through inhibition of AMP deaminase." J Biol Chem 286(1): 1-11.

- Panayiotou, C., N. Solaroli, et al. (2014). "The many isoforms of human adenylate kinases." Int J Biochem Cell Biol 49: 75-83.
- Park, S. Y., J. R. Gifford, et al. (2014). "Cardiac, skeletal, and smooth muscle mitochondrial respiration: are all mitochondria created equal?" Am J Physiol Heart Circ Physiol 307(3): H346-352.
- Patra, S., S. Bera, et al. (2008). "Progressive decrease of phosphocreatine, creatine and creatine kinase in skeletal muscle upon transformation to sarcoma." FEBS J 275(12): 3236-3247.
- Pedersen, P. L. (2007). "Warburg, me and Hexokinase 2: Multiple discoveries of key molecular events underlying one of cancers' most common phenotypes, the "Warburg Effect", i.e., elevated glycolysis in the presence of oxygen." J Bioenerg Biomembr 39(3): 211-222.
- Pfeiffer, T., S. Schuster, et al. (2001). "Cooperation and competition in the evolution of ATP-producing pathways." Science 292(5516): 504-507.
- Phelps, M. E. (2000). "Positron emission tomography provides molecular imaging of biological processes." Proc Natl Acad Sci U S A 97(16): 9226-9233.
- Plaideau, C., Y. C. Lai, et al. (2014). "Effects of pharmacological AMP deaminase inhibition and Ampd1 deletion on nucleotide levels and AMPK activation in contracting skeletal muscle." Chem Biol 21(11): 1497-1510.
- Plaideau, C., J. Liu, et al. (2012). "Overexpression of AMP-metabolizing enzymes controls adenine nucleotide levels and AMPK activation in HEK293T cells." FASEB J 26(6): 2685-2694.
- Ponnuram, S., D. Standing, et al. (2013). "Tandutinib inhibits the Akt/mTOR signaling pathway to inhibit colon cancer growth." Mol Cancer Ther 12(5): 598-609.
- Postic, C., M. Shiota, et al. (2001). "Cell-specific roles of glucokinase in glucose homeostasis." Recent Prog Horm Res 56: 195-217.
- Qian, X. L., Y. Q. Li, et al. (2012). "Overexpression of ubiquitous mitochondrial creatine kinase (uMtCK) accelerates tumor growth by inhibiting apoptosis of breast cancer cells and is associated with a poor prognosis in breast cancer patients." Biochem Biophys Res Commun 427(1): 60-66.
- Ramaiah, A., J. A. Hathaway, et al. (1964). "Adenylate as a Metabolic Regulator. Effect on Yeast Phosphofructokinase Kinetics." J Biol Chem 239: 3619-3622.
- Reynolds, C. P., K. K. Matthay, et al. (2003). "Retinoid therapy of high-risk neuroblastoma." Cancer Lett 197(1-2): 185-192.
- Robey, R. B., B. J. Raval, et al. (2000). "Thrombin is a novel regulator of hexokinase activity in mesangial cells." Kidney Int 57(6): 2308-2318.
- Roesli, C., B. Borgia, et al. (2009). "Comparative analysis of the membrane proteome of closely related metastatic and nonmetastatic tumor cells." Cancer Res 69(13): 5406-5414.
- Ross, R. A. and B. A. Spengler (2007). "Human neuroblastoma stem cells." Semin Cancer Biol 17(3): 241-247.
- Rostovtseva, T. K., K. L. Sheldon, et al. (2008). "Tubulin binding blocks mitochondrial voltage-dependent anion channel and regulates respiration." Proc Natl Acad Sci U S A 105(48): 18746-18751.
- Rybakowska, I., E. M. Slominska, et al. (2014). "Activity of AMP-regulated protein kinase and AMP-deaminase in the heart of mice fed high-fat diet." Nucleosides Nucleotides Nucleic Acids 33(4-6): 347-352.

- Saks, V. A., Y. O. Belikova, et al. (1991). "In vivo regulation of mitochondrial respiration in cardiomyocytes: specific restrictions for intracellular diffusion of ADP." Biochim Biophys Acta 1074(2): 302-311.
- Saks, V. A., G. B. Chernousova, et al. (1975). "Studies of energy transport in heart cells. Mitochondrial isoenzyme of creatine phosphokinase: kinetic properties and regulatory action of Mg<sup>2+</sup> ions." Eur J Biochem 57(1): 273-290.
- Saks, V. A., Z. A. Khuchua, et al. (1994). "Metabolic compartmentation and substrate channelling in muscle cells. Role of coupled creatine kinases in in vivo regulation of cellular respiration--a synthesis." Mol Cell Biochem 133-134: 155-192.
- Saks, V. A., A. V. Kuznetsov, et al. (2004). "Functional coupling as a basic mechanism of feedback regulation of cardiac energy metabolism." Mol Cell Biochem 256-257(1-2): 185-199.
- Sato, C., T. Matsuda, et al. (2002). "Neuronal differentiation-dependent expression of the disialic acid epitope on CD166 and its involvement in neurite formation in Neuro2A cells." J Biol Chem 277(47): 45299-45305.
- Schlitter, A. M., C. Dornenburg, et al. (2012). "CD57(high) neuroblastoma cells have aggressive attributes ex situ and an undifferentiated phenotype in patients." PLoS One 7(8): e42025.
- Shackleton, M. (2010). "Normal stem cells and cancer stem cells: similar and different." Semin Cancer Biol 20(2): 85-92.
- Shaw, R. J., M. Kosmatka, et al. (2004). "The tumor suppressor LKB1 kinase directly activates AMP-activated kinase and regulates apoptosis in response to energy stress." Proc Natl Acad Sci U S A 101(10): 3329-3335.
- Shinohara, Y., K. Yamamoto, et al. (1994). "Steady state transcript levels of the type II hexokinase and type 1 glucose transporter in human tumor cell lines." Cancer Lett 82(1): 27-32.
- Simamura, E., H. Shimada, et al. (2008). "Mitochondrial voltage-dependent anion channels (VDACs) as novel pharmacological targets for anti-cancer agents." J Bioenerg Biomembr 40(3): 213-217.
- Singer, K., M. Kastenberger, et al. (2011). "Warburg phenotype in renal cell carcinoma: high expression of glucose-transporter 1 (GLUT-1) correlates with low CD8(+) T-cell infiltration in the tumor." Int J Cancer 128(9): 2085-2095.
- Speers, C., A. Tsimelzon, et al. (2009). "Identification of novel kinase targets for the treatment of estrogen receptor-negative breast cancer." Clin Cancer Res 15(20): 6327-6340.
- Zarghami, N., M. Giai, et al. (1996). "Creatine kinase BB isoenzyme levels in tumour cytosols and survival of breast cancer patients." Br J Cancer 73(3): 386-390.
- Zarghami, N., H. Yu, et al. (1995). "Quantification of creatine kinase BB isoenzyme in tumor cytosols and serum with an ultrasensitive time-resolved immunofluorometric technique." Clin Biochem 28(3): 243-253.
- Zeleznikar, R. J., P. P. Dzeja, et al. (1995). "Adenylate kinase-catalyzed phosphoryl transfer couples ATP utilization with its generation by glycolysis in intact muscle." J Biol Chem 270(13): 7311-7319.
- Zhang, S., E. Nemetlu, et al. (2010). "Metabolomic Profiling of Adenylate Kinase AK1-/- and AK2+/- Transgenic Mice: Effect of Physical Stress." Circulation 122(21).
- Zhao, R. X. and Z. X. Xu (2014). "Targeting the LKB1 tumor suppressor." Curr Drug Targets 15(1): 32-52.

- Zhdanov, A. V., A. H. Waters, et al. (2014). "Availability of the key metabolic substrates dictates the respiratory response of cancer cells to the mitochondrial uncoupling." Biochim Biophys Acta 1837(1): 51-62.
- Zheng, J. (2012). "Energy metabolism of cancer: Glycolysis versus oxidative phosphorylation (Review)." Oncol Lett 4(6): 1151-1157.
- Zielinski, L. P., A. C. Smith, et al. (2016). "Metabolic flexibility of mitochondrial respiratory chain disorders predicted by computer modelling." Mitochondrion 31: 45-55.
- Zu, X. L. and M. Guppy (2004). "Cancer metabolism: facts, fantasy, and fiction." Biochem Biophys Res Commun 313(3): 459-465.
- Takeuchi, T., A. Fujita, et al. (1995). "Necessity of newly synthesized ATP by creatine kinase for contraction of permeabilized longitudinal muscle preparations of rat proximal colon." J Pharmacol Exp Ther 275(1): 429-434.
- Tan, A. S., J. W. Baty, et al. (2014). "The role of mitochondrial electron transport in tumorigenesis and metastasis." Biochim Biophys Acta 1840(4): 1454-1463.
- Tanabe, T., M. Yamada, et al. (1993). "Tissue-specific and developmentally regulated expression of the genes encoding adenylate kinase isozymes." J Biochem 113(2): 200-207.
- Tepp, K., I. Shevchuk, et al. (2011). "High efficiency of energy flux controls within mitochondrial interactosome in cardiac intracellular energetic units." Biochim Biophys Acta 1807(12): 1549-1561.
- Timohhina, N., R. Guzun, et al. (2009). "Direct measurement of energy fluxes from mitochondria into cytoplasm in permeabilized cardiac cells in situ: some evidence for Mitochondrial Interactosome." J Bioenerg Biomembr 41(3): 259-275.
- Uranbileg, B., K. Enooku, et al. (2014). "High ubiquitous mitochondrial creatine kinase expression in hepatocellular carcinoma denotes a poor prognosis with highly malignant potential." Int J Cancer 134(9): 2189-2198.
- Utech, M., A. I. Ivanov, et al. (2005). "Mechanism of IFN-gamma-induced endocytosis of tight junction proteins: myosin II-dependent vacuolarization of the apical plasma membrane." Mol Biol Cell 16(10): 5040-5052.
- Wallimann, T. and W. Hemmer (1994). "Creatine kinase in non-muscle tissues and cells." Mol Cell Biochem 133-134: 193-220.
- Wallimann, T., M. Wyss, et al. (1992). "Intracellular compartmentation, structure and function of creatine kinase isoenzymes in tissues with high and fluctuating energy demands: the 'phosphocreatine circuit' for cellular energy homeostasis." Biochem J 281 ( Pt 1): 21-40.
- Vander Heiden, M. G., L. C. Cantley, et al. (2009). "Understanding the Warburg effect: the metabolic requirements of cell proliferation." Science 324(5930): 1029-1033.
- Warburg, O. (1956). "On respiratory impairment in cancer cells." Science 124(3215): 269-270.
- Varikmaa, M., R. Bagur, et al. (2014). "Role of mitochondria-cytoskeleton interactions in respiration regulation and mitochondrial organization in striated muscles." Biochim Biophys Acta 1837(2): 232-245.
- Vasseur, S., C. Malicet, et al. (2005). "Gene expression profiling of tumours derived from rasV12/E1A-transformed mouse embryonic fibroblasts to identify genes required for tumour development." Mol Cancer 4(1): 4.



- Vendelin, M., M. Lemba, et al. (2004). "Analysis of functional coupling: mitochondrial creatine kinase and adenine nucleotide translocase." *Biophys J* 87(1): 696-713.
- WHO. (2018). "Cancer key facts." from <http://www.who.int/en/news-room/factsheets/detail/cancer>.
- Wilson, C. D., W. Shen, et al. (1997). "Expression of the brain creatine kinase gene is low in neuroblastoma cell lines." *Dev Neurosci* 19(5): 375-383.
- Wilson, J. E. (2003). "Isozymes of mammalian hexokinase: structure, subcellular localization and metabolic function." *J Exp Biol* 206(Pt 12): 2049-2057.
- Wise, D. R., R. J. DeBerardinis, et al. (2008). "Myc regulates a transcriptional program that stimulates mitochondrial glutaminolysis and leads to glutamine addiction." *Proc Natl Acad Sci U S A* 105(48): 18782-18787.
- Woods, A., K. Dickerson, et al. (2005). "Ca<sup>2+</sup>/calmodulin-dependent protein kinase kinase-beta acts upstream of AMP-activated protein kinase in mammalian cells." *Cell Metab* 2(1): 21-33.
- Woods, A., S. R. Johnstone, et al. (2003). "LKB1 is the upstream kinase in the AMP-activated protein kinase cascade." *Curr Biol* 13(22): 2004-2008.
- Xun, Z., D. Y. Lee, et al. (2012). "Retinoic acid-induced differentiation increases the rate of oxygen consumption and enhances the spare respiratory capacity of mitochondria in SH-SY5Y cells." *Mech Ageing Dev* 133(4): 176-185.

## Acknowledgements

For this thesis the experiments were performed in the National Institute of Chemical Physics and Biophysics in the laboratory of Bioenergetics in Tallinn, Estonia.

Firstly, my sincere gratitude and respect belongs to my academic supervisor Dr. Tuuli Kaambre who has guided me during my young scientist career since master study until the end of PhD study. She motivated me always to go on. Moreover, I would like to thank my co-supervisor Dr. Anu Planken for guiding PCR experiments.

My gratitude also extends to opponents of my theses, Professor Allen Kaasik and Dr Emirhan Nemutlu for accepting to review this work.

My special thanks belong to my colleagues from Bioenergetics lab: Dr Vladimir Chekulayev for helping to grow cell lines and for interesting scientific discussions, Dr Natalja Timohhina for guiding spectrophotometric experiments, Laura Truu who taught me PCR method, Dr Kersti Tepp who helped to isolate rat cardiomyocytes and liver mitochondria and Igor Shevchuk for introducing me a wonderful world of confocal microscopy. I wish to express my special thanks to Maire Peitel for her assistance with everyday work.

I wish to thank MD PhD Vahur Valvere, MD Vladimir Afanasjev and MD Karoliina Heck from the North Estonian Medical Center for providing the post-operational material. Moreover, I would like to thank my collaboration partners from University of Joseph Fourier in Grenoble Professor Uwe Schlattner and Dr Rita Guzun.

My warmest thanks go to Ljudmila for love and understanding and giving me energy to complete this work. Deep thanks belong to my grandparents, parents, brothers and sisters endless support and understanding.

I am very grateful also to the Archimedes Foundation, the Dora Program, and the graduate school of Biomedicine and Biotechnology for supporting my participation in conferences and my study abroad.

This work was supported by grants: No. 8987 from the Estonian Science Foundation, SF0180114Bs08 and institutional research funding IUT (IUT23-1) from Estonian Ministry of Education and Research, and by the project "Aid for research and development in health care technology" of Archimedes foundation No. 3.2.1001.11-0027.

## Abstract

Both adenylate (AK) and creatine kinase (CK) networks play important roles in cellular energy metabolism of fully-differentiated cells. Under poor-energy supply conditions AK(s) also mediate intracellular AMP signaling *via* activation of the energy-sensing AMP-activated protein kinase (AMPK). It has been found that AMPK behaves as a tumor suppressor gene. However, the role of the AK and CK networks in cancer formation have remained unclear.

The aim of this study was to analyze the kinetics of the mitochondrial metabolism, as well as to evaluate which changes within the interplay between the AK and CK networks play a role in neuroblastoma (NB), human colorectal cancer (HCC) and human breast cancer (HBC) formation. Experiments were performed on permeabilized material, including undifferentiated and differentiated NB Neuro-2a cells, as well as on (HBC) and (HCC) postoperative samples.

The current study demonstrated that in NB and HCC cells a considerable amount of ATP is produced *via* aerobic glycolysis, where mitochondria oxidative phosphorylation linked with glycolytic pathway supports the high glycolytic rate in cancer cells. Mitochondrial respiration kinetic analysis revealed that the malignant transformation of cells caused rearrangement of mitochondrial permeability for adenine nucleotides.

Experiments demonstrated plasticity of the phosphotransfer network in cells. If colon tissue cells predominantly used CK pathway to maintain cell energy homeostasis, then during colorectal cancer formation an energetic shift occurred from the CK to the AK pathway in malignant cells. The respirometric study showed that in neuroblastoma cells the mitochondrial energy is transferred to cytosolic compartment *via* AK network instead of the CK network.

Furthermore, a semi-quantitative oxygraphic method was developed to estimate the distribution of cytosolic AK1 and mitochondrial AK2 in permeabilized cells and tissue samples. The method is based on AK functional coupling with mitochondrial oxidative phosphorylation. To differentiate AK1 and AK2 dependent respiration, the extra-mitochondrial ADP is eliminated by pyruvate kinase and its substrate phosphoenolpyruvate.

An oxygraphic study on post-operative samples revealed that in both HCC and HBC the AK pathway was up-regulated. Moreover, it was found that the mitochondrial kinase AK2 was expressed predominantly in poorly differentiated cells with a high proliferative index. The up-regulation of AK2 is associated with rearrangement of mitochondrial affinity for AMP.

Finally, it was hypothesized in the current study that malignant cells can avoid AK-AMP-AMPK intracellular signal activation and its tumor suppressor action *via* overexpression of AK2 and changes of mitochondrial affinity for AMP.

## Lühikokkuvõte

Adenülaat- (AK) ja kreatiinkinaas (CK, *creatine kinase*) energiaülekande võrgustik omab tähtsat rolli raku energeetilise homöostaasi säilitamises. Stressi tingimustes AK vahendab adenülaatkinaas AMP signaalirada, mille käigus aktiveeritakse rakusisene molekulaarne energiasensor AMP-aktiveeritud proteiin kinaas (AMPK). Paljud tööd on näidanud, et AMPK käitub nagu tuumor suppressor geen. Paraku on AK ja CK energiaülekande võrgustiku roll vähi tekkes jäänud siiani ebaselgeks.

Töö eesmärk oli läbi viia mitokondri metabolismi kineetiline analüüs ja selgitada välja millised muutused AK ja CK energiaülekande võrgustike vastasmõjus toovad kaasa neuroblastoomi ja jämesoole- ning rinnavähi tekke. Uuringud viidi läbi permeabiliseeritud rakkudel ja kudedel: diferentseerimata ja diferentseeritud neuroblastoomi rakuliinil Neuro-2A, ning rinna- ja jämesoolevähi operatsioonijärgsel materjalil .

Töö näitas, et neuroblastoomi ja jämesoole vähi rakkudes energiat osaliselt toodetakse aeroobse glükolüüsi abil. Antud vähi tüüpides on arvukalt mitokondreid, mille üheks funktsiooniks on toetada kõrget glükolüüsi taset neis maliigsetes rakkudes. Mitokondriaalse hingamise kineetiline analüüs näitas, et jämesoole ja neuroblastoomi mitokondri välismembraani läbitavus ADP suhtes on suur.

Töö tulemusel saab järeldada, et rakkude energiaülekande võrgustik on paindlik. Kui jämesoole epiteeli rakud kasutavad pealmiselt CK energialülekande rada energia homöostaasi säilitamiseks, siis jämesoole epiteeli kartsinogenees toob kaasa muutusi raku energia metabolismis, mille käigus asendatakse CK poolt vahendatud rada AK rajaga, mis on väga oluline ka neuroblastoomi rakkudes .

Töötati välja ka poolkvantitatiivne oksügraafial põhinev meetod, et välja selgitada tsütosoolset AK1 ja mitokondiaalset AK2 isoformide jaotus erinevates rakkudes ja kudedes. Antud meetod põhineb sellel, et AK poolt katalüüsitud reaktsioon on tugevasti sidestatud mitokondriaalse oksüdatiivse fosforüülimisega. Selleks, et elimineerida mitokondri välist ADP-d kasutati püruvaatkinaasi ja selle ensüümi substraati fosfoenoolpüruvaati.

Meetod kontrolliti ka kasvajate operatsioonijärgsel materjalil, ning selgus, et antud meetod on piisaval tundlik, et uurida AK poolt vahendatud energiatransporti. Eksperimendid näitasid, et AK roll energia metabolismis on suurenenud jämesoole ja rinnavähis tekkimisel. Lisaks sellele selgus ka, et mitokondriaalne AK2 ekspresseeritakse eelistatult kõrge proliferatsiooni indeksiga ning diferentseerimata vähirakkudes. Neile rakkudele on omane ka kõrge mitokondri välismembraani läbitavus AMP suhtes.

Lähtuvalt töö tulemustes püstitati hüpotees, et kasvajates esineb AK2 isovormi üleekspressioon ning suurenenud mitokondri välismembraani läbitavus AMP suhtes aitab ära hoida AK-AMP-AMPK signaaliraja aktivatsiooni maliigsetes rakkudes.

## Appendix




### **Publication I**

**Aleksandr Klepinin**, Lyudmila Ounpuu, Rita Guzun, Vladimir Chekulayev, Natalja Timohhina, Kersti Tepp, Igor Shevchuk, Uwe Schlattner, Tuuli Kaambre. (2016) Simple oxygraphic analysis for the presence of adenylate kinase 1 and 2 in normal and tumor cells. *Journal of Bioenergetics and Biomembranes*, 48 (5), 531–548.





# Simple oxygraphic analysis for the presence of adenylate kinase 1 and 2 in normal and tumor cells

Aleksandr Klepinin<sup>1</sup> · Lyudmila Ounpuu<sup>1</sup> · Rita Guzun<sup>2,3</sup> · Vladimir Chekulayev<sup>1</sup> · Natalja Timohhina<sup>1</sup> · Kersti Tepp<sup>1</sup> · Igor Shevchuk<sup>1</sup> · Uwe Schlattner<sup>2,3</sup> · Tuuli Kaambre<sup>1,4</sup> 

Received: 28 June 2016 / Accepted: 31 October 2016  
© Springer Science+Business Media New York 2016

**Abstract** The adenylate kinase (AK) isoforms network plays an important role in the intracellular energy transfer processes, the maintenance of energy homeostasis, and it is a major player in AMP metabolic signaling circuits in some highly-differentiated cells. For this purpose, a rapid and sensitive method was developed that enables to estimate directly and semi-quantitatively the distribution between cytosolic AK1 and mitochondrial AK2 localized in the intermembrane space, both in isolated cells and tissue samples (biopsy material). Experiments were performed on isolated rat mitochondria or permeabilized material, including undifferentiated and differentiated neuroblastoma Neuro-2a cells, HL-1 cells, isolated rat heart cardiomyocytes as well as on human breast cancer post-operative samples. In these samples, the presence of AK1 and AK2 could be detected by high-resolution respirometry due to the functional coupling of these enzymes with ATP synthesis. By eliminating extra-mitochondrial ADP with an excess of pyruvate kinase and its substrate phosphoenolpyruvate, the coupling of the AK reaction with mitochondrial ATP synthesis could be quantified for total AK and mitochondrial AK2 as a specific AK index. In contrast to the creatine kinase pathway,

the AK phosphotransfer pathway is up-regulated in murine neuroblastoma and HL-1 sarcoma cells and in these malignant cells expression of AK2 is higher than AK1. Differentiated Neuro-2a neuroblastoma cells exhibited considerably higher OXPHOS capacity than undifferentiated cells, and this was associated with a remarkable decrease in their AK activity. The respirometric method also revealed a considerable difference in mitochondrial affinity for AMP between non-transformed cells and tumor cells.

**Keywords** Adenylate kinase · Cardiomyocytes; mitochondria · Neuroblastoma · Breast cancer

## Introduction

Adenylate kinases (AKs) are members of an evolutionary conserved family of enzymes that catalyze the phosphoryl transfer between adenylates ( $\text{AMP} + \text{ATP} \leftrightarrow 2\text{ADP}$ ) and could facilitate the intracellular energetic communication (Carrasco et al. 2001; Dzeja and Terzic 2009; Dzeja and Terzic 2003). The main function of AK is to maintain the cellular energy state through regulation of nucleotide ratios in different intracellular compartments (Dzeja and Terzic 2009). AK(s) also mediate intracellular AMP signaling, e.g. via the membrane metabolic sensor ATP-sensitive potassium channel, the energy-sensing AMP-activated protein kinase (AMPK), and other AMP-sensitive metabolic enzymes which collectively form a key metabolic sensing system to regulate a number of vital cellular processes (Dzeja and Terzic 2009; Dzeja et al. 2007; Dyck and Lopaschuk 2006). For example, regulation of AMPK by AMP is involved in its tumor suppressor functions under energy-poor conditions in several types of tumors (Dasgupta and Chhipa 2016; Hardie and Alessi 2013; Shackelford and Shaw 2009). In cells, AMPK

**Electronic supplementary material** The online version of this article (doi:10.1007/s10863-016-9687-3) contains supplementary material, which is available to authorized users.

✉ Tuuli Kaambre  
tuuli.kaambre@kbfi.ee

<sup>1</sup> Laboratory of Bioenergetics, National Institute of Chemical Physics and Biophysics, Akadeemia tee 23, 12618 Tallinn, Estonia

<sup>2</sup> Laboratory of Fundamental and Applied Bioenergetics, Univ. Grenoble Alpes, Grenoble, France

<sup>3</sup> Inserm, U1055, Grenoble, France

<sup>4</sup> Tallinn University, Tallinn, Estonia

is activated through increased AK-catalyzed AMP generation or suppression of AMP removal catalyzed by 5'-nucleotidase (5'-NT) and AMP-deaminase (AMPD<sup>1</sup>) which all regulate cellular AMP concentration (Dzeja and Terzic 2009; Plaideau et al. 2014; Plaideau et al. 2012).

The AK family includes nine major isoforms (AK1 - AK9), and several sub-forms with distinct intracellular localization and kinetic properties (Amiri et al. 2013; Dzeja and Terzic 2009; Panayiotou et al. 2014). These isoenzymes support specific cellular processes ranging from muscle contraction, electrical activity, cell motility, unfolded protein response and mitochondrial energetics (Burkart et al. 2011; Zhang et al. 2014). Different isoforms of AK have been found in distinct cell compartments such as cell membranes, cytosol, mitochondria and also nucleus, thereby creating an integrated phosphotransfer network. Tissues with high energy demand, such as brain, heart and skeletal muscles are rich in AK1, the major isoform located in the cytosol (Tanabe et al. 1993). In striated muscle cells (e.g., cardiomyocytes (Noma 2005)), AK1 contributes to energy transfer from ATP-producing sites (mitochondria) to the ATP-consuming sites (actomyosin) (Dzeja et al. 1999). Mitochondria harbor three different isoforms: AK2 in the intermembrane space and AK3 and AK4 in the matrix. AK2 is predominantly expressed in liver, kidney, spleen, large intestine and stomach (Tanabe et al. 1993). Due to its localization at the mitochondria/cytosol interface, AK2 plays a unique role in the regulation of energy transfer between these two compartments and cellular energy homeostasis in general (Gellerich 1992). AK3, which uses GTP instead of ATP, is expressed in all tissues except red blood cells. AK4 is expressed mainly in kidney, brain, heart, and liver, however it is unsure whether it functions as a kinase (Liu et al. 2009). Expression of AK1, AK2 and AK4 is regulated and shows a certain tissue-specificity, while AK3 is ubiquitously expressed and can be considered as a housekeeping enzyme.

AK2 and enzymatically-inactive AK4 are considered (Eimre et al. 2008; Liu et al. 2009) to be the components of the Mitochondrial Interactosome - a large mitochondrial

transmembrane complex consisting of ATP-synthasome, mitochondrial creatine kinase (MtCK), voltage dependent anion channel (VDAC), and some protein factors which regulate the mitochondrial outer membrane (MOM) permeability by interacting with VDAC from the cytosolic side (Guzun et al. 2012; Martel et al. 2014). It was reported that within this mitochondrial supercomplex, AK4 interacted with mitochondrial ADP/ATP-translocase which protected the neural cells against oxidative stress (Liu et al. 2009). The mitochondrial supercomplex may also include some cytosolic hexokinase (HK) isoforms HK-1 or -2 (Mathupala et al. 2006) which in hepatomas bind to mitochondria and use mitochondrially produced ATP, where up to ~50% of total ATP provided by AK2 (Nelson and Kabir 1985).

For a long time, the main function of AK has been associated solely with efficient transfer and equilibrium of high-energy phosphates in different micro-compartments within the cell. During the last decade, several new functions of AK have been identified. Firstly, AK has an important role in cell proliferation where AK1 associated with the mitotic spindle apparatus, to supply energy for cell division (Dzeja et al. 2011). Secondly, AK2 plays an important role in differentiation of neural, cardiac and haematopoietic stem cells, by providing the energy required for cell cycle, DNA synthesis and repair (Dzeja and Terzic 2009; Inouye et al. 1998; Zhang et al. 2014; Tanimura et al. 2014). Adipocyte differentiation was also shown to be associated with a remarkable increase in the levels of AK2 (Burkart et al. 2011). Thirdly, mitochondrially-associated AK2 is one of the components of the apoptotic complex where AK2 released into cytosol initiates cell death (Lee et al. 2007; Mather and Rottenberg 2001).

Deficiencies of AK expression or mutations in AK genes are associated with several diseases such as hemolytic anemia, reticular dysgenesis and ciliary dyskinesia (Dzeja and Terzic 2009). Park et al. (Park et al. 2012) have reported that AK1 could play a neuropathogenic role in Alzheimer's disease due to hyperphosphorylation of tau proteins. In cells, AK is functionally coupled to mitochondrial oxidative phosphorylation (OXPHOS), where during cellular stress conditions a small decrease in ATP induces a large increase in AMP which stimulates OXPHOS through AK-catalyzed ADP regeneration in mitochondria (Dzeja and Terzic 2009). This is in particular true for highly-differentiated cells such as adult cardiomyocytes (CM) and hepatocytes (Gellerich 1992), but has also been found for some sarcoma cells and other neoplasms (Chekulayev et al. 2015; Eimre et al. 2008; Klepinin et al. 2014). Previous studies have shown that increased AK expression, associated with changes in the expression profile of creatine kinase (CK) isoforms (Chekulayev et al. 2015; Greengard et al. 1980; Patra et al. 2012), can promote tumor progression. Moreover, in human prostate cancer (Hall et al. 1985) it was shown that AK may serve as an onco-

#### <sup>1</sup> Abbreviations:

AK, adenylate kinase; AMPD, AMP deaminase; AMPK, AMP-activated protein kinase; ANT, adenine nucleotide translocator; AP5A, diadenosine pentaphosphate; BSA, bovine serum albumin; CAT, carboxyatractyloside; CK, creatine kinase; CM, cardiomyocyte; CSC, cancer stem cells; Cyt-c, cytochrome c; DMEM, Dulbecco's Modified Eagle Medium; dN2a, differentiated N2a cells; DTT, dithiothreitol; FBS, fetal bovine serum; HBC, human breast cancer; HK, hexokinase; I<sub>AK</sub>, adenylate kinase index; IMP, inosine monophosphate; Km, Michaelis-Menten constant; MIM, mitochondrial inner membrane; MOM, mitochondrial outer membrane; MtCK, mitochondrial creatine kinase; N2a, Neuro-2a; NB, neuroblastoma; NEM, N-ethylmaleimide; OXPHOS, oxidative phosphorylation; PBS, phosphate buffered saline; PEP, phosphoenolpyruvate; PK, pyruvate kinase; RA, all-trans-retinoic acid; RCI, respiratory control index; SNS, sympathetic nerve system; uN2a, undifferentiated N2a cells; VDAC, voltage dependent anion channel; V<sub>m</sub>, rates of maximal respiration; V<sub>o</sub>, rates of basal respiration.

developmental marker. However, also the opposite has been found; in lung and hepatoma cancers, AK is down-regulated as compared to normal tissue (Balinsky et al. 1984; Criss et al. 1970).

To date, a variety of different analytical methods have been applied for evaluating the functional state of the AK phosphotransfer system such as: spectrophotometric measurements (Dzeja et al. 1999; Tanabe et al. 1993), gel-electrophoresis (Criss et al. 1970), immuno-histochemical analysis and Western blotting (Burkart et al. 2011; Carrasco et al. 2001; Dzeja et al. 1999; Liu et al. 2009; Tanabe et al. 1993), two-dimensional SDS-PAGE along with subsequent MALDI-MS/MS or LC-MS/MS (Fukada et al. 2004), RT-PCR (Noma et al. 2001),  $^{18}\text{O}$  isotopic tracer studies (Dzeja et al. 1999), as well as two-photon excitation fluorescence imaging and fluorescence correlation spectroscopy (Ruan et al. 2002). These analytical procedures are mostly invasive, thus require extraction of tissue proteins or mRNA and in some cases also very expensive equipment. Finally, there are some known global inhibitors of the AK reaction like Ap5A (Daniel et al. 2003; Hampton et al. 1976; Rosano et al. 1976), but isoform-specific inhibitors for AK1 or AK2 are lacking.

In this study, we have developed a simple and rapid method for semi-quantifying the activity of AK1 and AK2 separately in different biological samples. This method is based on measuring the rate of cellular/tissue respiration due to stimulation of the mitochondrial respiration by ADP released via AK-catalyzed reactions, stimulated by external ATP and AMP. For this objective, corresponding experiments were carried out on a large set of normal and tumor cells with known and unknown profile of AK1/AK2 expression. In the present work, we also demonstrate that the elaborated analytical approach can be successfully applied for evaluating these AK isoforms activities in postoperative tissues of breast cancer patients.

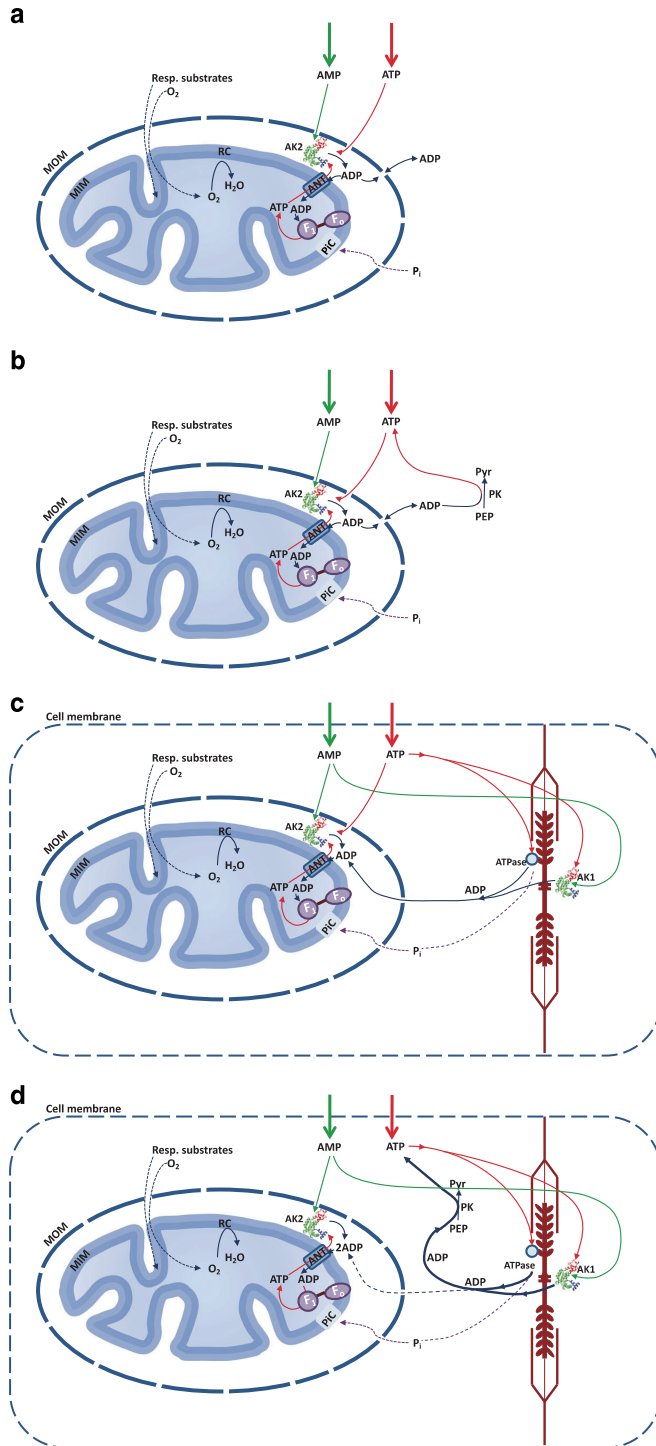
## Results

Scheme 1 depicts our approach to quantify *in vitro* the presence of cytosolic AK1 and mitochondrial AK2 in mammalian cells and tissues. The basic principle is oxygraphic analysis of the connections between AK1/AK2 catalyzed reactions and mitochondrial OXPHOS, for this purpose permeabilized cells method are used since the plasma membrane is impermeable for adenine nucleotides. AMP can support ATP synthesis in mitochondria in the presence of endogenous ATP due to AK coupling with OXPHOS. According to Scheme 1, the ADP formed by the AK-catalyzed reaction (in the presence of exogenously-added ATP and AMP), either directly in the mitochondrial intermembrane space (AK2) (Scheme 1a), or in the cytosol (AK1) and accessing mitochondria via the VDAC pore (Scheme 1c), is finally using ADP/ATP exchange via the adenine nucleotide translocator (ANT) to stimulate

mitochondrial respiration. Since isoform-specific AK inhibitors do not exist, another approach is required to estimate non-invasively the contributions of AK1 and AK2 to total AK activity. Here, we use the phosphoenolpyruvate (PEP) – pyruvate kinase (PK) ADP trapping system in combination with respirometry (Saks et al. 2010; Timohhina et al. 2009). This system efficiently eliminates extra-mitochondrial ADP (Schemes 1b, d). It allows us to measure, in permeabilized cells, the total AK pool (AK1 + AK2) in absence of PEP-PK system (Scheme 1c) as well as specifically the mitochondrial AK2 coupled with OXPHOS in presence of PEP-PK system, which traps all cytosolic ADP accessible to AK1 (Scheme 1d).

The main isoform of adenylate kinase in a rat liver is AK2 (Supplement Fig. 1) (Noma 2005). Figure 1 shows oxygraph recording of isolated rat liver mitochondria. The mitochondrial respiration was activated by AMP and ATP via AK2 where AK2 produced 2 molecules ADP which directly transfer through adenine nucleotide translocator (ANT) into the mitochondria matrix (Scheme 1a). The respiratory control index (RCI) for the given mitochondrial preparations exceeded 8 (Table 1). Addition of exogenous Cyt-c did not increase the respiration rate, showing the intactness of the mitochondrial outer membrane (MOM) (Fig. 1a). Addition of carboxyatractyloside (CAT) decreased respiration rate back to the State II respiration level ( $V_0$ ), indicating that the mitochondrial inner membrane (MIM) is also intact. Next, in the presence of the PK-PEP system (Fig. 1b) and under the same condition as Fig. 1a, (except using 2 mM ATP instead of 0.1 mM ATP) 80% of ADP formed in mitochondrial intermembrane space via AK2 were trapped by PK due to the high permeability of VDAC for adenine nucleotides (Scheme 1b). Thus, in presence of the PK-PEP system, the exogenous AMP activates only 20% of the maximal respiration, which is the part of AK2-generated ADP functionally coupled with OXPHOS. Addition of the AK inhibitor AP5A to the mitochondria almost entirely eliminated also these 20% of respiratory stimulation (Fig. 1b). This data is in correlation with Dr. F.N. Gellerich results (Gellerich 1992). Dr. F.N. Gellerich studied dynamic adenine nucleotide compartmentation in 1992, and found that ADP generated by AK2 in the mitochondrial intermembrane space can be channeled into mitochondrial matrix (Gellerich 1992).

Not only ADP but also AMP can control mitochondrial respiration due to AK functional coupling with OXPHOS. We hypothesized that the sensitivity of the proposed method could be applied at the cellular level to measure the ratio of AK1 and AK2, which is determined among others by the intracellular content of mitochondria and their OXPHOS capacity. For this purpose, a broad panel of normal and tumor cells with different OXPHOS rates was studied, including rat cardiomyocytes (CM) and human breast cancer (HBC) tissue samples. Heart muscle cells produce more than 90% of their



◀ **Scheme 1** The principles of this study are illustrated by four schemes of increasing complexity: Schemes A and B represent isolated liver mitochondrion as a reference system. Schemes C and D illustrate permeabilized cells chosen as experimental study model. Experiments were performed in two types of conditions: in the presence of ADP trapping system after or before activation cytosolic (AK1) and mitochondrial (AK2) adenylate kinase isoform. The ADP tapping system consist of phosphoenolpyruvate (PEP) and pyruvate kinase (PK), traps extramitochondrial ADP produced by AK1 and MgATPase reactions and subsequently regenerates extramitochondrial ATP. In mitochondrial AK2 forms micro-domain within the intermembrane space where AK2 produces 2 molecules ADP which is re-imported into the matrix via adenine nucleotide translocator (ANT) due to its functional coupling with AK2

ATP via mitochondrial respiration (Ventura-Clapier et al. 2011), whereas tumor cells are usually highly glycolytic and have low rates of mitochondrial respiration (Hanahan and Weinberg 2011). The following parameters were measured for every cell model: the rates of basal respiration ( $V_o$ ) and maximal AMP- and ADP-activated respiration ( $V_{AMP}$ ,  $V_{ADP}$ ), as well as the respiratory control index (RCI) (Table 1). Among the studied cells, adult rat CM(s) were characterized by the highest  $V_{ADP}$  and RCI values. The RCI exceeded about 5–7 times those for human HBC tissue cells. Although, HL-1 cardiac sarcoma cells have relatively high rates of mitochondrial respiration, their  $V_{ADP}$  values were nearly 10 times lower as compared to normal CM(s). This result is consistent with several studies which showed reprogramming of mitochondrial morphology and function during carcinogenesis. It is important to emphasize that in cardiomyocytes  $V_{ADP}$  was at a similar level as AMP induced respiration ( $V_{AMP}$ ), while HL-1 cells showed decreased  $V_{AMP}$  (Table 1). This indicates that there is decreased AK expression in HL-1 cells as compared to cardiomyocytes, but it is not clear, how exactly the AK profile changes in cardiac sarcoma cells. This question can be addressed by introducing the PEP-PK trapping system as outlined above.

Respiratory measurements were conducted with permeabilized cells, and AK1/AK2 distribution was first analyzed in rat heart CM(s) and in HL-1 tumor cells of the cardiac origin (Fig. 2). Functional coupling between ANT and mitochondrial AK2 is known to exist in human CM(s) (Seppet et al. 2005). In permeabilized CM and HL-1 cells, the addition of AMP and ATP activated AK1 and AK2 (Scheme 1c). This activation led to increased rates of cellular  $O_2$  consumption ( $V_{AMP}$ ) (Fig. 2) as a result of ADP produced and transported into the mitochondrial matrix via VDAC and/or ANT. Subsequent addition of PK to the assay systems (Scheme 1d) decreased the rates of  $O_2$  consumption ( $V_{PK}$ ) (Fig. 2), since the added PK removes efficiently extramitochondrially-generated ADP generated by AK1 and MgATPases (Scheme 1d), as well as intra-mitochondrially-generated ADP not coupled to respiration and escaping mitochondria. A PK activity of 10 U/ml was sufficient to trap all ADP available in the bulk phase of the cytoplasm. Residual respiration is associated with AK2 fully coupled with

OXPHOS. That functional coupling between AK2 and mitochondrial respiration is indeed responsible for this residual respiration was confirmed by AP5A which decreased respiration back to  $V_o$  (Fig. 2). According to this protocol, AK indexes ( $I_{AK1}$  and  $I_{AK2}$ ) were defined which semi-quantify distribution of AK1 and AK2 in cells (Fig. 3a, see also Material and Methods) and calculated for adult rat CM(s) and HL-1 tumor cells (Fig. 3a). These values were in a good agreement with the results of standard spectrophotometric activity assays in cell extracts (Table 2). This method provides information on the distribution of AK1 and coupled AK2 in cells. It is known that AK1 is the predominant AK isoform in cardiac muscle cells with only a minor level of mitochondrial AK2 (Tanabe et al. 1993), and this observation is in accordance with our oxygraphic studies (Table 2). The specificity of current oxygraphic method was confirmed by western blot and spectrophotometric methods (Fig. 4) which showed that in rat cardiomyocytes main AK isoform was AK1 as well as only AK1 was present in cytosol. HL-1 cardiac tumor cells have decreased  $V_{AMP}$  which is associated with downregulation of AK1 (Fig. 3a, Table 2). Here, carcinogenesis shifts the AK profile from AK1 to AK2.

The current study revealed few differences in the ratio of AK1 and AK2 in rat cardiomyocytes when comparing oxygraphic (Fig. 3a) and spectrophotometric AK activity assays (Table 2). Therefore to control specificity of N-ethylmaleimide (NEM) in inhibition of AK1 (Khoo and Russell 1972) rat liver where only AK2 expressed (Noma 2005) and rat skeletal muscle soleus where predominantly expressed AK 1 (Makarchikov et al. 2002) were used. Our study confirmed specificity of NEM to inhibit AK1 (Supplement Fig.1). Incubation with NEM decreased 99% of total AK activity in rat soleus homogenate, at the same time NEM did not influence on rat liver AK activity (Supplement Fig.1) In addition, commercial pure AK1 enzyme from rabbit muscle (Sigma-Aldrich) was used where NEM fully inhibited AK activity (data not shown).

The PK-PEP protocol, which enables the determination of cytosolic (mainly AK1) and coupled mitochondrial AK2 activity in the same sample, was also applied to examine the effect of neuroblastoma (NB) N2a cell differentiation induced by all-trans-retinoic acid (RA) on AK isoenzymes. Earlier, we had shown that the treatment of undifferentiated N2a cells with RA led to formation of a cell population morphologically similar to mature neurons of the sympathetic nerve system (SNS) and characterized by elevated acetylcholinesterase activity, a marker enzyme for the SNS cells (Klepini et al. 2014). The elaborated oxygraphic method demonstrated that RA had no effect on the profile of AK1 and coupled AK2 activities in these NB cells (Fig. 3b). Western blot and spectrophotometric analysis (Fig. 4) confirmed that AK1 and AK2 expressed equally in N2a cells and that AK1 indeed localized to the cytosol. The spectrophotometric activity assays also

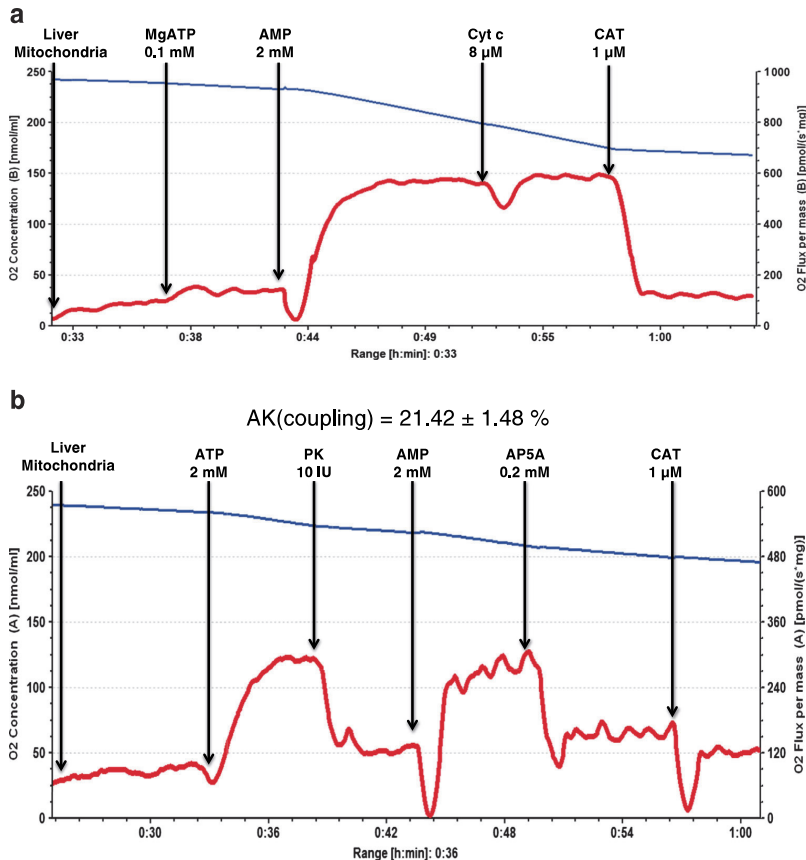


**Fig. 1** Oxygraphic analysis of the functional coupling between the AK pathway and OXPHOS in isolated rat liver mitochondria: A – Recording of original traces of AMP-activated respiration; the addition of 2 mM AMP to mitochondria (in the presence of 0.1 mM ATP) resulted in a ~ 5 times increase in the rate  $O_2$  consumption due to activation of mitochondrial AK2 which coupled with OXPHOS. Outer mitochondrial intactness was controlled by exogenously-added cytochrome c (Cyt-c). The AMP-activated respiration was inhibited by carboxyatractyloside (CAT; final concentration, 1  $\mu$ M) to the initial level showing that the respiration is well controlled by adenine nucleotide translocator in the intact inner mitochondrial membrane. B – Testing the influence of a pyruvate kinase (PK)–phosphoenolpyruvate (PEP) ADP trapping

system on the coupling of AK-catalyzed processes with OXPHOS. The addition of PK to isolated mitochondria suppressed almost completely the ATP (2 mM) activated respiration due to elimination of ADP formed in ATPase reactions, further addition of AMP (final concentration, 2 mM) caused a powerful increase in the rate of  $O_2$  consumption due to local release of ADP in AK2-catalyzed processes. Part ADP, which was produced via AK2 was trapped by PK. The presence of AK2 activity was confirmed by addition of diadenosine pentaphosphate (AP5A, an inhibitor of AK). This inhibitor, at a concentration of 0.2 mM, suppressed the AMP-stimulated respiration up to initial level indicating thereby that it was largely mediated by ADP produced in AK reactions

revealed a decrease in total AK activity during NB cell differentiation (Table 2).

We finally applied high-resolution respirometry for estimating the AK activity distribution in cancerous tissue biopsy material. Unfortunately, it was not possible to measure the rate  $V_{AMP}$  for adjacent normal tissue. This tissue consists of a mix of connective and adipose tissue and exhibited low rates of State II and State III respiration. Since our previous work on human HBC showed that MtCK plays a minor role in cellular energy transfer (Kaambre et al. 2012), we examined here the

coupling of AK with OXPHOS. Respirometry experiments suggested that the mitochondrial respiration rate in the presence of 2 mM AMP is close to maximal rate with 2 mM ADP (Table 1) which indicated that the AK system is a main energy transfer system in HBC. The spectrophotometrically determined activities demonstrated that both AK1 and AK2 increased 5- to 7-fold during breast carcinogenesis with AK1 remaining the predominant isoform (Table 2).

The main limiting factor for the described AK respirometric assay is the low mitochondrial respiration of an examined

**Table 1** Rates of basal ( $V_0$ ), ADP ( $V_{ADP}$ )- and AMP ( $V_{AMP}$ )-activated respiration, respiratory control index (RCI) and apparent  $K_m$  (AMP) values for human breast cancer tissue, isolated rat liver mitochondria and cardiomyocytes (CMs) as well as some tumor cells of different histological type

Cells and tissues	$V_0^{(a)}$ mean $\pm$ SEM	$V_{ADP}^{(b)}$ mean $\pm$ SEM	RCI <sup>(b)</sup> , ADP	$V_{AMP}^{(c)}$ mean $\pm$ SEM	$K_m$ (AMP) mean $\pm$ SEM
Mitochondria	4.75 $\pm$ 0.44	42.4 $\pm$ 4.06	8.88 $\pm$ 0.72	41.5 $\pm$ 6.3	23.5 $\pm$ 6.9
Rat CM(s)	7.5 $\pm$ 1.6 <sup>(d)</sup>	84.5 $\pm$ 13.9 <sup>(d)</sup>	11.2 $\pm$ 4.2 <sup>(d)</sup>	88.1 $\pm$ 2.7	369 $\pm$ 88
HL-1 cells	1.91 $\pm$ 0.8	9.12 $\pm$ 2.3	4.51 $\pm$ 0.63	2.9 $\pm$ 0.2	67 $\pm$ 9.3
uN2a cells	3.38 $\pm$ 0.12	11.0 $\pm$ 0.43	3.28 $\pm$ 0.05	7.2 $\pm$ 0.40	92 $\pm$ 14
dN2a cells	4.07 $\pm$ 0.46	12.05 $\pm$ 1.06	3.13 $\pm$ 0.16	6.8 $\pm$ 0.5	207 $\pm$ 24
Breast cancer	0.56 $\pm$ 0.04 <sup>(e)</sup>	1.09 $\pm$ 0.04 <sup>(f)</sup> (range, 0.10–2.02) <sup>(f)</sup>	1.95 $\pm$ 0.21	0.72 $\pm$ 0.07 <sup>(f)</sup> (range, 0.59–1.03)	-
Breast control tissue	0.02 $\pm$ 0.01 <sup>(f)</sup>	-	-	-	-

<sup>a</sup>Rates of  $O_2$  consumption are expressed in nmol  $O_2$ /min per mg protein

<sup>b</sup> $V_{ADP}$  and RCI values were measured in the presence of 2 mM ADP

<sup>c</sup>These values were obtained in the presence of 2 mM AMP

<sup>d</sup>From (Timohhina et al. 2009)

<sup>e</sup>From (Kaambre et al. 2012)

<sup>f</sup>Rates of respiration in nmol  $O_2$ /min per mg dry weight of the tissue

biomaterial - cells or tissues with low ( $< 2$ ) RCI values. In this respect, also ATP concentration should be adapted to the respiratory capacity of the cells to avoid interfering effects of ADP released by non-specific ATPase reactions. Cells with a decreased number of mitochondria and/or with low OXPHOS rates and RCI values in the range of 2–4 should be measured at low (0.1 mM) ATP concentrations, while for cells with higher RCI values the use of higher (2 mM) ATP concentrations is recommended.

In a previous study, Gellerich (Gellerich 1992) showed that PEP-PK could be used to examine the affinity of mitochondria for exogenously added AMP. However, the roles of AK2 in the regulation of OXPHOS and mitochondrial MOM permeability for AMP have remained unclear. Here we have determined mitochondrial AMP affinity in isolated rat liver mitochondria and permeabilized rat heart muscle fibers (Figs. 5a and b) using the PK-PK protocol. Isolated liver mitochondria had high affinity for AMP with a Michaelis-Menten constant ( $K_m$ ) for AMP of  $23.5 \pm 6.9 \mu\text{M}$  (Fig. 6a). This value is close to isolated AK2 enzymes ( $\leq 10 \mu\text{M}$ ) (Dzeja and Terzic 2009). The same result was obtained in isolated heart mitochondria ( $\sim 20 \mu\text{M}$ ) (Doliba et al. 2015). However, in permeabilized adult rat heart muscle fibers and tumor cells,  $K_m$  (AMP) values were significantly higher and seem to depend on their proliferation and differentiation status. Non-proliferating, highly-differentiated adult rat heart muscle have the highest  $K_m$  value ( $369 \pm 88 \mu\text{M}$ ) (Fig. 6b) for exogenously-added AMP, whereas the  $K_m$  values found for rapidly-proliferating HL-1 cardiac sarcoma and NB cells were at least 4- times lower (Fig. 6b, c). It was also found that N2a cell differentiation induced by RA is

associated with suppression of their proliferative activity (Klepinin et al. 2014) and accompanied by a 2-fold increase in the  $K_m$ (AMP) value (Fig. 6c).

In resting muscle, cellular AMP concentration is  $\sim 10 \mu\text{M}$ , while during muscle contraction AMP concentration increases up to  $100 \mu\text{M}$  (Plaideau et al. 2014). Since our data for heart muscle and dN2a cells suggest an apparent  $K_m$ (AMP) that is several times higher than the physiological AMP concentration, we became interested in reactions that could compete for the AMP substrate, such as AMPD. Total AMPD activity was about 2.5-fold higher in HL-1 and uN2a cells as compared to CM, and decreased during N2a cell differentiation with RA about 2.4-fold (Table 3).

## Discussion

In the present work, a simple new method is used for quantitative estimation of cellular compartmentation of AK activity in permeabilized mammalian cells or tissues. It distinguishes between mitochondrial AK2-dependent activity strongly coupled to mitochondrial respiration, and less coupled AK activity mainly dependent on cytosolic AK1 activity. It is based on ATP/AMP-stimulated AK-catalyzed reactions delivering ADP to OXPHOS, cytosolic ADP trapping by the PEP/PK system and measurements of  $O_2$  consumption rates. The main advantage of this method is its capacity to estimate the relative ratio of AK1 and AK2 activities in one sample without extraction of cellular protein(s). However, the method is limited by poor mitochondrial respiration of an examined biomaterial, i.e. by a RCI below 2.

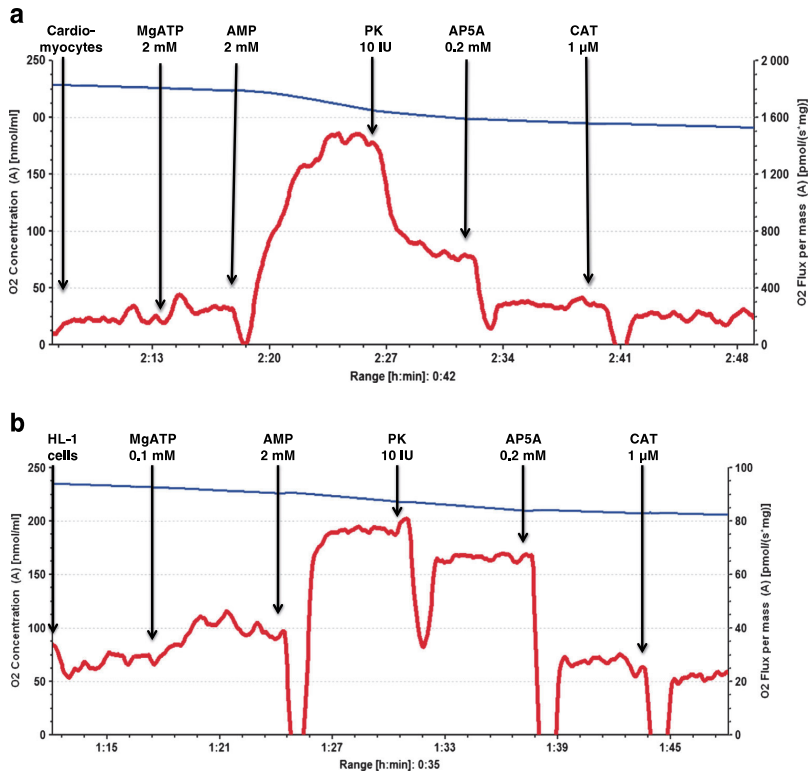


**Fig. 2** Illustration of analytical protocols (original recording of rates of O<sub>2</sub> uptake, in red) applied to permeabilized rat cardiomyocytes (a) and HL-1 tumor cells (b) which permit to estimate, quantitatively, the presence of AK-1 and -2 isoforms in studied cell or tissue material. This can be accomplished through analysis of these isoenzymes functional coupling with the OXPHOS system. The addition of AMP (final concentration, 2 mM) to the model cells (in the presence of ATP (0.1 mM) and PEP at a final concentration of 5 mM) which increased mitochondrial respiration due to activation both AK1 and AK2.

Subsequent addition of pyruvate kinase (PK) decreases O<sub>2</sub> consumption since the added PK removes efficiently extramitochondrially-generated ADP from AK1 and MgATPases. Remain respiration is associated with AK2 coupling with OXPHOS. The functional coupling between AK2 and mitochondrial respiration was confirmed by diadenosine pentaphosphate (AP5A, a selective inhibitor of AK) which decreased respiration back to basal respiration. Finally, carboxyatractylsilde (CAT) was added in order to control mitochondrial inner membrane intactness

In human HBC which has low mitochondrial respiration ( $RCI < 2$ ) only total AK mediated respiration can be measured by the respirometry method. In such cases, as we have shown earlier (Kaldma et al. 2014), the functional coupling between AK and OXPHOS can be estimated by the adenylate kinase index ( $I_{AKtotal}$ ) without PK-PEP system. The  $I_{AKtotal}$  value for HBC ( $I_{AKtotal} = 0.37 \pm 0.06$ ) was 1.35 times lower than in human colorectal cancer ( $I_{AKtotal} = 0.50 \pm 0.06$ ) but close to normal large intestine tissue ( $I_{AKtotal} = 0.31 \pm 0.03$ ) (Kaldma et al. 2014). These respirometry data correlate well with total AK activity in HBC (Table 2), large intestine and colorectal tissue (Kaldma et al. 2014). This result indicates that the respirometry methods can be used to detect changes in AK activity in clinical postoperative tissues.

Although, the AK phosphotransfer network has been well studied in heart muscle (Dzeja and Terzic 2009), the expression of AK isoforms and their putative role in carcinogenesis is much less clear. In this work, we have demonstrated that the oxygraphic assay can be successfully applied for estimating the alterations in AK1 and AK2 activities in cardiac muscle cells, differentiating N2a cells and cancer cells in vitro and in situ (on biopsy material). Furthermore, in presence of the PK-PEP system, the method can determine permeability of MOM for exogenous AMP.

AK1 is predominantly expressed in cells and organs with a high energy consumption (such as CM(s) and mature neural cells) (Tanabe et al. 1993), while AK2 expression is rather pronounced in rapidly proliferating



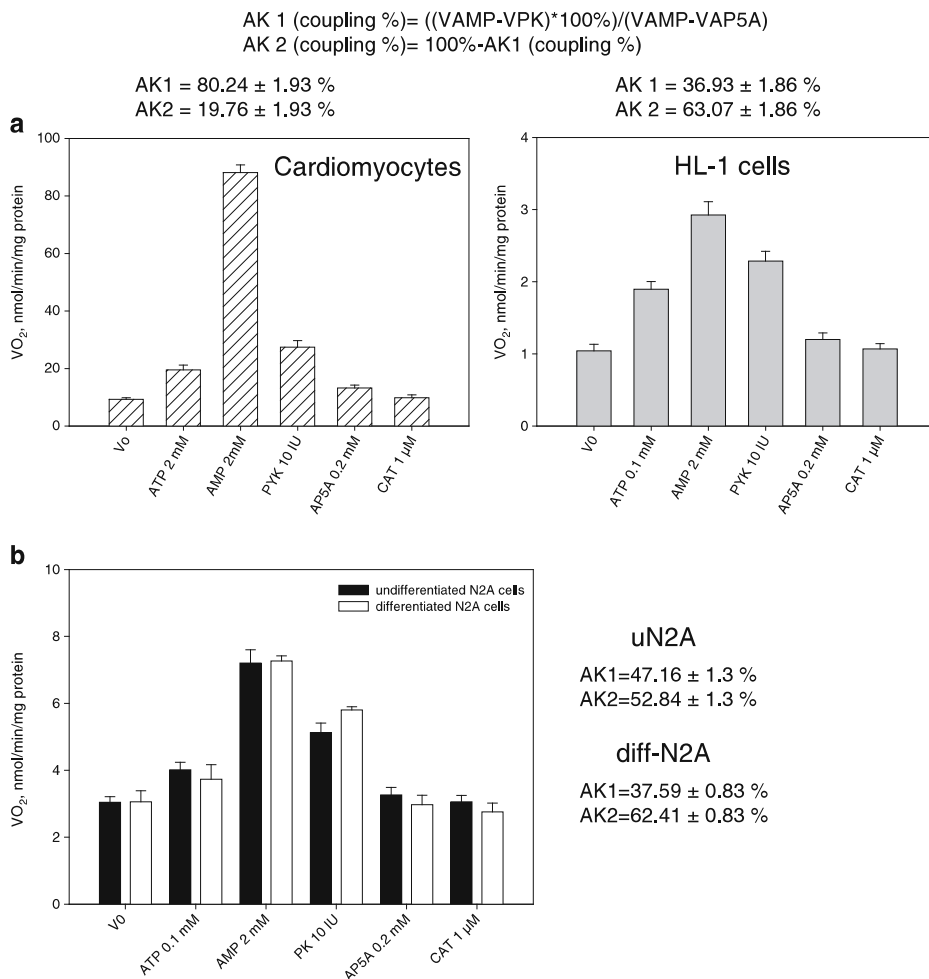


**Fig. 3** Application of a pyruvate kinase (PK)–phosphoenolpyruvate (PEP) protocol for determination of the presence of cytosolic (AK1) and mitochondrial (AK2) isoforms in one sample: **(a)** rat cardiomyocytes and HL-1 cardiac sarcoma cells; **(b)** undifferentiated and retinoic acid differentiated N2a cells (uN2a and dN2a,

respectively). The presence of AK1 and AK2 in studied material can be quantified as the adenylate kinase index ( $I_{AK}$ ) that reflects the strength of AK coupling with the OXPHOS system; the value of  $I_{AK}$  for AK1 and AK2 can be calculated as indicated in the corresponding section of “Materials and methods”. On these charts, bars are SEM,  $n = 5$

cells (Abdul Khalek et al. 2010; Bjorkholm et al. 2003). Consistent with these data, we found high values of AK1 activity and minor levels of AK2 in fully-differentiated rat CM(s), but more important AK2 activity in HL-1 tumor cells from adult rat ventricular myocardium and poorly-differentiated rapidly proliferating neuroblastoma cells (N2a line). Mature neurons in contrast to N2a cells mature neurons, the prevailing isoenzyme is cytosolic AK1 (Noma 2005).

It is important to emphasize that in several tumors, including NB(s) and HL-1 cells, the up-regulation of AK2 is associated with a loss of mitochondrial creatine kinase (Eimre

et al. 2008; Kaambre et al. 2012; Kaldma et al. 2014; Klepinin et al. 2014; Patra et al. 2012). The current study shows that during breast cancer carcinogens the AK1/AK2 ratio did not change, while the AK1 and AK2 activities were higher than in normal tissue, with AK1 remaining the predominant isoform. Previously, it was shown that in breast cancer the up-regulation of AK2 was associated with an increase in cancer stem cells (CSC) (Lamb et al. 2015), NB also contains numerous CSC (Ross and Spengler 2007).

Although, AK1 associates with the mitotic spindle apparatus, probably to supply energy for cell proliferation (Dzeja et al. 2011), but AK1 knockout in NB cells did not affect

**Table 2** The activity of adenylate kinase (AK) in human breast cancer tissue, adult rat cardiomyocytes (CMs), and some tumor cells of different histological type along with corresponding adenylate kinase indexes ( $I_{AK}$ )

Cells and tissues	Total activity, mU/mg protein*	AK1, mU/mg protein	AK2, mU/mg protein	$I_{AK1}$ , %	$I_{AK2}$ , %
Rat CM(s)	2493 ± 113; <i>n</i> = 5	2394 ± 102 (96%**)	99 ± 18 (4%**)	80	20
HL-1 cells	311 ± 10; <i>n</i> = 5	174 ± 9 (56%)	137 ± 2 (44%)	37	63
uN2a cells	245 ± 12; <i>n</i> = 5	136 ± 9 (56%)	109 ± 8 (44%)	53	47
dN2a cells	172 ± 15; <i>n</i> = 5	81 ± 10 (47%)	91 ± 8 (53%)	39	61
Breast cancer	290 ± 89; <i>n</i> = 6	208 ± 64 (69%)	82 ± 15 (31%)	-	-
Non-tumor tissue	53 ± 5; <i>n</i> = 6	42 ± 4 (80%)	11 ± 2 (20%)	-	-

\*all data presented in the Table 2 are mean values ± SEM from at least 5 independent experiments; \*\* % from the total AK activity; uN2a and dN2a are undifferentiated and retinoic acid differentiated Neuro-2A cells, respectively

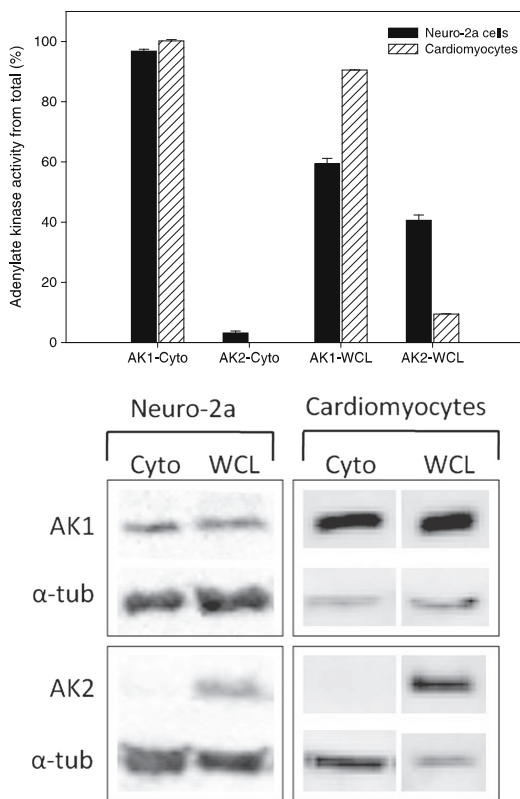


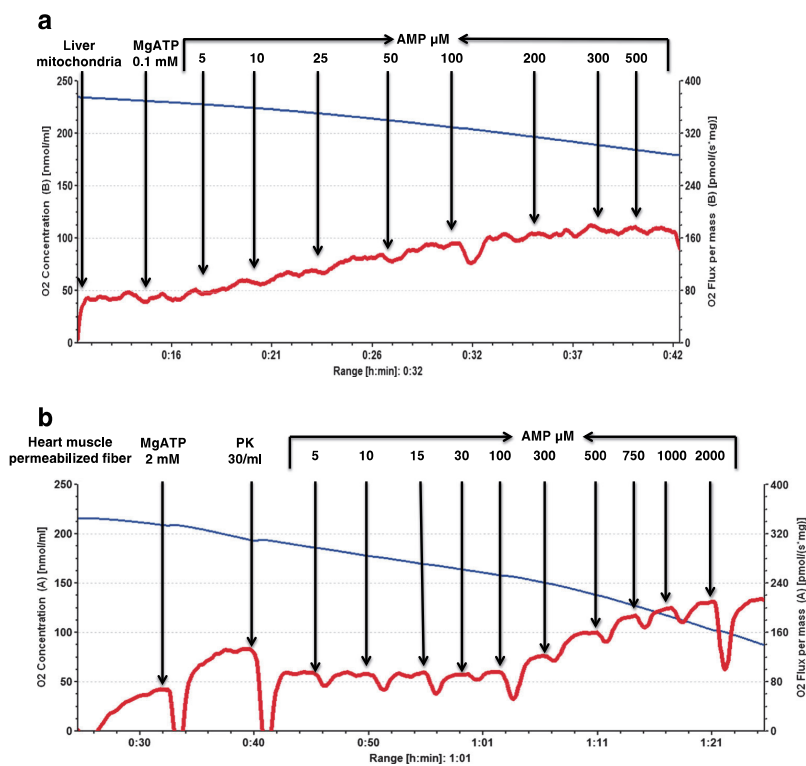
**Fig. 4** Intracellular localization of adenylate kinase 1 (AK1) and adenylate kinase 2 (AK2) in Neuro-2a cell line and cardiomyocytes. The 10,000 × g supernatants of cytosolic fraction (Cyto) from digitonin permeabilized Neuro-2a and cardiomyocytes were prepared for adenylate kinase (AK) spectrophotometric assay (upper panel) and Western blot analysis (lower panel). Whole cell lysates (WCL) of Neuro-2a and cardiomyocytes were used as a control. Enzymes samples for AK1 and AK2 activity assay were incubated in the presence or absence of specific AK1 inhibitor N-ethylmaleimide for 1 h at 25°C. For Western blot analysis, α-tubulin was used as a loading control, bars are SEM, *n* = 3

cancer cells growth (de Bruin et al. 2004). Proteomics studies have also revealed the up-regulation of AK2 in human prostate and pancreatic cancer cells (Lam et al. 2010; Liu et al. 2010). It was shown that AK2 can promote cell proliferation under normal circumstances (Dzeja and Terzic 2009; Lagresle-Peyrou et al. 2009) and full AK2 deletion (AK2<sup>-/-</sup>) in mice is embryonically lethal (Zhang et al. 2010). Although, this would suggest AK2 as a target for antitumor therapy, literature data on its association with tumor progression remain contradictory. Kim and colleagues have postulated that AK2 is rather a negative regulator of tumor growth (Kim et al. 2014). They showed that AK2 can interact with dual-specificity phosphatase 26 in the nucleus and this protein complex can dephosphorylate fas-associated protein with death domain leading to suppressed cell growth.

Adenine nucleotides and some respiratory substrates are transported into mitochondria via VDAC (Maldonado et al. 2013) which is also the binding partner for HK-1/2 (Pastorino and Hoek 2008). Hence, in tumor cells, the observed increased level of VDAC(s) (Simamura et al. 2008) can enhance the binding of HK-2 to mitochondria and, according to the model proposed by Majewski and coauthors (Majewski et al. 2004), this interaction would support VDAC in the open state. It was reported (Simamura et al. 2008) that tumor cells contain an increased amount of VDAC(s) per mitochondrion, and this circumstance could be responsible for the higher permeability of tumor mitochondria for ADP and AMP.

Further, it is well-known that the lipid composition of tumor mitochondria differs substantially from that in normal cells (Baggetto et al. 1992; Kiebish et al. 2008; Park and Wenner 1970). This could also affect adenine nucleotide permeability of MOM in malignant cells. Finally, the difference in the  $K_m$ (AMP) values between poorly-differentiated tumor cells and highly-differentiated cells could be due to varying AMPD activity. This enzyme catalyzes the deamination of AMP to inosine monophosphate and plays an important role

**Fig. 5** Measurements of the apparent  $K_m$  (AMP) value (a) for rat liver mitochondria and (b) for rat heart fiber; representative oxygraphic tracings. The right scale show the rate of oxygen uptake expressed in  $\text{pmol O}_2 \text{ sec}^{-1}$  per mg protein. Samples were incubated in respiratory buffer (with 2 mM malate and 5 mM glutamate as respiratory substrates) in the presence of a PK-PEP system and 0.1 mM ATP (for rat heart fiber 2 mM ATP), the rates of  $\text{O}_2$  consumption were recorded after a step-wise addition of AMP



in the purine nucleotide cycle (Morisaki et al. 1992). The highest expression of AMPD was found in muscle where main isoform was AMPD1. Other tissues have much lower activity of AMPD. AMPD2 is predominant in nonmuscle tissues, and AMPD3 is found in erythrocytes (Plaideau et al. 2012). In 2014 Catheline Plaideau showed pharmacological inhibition of AMPD or AMPD 1 deletion in muscle increased nucleotide level especially AMP (Plaideau et al. 2014). Our work suggested that in HL-1 cells AMPD activity (Table 3) was 6 times higher than previously reported for mouse heart muscle (Rybakowska et al. 2014). Similarly, in NB cells had 2.4 times higher AMPD activity that RA-treated N2a cells (Table 3). At the same time, we did not find correlation between AMPD activity and increased  $K_m$  values for AMP in heart muscle and RA-differentiated N2a cells (Tables 1, 3). There is presumably another AMP removal pathway which can regulate cellular AMP concentration. Altogether, further work is needed to understand the role of increased MOM permeability for ADP and AMP as well as AMP remove pathway different enzymes in the regulation of adenine nucleotides level in malignant cells.

In summary, we developed here a simple oxygraphic method for semi-quantifying the ratio between mostly AK1- and AK2-related activities in mammalian tissues and cultured cells. This method is rapid and enables to estimate the activities related to these two AK isoforms in one sample. We tested this method on two tumor cell lines, isolated cardiac muscle cells, and human breast cancer postoperative material. The method is sensitive enough to be performed on tumor biopsies. The data show that AK2 is expressed predominantly in poorly differentiated cells with high proliferative index, and that strong differences exist between highly-differentiated and tumor cells in the affinity of their mitochondrial respiration for exogenous AMP. Further studies will be required to identify the underlying molecular mechanisms and to evaluate their value for cancer diagnosis and therapy.

## Materials and methods

### Chemicals

Unless otherwise stated, all materials and reagents were purchased from Sigma-Aldrich Company (St. Louis USA).

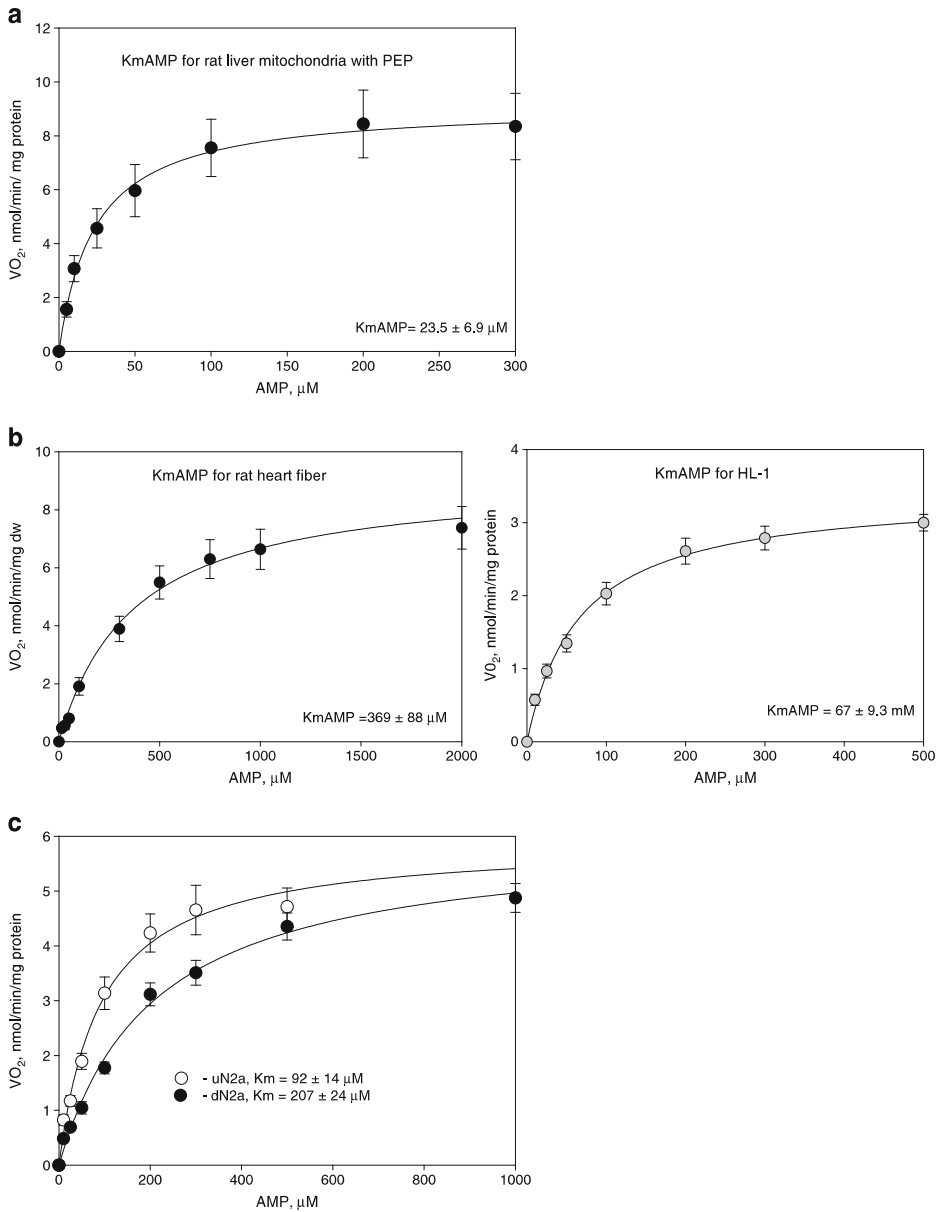


**Fig. 6** Kinetic analysis of regulation of the AMP-activated respiration in isolated rat liver mitochondria (a), for skinned rat heart myocytes (b) and HL-1 cardiac tumor cells (c) as well as for undifferentiated or retinoic acid differentiated murine neuroblastoma cells; uN2a and dN2a, respectively

(d). The corresponding apparent Michaelis-Menten constant ( $\text{Km}$ ) values towards exogenously-added AMP were determined. These measurements were performed in the presence of a PEP-PK ADP-trapping system, bars are SEM,  $n = 5$

Dulbecco's Modified Eagle Medium (DMEM) and phosphate buffered saline (PBS, Ca/Mg free) were obtained from Corning (USA) whereas heat-inactivated fetal bovine serum

(FBS), accutase, penicillin-streptomycin solution (100 $\times$ ), gentamicin and 0.05% Trypsin-EDTA were purchased from Gibco Life Technologies (Grand Island, NY).

**Table 3** The activity of AMP deaminase (AMPD) in differentiated neuron and adult rat cardiomyocytes (CM) cells and appropriate cancer cells

Enzyme activities, mU(s)/mg protein	HL-1 cells mean ± SEM, <i>n</i> = 3	Rat CM(s) mean ± SEM, <i>n</i> = 3	uN2a cells mean ± SEM, <i>n</i> = 3	dN2a cells mean ± SEM, <i>n</i> = 3
AMPD	40.1 ± 2.6 *	16.4 ± 0.4	36.0 ± 1.7 **	15.1 ± 1.3

\**P* < 0.001 vs Rat CM(s), \*\**P* < 0.001 vs dN2a cells; uN2a and dN2a are undifferentiated and retinoic acid differentiated Neuro-2A cells, respectively

### Clinical material and patients

All women (with ages ranging from 50 to 71 years, *n* = 10) had local or locally advanced disease (T1-4 N0-2 M0, st. IA-IIIb). Invasive ductal carcinoma accounted for 87% and lobular carcinoma for 13% of these tumors. These patients had not received prior radiation or chemotherapy. Postoperational samples of human HBC and normal tissue (0.1–0.5 g) were acquired by the Oncology and Hematologic Clinic at the North Estonia Medical Centre (NEMC, Tallinn). They were obtained under general anesthesia and then within 1 h after surgery were delivered to the Laboratory of Bioenergetics for corresponding studies. During transportation, clinical material was stored on ice in solution consisting of 0.5 mM EGTA, 3 mM MgCl<sub>2</sub>, 60 mM K-lactobionate, 3 mM KH<sub>2</sub>PO<sub>4</sub>, 20 mM taurine, 20 mM HEPES (pH 7.1), 110 mM sucrose, 0.5 mM dithiothreitol (DTT) and 5 mg/ml fatty acid free bovine serum albumin (BSA).

### Cell cultures

Our in vitro studies were carried out on several different cell types, such as mouse neuroblastoma Neuro-2A (N2a) cells, both undifferentiated and subjected to retinoic acid-induced differentiation, HL-1 cardiac sarcoma cells as well as on isolated rat heart CM(s).

Stock culture of N2a cells was obtained from American Type Culture Collection, Cat. No CCL-131. These NB cells were grown as a loosely adhering monolayer in T75 plates (Greiner bio-one) in high glucose DMEM with L-glutamine supplemented with 10% heat inactivated fetal bovine serum (FBS) and antibiotics: penicillin (100 U/ml), streptomycin (100 µg/ml) and 50 µg/ml gentamicin (complete growth medium). N2a cells were grown and maintained at 37°C in a humidified incubator containing 5% CO<sub>2</sub> in air. The cells were sub-cultured at 3 day intervals and had received no more than 20 cell culture passages. Neural differentiation of N2a cells to cholinergic neurons was induced by their treatment with 10 µM all-trans-retinoic acid (RA) in complete growth medium, for details see in (Blanco et al. 2001; Klepinin et al. 2014).

The HL-1 cardiac sarcoma cell line was originally established by William Claycomb (Claycomb et al. 1998) and was kindly provided to us by Dr. Andrey V. Kuznetsov (Innsbruck Medical University, Austria). These tumor cells

were grown in fibronectin–gelatin (5 µg/ml/0.2%) coated T75 flasks containing Claycomb medium (Sigma-Aldrich), supplemented with 10% FBS, 100 U/ml penicillin, 100 µg/ml streptomycin, 50 µg/ml gentamicin, 2 mM L-glutamine, 0.1 mM norepinephrine, and 0.3 mM ascorbic acid. HL-1 cells were cultured at 37°C in humid air with 5% CO<sub>2</sub>.

### Isolation of rat cardiomyocytes and liver mitochondria

Adult (3-month-old) male Wistar rats weighing about 350 g were used in experiments. These animals were kept on a standard laboratory diet and given tap water ad libitum. The organs (heart or liver) were removed for sacrificed animals under deep anesthesia; 50 mg/kg of Bioketan® plus 0.6 mg/kg of Dexamitor®, intraperitoneally.

CMs were obtained after perfusion of the isolated rat heart with collagenase-A (Roche) as described in our previous studies (Saks et al. 1991; Tepp et al. 2010). Isolated CMs contained approximately 90% of rod-like cells when observed under the light microscope. In order to examine the functional coupling of AK-catalyzed processes with OXPHOS in CM(s), the cells sarcolemma was permeabilized by saponin treatment. The permeabilization procedure was carried out directly in oxygraph chambers with 25 µg/ml saponin during 10 min before starting the measurements of respiration rates at 25°C with continuous magnetic stirring; it is important to note that the applied parameters of saponin treatment of CM(s) keep the intactness of their mitochondrial membranes (Guzun et al. 2009).

Rat liver mitochondria were isolated by mild protease digestion (trypsin, at a final concentration of 1 mg/ml for 10 min on melting ice) of the tissue homogenate, exactly as described previously (Saks et al. 1975; Timohhina et al. 2009). After differential centrifugation, the final mitochondrial pellet was suspended in isolation medium containing 1 mg/ml BSA to a mitochondrial protein concentration of 10–15 mg/ml, and this suspension was stored on melting ice until use.

### Preparation of skinned tumor and rat heart fibers, cell permeabilization, and high-resolution respirometry

Skinned fibers from human HBC postoperative samples and adult rat heart tissue were prepared according to the method described earlier (Kaambre et al. 2012; Kuznetsov et al. 2008).

In order to study the ADP- or AMP-mediated mitochondrial respiration in tumor tissues, the plasma membranes in HBC fibers was completely permeabilized by saponin treatment (50  $\mu\text{g/ml}$ ; for 30 min at 4°C upon mild stirring) exactly as described in our prior work (Kaambre et al. 2012). This permeabilization procedure had no effect on the intactness of mitochondrial membranes in the obtained HBC tissue fibers (Kaambre et al. 2012). Prior to respiratory experiments, N2a cells were permeabilized by saponin (40  $\mu\text{g/ml}$ ) treatment for 5 min at 25°C directly in oxygraphic chambers, whereas the plasma membrane in HL-1 tumor cells was permeabilized in similar manner but in the presence of digitonin (25  $\mu\text{g/ml}$ ). All protocols used for cell permeabilization provided the maximal respiratory response for exogenously-added ADP, whereas the integrity of the mitochondrial membranes was preserved. Measurements of cellular  $\text{O}_2$  consumption rates in the presence of exogenous ADP (2 mM) served as an indicator for mitochondrial respiratory chain function.

Rates of  $\text{O}_2$  consumption by the permeabilized, N2a, HL-1 tumor cells (at a density of  $\sim 0.5\text{--}1.0 \times 10^6$  cells/ml), CMs, HBC samples or liver mitochondria were measured under magnetic stirring (300 rpm) at 25°C in 2-ml glass chambers of a two-channel titration-injection respirometer (Oxygraph-2 K, OROBOROS Instruments, Austria) in medium-B supplemented with 5 mM glutamate, 2 mM malate and 10 mM succinate as respiratory substrates; solubility of oxygen was taken as 240 nmol/ml (Gnaiger 2001). All respiration rates of tissue samples and cells were normalized per mg dry weight or mg protein respectively.

### Oxygraphic analysis for the presence AK1 and mitochondrially-bound AK-2 in normal and tumor cells

Total adenylate kinase coupling with OXPHOS was measured by respirometry in permeabilized human HBC fibers according to our previous study (Kaldma et al. 2014). The total AK coupling with OXPHOS is expressed by adenylate kinase index ( $I_{AK \text{ total}}$ ):  $[I_{AK \text{ total}} = (V_{AMP} - V_{AP5A}) / V_{AP5A}]$  where  $V_{AMP}$  is mitochondrial respiration rate in the presence of 2 mM AMP and  $V_{AP5A}$  remain respiration rate after inhibition total AK by 0.2 mM diadenosine pentaphosphate (AP5A). AK coupling with OXPHOS is measured in the presence of 0.1 mM ATP.

The presence of cytosolic (AK1) and mitochondrial AK2 (which catalyze the phosphotransfer reaction of “AMP + ATP  $\leftrightarrow$  2ADP”) in permeabilized tumor and normal cells was assayed quantitatively by respirometry through their coupling with OXPHOS due to the formation of ADP in these enzymes catalyzed reactions. These measurements were performed in medium-B in the presence or absence of phosphoenolpyruvate (PEP, 5 mM) – pyruvate kinase (PK, 10 U/ml) ADP trapping system (Tepp et al. 2011; Timohhina et al. 2009).

The mitochondrial respiration assay is performed in medium-B. Respiration was activated by addition of 0.1 mM ATP or 2 mM ATP to initiate the endogenous ADP production by ATPases. Then AMP (up to a final concentration of 2 mM) was added to activate the coupled reaction of AK (AK1 and AK2) system with adenine nucleotide translocator (ANT). Next addition of PK removes ADP from cytosolic which is produced by AK1. Residual respiration which is associated with specific coupling of AK2 with OXPHOS is inhibited by 0.2 mM AP5A. Finally, CAT 1  $\mu\text{M}$  is added to control mitochondrial inner membrane intactness.

The AK1 functional coupling with OXPHOS system, linked with this isoenzyme activity, was characterized by the corresponding AK index ( $I_{AK1}$ ). The  $I_{AK1}$  was calculated according to the equation:  $[I_{AK1} = ((V_{AMP} - V_{PK}) / (V_{AMP} - V_{AP5A}) \times 100\%]$ , where  $V_{AMP}$ ,  $V_{PK}$  and  $V_{AP5A}$  are rates of  $\text{O}_2$  consumption that were measured after subsequent addition of 2 mM AMP, 10 U/ml PK and 0.2 mM AP5A, respectively.

The AK2 functional coupling with OXPHOS was calculated as  $I_{AK2} = 100\% - I_{AK1}$ . The use of PEP–PK ADP-trapping system allows us to distinguish the rate of cellular  $\text{O}_2$  consumption associated with the presence of AK2 from cytosolic AK1 mediated respiration. Thus, in our assay system the inhibitory effect of PK on the AMP-mediated  $\text{O}_2$  consumption correlate with intracellular AK1/AK2 ratio. In cells where mitochondrial AK2 is the predominant AK isoenzyme, the effect of PK addition on AMP-activated respiration will be negligible.

### Determination of apparent Michaelis-Menten constant values for exogenously-added AMP as well as rates of maximal ADP- or AMP-activated respiration for normal and malignant cells

The maximal respiration with ADP (final concentration, 2 mM) was measured in the presence of respiratory substrate (5 mM glutamate, 2 mM malate and 10 mM succinate). The maximal AMP-activated respiration rates were assayed in the same medium after preliminary addition of 0.1 mM ATP (or 2 mM ATP for CMs) in the presence of 2 mM AMP.

To determine the Michaelis-Menten constants ( $K_m$ ) for AMP the respiration rate of permeabilized fiber is measured in medium-B in the presence of PK–PEP ADP trapping system with exogenously-added ATP at a final concentration of 2 mM (0.1 mM ATP for isolated mitochondria). Due to the presence of PK-PEP (trapped ADP produced from AK1) addition of ATP with AMP activates only AK2. Using AK2 coupling with OXPHOS is able to determinate mitochondrial affinity for AMP via stepwise increased AMP concentration. Corresponding  $K_m$  (AMP) values were calculated by fitting experimental data to a non-linear regression.

## Immunoblot analysis

Fresh cells were washed with PBS and pelleted by centrifugation at 150 x g for 7 min. Cytosolic fractions were isolated by selective lysis of the plasma membrane with 35 µg of digitonin per  $4 \times 10^6$  N2a cells (Single et al. 1998) or with 25 µg/ml of digitonin for rat cardiomyocytes (Dedkova and Blatter 2012) followed by centrifugation at 1000 x g for 10 min. Supernatants containing cytosolic fraction of proteins were centrifuged at 10,000 g for 15 min to pellet any remaining cellular debris.

Whole cell extracts were isolated using Tris-Triton X lysis buffer (10 mM Tris pH 7.4, 100 mM NaCl, 1 mM EDTA, 1% Triton X-100, 10% glycerol, 0.1% SDS) supplemented with protease inhibitors (Cytoskeleton). Lysates were homogenized by Retsch Mixer Mill at 25 Hz for 2 min, incubated for 20 min on ice, and clarified by centrifugation at 21,000 x g for 30 min at 4°C. The concentration of the isolated proteins was determined using BCA Protein Assay Reagent (Pierce, Rockford, IL). Protein samples (20 µg per fraction) were separated by a 12% Tris-Glycine SDS-PAGE and electrophoretically transferred onto PVDF membrane (Millipore) by Trans-Blot Semi-Dry Transfer system (Bio-Rad). Membranes were then incubated with the primary antibodies against AK1 (sc365316), AK2 (sc374095) or  $\alpha$ -tubulin (ab7291) and the appropriate secondary antibodies.

## Enzymatic activities

AMPD activity was measured spectrophotometrically in whole cell or tissue extract by an enzyme-coupled spectrophotometric assay in the direction of IMP formation in the presence of 50 mM Hepes (pH 7.1), 100 mM KCl, 1 mM EDTA, 1 mM DTT, 5 mM  $\alpha$ -ketoglutarate, 0.15 mM NADH, and 5 U of glutamate dehydrogenase containing 0.25 mg of extract protein and reaction was initiated by 10 mM AMP and following the decrease in absorbance at 340 nm at 25°C (Ashby and Frieden 1978) One unit of AMPD activity was defined as 1 µmole of AMP deaminated to IMP.

AK1 and AK2 activities were measured in whole cell or tissue extracts at 25°C by an enzyme-coupled spectrophotometric assay in the direction of ATP formation, essentially as described earlier by Dzeja et al. and Tanabe et al. (Dzeja et al. 1999; Tanabe et al. 1993). The reaction mixture contained 20 mM Hepes (pH 7.5), 0.1 M KCl, 4 mM Mg-acetate, 1 mM EDTA, 20 mM glucose, 2 mM NADP<sup>+</sup>, 4.5 units/ml hexokinase, and 2 units/ml glucose-6-phosphate dehydrogenase as the coupled enzymes. The reaction was initiated with 2 mM ADP, and the increase in absorbance at 340 nm was recorded using a Cary 100 Bio UV-visible spectrophotometer. One unit of AK activity was defined as 1 µmole of ATP produced per minute at 25°C. The extinction coefficient of

NADPH ( $6.22 \times 10^3 \text{ M}^{-1} \text{ cm}^{-1}$ ) was used to convert its absorbance to molar concentration of the product formed.

AK1 is a thiol-containing enzyme that is inhibited by N-ethylmaleimide (NEM), while AK2 is not (Khoo and Russell 1972). For the NEM treatment, enzyme samples (in 20 mM MOPS-buffered solution with 0.2 M NaCl, pH 8.0) were incubated in the presence of 1 mM NEM for 1 h at 25°C before assay. AK2 activity was determined as the activity remaining after the NEM treatment of cell/tissue extracts. AK1 activity was measured as total AK activity minus activity remaining after the NEM treatment. For the NEM treatment, enzyme samples (in 20 mM MOPS-buffered solution with 0.2 M NaCl, pH 8.0) were incubated in the presence of 1 mM NEM for 1 h at 25°C before assay. Protein concentration of the used cell/tissue homogenates was determined by a Pierce BCA Protein Assay Kit according to the manufacturer recommendations using BSA as a standard.

## Statistical analysis of data

All data points are presented as means  $\pm$  standard error (SEM) from at least five parallel experiments. Significance was calculated by Student's t-test; differences between two data groups were considered to be statistically significant when  $P < 0.05$ .

**Acknowledgements** This work was supported by institutional research funding IUT23-1 of the Estonian Ministry of Education and Research and the Estonian Science Foundation grant No.8987.

**Compliance with ethical standards** Aleksandr Klepinin, Lyudmila Ounpuu, Rita Guzun, Vladimir Chekulayev, Natalja Timohhina, Kersti Tepp, Igor Shevchuk, Uwe Schlattner, and Tuuli Kaambre declare that they have no conflict of interest.

All institutional and national guidelines for the care and use of laboratory animals were followed.

All procedures followed were in accordance with the ethical standards of the responsible committee on human experimentation (institutional and national) and with the Helsinki Declaration of 1975, as revised in 2000 (5). Informed consent was obtained from all patients for being included in the study.

## References

- Abdul Khalek FJ, Gallicano GI, Mishra L (2010) Colon Cancer stem cells. *Gastrointestinal cancer research*, GCR, pp. S16–S23
- Amiri M, Conserva F, Panayiotou C, Karlsson A, Solaroli N (2013) The human adenylate kinase 9 is a nucleoside mono- and diphosphate kinase. *Int J Biochem Cell Biol* 45:925–931
- Ashby B, Frieden C (1978) Adenylate deaminase. Kinetic and binding studies on the rabbit muscle enzyme *J Biol Chem* 253:8728–8735
- Baggetto LG, Clottes E, Vial C (1992) Low mitochondrial proton leak due to high membrane cholesterol content and cytosolic creatine kinase as two features of the deviant bioenergetics of Ehrlich and AS30-D tumor cells. *Cancer Res* 52:4935–4941

- Balinsky D, Greengard O, Cayanis E, Head JF (1984) Enzyme activities and isozyme patterns in human lung tumors. *Cancer Res* 44:1058–1062
- Bjorkholm B, Falk P, Engstrand L, Nyren O (2003) *Helicobacter pylori*: resurrection of the cancer link. *J Intern Med* 253:102–119
- Blanco V, Lopez Camelo J, Carri NG (2001) Growth inhibition, morphological differentiation and stimulation of survival in neuronal cell type (neuro-2a) treated with trophic molecules. *Cell Biol Int* 25:909–917
- Burkart A, Shi X, Chouinard M, Corvera S (2011) Adenylate kinase 2 links mitochondrial energy metabolism to the induction of the unfolded protein response. *J Biol Chem* 286:4081–4089
- Carrasco AJ, Dzeja PP, Alekseev AE, Pucar D, Zingman LV, Abraham MR, Hodgson D, Bienengraeber M, Puceat M, Janssen E et al (2001) Adenylate kinase phosphotransfer communicates cellular energetic signals to ATP-sensitive potassium channels. *Proc Natl Acad Sci U S A* 98:7623–7628
- Chekulayev V, Mado K, Shevchuk I, Koit A, Kaldma A, Klepinin A, Timohhina N, Tepp K, Kandashvili M, Ounpuu L et al (2015) Metabolic remodeling in human colorectal cancer and surrounding tissues: alterations in regulation of mitochondrial respiration and metabolic fluxes. *Biochemistry and Biophysics Reports* 4:111–125
- Claycomb WC, Lanson NA Jr, Stallworth BS, Egeland DB, Delcarpio JB, Bahinski A, Izzo NJ Jr (1998) HL-1 cells: a cardiac muscle cell line that contracts and retains phenotypic characteristics of the adult cardiomyocyte. *Proc Natl Acad Sci U S A* 95:2979–2984
- Criss WE, Litwack G, Morris HP, Weinhouse S (1970) Adenosine triphosphate: adenosine monophosphate phosphotransferase isozymes in rat liver and hepatomas. *Cancer Res* 30:370–375
- Daniel JM, McCombie G, Wendt S, Zenobi R (2003) Mass spectrometric determination of association constants of adenylate kinase with two noncovalent inhibitors. *J Am Soc Mass Spectrom* 14:442–448
- Dasgupta B, Chhipa RR (2016) Evolving lessons on the complex role of AMPK in normal physiology and cancer. *Trends Pharmacol Sci* 37:192–206
- de Bruin W, Oerlemans F, Wieringa B (2004) Adenylate kinase I does not affect cellular growth characteristics under normal and metabolic stress conditions. *Exp Cell Res* 297:97–107
- Dedkova EN, Blatter LA (2012) Measuring mitochondrial function in intact cardiac myocytes. *J Mol Cell Cardiol* 52:48–61
- Doliba NM, Babsky AM, Doliba NM, Wehrli SL, Osbakken MD (2015) AMP promotes oxygen consumption and ATP synthesis in heart mitochondria through the adenylate kinase reaction: an NMR spectroscopy and polarography study. *Cell Biochem Funct* 33:67–72
- Dyck JR, Lopuschuk GD (2006) AMPK alterations in cardiac physiology and pathology: enemy or ally? *J Physiol* 574:95–112
- Dzeja PP, Terzic A (2003) Phosphotransfer networks and cellular energetics. *J Exp Biol* 206:2039–2047
- Dzeja P, Terzic A (2009) Adenylate kinase and AMP signaling networks: metabolic monitoring, signal communication and body energy sensing. *Int J Mol Sci* 10:1729–1772
- Dzeja PP, Vitkevicius KT, Redfield MM, Burnett JC, Terzic A (1999) Adenylate kinase-catalyzed phosphotransfer in the myocardium: increased contribution in heart failure. *Circ Res* 84:1137–1143
- Dzeja, P.P., Chung, S., and Terzic, A. (2007). Integration of Adenylate Kinase and Glycolytic and Glycogenolytic Circuits in Cellular Energetics. In *Molecular system bioenergetics: energy for life*, S. Prof. Valdur, ed. (Weinheim, Germany, Wiley-VCH Verlag GmbH & Co. KGaA), pp. 265–301.
- Dzeja PP, Chung S, Faustino RS, Behfar A, Terzic A (2011) Developmental enhancement of adenylate kinase-AMPK metabolic signaling axis supports stem cell cardiac differentiation. *PLoS One* 6:e19300
- Eimre M, Paju K, Pelloux S, Beraud N, Roosimaa M, Kadaja L, Gruno M, Peet N, Orlova E, Rimmelkoor R et al (2008) Distinct organization of energy metabolism in HL-1 cardiac cell line and cardiomyocytes. *Biochim Biophys Acta* 1777:514–524
- Fukada K, Zhang F, Vien A, Cashman NR, Zhu H (2004) Mitochondrial proteomic analysis of a cell line model of familial amyotrophic lateral sclerosis. *Mol Cell Proteomics* 3:1211–1223
- Gellerich FN (1992) The role of adenylate kinase in dynamic compartmentation of adenine nucleotides in the mitochondrial intermembrane space. *FEBS Lett* 297:55–58
- Gnaiger E (2001) Oxygen solubility in experimental media. *OROBOROS Bioenerg News* 6:1–6
- Greengard O, Head JF, Goldberg SL (1980) Uridine kinase, adenylate kinase, and guanase in human lung tumors. *Cancer Res* 40:2295–2299
- Guzun R, Timohhina N, Tepp K, Monge C, Kaambre T, Sikk P, Kuznetsov AV, Pison C, Saks V (2009) Regulation of respiration controlled by mitochondrial creatine kinase in permeabilized cardiac cells in situ. Importance of system level properties. *Biochim Biophys Acta* 1787:1089–1105
- Guzun R, Gonzalez-Granillo M, Karu-Varikmaa M, Grichine A, Usson Y, Kaambre T, Guerrero-Roesch K, Kuznetsov A, Schlattner U, Saks V (2012) Regulation of respiration in muscle cells in vivo by VDAC through interaction with the cytoskeleton and MtCK within mitochondrial interactosome. *Biochim Biophys Acta* 1818:1545–1554
- Hall M, Mickey DD, Wenger AS, Silverman LM (1985) Adenylate kinase: an oncogene marker in an animal model for human prostatic cancer. *Clin Chem* 31:1689–1691
- Hampton A, Slotin LA, Kappler F, Sasaki T, Perini F (1976) Design of substrate-site-directed inhibitors of adenylate kinase and hexokinase. Effect of substrate substituents on affinity for the adenine nucleotide sites *Journal of medicinal chemistry* 19:1371–1377
- Hanahan D, Weinberg RA (2011) Hallmarks of cancer: the next generation. *Cell* 144:646–674
- Hardie DG, Alessi DR (2013) LKB1 and AMPK and the cancer-metabolism link - ten years after. *BMC Biol* 11:36
- Inouye S, Seo M, Yamada Y, Nakazawa A (1998) Increase of adenylate kinase isozyme I protein during neuronal differentiation in mouse embryonal carcinoma P19 cells and in rat brain primary cultured cells. *J Neurochem* 71:125–133
- Kaambre T, Chekulayev V, Shevchuk I, Karu-Varikmaa M, Timohhina N, Tepp K, Bogovskaja J, Kutner R, Valvere V, Saks V (2012) Metabolic control analysis of cellular respiration in situ in intraoperational samples of human breast cancer. *J Bioenerg Biomembr* 44:539–558
- Kaldma A, Klepinin A, Chekulayev V, Mado K, Shevchuk I, Timohhina N, Tepp K, Kandashvili M, Varikmaa M, Koit A et al (2014) An in situ study of bioenergetic properties of human colorectal cancer: the regulation of mitochondrial respiration and distribution of flux control among the components of ATP synthasome. *Int J Biochem Cell Biol* 55:171–186
- Khooc JC, Russell PJ (1972) Isoenzymes of adenylate kinase in human tissue. *Biochim Biophys Acta* 268:98–101
- Kiebish MA, Han X, Cheng H, Chuang JH, Seyfried TN (2008) Cardiolipin and electron transport chain abnormalities in mouse brain tumor mitochondria: lipidomic evidence supporting the Warburg theory of cancer. *J Lipid Res* 49:2545–2556
- Kim H, Lee HJ, Oh Y, Choi SG, Hong SH, Kim HJ, Lee SY, Choi JW, Su Hwang D, Kim KS et al (2014) The DUSP26 phosphatase activator adenylate kinase 2 regulates FADD phosphorylation and cell growth. *Nat Commun* 5:3351
- Klepinin A, Chekulayev V, Timohhina N, Shevchuk I, Tepp K, Kaldma A, Koit A, Saks V, Kaambre T (2014) Comparative analysis of some aspects of mitochondrial metabolism in differentiated and undifferentiated neuroblastoma cells. *J Bioenerg Biomembr* 46:17–31



- Kuznetsov AV, Veksler V, Gellerich FN, Saks V, Margreiter R, Kunz WS (2008) Analysis of mitochondrial function in situ in permeabilized muscle fibers, tissues and cells. *Nat Protoc* 3:965–976
- Lagresle-Peyrou C, Six EM, Picard C, Rieux-Laucat F, Michel V, Ditadi A, Demerens-de Chappedelaine C, Morillon E, Valensi F, Simon-Stoos KL et al (2009) Human adenylate kinase 2 deficiency causes a profound hematopoietic defect associated with sensorineural deafness. *Nat Genet* 41:106–111
- Lam YW, Yuan Y, Isaac J, Babu CV, Meller J, Ho SM (2010) Comprehensive identification and modified-site mapping of S-nitrosylated targets in prostate epithelial cells. *PLoS One* 5:e9075
- Lamb R, Bonuccelli G, Ozsvari B, Peiris-Pages M, Fiorillo M, Smith DL, Bevilacqua G, Mazzanti CM, McDonnell LA, Naccarato AG et al (2015) Mitochondrial mass, a new metabolic biomarker for stem-like cancer cells: understanding WNT/FGF-driven anabolic signaling. *Oncotarget* 6:30453–30471
- Lee HJ, Pyo JO, Oh Y, Kim HJ, Hong SH, Jeon YJ, Kim H, Cho DH, Woo HN, Song S et al (2007) AK2 activates a novel apoptotic pathway through formation of a complex with FADD and caspase-10. *Nat Cell Biol* 9:1303–1310
- Liu R, Strom AL, Zhai J, Gal J, Bao S, Gong W, Zhu H (2009) Enzymatically inactive adenylate kinase 4 interacts with mitochondrial ADP/ATP translocase. *Int J Biochem Cell Biol* 41:1371–1380
- Liu X, Zhang M, Go VL, Hu S (2010) Membrane proteomic analysis of pancreatic cancer cells. *J Biomed Sci* 17:74
- Majewski N, Nogueira V, Bhaskar P, Coy PE, Skeen JE, Gottlob K, Chandel NS, Thompson CB, Robey RB, Hay N (2004) Hexokinase-mitochondria interaction mediated by Akt is required to inhibit apoptosis in the presence or absence of Bax and Bak. *Mol Cell* 16:819–830
- Makarchikov AF, Wins P, Janssen E, Wieringa B, Grisar T, Bettendorff L (2002) Adenylate kinase 1 knockout mice have normal thiamine triphosphate levels. *Biochim Biophys Acta* 1592:117–121
- Maldonado EN, Sheldon KL, DeHart DN, Patnaik J, Manevich Y, Townsend DM, Bezrukov SM, Rostovtseva TK, Lemasters JJ (2013) Voltage-dependent anion channels modulate mitochondrial metabolism in cancer cells: regulation by free tubulin and erastin. *J Biol Chem* 288:11920–11929
- Martel C, Wang Z, and Brenner C. (2014). VDAC phosphorylation, a lipid sensor influencing the cell fate. *Mitochondrion* 19 Pt A, 69–77.
- Mather M, Rottenberg H (2001) Polycations induce the release of soluble intermembrane mitochondrial proteins. *Biochim Biophys Acta* 1503:357–368
- Mathupala SP, Ko YH, Pedersen PL (2006) Hexokinase II: cancer's double-edged sword acting as both facilitator and gatekeeper of malignancy when bound to mitochondria. *Oncogene* 25:4777–4786
- Morisaki T, Gross M, Morisaki H, Pongratz D, Zollner N, Holmes EW (1992) Molecular basis of AMP deaminase deficiency in skeletal muscle. *Proc Natl Acad Sci U S A* 89:6457–6461
- Nelson BD, Kabir F (1985) Adenylate kinase is a source of ATP for tumor mitochondrial hexokinase. *Biochim Biophys Acta* 841:195–200
- Noma T (2005) Dynamics of nucleotide metabolism as a supporter of life phenomena. *The journal of medical investigation* : JMI 52:127–136
- Noma T, Fujisawa K, Yamashiro Y, Shinohara M, Nakazawa A, Gondo T, Ishihara T, Yoshinobu K (2001) Structure and expression of human mitochondrial adenylate kinase targeted to the mitochondrial matrix. *Biochem J* 358:225–232
- Panayiotou C, Solaroli N, Karlsson A (2014) The many isoforms of human adenylate kinases. *Int J Biochem Cell Biol* 49:75–83
- Park CE, Wenner CE (1970) Mitochondrial lipids of Ehrlich letre ascites tumor cells. *Oncology* 24:241–260
- Park H, Kam TI, Kim Y, Choi H, Gwon Y, Kim C, Koh JY, Jung YK (2012) Neuropathogenic role of adenylate kinase-1 in Abeta-mediated tau phosphorylation via AMPK and GSK3beta. *Hum Mol Genet* 21:2725–2737
- Pastorino JG, Hoek JB (2008) Regulation of hexokinase binding to VDAC. *J Bioenerg Biomembr* 40:171–182
- Patra S, Ghosh A, Roy SS, Bera S, Das M, Talukdar D, Ray S, Wallimann T, Ray M (2012) A short review on creatine-creatine kinase system in relation to cancer and some experimental results on creatine as adjuvant in cancer therapy. *Amino Acids* 42:2319–2330
- Plaideau C, Liu J, Hartleib-Geschwindner J, Bastin-Coyette L, Bontemps F, Oscarsson J, Hue L, Rider MH (2012) Overexpression of AMP-metabolizing enzymes controls adenine nucleotide levels and AMPK activation in HEK293T cells. *FASEB J* 26:2685–2694
- Plaideau C, Lai YC, Kviklyte S, Zanou N, Lofgren L, Andersen H, Vertommen D, Gailly P, Hue L, Bohlooly YM et al (2014) Effects of pharmacological AMP deaminase inhibition and Ampd1 deletion on nucleotide levels and AMPK activation in contracting skeletal muscle. *Chem Biol* 21:1497–1510
- Rosano TG, Clayson KJ, Strandjord PE (1976) Evaluation of adenosine 5'-monophosphate and fluoride as adenylate kinase inhibitors in the creatine kinase assay. *Clin Chem* 22:1078–1083
- Ross RA, Spengler BA (2007) Human neuroblastoma stem cells. *Semin Cancer Biol* 17:241–247
- Ruan Q, Chen Y, Gratton E, Glaser M, Mantulin WW (2002) Cellular characterization of adenylate kinase and its isoform: two-photon excitation fluorescence imaging and fluorescence correlation spectroscopy. *Biophys J* 83:3177–3187
- Rybakowska I, Slominska EM, Romaszko P, Lipinski M, Zukowska P, Smolenski RT (2014) Activity of AMP-regulated protein kinase and AMP-deaminase in the heart of mice fed high-fat diet. *Nucleosides Nucleotides Nucleic Acids* 33:347–352
- Saks VA, Chernousova GB, Gukovsky DE, Smirnov VN, Chazov EI (1975) Studies of energy transport in heart cells. Mitochondrial isoenzyme of creatine phosphokinase: kinetic properties and regulatory action of Mg<sup>2+</sup> ions. *Eur J Biochem* 57:273–290
- Saks VA, Belikova YO, Kuznetsov AV (1991) In vivo regulation of mitochondrial respiration in cardiomyocytes: specific restrictions for intracellular diffusion of ADP. *Biochim Biophys Acta* 1074:302–311
- Saks V, Guzun R, Timohhina N, Tepp K, Varikmaa M, Monge C, Beraud N, Kaambre T, Kuznetsov A, Kadaja L et al (2010) Structure-function relationships in feedback regulation of energy fluxes in vivo in health and disease: mitochondrial interactome. *Biochim Biophys Acta* 1797:678–697
- Seppet E, Eimre M, Peet N, Paju K, Orlova E, Ress M, Kovask S, Piirsoo A, Saks VA, Gellerich FN et al (2005) Compartmentation of energy metabolism in atrial myocardium of patients undergoing cardiac surgery. *Mol Cell Biochem* 270:49–61
- Shackelford DB, Shaw RJ (2009) The LKB1-AMPK pathway: metabolism and growth control in tumour suppression. *Nat Rev Cancer* 9:563–575
- Simamura E, Shimada H, Hatta T, Hirai K (2008) Mitochondrial voltage-dependent anion channels (VDACs) as novel pharmacological targets for anti-cancer agents. *J Bioenerg Biomembr* 40:213–217
- Single B, Leist M, Nicotera P (1998) Simultaneous release of adenylate kinase and cytochrome c in cell death. *Cell Death Differ* 5:1001–1003
- Tanabe T, Yamada M, Noma T, Kajii T, Nakazawa A (1993) Tissue-specific and developmentally regulated expression of the genes encoding adenylate kinase isozymes. *J Biochem* 113:200–207
- Tanimura A, Horiguchi T, Miyoshi K, Hagita H, Noma T (2014) Differential expression of adenine nucleotide converting enzymes in mitochondrial intermembrane space: a potential role of adenylate kinase isozyme 2 in neutrophil differentiation. *PLoS One* 9:e89916
- Tepp K, Timohhina N, Chekulayev V, Shevchuk I, Kaambre T, Saks V (2010) Metabolic control analysis of integrated energy metabolism in permeabilized cardiomyocytes - experimental study. *Acta Biochim Pol* 57:421–430

- Tepp K, Shevchuk I, Chekulayev V, Timohhina N, Kuznetsov AV, Guzun R, Saks V, Kaambre T (2011) High efficiency of energy flux controls within mitochondrial interactosome in cardiac intracellular energetic units. *Biochim Biophys Acta* 1807:1549–1561
- Timohhina N, Guzun R, Tepp K, Monge C, Varikmaa M, Vija H, Sikk P, Kaambre T, Sackett D, Saks V (2009) Direct measurement of energy fluxes from mitochondria into cytoplasm in permeabilized cardiac cells in situ: some evidence for mitochondrial interactosome. *J Bioenerg Biomembr* 41:259–275
- Ventura-Clapier R, Garnier A, Veksler V, Joubert F (2011) Bioenergetics of the failing heart. *Biochim Biophys Acta* 1813:1360–1372
- Zhang S, Nemetlu E, Dzeja P (2010) Metabolomic profiling of adenylate kinase AK1<sup>-/-</sup> and AK2<sup>+/-</sup> transgenic mice: effect of physical stress. *Circulation* 122
- Zhang S, Nemetlu E, Terzic A, Dzeja P (2014) Adenylate kinase isoform network: a major hub in cell energetics and metabolic signaling. In: Aon MA, Saks V, Schlattner U (eds) *Systems biology of metabolic and signaling networks*. Springer, Berlin Heidelberg, pp. 145–162

## **Publication II**

Kaldma, Andrus; **Klepinin, Aleksandr**; Chekulayev, Vladimir; Mado, Kati; Shevchuk, Igor; Timohhina, Natalja; Tepp, Kersti; Kandashvili, Manana; Varikmaa, Minna; Koit, Andre; Planken, Margus; Heck, Karoliina; Truu, Laura; Planken, Anu; Valvere, Vahur; Rebane, Egle; Kaambre, Tuuli. (2014). An in situ study of bioenergetic properties of human colorectal cancer: The regulation of mitochondrial respiration and distribution of flux control among the components of ATP synthasome. *The International Journal of Biochemistry & Cell Biology*, 55, 171–186.





Contents lists available at ScienceDirect

# The International Journal of Biochemistry & Cell Biology

journal homepage: [www.elsevier.com/locate/biocel](http://www.elsevier.com/locate/biocel)

## An *in situ* study of bioenergetic properties of human colorectal cancer: The regulation of mitochondrial respiration and distribution of flux control among the components of ATP synthasome



Andrus Kaldma<sup>a</sup>, Aleksandr Klepinin<sup>a</sup>, Vladimir Chekulayev<sup>a</sup>, Kati Mado<sup>a</sup>, Igor Shevchuk<sup>a</sup>, Natalja Timohhina<sup>a</sup>, Kersti Tepp<sup>a</sup>, Manana Kandashvili<sup>b</sup>, Minna Varikmaa<sup>a</sup>, Andre Koit<sup>a</sup>, Margus Planken<sup>e</sup>, Karoliina Heck<sup>d</sup>, Laura Truu<sup>e</sup>, Anu Planken<sup>c</sup>, Vahur Valvere<sup>d</sup>, Egle Rebane<sup>c</sup>, Tuuli Kaambre<sup>a,b,\*</sup>

<sup>a</sup> Laboratory of Bioenergetics, National Institute of Chemical Physics and Biophysics, Tallinn, Estonia

<sup>b</sup> Tallinn University, Tallinn, Estonia

<sup>c</sup> Cancer Research Competence Center, Tallinn, Estonia

<sup>d</sup> North Estonian Regional Hospital, Tallinn, Estonia

<sup>e</sup> Tallinn University of Technology, Tallinn, Estonia

### ARTICLE INFO

#### Article history:

Received 15 May 2014

Received in revised form 12 August 2014

Accepted 2 September 2014

Available online 10 September 2014

#### Keywords:

Energy metabolism

Metabolic control analysis

Colorectal cancer

Mitochondria

VDAC

Hexokinase

Tubulin

Warburg effect

### ABSTRACT

The aim of this study is to characterize the function of mitochondria and main energy fluxes in human colorectal cancer (HCC) cells. We have performed quantitative analysis of cellular respiration in post-operative tissue samples collected from 42 cancer patients. Permeabilized tumor tissue in combination with high resolution respirometry was used.

Our results indicate that HCC is not a pure glycolytic tumor and the oxidative phosphorylation (OXPHOS) system may be the main provider of ATP in these tumor cells. The apparent Michaelis–Menten constant ( $K_m$ ) for ADP and maximal respiratory rate ( $V_m$ ) values were calculated for the characterization of the affinity of mitochondria for exogenous ADP: normal colon tissue displayed low affinity ( $K_m = 260 \pm 55 \mu\text{M}$ ) whereas the affinity of tumor mitochondria was significantly higher ( $K_m = 126 \pm 17 \mu\text{M}$ ). But concurrently the  $V_m$  value of the tumor samples was 60–80% higher than that in control tissue. The reason for this change is related to the increased number of mitochondria. Our data suggest that in both HCC and normal intestinal cells tubulin  $\beta$ -II isoform probably does not play a role in the regulation of permeability of the MOM for adenine nucleotides.

The mitochondrial creatine kinase energy transfer system is not functional in HCC and our experiments showed that adenylate kinase reactions could play an important role in the maintenance of energy homeostasis in colorectal carcinomas instead of creatine kinase.

Immunofluorescent studies showed that hexokinase 2 (HK-2) was associated with mitochondria in HCC cells, but during carcinogenesis the total activity of HK did not change. Furthermore, only minor alterations in the expression of HK-1 and HK-2 isoforms have been observed.

Metabolic Control analysis showed that the distribution of the control over electron transport chain and ATP synthasome complexes seemed to be similar in both tumor and control tissues. High flux control coefficients point to the possibility that the mitochondrial respiratory chain is reorganized in some way or assembled into large supercomplexes in both tissues.

© 2014 Elsevier Ltd. All rights reserved.

**Abbreviations:** AK, adenylate kinase; ANT, adenine nucleotide translocator; BSA, bovine serum albumin; CAT, carboxyatractylidase; COX, cytochrome c oxidase; CK, creatine kinase; ETC, electron transport chain; FDG, 18-fluorodeoxyglucose; FCC, flux control coefficient; HCC, human colorectal cancer; HK, hexokinase;  $K_m$ , Michaelis–Menten constant; uMtCK, ubiquitous mitochondrial creatine kinase; MCA, Metabolic Control Analysis; 3-NP, 3-nitropropionic acid; OXPHOS, oxidative phosphorylation; MOM, mitochondrial outer membrane; PCR, phosphocreatine; PET, positron emission tomography; Pi, inorganic phosphate; PIC, inorganic phosphate carrier; PEP, phosphoenolpyruvate; PYK, pyruvate kinase; RCI, respiratory control index; TMPD, N,N,N',N'-tetramethyl-p-phenylenediamine; VDAC, voltage dependent anion channel;  $V_0$ , basal respiration level;  $V_m$ , maximal respiration rate.

\* Corresponding author at: Laboratory of Bioenergetics, National Institute of Chemical Physics and Biophysics, Akadeemia tee 23, 12618 Tallinn, Estonia.

E-mail address: [tuuli.kaambre@kbfi.ee](mailto:tuuli.kaambre@kbfi.ee) (T. Kaambre).

<http://dx.doi.org/10.1016/j.biocel.2014.09.004>

1357-2725/© 2014 Elsevier Ltd. All rights reserved.

## 1. Introduction

Human colorectal cancer (HCC) is a malignant tumor caused by uncontrolled growth of mutated cells in the colon, rectum or vermiform appendix. It is highly resistant to chemotherapy, has strong inclination to metastasis and is one of the main causes of cancer death worldwide which necessitate for new strategies of the HCC treatment. Studies performed during the past decade demonstrated that targeting cancer cell energy metabolism might be a new and very effective therapeutic approach for selective ablation of malignancies (Geschwind et al., 2004; Gogvadze et al., 2009). Today, however, little is known about the key processes involved in the maintenance of energy homeostasis in HCC cells as well as the bioenergetic function of their mitochondria.

In the 1920s, Warburg et al. (1927) observed that tumor cells consumed a large amount of glucose and converted most of it to lactic acid even in the presence of oxygen which was contrary to Pasteur observation (“Pasteur effect”), who found that in most eukaryotic cells the rate of glycolysis decreases significantly in the presence of oxygen.

According to the model proposed by Pedersen and co-workers (Pedersen, 2008), the interaction of voltage dependent anionic channel (VDAC), located within the outer mitochondrial membrane (MOM) with hexokinase-2 (HK-2) (a key glycolytic enzyme that is usually upregulated in tumor cells), is one of the main pathways mediating the “Warburg effect” in cancer (Pedersen, 2007a,b). It was shown that mitochondrially-bound HK uses exclusively intramitochondrially compartmented ATP (Cesar Mde and Wilson, 1998). It was reported (Majewski et al., 2004) that the binding of HK-2 to mitochondria through VDAC supported this porin complex in an open state. Another consequence of HK–VDAC interaction is that it prevents binding of pro-apoptotic proteins to VDAC (a component of the MPT pore) and thereby protects cell from the induction of apoptosis (Pastorino and Hoek, 2008).

Our recent studies have shown that alterations in the expression profile of some tubulin isotypes in tumor cells could induce their Warburg behavior (Guzun et al., 2011a; Rostovtseva et al., 2008). We found (Guzun et al., 2012) that the localization and function of  $\beta$ -tubulin isotypes varied in different muscle tissues and malignant cells. The absence of  $\beta$ II-tubulin in cancer cells permits binding of HK-2 to VDAC mediating thereby the initiation of the Warburg effect. At the same time, it was shown (Rodríguez-Enriquez et al., 2011; Rodríguez-Enriquez et al., 2006; Zu and Guppy, 2004) that chemotherapeutic strategies using glycolytic inhibitors can often be inefficient in arresting tumor proliferation and the Warburg hypothesis may not be applicable to all existing malignancies. The concept of glycolytic cancer cells has been recently brought into question; Zu and Guppy (2004) concluded that the data from the last 40 years provided no evidence that cancer cells were inherently glycolytic but some tumors might indeed be glycolytic *in vivo* as a result of their adaptation to the hypoxic environment. Mitochondria, besides their role in cellular energy metabolism also play a critical role in many regulatory and signaling events in the response to a multiplicity of physiological and genetic stress factors, inter-organelle communication, cell proliferation and cell death (Goldenthal and Marín-García, 2004). To date, a new concept for cancer treatment focused on targeting tumor cell mitochondria has been elaborated, which may prove to be a very effective therapeutic approach for selective ablation of malignancies (Fulda et al., 2010; Gogvadze et al., 2009).

It has now become obvious that some cancer cells, like normal proliferating cells, can reprogram carbon metabolism by reducing energy production of oxidative phosphorylation (OXPHOS) and simultaneously up-regulating glycolysis. All this drives glycolytic and tricarboxylic acid cycle (TCA) intermediates into biosynthetic

pathways (Lunt and Vander Heiden, 2011; Vander Heiden et al., 2009); possible signaling pathways of this phenomenon are the object of intensive studies (Agathocleous and Harris, 2013).

During the last years, the concept of aerobic glycolysis as the framework of tumor cell metabolism has been challenged, as some tumor cells exhibit high rates of OXPHOS (Diers et al., 2012; Klepinin et al., 2014; Moreno-Sánchez et al., 2009). Also, our recent studies on clinical material have shown that human breast cancer is a non-hypoxic oxidative tumor in which the mitochondrial respiration is significantly increased and is sensitive to respiratory chain inhibitors (Kaambre et al., 2012; Sotgia et al., 2012). Our results show that in these carcinoma cells the OXPHOS system, but not glycolysis, is the major source of ATP. Recently, a new two-compartment model has been proposed to understand the Warburg effect in tumor metabolism, which is referred to as “reverse Warburg” effect (Sotgia et al., 2012; Witkiewicz et al., 2012). In this model, glycolytic stromal cells produce mitochondrial fuels which are then transferred into oxidative cancer cells, driving OXPHOS and fueling tumor growth and metastasis (Martínez-Outschoorn et al., 2012; Sotgia et al., 2012; Whitaker-Menezes et al., 2011; Witkiewicz et al., 2012). Although, the first studies on two-compartment tumor metabolism were first performed on fibroblasts and breast cancer cells (Martínez-Outschoorn et al., 2011; Sotgia et al., 2011, 2012; Whitaker-Menezes et al., 2011), this emerging paradigm has already expanded to other malignancies like adipocytes and ovarian cancer cells, head and neck tumors and cancer lymph node metastases (Curry et al., 2013; Nieman et al., 2011; Sotgia et al., 2012).

For better understanding functional centers, which control and regulate the energy fluxes in cancer cells *in vivo*, analytical tools are needed to link the properties of metabolic systems with the kinetic characteristics of the component enzymes and their impact on network function. A potent experimental approach for this is Metabolic Control Analysis (MCA) (Fell, 2005). MCA has been shown to be very helpful for understanding the enzymatic abnormalities in syndromes associated with mitochondrial dysfunction (Kuznetsov et al., 2008). Moreno-Sánchez and colleagues have applied MCA to investigate the control of glycolytic flux and mitochondrial respiration in different types of tumor cells growing in culture. Main conclusion of these studies was that the significance of OXPHOS in bioenergetics of cancer cells should be re-evaluated and experimentally determined for each particular type of neoplasm (Marín-Hernández et al., 2006; Moreno-Sánchez et al., 2007, 2010; Moreno-Sánchez et al., 2009). Recently in our laboratory, MCA was successfully used to study the bioenergetic function of mitochondria in human breast cancer postoperative samples (Kaambre et al., 2012).

In the present work, MCA was applied to characterize the function of OXPHOS in HCC cells *in situ*. We quantified the control exerted by different components of the respiratory chain and the ATP synthasome complex (a large mitochondrial complex consisting of ATP synthase, adenine nucleotide transporter (ANT) and inorganic phosphate carrier (Pedersen, 2008)) in these carcinoma cells as compared with normal colon tissue. To determine the flux control coefficients, the flux was measured as the rate of O<sub>2</sub> consumption by permeabilized tissue fibers derived from HCC patients when all components of the OXPHOS system were titrated with specific inhibitors to stepwise decrease selected respiration complex activities. It is important to note that the use of MCA and the permeabilization techniques permit to estimate the function of OXPHOS system without isolation of mitochondria and thereby avoiding artifacts linked to their isolation procedure and the loss of components involved in the regulation. Besides, such a methodology preserves intimate interactions between mitochondria within the cell as well as the intactness of their cytoskeletal structures.

The present work also evaluated the significance of creatine kinase (CK) and adenylate kinase (AK) reactions in the maintenance of energy homeostasis in HCC cells.

## 2. Materials and methods

### 2.1. Reagents

Chemicals were purchased from Sigma–Aldrich Chemical Com. (USA) and were used directly without further purification. Primary and secondary antibodies were obtained from Santa Cruz Biotechnology Inc. or Abcam PLC, whereas rabbit polyclonal antibodies vs. VDAC were kindly donated by Dr. Catherine Brenner from Paris-Sud University, France.

### 2.2. Clinical materials and patients

All patients examined ( $n=42$ , with ages ranging from 63 to 92 years) had local or locally advanced disease (T2–4 N0–1, M0–1). The patients in the study had not received prior radiation or chemotherapy.

HCC postoperative and normal tissue samples (0.1–0.5 g) were provided by the Oncology and Hematologic Clinic at the North Estonia Medical Centre (NEMC, Tallinn). Pathology reports were provided by the NEMC for each tissue sample. Only primary tumor samples were examined. All investigations were approved by the Medical Research Ethics Committee (National Institute for Health Development, Tallinn) and were in accordance with Helsinki Declaration and Convention of the Council of Europe on Human Rights and Biomedicine.

Normal tissue samples were taken from the same location at sites distant from the tumor by 5 cm and they were evaluated for presence of malignant cells. The adjacent control tissues consisted of colonocytes and smooth muscle cells. Images of hematoxylin-eosin stained preparations of tumor and surrounding normal tissues are shown in Fig. 1 in supplement. In addition, we performed molecular characterization of tissue samples from 35 patients (both tumor and normal) using microsatellite instability, CpG island methylator (CIMP) phenotype and 5-hydroxymethylation assay. They showed that all control samples had a stable microsatellite profile and no CIMP phenotype. Also the 5-hydroxymethylation expression was statistically significantly higher in normal tissue samples as compared to tumor tissue, as analyzed in 13 patients (Supplementary Fig. 2). 5-Hydroxymethylation analysis was carried out according to manufacturer instructions provided with the MethylFlash Hydroxymethylated DNA Quantification Kit (Epigenetek, USA).

Supplementary material related to this article can be found, in the online version, at <http://dx.doi.org/10.1016/j.biocel.2014.09.004>.

### 2.3. Preparation of skinned tumor fibers and permeabilization procedure

Immediately after the surgery the tissue samples were placed into pre-cooled (on melting ice) medium-A (Kaambre et al., 2012), dissected into small fiber bundles (10–20 mg) and permeabilized in the same medium with 50  $\mu\text{g/ml}$  saponin upon mild stirring for 30 min at 4 °C (Kaambre et al., 2012; Kuznetsov et al., 2008). The obtained permeabilized (skinned) fibers were then washed three times for 5 min in pre-cooled solution containing: 20 mM imidazole, 3 mM  $\text{KH}_2\text{PO}_4$ , 0.5 mM DTT, 20 mM taurine, 4 mM  $\text{MgCl}_2$ , 100 mM 2-morpholinoethanesulfonic acid, 2.74 mM  $\text{K}_2\text{Ca-EGTA}$ , 4.72 mM  $\text{K}_2\text{-EGTA}$ , and 5 mg/ml fatty acids free bovine serum albumin (BSA); medium-B, pH 7.1. After that samples were kept in medium-B at 4 °C until use. Typical dimension of skinned fibers

was about 2 mm  $\times$  2 mm  $\times$  2 mm, and one of these pieces was used in oxygraphic experiments.

### 2.4. Oxygraphic measurements

Mitochondrial respiration of tissue samples was measured at 25 °C in medium-B supplemented with 5 mM glutamate, 2 mM malate and 10 mM succinate as respiratory substrates using high-resolution respirometer Oxygraph-2k (Oroboros Instruments, Innsbruck, Austria) as described previously (Kuznetsov et al., 2008). The solubility of oxygen at 25 °C was taken as 240 nmol/ml (Gnaiger, 2001). All respiration rates were normalized per mg dry weight of tissue.

#### 2.4.1. Analysis of OXPHOS coupling with adenylate kinase

The adenylate kinase coupling with OXPHOS was measured by respirometry using modified protocols of Gruno et al. (2006). Mitochondrial basal respiration was activated by glutamate, malate and succinate (at a final concentration of 5, 2 and 10 mM, respectively), 100  $\mu\text{M}$  ATP was added to produce a minimum amount of endogenous ADP to stimulate mitochondria, AMP (2 mM) activated the coupled reaction of adenylate kinase system with ANT followed by addition of 0.2 mM diadenosine pentaphosphate (AP5A) to inhibit total AK reaction. Then AK index (IAK):  $[\text{IAK} = (\text{VAMP} - \text{VAP5A})/\text{VAP5A}]$  was calculated, where it expressed the strength of the AK functional coupling with OXPHOS. A rate of AMP activated respiration (VAMP) was normalized for the respiration after total inhibition of AK by AP5A (VAP5A).

#### 2.4.2. Analysis of OXPHOS coupling with creatine kinase (MtCK)

The steady state kinetics of MtCK reaction coupled to oxidative phosphorylation via ANT in permeabilized HCC and control tissue *in situ* was studied using the protocol described earlier by Guzun et al. (2009) and Gellerich et al. (2002).

### 2.5. Immunofluorescence and confocal microscopy

Confocal microscopy was applied to immunostained skinned fibers and paraffin-embedded sections of HCC and normal colorectal tissue to assess the presence and intracellular localization of mitochondria (via VDAC immunolabeling), HK-2, and  $\beta$ II-tubulin. For immunocytochemistry, skinned fibers were fixed with 4% paraformaldehyde (PFA) for 15 min at 37 °C, treated with an antigen retrieval buffer (ARB, 100 mM Tris buffer with 5%, w/v urea, pH 9.5) and permeabilized with 1.0% Triton X-100 for 15 min at room temperature (RT). For immunohistochemistry, formalin fixed paraffin-embedded tissue sections were rinsed with xylene for 4–5 min, rehydrated step-by-step by ethanol (at 100% and 50%) and treated with ARB at 98 °C for 15 min.

Fibers and tissue sections were then blocked with 2% BSA in PBS and incubated overnight at 4 °C with primary antibodies. Monoclonal mouse anti-tubulin  $\beta$ II (Abcam®, ab92857), polyclonal rabbit antibody vs. VDAC and polyclonal goat antibodies vs. HK-2 (Santa Cruz Biotechnology Inc., sc-6521) were used. Thereafter fibers were washed and incubated for 2 hours at RT with following secondary antibodies: DyLight-488 goat anti-rabbit IgG (Abcam®, ab96899) or DyLight-549 goat anti-mouse IgG (Abcam®, ab96880). Thereafter fibers and tissue slides were mounted in Prolong® Gold Antifade Reagent supplemented with 4',6-diamidino-2-phenylindole dihydrochloride (DAPI, Life Technologies), deposited between glass coverslips and observed by confocal microscope. Confocal images were collected using Olympus FV10i-W inverted laser scanning confocal microscope equipped with a 60 $\times$  water immersion objective. Laser excitation was 488 nm for DyLight-488 and 561 nm for DyLight-549.

## 2.6. Quantification of mitochondrial content

The mitochondrial content was quantified in paraffin embedded neoplastic and normal colon tissue samples *via* selective marking of mitochondrial outer membrane translocase Tom20 (Santa Cruz Biotechnology, sc17764). The Tom20 fluorescence intensity was normalized against whole  $\beta$ -tubulin (Abcam®, ab6046) fluorescence.

## 2.7. Assessment of enzymatic activities

HK activity was measured as the total glucose phosphorylating capacity of whole tissue extracts, using a standard glucose-6-phosphate dehydrogenase (G6PDH)-coupled spectrophotometric assay (Robey et al., 2000).

The CK activity was assessed spectrophotometrically at 25 °C in the direction of ATP formation in the presence of di(adenosine-5') pentaphosphate (an adenylate kinase inhibitor (Lienhard and Secemski, 1973)), 20 mM phosphocreatine (PCr) and with 2 U/ml G6PDH and 2 U/ml HK as the coupled enzymes (Monge et al., 2009). One mU of CK activity represents the formation of 1 nmol of ATP per minute at 25 °C.

AK activity of whole-tissue extracts was measured at 25 °C by a coupled enzyme assay (Dzeja et al., 1999). The reaction was initiated with 2 mM ADP, and the arising changes in absorbance at 340 nm were recorded using a Cary 100 Bio UV-visible spectrophotometer. One mU of AK activity represents the formation of 1 nmole of ATP per minute at 25 °C.

All enzymatic activities were normalized per mg of tissue protein. The protein content of tissue extracts was determined by a Pierce BCA Protein Assay Kit according to the manufacturer recommendations using BSA as a standard.

## 2.8. RNA isolation and real-time quantitative RT-PCR

RNA from 29 human frozen colorectal cancer and normal colon tissue samples was isolated using Trizol (Life Technologies) solution, followed by purification using the RNeasy Mini Kit (QIAGEN Sciences) with DNase treatment. Extracted RNA was dissolved in RNase-free water, quality and concentration were measured using Nanodrop and RNA was stored at –80 °C until cDNA synthesis.

For cDNA synthesis 2  $\mu$ g of total RNA was used. cDNA was synthesized using High Capacity cDNA Reverse Transcription Kit with RNase Inhibitor (Applied Biosystems). cDNA was used as a template for TaqMan® quantitative RT-PCR (qRT-PCR) analysis in the Roche LightCycler 480 system (Roche). TaqMan® Gene Expression Master Mix and FAM labeled TaqMan® (Applied Biosystems) gene assays were used to detect the mRNA expression level of the gene of interest and of actin as a reference gene. The used TaqMan® probes were the following: actin beta – Hs01060665.g1; tubulin beta 2A – Hs00742533.s1; tubulin beta 2B – Hs00603550.g; tubulin beta 2C – Hs00607181.g1; tubulin beta 3 – Hs00801390.s1; tubulin beta 4 – Hs00760066.s1; tubulin beta 1/5 – Hs00742828.s1; hexokinase I – Hs00175976.m1; hexokinase II – Hs00606086.m1; creatine kinase, mitochondrial 1B – Hs00179727.m1; creatine kinase, mitochondrial 2 – Hs00176502.m1. Reactions were carried out in four replicates. Data was analyzed using the 2(–Delta Delta C(T)) method, where the gene expression levels were normalized to the level of actin beta housekeeping gene. The data of studied genes following normal distribution were parametrically tested by unpaired *t*-test.

## 2.9. Metabolic control analysis (MCA) and determination of flux control coefficients

MCA was performed as described previously (Fell, 1997; Groen et al., 1982; Kaambre et al., 2012; Moreno-Sanchez et al., 2008;

Tepp et al., 2011). Flux control coefficients (FCC) were calculated by using non-linear regression analysis by fitting experimental data to the mathematical model, as described by Gellerich et al. (1990) and Small and Fell (1990). The results were also verified by a graphical method (Fell, 2005; Gellerich et al., 1990).

## 2.10. Data analysis

Data in the text, tables and figures are presented as mean  $\pm$  standard error (SEM). Results were analyzed by Student's *t*-test. *p*-values <0.05 were considered statistically significant. Apparent  $K_m$  values for ADP were measured by fitting experimental data to a non-linear regression (according to a Michaelis–Menten model) equation.

## 3. Results

### 3.1. Mitochondrial respiration in colorectal carcinomas

#### 3.1.1. Quality test of intactness of mitochondrial membranes

We performed a comparative study to characterize the respiratory activities of mitochondria in HCC cells and adjacent normal tissue *in situ* using the permeabilized cell technique, which allows to study the mitochondrial function under conditions close to physiological ones (Kuznetsov et al., 2008). Fig. 1 shows the quality test of respiration of saponin permeabilized fibers prepared from HCC and normal colon tissue. The mitochondrial respiration activated by 2 mM ADP was not increased after addition of exogenous cytochrome-*c*, showing the intactness of the outer mitochondrial membrane. Mitochondrial inner membrane intactness was controlled by carboxyatractyloside (CAT) where the respiration rate decreased back to the basal respiration level ( $V_0$ ) due to inactivation of ANT (Saks et al., 1998; Timohhina et al., 2009).

Respiration rates of human colorectal cancer and normal tissue samples in the absence of saponin treatment were also estimated,

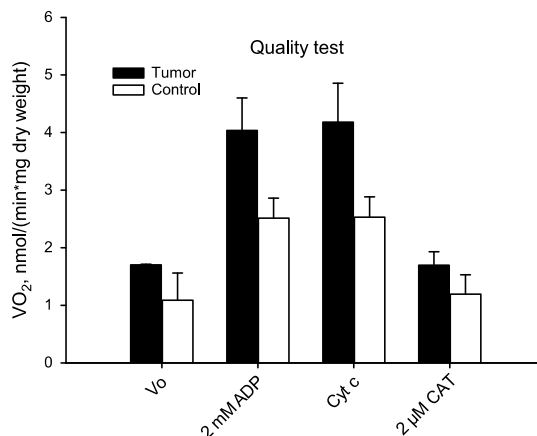


**Fig. 1.** Quality tests for the intactness of mitochondrial membranes in permeabilized human colorectal cancer and surrounding normal tissue fibers. These experiments were performed in medium-B with 5 mM glutamate, 2 mM malate, and 10 mM succinate as respiratory substrates. Respiration of permeabilized samples was activated by 2 mM ADP and the addition of cytochrome *c* (Cyt *c*, final concentration – 8  $\mu$ M) did not cause any marked increase in the rate of oxygen consumption, indicating the intactness of the outer mitochondrial membrane. Finally, addition of carboxyatractyloside (CAT, final concentration – 2  $\mu$ M) decreased the respiration rate back to the basal ( $V_0$ ) level showing that the inner membrane of the mitochondria was intact (bars are SEM, *n* = 11). All respiratory substrates and inhibitors were added sequentially as indicated in the X-axis.



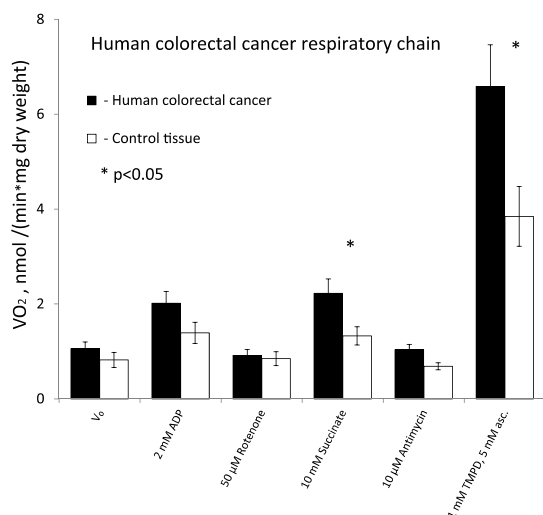


**Fig. 2.** Evaluation of the respiratory chain functions in permeabilized human colorectal cancer fibers and normal adjacent tissues. The experiment was performed in medium-B with 5 mM glutamate and 2 mM malate as respiratory substrates. TMPD is N,N,N',N'-tetramethyl-phenylenediamine, and asc – ascorbate (bars are SEM,  $n = 7$ ,  $p < 0.05$ ).

and there is only a minor activation in comparison with permeabilized tissue samples (Supplementary Fig. 3). The unambiguous analysis of respiratory parameters is possible solely after permeabilization of the cell membrane with saponin or another suitable detergent, since it is impermeable to the adenine nucleotides.

Supplementary material related to this article can be found, in the online version, at <http://dx.doi.org/10.1016/j.biocel.2014.09.004>.

### 3.1.2. Activities of respiratory chain complexes in HCC and non-neoplastic tissue samples

Activities of segments of the mitochondrial respiratory chain were analyzed by using a specific step-by-step substrate inhibitor titration oxygraphic protocol. It was found (Fig. 2) that the mean value ( $1.06 \pm 0.14$  nmol O<sub>2</sub>/min/mg dry weight) of basal respiration in skinned fibers of HCC exceeded slightly that in non-tumorous tissues ( $0.82 \pm 0.16$  nmol O<sub>2</sub>/min/mg dry weight). The addition of 2 mM Mg-ADP resulted in a strong increase in the rates of O<sub>2</sub> consumption by both HCC and normal tissue fibers. The maximal ADP-stimulated (state 3) respiration rate for HCC samples exceed that measured for non-neoplastic tissue;  $2.02 \pm 0.14$  nmol O<sub>2</sub>/min/mg vs.  $1.39 \pm 0.22$  nmol O<sub>2</sub>/min/mg dry weight, correspondingly. The ADP activated respiration was strongly inhibited in both HCC and normal tissue samples by rotenone; this was a characteristic feature of cells with active Complex-I (Fig. 2). Addition of succinate (Complex-II substrate) resulted in reactivation of oxygen consumption showing that the Complex-II of the mitochondrial respiratory chain is functionally active in both normal and tumor tissues. The addition of 10 μM antimycin-A inhibited the electron flow from Complex-III to cytochrome c. Mitochondrial Complex IV was activated by 1.0 mM N,N,N',N'-tetramethyl-p-phenylenediamine (TMPD) in the presence of 5 mM ascorbate, and this resulted in a very strong increase in the rate of O<sub>2</sub> consumption in HCC fibers (Fig. 2). Finally, exogenously added 8 μM cytochrome c had no effect on the TMPD ascorbate activated respiration, suggesting

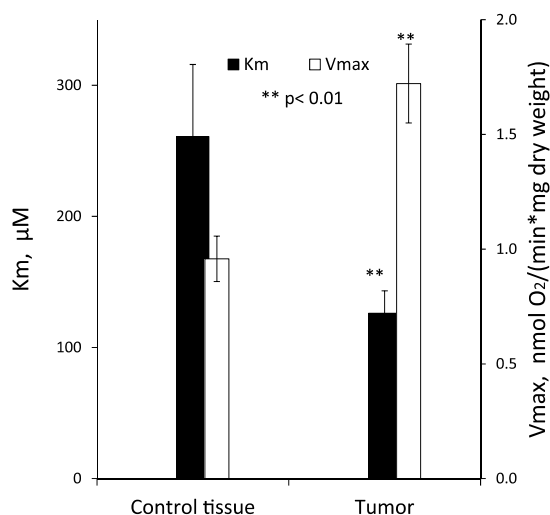


**Fig. 3.** Comparative analysis of the apparent  $K_m$  values for ADP and the maximal respiration rate ( $V_{max}$ ) for permeabilized skinned HCC and normal colon samples. Bars are SEM,  $n = 35$ ,  $p < 0.01$ .

that the applied permeabilization procedure did not damage the intactness of the external mitochondrial membrane in HCC cells.

### 3.2. Regulation of mitochondrial respiration in HCC cells

Fig. 3 summarizes the values of the apparent Michaelis–Menten constant ( $K_m$ ) and maximal respiration rate ( $V_m$ ) for exogenous ADP in tumor and adjacent normal colon tissue samples. From these data, the apparent  $K_m$  for ADP and  $V_m$  were calculated for characterization of the affinity of mitochondria for ADP. For skinned fibers from control tissue the statistical average apparent  $K_m$  for ADP is found to be  $260 \pm 55$  μM. The lower  $K_m$  value for ADP ( $126 \pm 17$  μM) in HCC cells, as compared with control tissue, suggests that in cancer cells the MOM has an increased permeability for adenine nucleotides.

Fig. 3 also demonstrates a striking difference in the values of  $V_m$  for ADP between normal and HCC tissue samples. There is an approximately 2-fold difference in mitochondrial respiration between control ( $V_m = 0.96 \pm 0.1$  nmol O<sub>2</sub>/min per mg dry weight of tissue) and tumor tissues ( $V_m = 1.72 \pm 0.13$  nmol O<sub>2</sub>/min per mg dry weight of tissue). The reason of this change is probably related with the increased number of mitochondria (Fig. 4). Therefore, mitochondrial content was estimated in HCC samples with immunocytochemistry and confocal microscopic imaging (Fig. 4). Differences in maximal respiration rates in tumor and control tissue were of the same order of magnitude than that in the number of mitochondria (by 60–70%). The immunocytochemical study used for analysis of the relative content of mitochondria in tumor and healthy tissues based on the expression of TOM20 (Fig. 4B) show statistical significance of the differences in obtained, values ( $p < 0.05$ ) of fluorescence signals.

The presented data clearly show that *in situ* there are striking differences between the kinetics of regulation of mitochondrial respiration by ADP in colorectal carcinomas and adjacent healthy tissue.

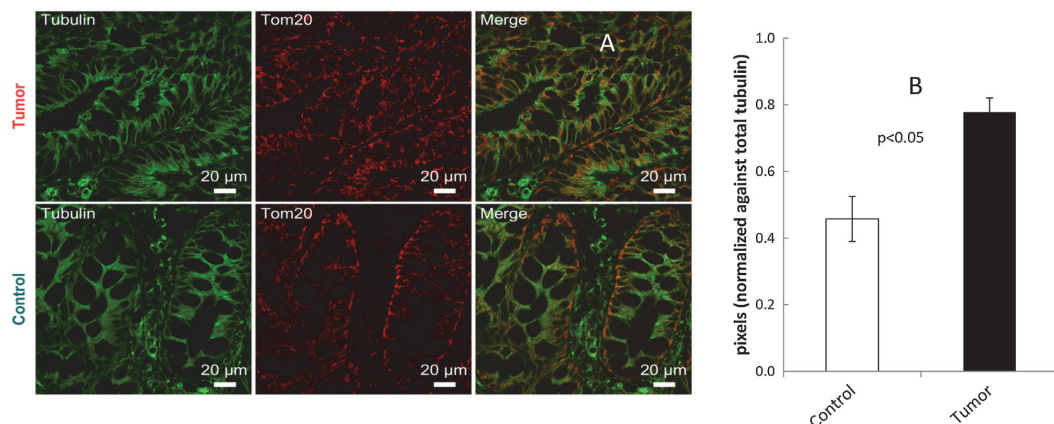


**Fig. 4.** Immunohistochemistry quantification of the total mitochondrial content in postoperative tissue samples; this was performed *via* measurements of Tom20 expression levels. (A) Representative confocal images of paraffin-embedded sections of HCC and normal colorectal tissue preloaded with anti-tubulin  $\beta$ II and anti Tom20 antibodies. Fluorescence signal intensities in normal and cancerous colorectal tissue where normalized against total  $\beta$ -tubulin fluorescence intensities (B); bars are SEM,  $n = 7$ ,  $p < 0.05$ .

### 3.2.1. Coupling of OXPHOS with creatine and adenylate kinase systems

Decreased permeability of MOM for adenine nucleotides significantly enhances the functional coupling between MtCK and ANT. Thus, adenine nucleotides are compartmented in mitochondrial matrix-inner membrane space where ADP and ATP recycling is ensured between OXPHOS and MtCK (Guzun et al., 2009; Saks et al., 2010). The changes in the CK energy transfer pathway in HCC could be responsible for changes in regulation of mitochondrial respiration during carcinogenesis. Especially CK is a ubiquitous enzyme that catalyses the reversible transphosphorylation reaction between ATP and Cr, generating ADP and phosphocreatine (PCr) (Dzeja and Terzic, 2003). Human colonocytes express all types of CK isoenzymes and are capable to produce PCr. BB-CK, which is characteristic for the brain, is the predominant isoenzyme in normal colon tissue (Joseph et al., 1997; Kasimos et al., 1990).

Our results show that the total CK activity in HCC samples is considerably (by  $\sim 2.5$  times) lower in comparison with normal colon tissues (Table 1). By means of qRT-PCR, we revealed that at gene level sMtCK (CKMT2) mRNA is remarkably upregulated (by 6.8-fold,  $p = 0.06$ ) in tumor tissue (Fig. 5); the uMtCK (CKMT1) expression is 2-fold higher ( $p = 0.009$ ) in normal colon tissue. The general expression level for this gene is significantly higher than for sMtCK. Therefore, we performed a study to estimate the potential role of MtCK in maintenance of energy homeostasis in HCC tissue as compared with normal colon sample. In these experiments, mitochondrial respiration was activated with 10 mM Cr and MgATP (final concentration, 0.2 mM) in the presence of pyruvate kinase (PYK, 30 U/ml) and phosphoenolpyruvate (PEP, 5 mM) for trapping extramitochondrial ADP to follow control of mitochondrial oxygen consumption only by uMtCK (Gellerich and Saks, 1982). The obtained results showed that addition Cr (in the presence of PYK-PEP system and exogenously added MgATP) to normal colon tissue

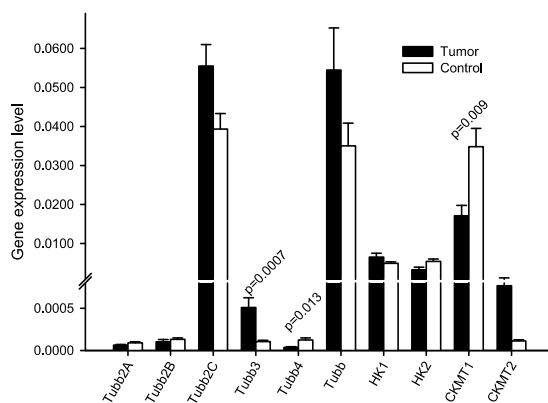


**Fig. 5.** Expression profile of various  $\beta$ -tubulin isotypes, some creatine kinase and hexokinase isoforms in human colorectal cancer and normal tissue; mRNA levels were assayed by real-time quantitative RT-PCR (bars are SEM,  $n = 29$ ). Here: HK-1 and HK-2 are hexokinase-1 and -2; CKMT1 and CKMT2 are ubiquitous and sarcomeric mitochondrial creatine kinase, respectively.

fibers caused an increase in the rate of ADP-mediated oxygen consumption nearly 60% due to the activation of MtCK and this effect was not observed in cancerous tissues (Fig. 6). These *in situ* experiments indicate that mitochondria in HCC cells have a decreased capacity for the production of PCr which is in a good agreement with some literature data (Kasimos et al., 1990; Monge et al., 2009).

It is well-known that AK-catalyzed phosphotransfer plays one of the key roles in the maintenance of energy homeostasis in fully differentiated cells with a high-energy demand, such as neural, cardiac and some skeletal muscle cells (Ames, 2000; Dzeja and Terzic, 2009). Due to decreased CK activity and the absence of MtCK coupling with OXPHOS in HCC cells, the functional coupling of AK-catalyzed processes with the OXPHOS system was estimated in both tumor and normal colon tissues. The total AK activity (Table 1) of HCC tissue extracts exceeded substantially (by  $\sim 40\%$ ) that of adjacent normal tissue. In addition, the coupling between AK and OXPHOS was expressed with AK index (IAK) proposed by Gruno et al. (2006). The value of IAK, which is independent of the tissues mitochondrial content, was substantially smaller for

**Table 1**  
Enzymatic activities in human colorectal cancer and adjacent normal tissue samples.

Enzyme activities, mU(s) per mg protein	Normal tissue, mean $\pm$ SE, $n = 11$	Tumor, mean $\pm$ SE, $n = 11$	$p$ -values
Hexokinase	244 $\pm$ 50	215 $\pm$ 40	0.33
Creatine kinase	497 $\pm$ 142	204 $\pm$ 84	<0.05
Adenylate kinase	257 $\pm$ 35	411 $\pm$ 43	<0.05

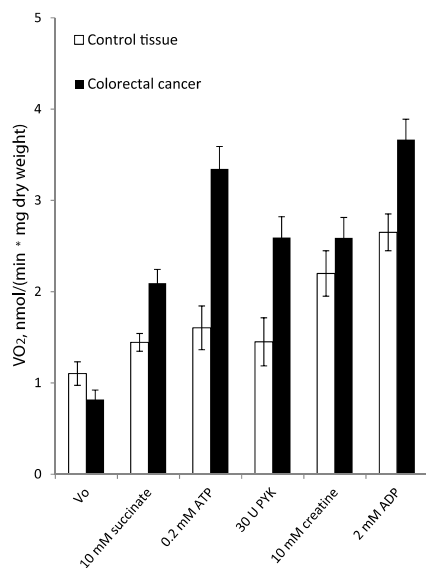


**Fig. 6.** Efficiency of creatine in the control of OXPHOS by mitochondrial creatine kinase (uMtCK) via local ADP production in permeabilized HCC and normal tissue fibers. The experiment was performed in medium-B with 5 mM glutamate and 2 mM malate and 10 mM succinate as respiratory substrates. Creatine under these conditions rapidly activates MtCK reaction and subsequently local MgADP recycling and oxygen consumption rate to the maximal values. First, the respiration is activated by addition of 0.2 mM MgATP after permeabilization of tumor and control samples inducing production of endogenous ADP in MgATPase reaction. Then PEP–PYK is added to trap all extramitochondrial free ADP. Finally, 2 mM exogenous ADP was added to activate maximal respirator rate. Bars are SEM,  $n=8$ .

non-neoplastic tissue comparing to HCC (Fig. 7). This strong difference between the values of AK indexes indicates that the AK system may be upregulated; i.e., AK and OXPHOS systems are stronger in HCC cells than in normal tissue. This could be partly mediated by higher activity of AK2 in carcinoma cells in comparison with non-transformed cells.

Further work is needed to clarify mechanisms and functional significance of these changes in the interaction and coupling between CK and AK energy transfer systems during carcinogenesis.

### 3.2.2. Coupling of OXPHOS with HK reactions, $\beta$ -tubulin mRNA expression in tumor and normal tissues

Our qRT-PCR and immunocytochemistry studies have shown that HCC cells express genes encoding HK-1 and 2 (Fig. 5); in these malignant cells HK-2 may be presumably bound to mitochondria. Indeed, in Fig. 9 the colocalization of the HK-2 isoenzyme with VDAC is demonstrated. HK could play an important role in energy metabolism of HCC cells. Since, it has been proposed by Pedersen and colleagues that in tumor cells the binding of HK to the VDAC in the mitochondrial outer membrane (MOM) can mediate their Warburg phenotype (Pedersen, 2008), in this study was therefore investigated coupling between HK and OXPHOS in HCC cells. Glucose (10 mM) exerted some stimulatory effect in HCC mitochondrial respiration at 0.1 mM MgATP, but its effect was negligible in permeabilized fibers derived from normal tissue (Fig. 8). The stimulating effect of glucose on mitochondrial respiration rate in HCC fibers was about 30–35% of the ADP-mediated (2 mM) activation. Consequently, in HCC cells either one or both isoforms of both HK-2 and HK-1 are associated with VDAC in the MOM. Thus, this interaction of HK with mitochondria allows exerting control

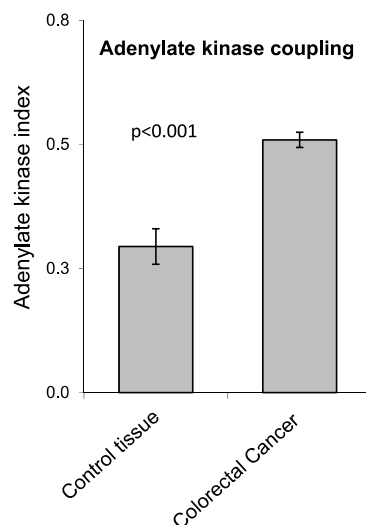


**Fig. 7.** Adenylylate kinase (AK) functional coupling in permeabilized control and HCC tissues. Adenylylate kinase coupling with mitochondria was expressed using AK index. Outer mitochondrial intactness was controlled by effect of exogenously-added cytochrome c (cytochrome c effect <math><20\%</math>). Bars are SEM,  $n=6$ , and  $p<0.001$ .

over OXPHOS so that HK uses mitochondrially-generated ATP for glucose phosphorylation.

Although, in HCC the expression levels of HK-1 and 2 as well as total glucose phosphorylating activity are similar to those in non-tumorous tissue (Fig. 5 and Table 1), we did not registered any stimulatory effect of glucose on mitochondrial respiration in the normal colon tissue (Fig. 8).

Altered profiles of some cytoskeletal protein ( $\beta$ -tubulin isotypes) expression could explain this difference in the coupling of OXPHOS with HK reactions in HCC cells as compared to non-tumorous tissues. Previous studies have shown that the cytoskeletal tubulin–microtubular system has considerable role in the regulation of mitochondrial respiration *in vivo* (Guzun et al., 2009, 2011a,b, 2012). It was demonstrated that tubulin could compete with HK-2 for the binding sites on VDAC. Therefore, in cancer cells decreased levels of tubulin favor the HK binding and thus explain the Warburg effect of increased glycolytic lactate production in these cells (Guzun et al., 2011a, 2012).

We further investigated the spectrum of  $\beta$ -tubulins by comparing the mRNA expression of the five human  $\beta$ -tubulin isotypes encoding class I IIa, IIb, III, IVa, and IVb, in colorectal carcinomas with that in non-tumorous tissue. It was found that in tumor tissues TUBB3 (gene encoding  $\beta$ III-tubulin) had statistically significantly increased expression levels compared to normal tissue (by 4.8-fold,  $p=0.0007$ ), TUBB4 ( $\beta$ IVa) was significantly decreased (by 3.4-fold,  $p=0.013$ ) in tumor tissue, whereas the levels of mRNA expression for other tubulin isotypes TUBB2A (II) and TUBB2B (II) TUBB2C (IVb) and TUBB (I) were not significantly changed in both studied tissues (Fig. 5). We found that HCC is characterized by a significant increase in the expression of TUBB3 (Fig. 5) which is the marker cell invasiveness as shown in the literature (Leandro-Garcia et al., 2010; Mozzetti et al., 2005).

The association of  $\beta$ II-tubulin with mitochondria (immunolabeled with anti-VDAC anti-body) was determined by immunohistochemistry and confocal microscopy. In both tissue types, mitochondria were showing frequent alignment along  $\beta$ II-tubulin

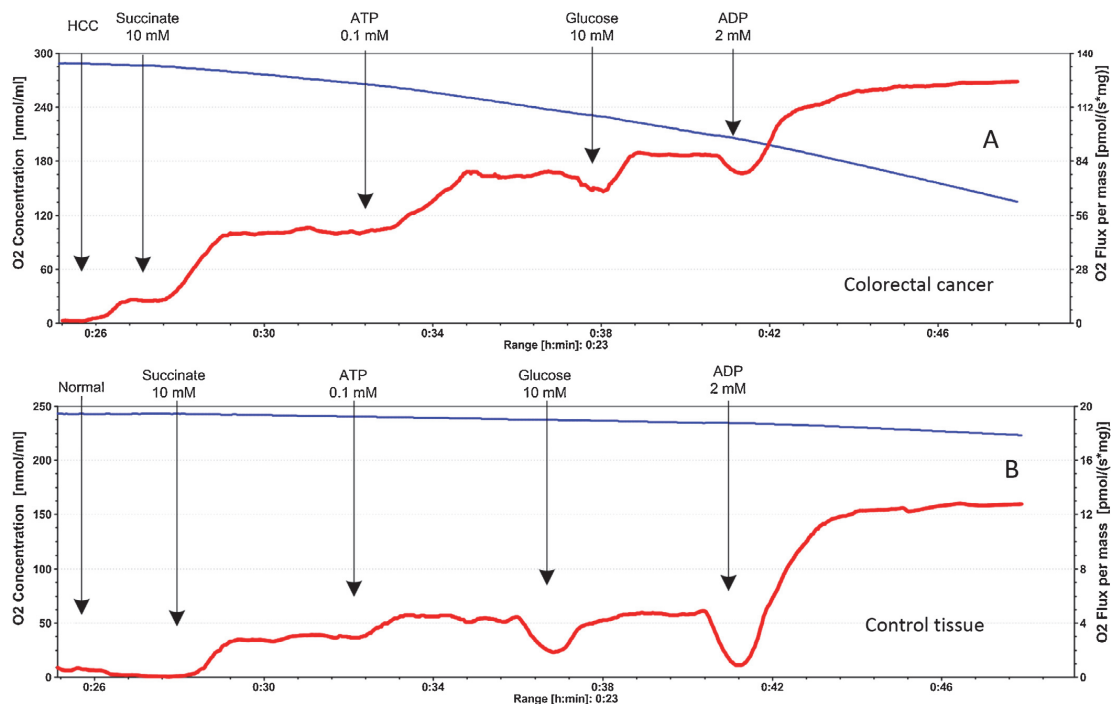


**Fig. 8.** Oxygraphic analysis of coupling of HK to OXPHOS in permeabilized HCC (A) and normal tissue fibers (B); recording of original traces of O<sub>2</sub> consumption. The addition of 10 mM glucose to HCC fibers in the presence of 0.1 mM Mg-ATP caused a stimulatory effect on mitochondrial respiration, but this HK coupling with OXPHOS was not observed in the case of fibers derived from normal adjacent tissue. Blue line – O<sub>2</sub> concentration, red – rates of O<sub>2</sub> consumption. (For interpretation of the references to color in this figure legend, the reader is referred to the web version of the article.)

containing microfilaments, but no direct association between the two was noticed (Fig. 10). This was further confirmed with comparison of the pixel intensity profiles of both dye channels, demonstrating that the signal intensity levels of the two were co-varying in random fashion. Thus, in contrast to our previous observations which were made on cardiac cells (Guzun et al., 2011a),  $\beta$ II-tubulin did not seem to be involved in regulation of VDAC conductance in colorectal tissue. Some differences between normal and HCC samples were also observed in respect to  $\beta$ II-tubulin network morphology and nuclei distribution. In particular, in normal colorectal tissue  $\beta$ II-tubulin appeared to form dense microtubular network that spread uniformly throughout the cytoplasm, whereas in HCC, clustering and fragmentation of  $\beta$ II-tubulin filaments was seen, suggesting that some remodeling of its biochemical properties (e.g., dynamic stability) has occurred. In addition, HCC cells stand out also by their enlarged and stratified nuclei, which are one of the main signs of colorectal tissue malignancy. It is impossible to explain the enhanced control of HK-2 over mitochondrial respiration in HCC cells through downregulation of  $\beta$ II-tubulin expression as was observed earlier in tumor cells of another histological type (Guzun et al., 2011a).

### 3.3. Metabolic control analysis of respiration regulation in HCC and normal non-tumor tissues

The approach of MCA allows to identify the key regulatory complexes of the energy metabolism pathways and to find the best targets for effective antineoplastic treatment (Moreno-Sanchez et al., 2008, 2010). In our MCA studies, the mitochondrial

respiration in permeabilized HCC and normal tissue fibers was activated by exogenously added ADP (final concentration, 2 mM). The use of ADP for activation of respiration was mainly mediated by low expression levels of uMtCK and its negligible activity in HCC samples. Fig. 11 shows representative traces of O<sub>2</sub> consumption in permeabilized HCC and non-neoplastic tissue fibers upon their titration with increasing concentrations of 3-NP, an inhibitor of Complex-II (Huang et al., 2006). The respiration rate was registered in steady-state conditions (Fig. 11). The same titration curves were obtained for other inhibitors of the mitochondrial ETC and ATP synthasome complexes (Supplementary Fig. 4). They were plotted as relative rates of O<sub>2</sub> consumption ( $VO_2, J/J_0$ ) versus concentration of used inhibitors (Fig. 12A and B). The FCC(s) for tumor and non-tumorous samples were calculated by fitting experimental data to the mathematical model of Gellerich et al. (Gellerich et al., 1990; Wisniewski et al., 1995). We analyzed distribution of metabolic flux controls for all of mitochondrial respiratory chain and the ATP-Synthasome complexes as described previously in (Kaambre et al., 2012; Small, 1993; Tepp et al., 2011). Two ways of electron transfer were examined, namely, NADH and FADH (succinate dependent) electron transfers (Fig. 12C and D). The calculated values (Gellerich et al., 1990; Small, 1993) FCC(s), were found to be comparable in control and tumor tissues, only FCCs for the mitochondrial respiratory chain Complex-III differ from each slightly. The sums of FCC(s) calculated for HCC cells (NADH dependent pathway,  $3.05 \pm 0.23$ ; succinate dependent pathway,  $3.03 \pm 0.20$ ) and normal colonic cells (NADH dependent,  $3.15 \pm 0.50$ ; succinate dependent,  $3.25 \pm 0.49$ ) had similar values, and was found to exceed significantly the theoretic value for linear systems (close to 1)

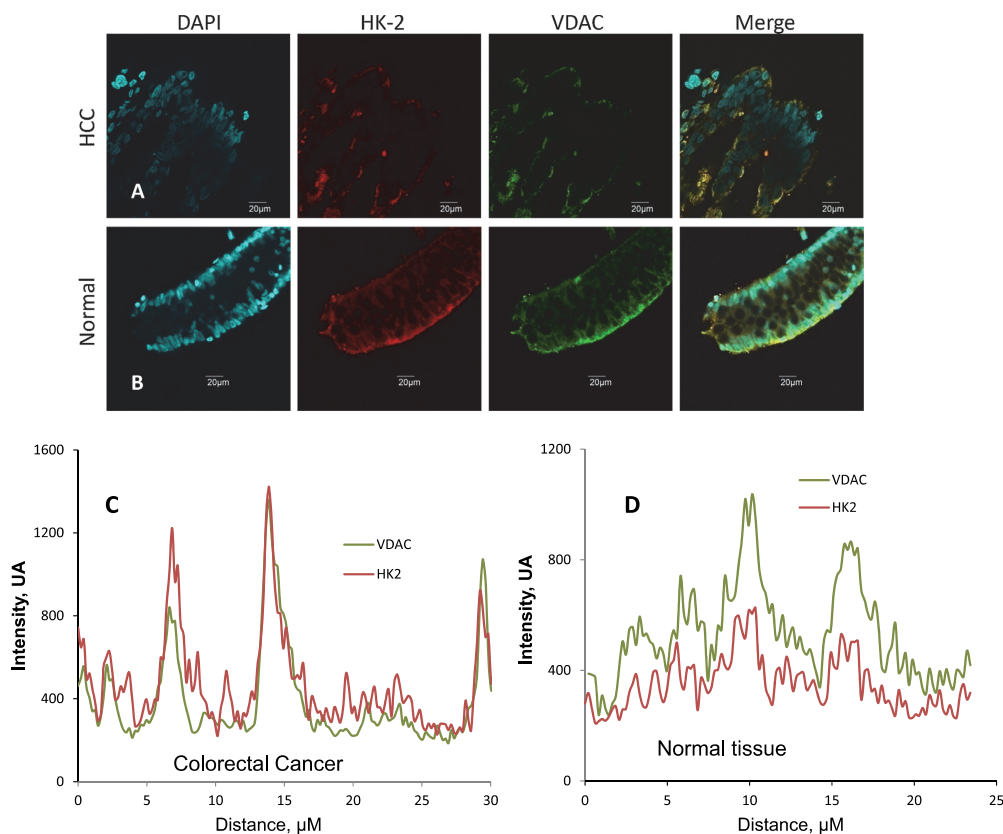


**Fig. 9.** Confocal imaging immunofluorescence of hexokinase-2 (HK-2), mitochondrial VDAC and their colocalization in saponin-skinned human colorectal cancer (HCC) fibers (A) and adjacent normal tissue (B) obtained by immunocytochemistry: blue fluorescence (nucleus, DAPI), red color indicates the presence of HK-2 (Cy-3 labeled antibody), green fluorescence corresponds to the outer mitochondrial membrane VDAC (DyLight-488) and yellow color is superposition of HK-2 and VDAC. Parts C and D indicate the distribution of fluorescent signals derived from HK-2 and VDAC in tumor and normal tissue samples. The images clearly show that HCC cells contain a number of mitochondria and that in these cells the HK-2 is bound to VDAC. This can mediate, according to the hypothesis of Pedersen and colleagues (Pedersen, 2008), a Warburg phenotype of malignancies.

(Kholodenko and Westerhoff, 1993). These values are higher than for some normal non-proliferative cells with high rates of OXPHOS (for adult rat cardiomyocytes the  $\Sigma = 1.33$ ) (Tepp et al., 2011). It can be concluded that the function of respiratory chain and ATP synthasome complexes in intestinal cells may differ considerably from that in non-proliferative muscle cells of oxidative type. One possible explanation for the increased sum of the FCCs may be due to the existence of direct channeling of substrates between the protein complexes or formation of supercomplexes (Kholodenko and Westerhoff, 1993).

Supplementary material related to this article can be found, in the online version, at <http://dx.doi.org/10.1016/j.biocel.2014.09.004>.

#### 4. Discussion

So far, HCC was considered as a tumor of the Warburg phenotype having high rates of glucose consumption associated with the deregulated OXPHOS system (Chung et al., 1999; Dias et al., 2007; Haber et al., 1998; Izuishi et al., 2012; Jun et al., 2011; Koukourakis et al., 2005). Some *in vitro* studies suggest that HCC cells have gone through a metabolic shift from OXPHOS to aerobic glycolysis; so it was reported (Donohoe Dallas et al., 2012) that unlike normal

intestinal cells, colorectal carcinomas cannot utilize short-chain fatty acids (butyrate, propionic acid) as an energy source and carbon donor. Instead they utilize glucose and glutamine as the main providers of energy and carbon for biosynthetic processes (Zhdanov et al., 2014).

Our studies indicate that HCC is not a pure glycolytic tumor and that the OXPHOS system is the substantial source of ATP in these malignant cells; it was found that the cells contain an increased, in comparison with normal tissue, amount of mitochondria (Fig. 4), fully-functioning respiratory chain complexes, and display higher rates of basal and ADP-activated respiration (Figs. 1–3). Different authors have shown that the mitochondrial biogenesis may be up-regulated in some cancer types *versus* healthy tissues; e.g. (Jose and Rossignol, 2013). Unexpectedly, one of the reasons for this change may be related to stimulated mitochondrial biogenesis. Overexpression of MYC proto-oncogene is characteristic for human colorectal carcinomas (Dang et al., 2009) and this event could lead to a strong increase in the content of mitochondria, since native MYC (encoding a transcription factor c-MYC) is known to play a pivotal role in the regulation of mitochondrial biogenesis. It has been previously reported that MYC null rat fibroblasts have diminished mitochondrial mass and decreased number of normal mitochondria (Li et al., 2005). We found that the rate of

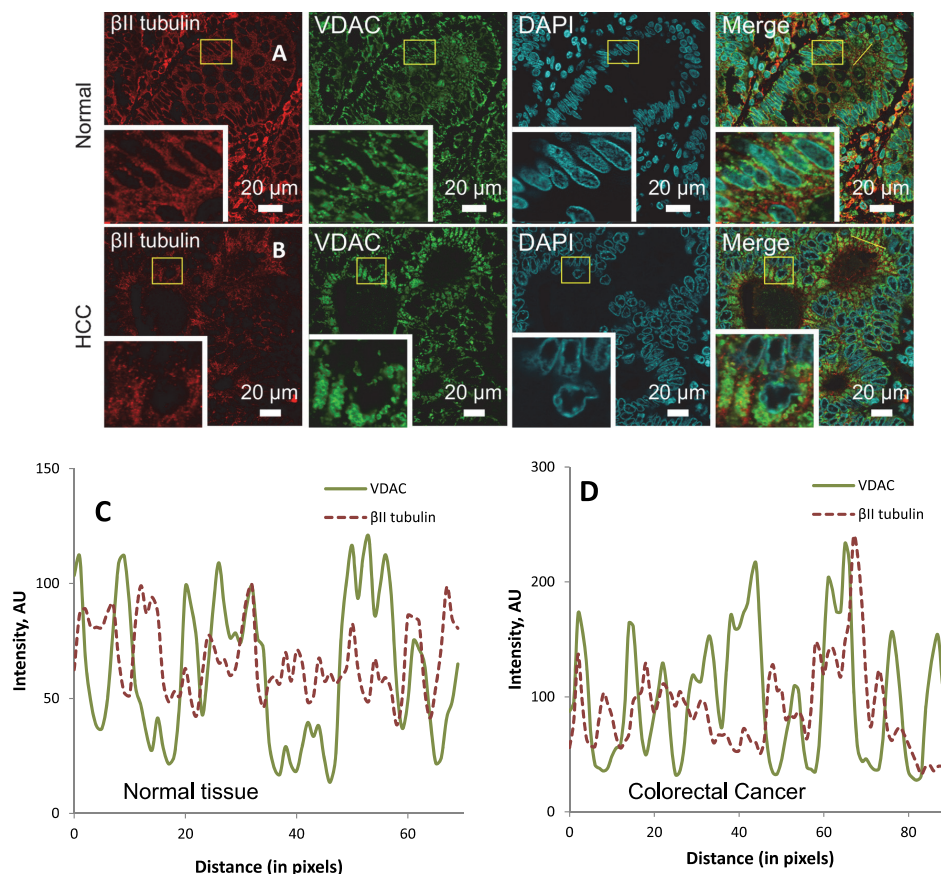


**Fig. 10.** Confocal imaging immunofluorescence of mitochondrial VDAC, cytoskeletal  $\beta$ II-tubulin, and their colocalization in normal (A) and human colorectal cancer (HCC) (B) tissue slices. Here: blue fluorescence (nucleus, DAPI); red color indicates the presence of  $\beta$ II-tubulin (Dylight-550 labeled Ig. ab96880), green color is the staining for VDAC, and yellow color is superposition of VDAC and  $\beta$ II-tubulin. Parts C and D indicate the distribution of fluorescent signals derived from VDAC and  $\beta$ II-tubulin in tumor and normal tissue samples. Immunofluorescence imaging showed a weak association between  $\beta$ II-tubulin and mitochondrial VDAC in the studied samples.

mitochondrial respiration in HCC fibers is higher than in surrounding normal tissues. It could be also hypothesized that a reverse Warburg effect occurs in colorectal carcinomas; *i.e.*, carcinoma cells cause reprogramming the energy metabolism of normal tissues from OXPHOS towards aerobic glycolysis (Bonuccelli et al., 2010a,b). However more extensive studies are needed to support this hypothesis.

It is clearly shown that there are striking differences between the kinetics of respiration regulation by ADP in colorectal carcinomas and in healthy tissue. In normal tissues, the apparent  $K_m$  value for exogenously added ADP was found to exceed nearly 2 times that for tumor tissue (Fig. 3). Low affinity of mitochondria for ADP in control tissue, in comparison with tumor tissue, is obviously a result of diffusion restriction of extracellular ADP. Several possible explanations can be proposed to clarify such changes in the regulation of ADP-activated respiration. The higher  $K_m$  value for ADP in normal tissue, as compared with HCC fibers, could be mediated by very rapid utilization of ADP in AK reactions, but this pathway may be excluded since the total AK activity in non-tumorous tissue was even smaller than in cancer (Table 1) and it has been shown that complete inhibition of AK by diadenosine pentaphosphate had no effect on the affinity of mitochondria for ADP in skinned

muscle fibers (Saks et al., 1991). The diffusion restrictions for extracellular ADP in non-transformed cells may be due to more dense and developed cytoskeleton which was extensively investigated in our previous works (Kaambre et al., 2012; Kuznetsov et al., 1996; Kuznetsov et al., 2008; Saks et al., 2003; Vendelin et al., 2004). Higher levels of  $\beta$ II-tubulin expression in normal intestinal tissues could be responsible for the observed high  $K_m$  value. It was recently shown that in normal oxidative muscle cells,  $\beta$ II-tubulin could bind to VDAC and selectively limit the permeability of the MOM for adenine nucleotides (Guzun et al., 2011a; Rostovtseva et al., 2008) and therefore mediate the high  $K_m$  values (about 300–500  $\mu$ M). The  $K_m$  for rat permeabilized cardiac non-beating HL-1 tumor cells was by more than order of magnitude lower (Anmann et al., 2006; Guzun et al., 2011a). Our previous studies of intracellular distribution of different  $\beta$ -tubulin isotypes using immunocytochemistry revealed the role of the  $\beta$ II-tubulin as one of the key potential regulatory proteins of VDAC channel permeability in adult rat cardiomyocytes (Gonzalez-Granillo et al., 2012; Guzun et al., 2012). Surprisingly the levels of  $\beta$ II-tubulin expression in HCC and normal adjacent tissue are comparable in spite of the differences in MOM permeability and  $\beta$ II-tubulin isotype does not display very clear colocalization with VDAC (Fig. 10). One possible explanation

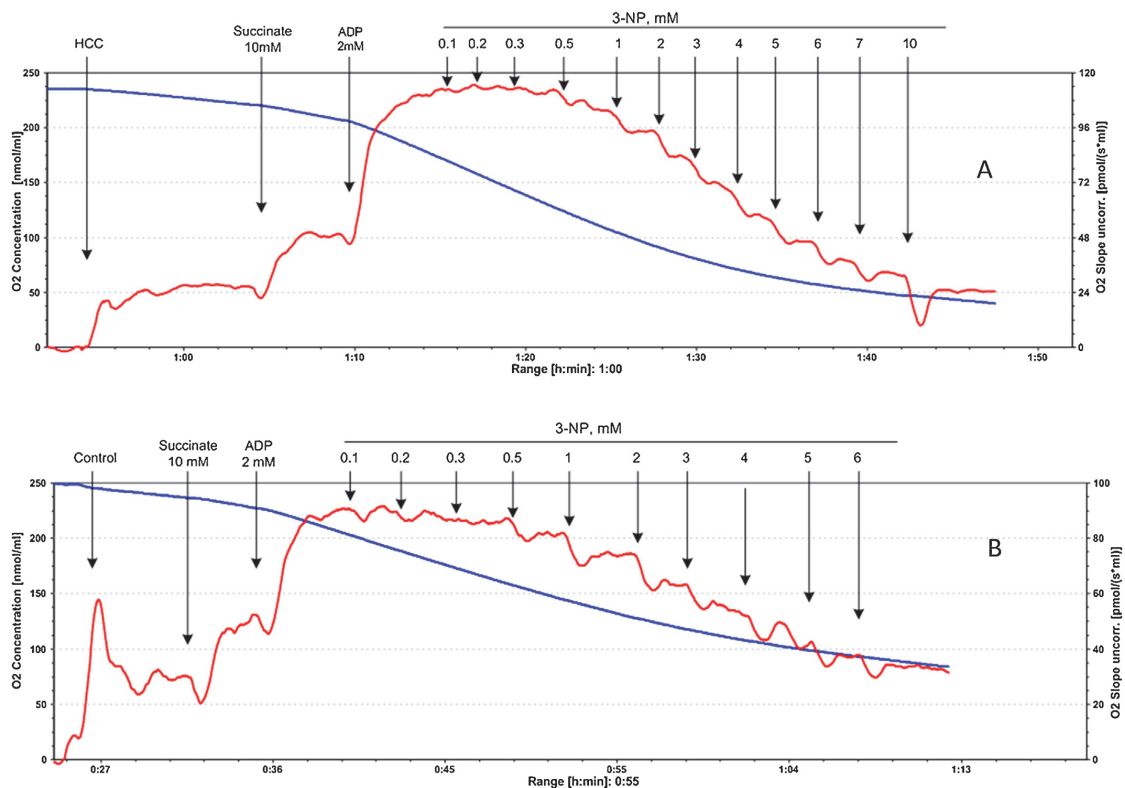


**Fig. 11.** Representative tracing of change in the rate of O<sub>2</sub> consumption (red lines) by permeabilized human colorectal cancer (A) and adjacent normal tissue fibers (B) during their titration with increasing concentrations of 3-nitropropionic acid (3-NP, a specific inhibitor of Complex-II) in the presence of 10 mM succinate, and direct activation of mitochondrial respiration with 2 mM ADP; on these figures, final concentrations of 3-NP are shown at every steady state. (For interpretation of the references to color in this figure legend, the reader is referred to the web version of the article.)

for this phenomenon is that some other proteins like actin, desmin, microtubule-associated proteins, plectin, other tubulin isoforms or their posttranslational modifications could be involved in the regulation of permeability of mitochondrial VDAC towards adenine nucleotides (Appaix et al., 2003; Guzun et al., 2012). Furthermore, it is possible that differences in MOM permeability for ADP and ATP could arise from distinct expression patterns of VDAC and/or ANT isoforms. Recently it was found that in some tissues of oxidative type –  $\alpha$ -enolase, a glycolytic enzyme – can bind with mitochondrial VDAC1, to display anti-apoptotic activity (Gao et al., 2014). Changed profile of this enzyme isotypes could also influence the VDAC selective permeability for adenine nucleotides.

And last, but not least, in our previous works it was shown that the  $\beta$ II isotype of tubulin is closely associated with mitochondria and co-expressed with mitochondrial creatine kinase (MtCK). MtCK coupled with ATP synthasome, as well as with VDAC, provide functional compartmentation of ATP in mitochondria and energy transfer into cytoplasm via phosphotransfer network. Therefore, direct transfer of mitochondrially produced ATP to sites of its utilization is largely avoided under physiological conditions, but may occur in pathology (Gonzalez-Granillo et al., 2012; Saks et al., 2010, 2012; Tepp et al., 2011; Timohhina et al., 2009).

The CK system, playing one of the key roles in production of PCr and maintaining the energy homeostasis in normal colonocytes and muscle cells, is downregulated in HCC cells and this result is in accordance with some literature data (Joseph et al.,

1997; Kasimos et al., 1990). Our studies showed that during carcinogenesis total CK activity was strongly decreased (Table 1). Furthermore, in normal intestinal cells elevated levels of uMtCK expressions were noticed together with tight coupling between the MtCK and OXPHOS system, but such functional coupling was absent in HCC cells (Figs. 5 and 6). The same functional coupling had been reported in cardiac and slow twitch skeletal muscle cells (Guzun et al., 2009; Monge et al., 2009; Seppet et al., 2001; Timohhina et al., 2009). Possible signaling pathways mediating the downregulation of CK system in HCC cells remain still unclear. These results lead to the conclusion that uMtCK plays a minor role in the cellular energy transfer and the functional coupling of MtCK with ANT in HCC cells. It was recently reported that in HCC cells BB-CK has an unusual profile of intracellular distribution, where BB-CK is expressed not only in the cytoplasm (characteristic for normal cells) but predominantly in the cell nucleus (Balasubramani et al., 2006). It was also suggested that the downregulation of BB-CK in HCC cells may play an important role in the tumor progression (Mooney et al., 2011).

AK isoenzymes are important regulators of the composition of the cellular adenine nucleotide pool and determinants of the energy charge of cells. The presence of nine AK isoenzymes have been reported in vertebrates (Panayiotou et al., 2011). Proteomics studies have shown that both cytosolic (AK1) and mitochondrial (AK2) isoenzymes are expressed in human colon epithelial cells (Birkenkamp-Demtroder et al., 2005; Li et al., 2004). But according to literature, little is known about the expression profile of

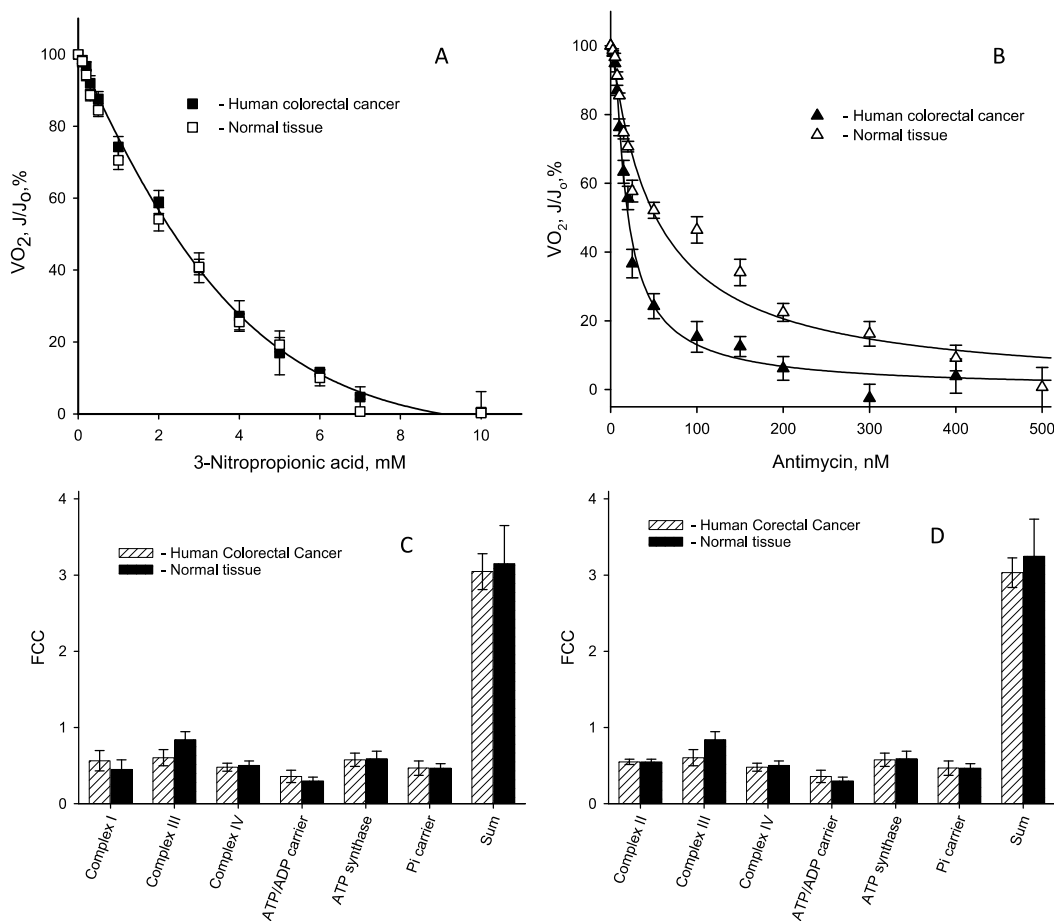


**Fig. 12.** Titration curves of inhibition of the mitochondrial respiratory chain complexes in permeabilized human colorectal cancer and non-tumorous adjacent tissue fibers with: (A) 3-nitropropionic acid, in the presence of 10 mM succinate as a respiratory substrate (without malate and glutamate); and (B) antimycin-A, respiratory substrates were 2 mM malate and 5 mM glutamate and 10 mM succinate. Similar titration curves were constructed for other mitochondrial respiratory chain and the ATP synthasome complexes; see in Supplementary Fig. 4. On the basis of these graphs, corresponding flux control coefficients were calculated. Two ways of electron transfer were examined: (C) NADH and (D) succinate dependent (FADH) electron transfers. On these figures, every data point was calculated as the mean of 10–15 independent experiments, bars are SEM.

AK isoenzymes and the role of AK system in maintaining energy homeostasis in colorectal carcinomas. Nevertheless, in some malignancies expression of AK2 was found, which had an important role in generation of ATP, providing up to 50% of the total ATP used by mitochondrially-bound HK (Nelson and Kabir, 1985).

Precise coupling of spatially separated intracellular ATP production and ATP-consuming processes is fundamental to the bioenergetics of living organisms, ensuring a fail-safe operation of the energetic system over a broad range of cellular functional activities. For this purpose colonic epithelial cells, like neurons, cardiac and skeletal muscles and many other cells, exert CK and AK systems (Dzeja and Terzic, 2003, 2009; Joseph et al., 1997; Saks et al., 2003). Previous studies on different types of carcinomas, such as human breast carcinoma (Kaambre et al., 2012), neuroblastoma (Klepinin et al., 2014), and sarcoma cells (Bera et al., 2008; Guzun et al., 2011b; Patra et al., 2008, 2012) showed that the suppression of the CK system is associated with loss of uMtCK. In addition, Dzeja et al. (1996) described that suppression of CK-catalyzed phosphotransfer

network might result in increased phosphoryl transfer by AK in intact skeletal muscle. Therefore, we propose that the revealed downregulation of CK system may be casually-linked with alterations of the AK phosphotransfer system. In this study we found that the total AK activity in HCC cells exceeds that of adjacent normal tissue cells (Table 1). Also, our respiratory experiments show that HCC cells have higher coupling between the OXPHOS and AK reactions than normal colon cells (Fig. 7). Further studies are needed to determine the profile of AK isoforms expression in HCC cells, as well as their role in tumor energy metabolism.

We evaluated the glycolytic capacity of human colorectal and adjacent normal tissue samples by using hexokinase activities (see Table 1). HCC cells express both HK-1 and HK-2, but levels of these isoenzymes as well as the total glycolytic activity in tumor tissue extracts, do not differ from those in normal tissue samples (Figs. 5 and 9 and Table 1). This obtained result is in a good agreement with some literature data (Chung et al., 1999).



Consequently another mechanism, besides high HK activity in the malignancy, could be responsible for the elevated rates of glucose consumption detected by FDG-PET in colorectal cancers. This could be mediated through increased expression of the plasma membrane glucose transporter GLUT-1, which has already been demonstrated in human colorectal carcinomas (Izuishi et al., 2012). Possible two-compartment energy metabolism also may be the reason of the positive FDG-PET analysis, where the elevated rate of glucose consumption is the feature of the stromal cells.

We established that HK-2 is associated with the mitochondria in HCC cells (Fig. 9). Possible coupling of HK reactions with the OXPHOS system in these malignant cells could explain, to some degree, increased inclination of HCC cells to aerobic glycolysis. The obtained results strongly suggest that in human HCC cells high levels of HK-1 or HK-2 expression could be associated with binding either one or both isoforms to VDAC in the MOM. The interaction of ATP synthase, ANT, VDAC and HK as a single functional complex results in a rapid and very efficient production of glucose-6-phosphate (Mathupala et al., 2006), a precursor for other glycolytic steps and key biosynthetic metabolites via the pentose phosphate pathway and Krebs cycle. The mechanism of the Warburg effect proposed by Pedersen and colleagues (Pedersen, 2008) could only partly explain high rates of aerobic glycolysis in human colorectal carcinomas. Although, the expression levels of HK-1 and HK-2 were similar in tumor and nontumorous tissue (Fig. 5), we did not observe any stimulatory effect of exogenously added glucose on mitochondrial respiration in normal tissue (Fig. 8B). One of the possible explanations for such difference could be that the mitochondria of colorectal carcinomas have an increased binding capacity towards HK-1 and HK-2 in comparison with normal intestinal cells. Indeed, according to some literature data, the increased affinity of tumor mitochondria to HK-2 has already been registered in tumors of another histological type. It was recently hypothesized that some tubulin isotypes ( $\beta$ -tubulin class II) could compete with HK-2 for the binding sites on VDAC and downregulation of the  $\beta$ II-tubulin isotype could promote the HK binding mediating Warburg effect (Guzun et al., 2011a, 2012). Therefore, we studied the levels of  $\beta$ II-tubulin expression (by measurements of its mRNA content) and no substantial differences in expression of  $\beta$ II-tubulin between HCC and normal adjacent tissue cells were found (Figs. 5 and 10). Thus, the proposed model, linked with the competition between HK-2 and  $\beta$ II-tubulin for binding sites on VDAC, does not function in the case of HCC. In cancer cells, other cytoskeletal proteins and mechanisms could control the binding of HK-2 to VDAC, but these mechanisms have not been cleared yet. Furthermore, it is known that various tubulin isotypes can undergo many post-translational modifications, such as deetyrosination, acetylation, polyglutamylation and polyglycylation (Janke and Bulinski, 2011). In cancer cells, a spectrum of post-translational modifications of tubulin may differ remarkably from that in normal cells. This could seriously affect the binding capacity of modified tubulins to VDAC, their ability to compete with HK-2 for the binding sites on VDAC as well as regulation of permeability of adenine nucleotides through MOM.

Our results show that although the regulation of mitochondrial respiration in HCC cells differs from the normal oxidative type tissues, the OXPHOS, but not glycolysis, could play a key role in the generation of ATP. Our MCA inhibitor titration studies were carried out on Complex I, II, III, IV, ATP synthase, ANT and PIC upon direct activation of mitochondrial respiration with exogenously added ADP. All these coefficients were found to be with high values. The reason for these high control coefficients is not simply the diffusion restriction, since nearly the same concentration range of inhibitors corresponding FCCs were determined for isolated rat cardiomyocytes and differentiated or undifferentiated

neuroblastoma cells (Klepinin et al., 2014). The presence of albumin in the assay medium of detergent-permeabilized cells cannot be the reason for the high FCCs as proposed in the recent work of Moreno-Sanchez et al. (2014). The sum of FCCs for permeabilized cardiomyocytes determined upon direct activation with 2 mM ADP differed, in terms of the sums, by three times despite the use of the same concentrations of albumin (Klepinin et al., 2014). We found that in human HCC cells the control was distributed across several ATP-Synthasome complexes rather evenly, and the key sites of the regulation of respiration were Complex-III and ATP synthase. The same results were achieved for normal tissue. Our MCA studies show that FCCs for Complex-V (ATP synthase) (Fig. 12) do not differ between tumor and control samples. This finding was surprising; it was reported (Sanchez-Cenizo et al., 2010; Willers et al., 2010) that  $\beta$ -F<sub>1</sub>-ATPase catalytic subunit of the mitochondrial H<sup>+</sup>-ATP synthase is downregulated in human colorectal carcinomas and this was associated with upregulation of the ATPase inhibitory factor 1 expression.

It is most interesting that the sum of FCC(s) for ADP activated respiration in HCC cells and in normal intestinal cells exceeds considerably (>3-times) the theoretic value for linear systems (close to 1) (Kholodenko et al., 1993) (Fig. 12C and D). The value close to 1 was registered for isolated mitochondria and permeabilized cardiac muscle cells during occurrence of ADP activated respiration (Tepp et al., 2011). Previously the large sum of FCC(s) was seen for Cr-activated respiration in permeabilized rat heart cells with ADP recycling inside the ATP synthasome and uMtCK reactions and in permeabilized neuroblastoma cells (Klepinin et al., 2014; Tepp et al., 2011). The theory of MCA claims that in an ideal linear system the sum of FCCs should be 1 (Fell, 1997; Groen et al., 1982; Rossignol et al., 2000; Westerhoff et al., 2009), but may become higher if the system includes enzyme-enzyme interactions, direct substrate channeling and recycling within multi-enzyme complexes (i.e., if system becomes non-linear) (Kholodenko et al., 1993, 1994). In isolated mitochondria or permeabilized highly differentiated cells from normal tissue, the system of OXPHOS works typically as a quasi-linear system with the sum of FCCs close to 1, if respiration is activated with ADP (Moreno-Sanchez et al., 1991; Rossignol et al., 2000; Tepp et al., 2011). The high value (>3) of the sum of FCCs in mitochondrial respiration activated by ADP clearly shows that HCC as well as normal cells of the colon may have an altered structure of the mitochondrial respiratory chain, as compared with non-proliferating highly-differentiated cardiac and some skeletal muscle cells. Our results support the hypothesis that in human colon cells the mitochondrial OXPHOS system may contain super-complexes with direct substrate (electron carrier) channeling. The veracity of this conclusion is supported by many recent studies (Bianchi et al., 2004; Dudkina et al., 2010, 2011; Genova et al., 2008; Lenaz and Genova, 2010; Quarato et al., 2011; Vonck and Schafer, 2009). Quarato et al. (2011) have examined kinetics of respiration regulation by applying MCA for permeabilized human hepatoma cells and found high FCCs in the de-energized state for three protonmotive Complexes I, III and IV, for which the sum of FCCs exceeded 1. Our results are in accordance with results from a series of studies performed by Lenaz and colleagues (Bianchi et al., 2004; Genova et al., 2008; Lenaz and Genova, 2009, 2010). These researchers, based on flux control analysis, showed that respiratory complexes might kinetically act as a single supramolecular unit, suggesting the existence of substrate channeling within supercomplexes. In this case, the sum of FCCs significantly exceeds 1 (Bianchi et al., 2004; Genova et al., 2008; Lenaz and Genova, 2009, 2010). The presence of supramolecular respiratory complexes (called respirasomes) in mitochondria has been confirmed by electron microscopy, native gel-electrophoresis and single particle image processing (Lenaz et al., 2010; Lenaz and Genova, 2009, 2010).

The formation of respirasomes may be characteristic for cells (both normal and tumorous) which have high proliferative rates. In MCA, high sums of FFC(s) (in the range of 3–5.5, upon direct activation of mitochondrial respiration with exogenously added ADP) have been registered not only for permeabilized HCC and normal colon cells (Fig. 12), but also in the permeabilized tissue of human breast cancer ( $\Sigma = \sim 4$  (Kaambre et al., 2012)), undifferentiated (line N2a,  $\Sigma = 5.06$ ), and differentiated neuroblastoma cells ( $\Sigma = 3.9$ ) (Klepinin et al., 2014) where all of them are having high proliferative activity. But for highly differentiated cardiac cells, which have low proliferative activity, the sum of FCCs was found to be substantially lower, close to 1 ( $\Sigma = 1.33$  (Tepp et al., 2011)). At present, the mechanism(s) of respirasomes formation is an object of intensive studies. Supercomplex formation and distribution of respiratory complexes between supercomplex and their free forms depend upon the protein/lipid ratio and phospholipid composition (Lenaz and Genova, 2009; Vartak et al., 2013).

Several important functions have been suggested for the formation of respiratory supercomplexes. First – channeling of ubiquinol and cytochrome c, avoiding competition from other enzymes. Second – catalytic enhancement from reduced diffusion times of substrates, and stabilization of the respiratory chain complexes. Third – preventing the generation of superoxide by sequestration of the reactive intermediate ubi-semiquinone (Dudkina et al., 2010; Hoefs et al., 2012). Finally, formation of respirasomes may also protect cells from the mitochondrially-induced apoptosis through suppression of the cytochrome-c release into the cytoplasm.

## 5. Conclusion

Several new important aspects were uncovered during bioenergetic profiling of HCC. We concluded that the rate of oxygen consumption is higher in colorectal carcinomas as compared to normal adjacent tissues, and that in these tumor cells the OXPHOS system serves as the main provider of ATP. So, immunocytochemical studies have shown that HCC cells contain increased number mitochondria. This is also supported by the hypothesis that the total glucose-phosphorylating capacity of colorectal carcinomas does not differ from surrounding normal tissues. Nevertheless, it was revealed that in HCC cells HK-2 is bound to VDAC, and this could lead to an increased production of lactate by the cells. The kinetics of respiration regulation by ADP is significantly changed during carcinogenesis. Low affinity of mitochondria for ADP in control tissue, in contrast to that of tumor tissue, is obviously a result of diffusion restriction of extracellular ADP and further work is needed to unfold the possible mechanisms of this phenomenon. Thus, during carcinogenesis some specific alterations arise in the regulation of permeability of mitochondrial outer membrane. Our MCA studies have shown that ATP synthasome complexes remain almost unchanged and only small differences were observed in the distribution of control between ETC complexes (small variations in complex III). In the presented work it was shown that there is functional coupling between AK-catalyzed processes and the OXPHOS system in HCC cells, and this could play an important role in maintaining the energy homeostasis in these malignant cells. In HCC cells there is upregulation of AK processes associated with downregulation of the CK system and these events could play an important role in the tumor progression. More extensive studies on HCC are required to identify the precise reasons for this disorganization of cell structure and metabolic compartmentation; remodeling of mitochondria-associated membrane interactions, impairment of intramitochondrial energy conversion and changes in metabolic fluxes.

## Conflict of interest

The authors declare no conflict of interest.

## Acknowledgements

This work was supported by institutional research funding IUT (IUT23-1) of the Estonian Ministry of Education and Research, the Estonian Science Foundation grant no. 8987, and by the project “Aid for research and development in healthcare technology” of Archimedes Foundation no. 3.2.1001.11-0027.

## References

- Agathocleous M, Harris WA. Metabolism in physiological cell proliferation and differentiation. *Trends Cell Biol* 2013;23:484–92.
- Ames A. CNS energy metabolism as related to function. *Brain Res Rev* 2000;34:42–68.
- Anmann T, Guzun R, Beraud N, Pelloux S, Kuznetsov AV, Kogerman L, et al. Different kinetics of the regulation of respiration in permeabilized cardiomyocytes and in HL-1 cardiac cells. Importance of cell structure/organization for respiration regulation. *Biochim Biophys Acta* 2006;1757:1597–606.
- Appaix F, Kuznetsov AV, Usson Y, Kay L, Andrienko T, Olivares J, et al. Possible role of cytoskeleton in intracellular arrangement and regulation of mitochondria. *Exp Physiol* 2003;88:175–90.
- Balashramani M, Day BW, Schoen RE, Getzenberg RH. Altered expression and localization of creatine kinase B, heterogeneous nuclear ribonucleoprotein F, and high mobility group box 1 protein in the nuclear matrix associated with colon cancer. *Cancer Res* 2006;66:763–9.
- Bera S, Wallimann T, Ray S, Ray M. Enzymes of creatine biosynthesis, arginine and methionine metabolism in normal and malignant cells. *FEBS J* 2008;275:5899–909.
- Bianchi C, Genova ML, Parenti Castelli G, Lenaz G. The mitochondrial respiratory chain is partially organized in a supercomplex assembly. *J Biol Chem* 2004;279:36562–9.
- Birkenkamp-Demtroder K, Olesen SH, Sorensen FB, Laurberg S, Laiho P, Aaltonen LA, et al. Differential gene expression in colon cancer of the caecum versus the sigmoid and rectosigmoid. *Gut* 2005;54:374–84.
- Bonucci G, Tsigirgos A, Whitaker-Menezes D, Pavlides S, Pestell RG, Chiavarina B, et al. Ketones and lactate “fuel” tumor growth and metastasis: evidence that epithelial cancer cells use oxidative mitochondrial metabolism. *Cell Cycle* 2010a;9:3506–14.
- Bonucci G, Whitaker-Menezes D, Castello-Cros R, Pavlides S, Pestell RG, Fatatis A, et al. The reverse Warburg effect: glycolysis inhibitors prevent the tumor promoting effects of caveolin-1 deficient cancer associated fibroblasts. *Cell Cycle* 2010b;9:1960–71.
- Cesar Mde C, Wilson JE. Further studies on the coupling of mitochondrially bound hexokinase to intramitochondrially compartmented ATP, generated by oxidative phosphorylation. *Arch Biochem Biophys* 1998;350:109–17.
- Chung JK, Lee YJ, Kim C, Choi SR, Kim M, Lee K, et al. Mechanisms related to [<sup>18</sup>F]fluorodeoxyglucose uptake of human colon cancers transplanted in nude mice. *J Nucl Med* 1999;40:339–46.
- Curry JM, Tuluc M, Whitaker-Menezes D, Ames JA, Anantharaman A, Butera A, et al. Cancer metabolism, stemness and tumor recurrence: MCT1 and MCT4 are functional biomarkers of metabolic symbiosis in head and neck cancer. *Cell Cycle* 2013;12:1371–84.
- Dang CV, Le A, Gao P. MYC-induced cancer cell energy metabolism and therapeutic opportunities. *Clin Cancer Res* 2009;15:6479–83.
- Dias AR, Nahas SC, Camargo EE, Nahas CS. Recent evidences of the use of [<sup>18</sup>F]fluorodeoxyglucose positron emission tomography in the management of colorectal cancer. *J Surg Educ* 2007;64:114–9.
- Diers AR, Broniowska KA, Chang CF, Hogg N. Pyruvate fuels mitochondrial respiration and proliferation of breast cancer cells: effect of monocarboxylate transporter inhibition. *Biochem J* 2012;444:561–71.
- Donohoe Dallas R, Collins Leonard B, Wali A, Bigler R, Sun W, Bultman Scott J. The Warburg effect dictates the mechanism of butyrate-mediated histone acetylation and cell proliferation. *Mol Cell* 2012;48:612–26.
- Dzeja P, Terzic A. Adenylate kinase and AMP signaling networks: metabolic monitoring, signal communication and body energy sensing. *Int J Mol Sci* 2009;10:1729–72.
- Dzeja PP, Zeleznikar RJ, Goldberg ND. Suppression of creatine kinase-catalyzed phosphotransfer results in increased phosphoryl transfer by adenylate kinase in intact skeletal muscle. *J Biol Chem* 1996;271:12847–51.
- Dzeja PP, Terzic A. Phosphotransfer networks, cellular energetics. *J Exp Biol* 2003;206:2039–47.
- Dzeja PP, Vitkevicius KT, Redfield MM, Burnett JC, Terzic A. Adenylate kinase-catalyzed phosphotransfer in the myocardium: increased contribution in heart failure. *Circ Res* 1999;84:1137–43.
- Dudkina NV, Koufil R, Peters K, Braun H-P, Boekema EJ. Structure and function of mitochondrial supercomplexes. *Biochim Biophys Acta (BBA): Bioenergetics* 2010;1797:664–70.

- Dudkina NV, Kudryashev M, Stahlberg H, Boekema EJ. Interaction of complexes I, III, and IV within the bovine respirasome by single particle cryoelectron tomography. *Proc Natl Acad Sci USA* 2011;108:15196–200.
- Fell D. Understanding the control of metabolism. London, Miami: Portland Press; 1997.
- Fell D. Metabolic control analysis. In: Alberghina L, Westerhoff HV, editors. *Systems biology*. Berlin: Springer Verlag; 2005. p. 69–80.
- Fulda S, Galluzzi L, Kroemer G. Targeting mitochondria for cancer therapy. *Nat Rev Drug Discov* 2010;9:447–64.
- Gao S, Li H, Cai Y, Ye J, -T, Liu Z, -P, Lu J, et al. Mitochondrial binding of  $\alpha$ -enolase stabilizes mitochondrial membrane: its role in doxorubicin-induced cardiomyocyte apoptosis. *Arch Biochem Biophys* 2014;542:46–55.
- Gellerich F, Saks VA. Control of heart mitochondrial oxygen consumption by creatine kinase: the importance of enzyme localization. *Biochem Biophys Res Commun* 1982;105:1473–81.
- Gellerich FN, Kunz WS, Bohnsack R. Estimation of flux control coefficients from inhibitor titrations by non-linear regression. *FEBS Lett* 1990;274:167–70.
- Gellerich FN, Laterveer FD, Zierz S, Nicolay K. The quantitation of ADP diffusion gradients across the outer membrane of heart mitochondria in the presence of macromolecules. *Biochim Biophys Acta* 2002;1554:48–56.
- Genova ML, Baracca A, Biondi A, Casalena G, Faccioli M, Falasca AI, et al. Is supercomplex organization of the respiratory chain required for optimal electron transfer activity? *Biochim Biophys Acta* 2008;1777:740–6.
- Geschwind JF, Georgiades CS, Ko YH, Pedersen PL. Recently elucidated energy catabolism pathways provide opportunities for novel treatments in hepatocellular carcinoma. *Expert Rev Anticancer Ther* 2004;4:449–57.
- Gnaiger E. Oxygen solubility in experimental media. *Mitochondrial Physiol Netw* 2001;6:1–6.
- Gogvadze V, Orrenius S, Zhivotovsky B. Mitochondria as targets for cancer chemotherapy. *Semin Cancer Biol* 2009;19:57–66.
- Goldenthal MJ, Marín-García J. Mitochondrial signaling pathways: a receiver/integrator organelle. *Mol Cell Biochem* 2004;262:1–16.
- Gonzalez-Granillo M, Grichine A, Guzun R, Ussov Y, Tepp K, Chekulayev V, et al. Studies of the role of tubulin beta II isotype in regulation of mitochondrial respiration in intracellular energetic units in cardiac cells. *J Mol Cell Cardiol* 2012;52:437–47.
- Groen AK, Wanders RJ, Westerhoff HV, van der Meer R, Tager JM. Quantification of the contribution of various steps to the control of mitochondrial respiration. *J Biol Chem* 1982;257:2754–7.
- Gruno M, Peet N, Seppet E, Kadaja L, Paju K, Eimre M, et al. Oxidative phosphorylation and its coupling to mitochondrial creatine and adenylate kinases in human gastric mucosa. *Am J Physiol Regul Integr Comp Physiol* 2006;291:R936–46.
- Guzun R, Gonzalez-Granillo M, Karu-Varikmaa M, Grichine A, Ussov Y, Kaambre T, et al. Regulation of respiration in muscle cells in vivo by VDAC through interaction with the cytoskeleton and MitCK within mitochondrial interactosome. *Biochim Biophys Acta* 2012;1818:1545–54.
- Guzun R, Karu-Varikmaa M, Gonzalez-Granillo M, Kuznetsov AV, Michel L, Cottet-Rousselle C, et al. Mitochondria-cytoskeleton interaction: distribution of beta-tubulins in cardiomyocytes and HL-1 cells. *Biochim Biophys Acta* 2011a;1807:458–69.
- Guzun R, Timohhina N, Tepp K, Gonzalez-Granillo M, Shevchuk I, Chekulayev V, et al. Systems bioenergetics of creatine kinase networks: physiological roles of creatine and phosphocreatine in regulation of cardiac cell function. *Amino Acids* 2011b;40:1333–48.
- Guzun R, Timohhina N, Tepp K, Monge C, Kaambre T, Sikk P, et al. Regulation of respiration controlled by mitochondrial creatine kinase in permeabilized cardiac cells in situ. Importance of system level properties. *Biochim Biophys Acta* 2009;1787:1089–105.
- Haber RS, Rathana A, Weiser KR, Pritsker A, Itzkowitz SH, Bodian C, et al. GLUT1 glucose transporter expression in colorectal carcinoma: a marker for poor prognosis. *Cancer* 1998;83:34–40.
- Hoefs SJG, Rodenburg RJ, Smeitink JAM, van den Heuvel LP. Molecular base of biochemical complex I deficiency. *Mitochondrion* 2012;12:520–32.
- Huang LS, Sun G, Cobessi D, Wang AC, Shen JT, Tung EY, et al. 3-Nitropropionic acid is a suicide inhibitor of mitochondrial respiration that, upon oxidation by complex II, forms a covalent adduct with a catalytic base arginine in the active site of the enzyme. *J Biol Chem* 2006;281:5965–72.
- Izuishi K, Yamamoto Y, Sano T, Takebayashi R, Nishiyama Y, Mori H, et al. Molecular mechanism underlying the detection of colorectal cancer by <sup>18</sup>F-2-fluoro-2-deoxy-D-glucose positron emission tomography. *J Gastrointest Surg* 2012;16:394–400.
- Janke C, Bulinski JC. Post-translational regulation of the microtubule cytoskeleton: mechanisms and functions. *Nat Rev Mol Cell Biol* 2011;12:773–86.
- Jose C, Rossignol R. Rationale for mitochondria-targeting strategies in cancer bioenergetic therapies. *Int J Biochem Cell Biol* 2013;45:123–9.
- Joseph J, Cardesa A, Carreras J. Creatine kinase activity and isoenzymes in lung, colon and liver carcinomas. *Br J Cancer* 1997;76:600–5.
- Jun YJ, Jiang SM, Han HL, Lee KH, Jung KS, Paik SS. Clinicopathologic significance of GLUT1 expression and its correlation with Apmf-1 in colorectal adenocarcinoma. *World J Gastroenterol* 2011;17:1866–73.
- Kaambre T, Chekulayev V, Shevchuk I, Karu-Varikmaa M, Timohhina N, Tepp K, et al. Metabolic control analysis of cellular respiration in situ in intraoperative samples of human breast cancer. *J Bioenerg Biomembr* 2012;44:539–58.
- Kasimos JN, Merchant TE, Gierke LW, Glonek T. 31P magnetic resonance spectroscopy of human colon cancer. *Cancer Res* 1990;50:527–32.
- Kholodenko BN, Cascante M, Westerhoff HV. Control theory of metabolic channelling. *Mol Cell Biochem* 1994;133–134:313–31.
- Kholodenko BN, Demin OV, Westerhoff HV. 'Channelled' pathways can be more sensitive to specific regulatory signals. *FEBS Lett* 1993;320:75–8.
- Kholodenko BN, Westerhoff HV. Metabolic channelling and control of the flux. *FEBS Lett* 1993;320:71–4.
- Klepinin A, Chekulayev V, Timohhina N, Shevchuk I, Tepp K, Kaldma A, et al. Comparative analysis of some aspects of mitochondrial metabolism in differentiated and undifferentiated neuroblastoma cells. *J Bioenerg Biomembr* 2014;46:17–31.
- Koukourakis MI, Giatromanolaki A, Simopoulos C, Polychronidis A, Sivridis E. Lactate dehydrogenase 5 (LDH5) relates to up-regulated hypoxia inducible factor pathway and metastasis in colorectal cancer. *Clin Exp Metastasis* 2005;22:25–30.
- Kuznetsov AV, Tiivel T, Sikk P, Kaambre T, Kay L, Daneshmand Z, et al. Striking differences between the kinetics of regulation of respiration by ADP in slow-twitch and fast-twitch muscles in vivo. *Eur J Biochem* 1996;241:909–15.
- Kuznetsov AV, Veksler V, Gellerich FN, Saks V, Margreiter R, Kunz WS. Analysis of mitochondrial function in situ in permeabilized muscle fibers, tissues and cells. *Nat Protoc* 2008;3:965–76.
- Leandro-García LJ, Leskela S, Landa I, Montero-Conde C, Lopez-Jimenez E, Leton R, et al. Tumoral and tissue-specific expression of the major human beta-tubulin isotypes. *Cytoskeleton (Hoboken)* 2010;6:214–23.
- Lenaz G, Baracca A, Barbero G, Bergamini C, Dalmondo ME, Del Sole M, et al. Mitochondrial respiratory chain super-complex I–III in physiology and pathology. *Biochim Biophys Acta (BBA): Bioenergetics* 2010;1797:633–40.
- Lenaz G, Genova ML. Structural and functional organization of the mitochondrial respiratory chain: a dynamic super-assembly. *Int J Biochem Cell Biol* 2009;41:1750–72.
- Lenaz G, Genova ML. Structure and organization of mitochondrial respiratory complexes: a new understanding of an old subject. *Antioxidants Redox Signal* 2010;12:961–1008.
- Li F, Wang Y, Zeller KI, Potter JJ, Wonsley DR, O'Donnell KA, et al. Myc stimulates nuclear encoded mitochondrial genes and mitochondrial biogenesis. *Mol Cell Biol* 2005;25:6225–34.
- Li XM, Patel BB, Blagoi EL, Patterson MD, Seeholzer SH, Zhang T, et al. Analyzing alkaline proteins in human colon crypt proteome. *J Proteome Res* 2004;3:821–33.
- Lienhard GE, Secemski II. P<sub>1</sub>P<sub>5</sub>-D(adenosine-5')pentaphosphate, a potent multi-substrate inhibitor of adenylate kinase. *J Biol Chem* 1973;248:1121–3.
- Lunt SY, VanderHeiden MG. Aerobic glycolysis: meeting the metabolic requirements of cell proliferation. *Annu Rev Cell Dev Biol* 2011;27:441–64.
- Majewski N, Nogueira V, Bhaskar P, Coy PE, Skeen JE, Gottlob K, et al. Hexokinase-mitochondria interaction mediated by Akt is required to inhibit apoptosis in the presence or absence of Bax and Bak. *Mol Cell* 2004;16:819–30.
- Marín-Hernández A, Rodríguez-Enriquez S, Vital-González PA, Flores-Rodríguez FL, Macías-Silva M, Sosa-Garrocho M, et al. Determining and understanding the control of glycolysis in fast-growing tumor cells. Flux control by an over-expressed but strongly product-inhibited hexokinase. *FEBS J* 2006;273:1975–88.
- Martínez-Outschoorn UE, Pavlides S, Howell A, Pestell RG, Tanowitz HB, Sotgia F, et al. Stromal-epithelial metabolic coupling in cancer: integrating autophagy and metabolism in the tumor microenvironment. *Int J Biochem Cell Biol* 2011;43:1045–51.
- Martínez-Outschoorn UE, Sotgia F, Lisanti MP. Power surge: supporting cells "fuel" cancer cell mitochondria. *Cell Metab* 2012;15:4–5.
- Mathupala SP, Ko YH, Pedersen PL. Hexokinase II: cancer's double-edged sword acting as both facilitator and gatekeeper of malignancy when bound to mitochondria. *Oncogene* 2006;25:4777–86.
- Monge C, Beraud N, Tepp K, Pelloux S, Chahboun S, Kaambre T, et al. Comparative analysis of the bioenergetics of adult cardiomyocytes and nonbeating HL-1 cells: respiratory chain activities, glycolytic enzyme profiles, and metabolic fluxes. *Can J Physiol Pharmacol* 2009;87:318–26.
- Mooney SM, Rajagopalan K, Williams BH, Zeng Y, Christudass CS, Li Y, et al. Creatine kinase brain overexpression protects colorectal cells from various metabolic and non-metabolic stresses. *J Cell Biochem* 2011;112:1066–75.
- Moreno-Sánchez R, Devars S, Lopez-Gomez F, Uribe A, Corona N. Distribution of control of oxidative phosphorylation in mitochondria oxidizing NAD-linked substrates. *Biochim Biophys Acta* 1991;1060:284–92.
- Moreno-Sánchez R, Marín-Hernández A, Saavedra E, Pardo JP, Ralph SJ, Rodríguez-Enriquez S. Who controls the ATP supply in cancer cells? Biochemistry lessons to understand cancer energy metabolism. *Int J Biochem Cell Biol* 2014;50:10–23.
- Moreno-Sánchez R, Rodríguez-Enriquez S, Marín-Hernández A, Saavedra E. Energy metabolism in tumor cells. *FEBS J* 2007;274:1393–418.
- Moreno-Sánchez R, Rodríguez-Enriquez S, Saavedra E, Marín-Hernández A, Gallardo-Pérez JC. The bioenergetics of cancer: is glycolysis the main ATP supplier in all tumor cells? *BioFactors* 2009;35:209–25.
- Moreno-Sánchez R, Saavedra E, Rodríguez-Enriquez S, Gallardo-Pérez JC, Quezada H, Westerhoff HV. Metabolic control analysis indicates a change of strategy in the treatment of cancer. *Mitochondrion* 2010;10:626–39.
- Moreno-Sánchez R, Saavedra E, Rodríguez-Enriquez S, Olin-Sandoval V. Metabolic control analysis: a tool for designing strategies to manipulate metabolic pathways. *J Biomed Biotechnol* 2008;2008:597913.
- Mozzetti S, Ferlini C, Concolino P, Filippetti F, Raspaglio G, Prislei S, et al. Class III beta-tubulin overexpression is a prominent mechanism of paclitaxel resistance in ovarian cancer patients. *Clin Cancer Res* 2005;11:298–305.
- Nelson BD, Kabir F. Adenylate kinase is a source of ATP for tumor mitochondrial hexokinase. *Biochim Biophys Acta* 1985;841:195–200.

- Nieman KM, Kenny HA, Penicka CV, Ladanyi A, Buell-Gutbrod R, Zillhardt MR, et al. Adipocytes promote ovarian cancer metastasis and provide energy for rapid tumor growth. *Nat Med* 2011;17:1498–503.
- Panayiotou C, Solaroli N, Xu Y, Johansson M, Karlsson A. The characterization of human adenylate kinases 7 and 8 demonstrates differences in kinetic parameters and structural organization among the family of adenylate kinase isoenzymes. *Biochem J* 2011;433:527–34.
- Pastorino JG, Hoek JB. Regulation of hexokinase binding to VDAC. *J Bioenerg Biomembr* 2008;40:171–82.
- Patra S, Bera S, SinhaRoy S, Ghoshal S, Ray S, Basu A, et al. Progressive decrease of phosphocreatine, creatine and creatine kinase in skeletal muscle upon transformation to sarcoma. *FEBS J* 2008;275:3236–47.
- Patra S, Ghosh A, Roy SS, Bera S, Das M, Talukdar D, et al. A short review on creatine-creatine kinase system in relation to cancer and some experimental results on creatine as adjuvant in cancer therapy. *Amino Acids* 2012;42:2319–30.
- Pedersen PL. The cancer cell's "power plants" as promising therapeutic targets: an overview. *J Bioenerg Biomembr* 2007a;39:1–12.
- Pedersen PL. Warburg, me and Hexokinase 2: multiple discoveries of key molecular events underlying one of cancers' most common phenotypes, the "Warburg Effect", i.e., elevated glycolysis in the presence of oxygen. *J Bioenerg Biomembr* 2007b;39:211–22.
- Pedersen PL. Voltage dependent anion channels (VDACs): a brief introduction with a focus on the outer mitochondrial compartment's roles together with hexokinase-2 in the "Warburg effect" in cancer. *J Bioenerg Biomembr* 2008;40:123–6.
- Quarato G, Piccoli C, Scrima R, Capitanio N. Variation of flux control coefficient of cytochrome c oxidase and of the other respiratory chain complexes at different values of protonmotive force occurs by a threshold mechanism. *Biochim Biophys Acta* 2011;1807:1114–24.
- Robey RB, Raval BJ, Ma J, Santos AV. Thrombin is a novel regulator of hexokinase activity in mesangial cells. *Kidney Int* 2000;57:2308–18.
- Rodríguez-Enríquez S, Gallardo-Pérez JC, Marín-Hernández A, Aguilar-Ponce JL, Mandujano-Tinoco EA, Meneses A, et al. Oxidative phosphorylation as a target to arrest malignant neoplasias. *Curr Med Chem* 2011;18:3156–67.
- Rodríguez-Enríquez S, Vital-González PA, Flores-Rodríguez FL, Marín-Hernández A, Ruiz-Azuara L, Moreno-Sánchez R. Control of cellular proliferation by modulation of oxidative phosphorylation in human and rodent fast-growing tumor cells. *Toxicol Appl Pharmacol* 2006;215:208–17.
- Rossignol R, Letellier T, Malgat M, Rocher C, Mazat J. Tissue variation in the control of oxidative phosphorylation: implication for mitochondrial diseases. *Biochem J* 2000;347(Pt 1):45–53.
- Rostovtseva TK, Sheldon KL, Hassanzadeh E, Monge C, Saks V, Bezrukov SM, et al. Tubulin binding blocks mitochondrial voltage-dependent anion channel and regulates respiration. *Proc Natl Acad Sci USA* 2008;105:18746–51.
- Saks V, Guzun R, Timohhina N, Tepp K, Varikmaa M, Monge C, et al. Structure-function relationships in feedback regulation of energy fluxes in vivo in health and disease: mitochondrial intercosome. *Biochim Biophys Acta* 2010;1797:678–97.
- Saks V, Kuznetsov A, Andrienko T, Usson Y, Appaix F, Guerrero K, et al. Heterogeneity of ADP diffusion and regulation of respiration in cardiac cells. *Biophys J* 2003;84:3436–56.
- Saks V, Kuznetsov AV, Gonzalez-Granillo M, Tepp K, Timohhina N, Karu-Varikmaa M, et al. Intracellular energetic units regulate metabolism in cardiac cells. *J Mol Cell Cardiol* 2012;52:419–36.
- Saks VA, Belikova YO, Kuznetsov AV. In vivo regulation of mitochondrial respiration in cardiomyocytes: specific restrictions for intracellular diffusion of ADP. *Biochim Biophys Acta* 1991;1074:302–11.
- Saks VA, Veksler VI, Kuznetsov AV, Kay L, Sikk P, Tiivel T, et al. Permeabilized cell and skinned fiber techniques in studies of mitochondrial function in vivo. *Mol Cell Biochem* 1998;184:81–100.
- Sanchez-Cenizo L, Formentini L, Aldea M, Ortega AD, Garcia-Huerta P, Sanchez-Arago M, et al. Up-regulation of the ATPase inhibitory factor 1 (IF1) of the mitochondrial H<sup>+</sup>-ATP synthase in human tumors mediates the metabolic shift of cancer cells to a Warburg phenotype. *J Biol Chem* 2010;285:25308–13.
- Seppet EK, Kaambre T, Sikk P, Tiivel T, Vija H, Tonkonogi M, et al. Functional complexes of mitochondria with Ca, MgATPases of myofibrils and sarcoplasmic reticulum in muscle cells. *Biochim Biophys Acta* 2001;1504:379–95.
- Small JR. Flux control coefficients determined by inhibitor titration: the design and analysis of experiments to minimize errors. *Biochem J* 1993;296(Pt 2):423–33.
- Small JR, Fell DA. Covalent modification and metabolic control analysis. Modification to the theorems and their application to metabolic systems containing covalently modifiable enzymes. *Eur J Biochem* 1990;191:405–11.
- Sotgia F, Martinez-Outschoorn UE, Pavlides S, Howell A, Pestell RG, Lisanti MP. Understanding the Warburg effect and the prognostic value of stromal caveolin-1 as a marker of a lethal tumor microenvironment. *Breast Cancer Res* 2011;13:213.
- Sotgia F, Whitaker-Menezes D, Martinez-Outschoorn UE, Flomenberg N, Birbe RC, Witkiewicz AK, et al. Mitochondrial metabolism in cancer metastasis: visualizing tumor cell mitochondria and the "reverse Warburg effect" in positive lymph node tissue. *Cell Cycle* 2012;11:1445–54.
- Zhdanov AV, Waters AHC, Golubeva AV, Dmitriev RI, Papkovsky DB. Availability of the key metabolic substrates dictates the respiratory response of cancer cells to the mitochondrial uncoupling. *Biochim Biophys Acta (BBA): Bioenergetics* 2014;1837:51–62.
- Zu XL, Guppy M. Cancer metabolism: facts, fantasy, and fiction. *Biochem Biophys Res Commun* 2004;313:459–65.
- Tepp K, Shevchuk I, Chekulayev V, Timohhina N, Kuznetsov AV, Guzun R, et al. High efficiency of energy flux controls within mitochondrial intercosome in cardiac intracellular energetic units. *Biochim Biophys Acta* 2011;1807:1549–61.
- Timohhina N, Guzun R, Tepp K, Monge C, Varikmaa M, Vija H, et al. Direct measurement of energy fluxes from mitochondria into cytoplasm in permeabilized cardiac cells in situ: some evidence for mitochondrial intercosome. *J Bioenerg Biomembr* 2009;41:259–75.
- Vander Heiden MG, Cantley LC, Thompson CB. Understanding the Warburg effect: the metabolic requirements of cell proliferation. *Science* 2009;324:1029–33.
- Warburg O, Wind F, Negelein E. The metabolism of tumors in the body. *J Gen Physiol* 1927;8:519–30.
- Vartak R, Porras C-M, Bai Y. Respiratory supercomplexes: structure, function and assembly. *Protein Cell* 2013;4:582–90.
- Vendelin M, Eimre M, Seppet E, Peet N, Andrienko T, Lemba M, et al. Intracellular diffusion of adenosine phosphates is locally restricted in cardiac muscle. *Mol Cell Biochem* 2004;256–257:229–41.
- Westerhoff HV, Winder C, Messiha H, Simeonidis E, Adamczyk M, Verma M, et al. Systems biology: the elements and principles of life. *FEBS Lett* 2009;583:3882–90.
- Whitaker-Menezes D, Martinez-Outschoorn UE, Lin Z, Ertel A, Flomenberg N, Witkiewicz AK, et al. Evidence for a stromal-epithelial "lactate shuttle" in human tumors: MCT4 is a marker of oxidative stress in cancer-associated fibroblasts. *Cell Cycle* 2011;10:1772–83.
- Willers IM, Isidoro A, Ortega AD, Fernandez PL, Cuezva JM. Selective inhibition of beta-F1-ATPase mRNA translation in human tumours. *Biochem J* 2010;426:319–26.
- Wisniewski E, Gellerich FN, Kunz WS. Distribution of flux control among the enzymes of mitochondrial oxidative phosphorylation in calcium-activated saponin-skinned rat musculus soleus fibers. *Eur J Biochem* 1995;230:549–54.
- Witkiewicz AK, Whitaker-Menezes D, Dasgupta A, Philp NJ, Lin Z, Gandara R, et al. Using the "reverse Warburg effect" to identify high-risk breast cancer patients: Stromal MCT4 predicts poor clinical outcome in triple-negative breast cancers. *Cell Cycle* 2012;11:1108–17.
- Vonck J, Schafer E. Supramolecular organization of protein complexes in the mitochondrial inner membrane. *Biochim Biophys Acta* 2009;1793:117–24.

### **Publication III**

**Klepinin, Aleksandr;** Chekulayev, Vladimir; Timohhina, Natalja; Shevchuk, Igor; Tepp, Kersti; Kaldma, Andrus; Koit, Andre; Saks, Valdur; Kaambre, Tuuli (2014). Comparative analysis of some aspects of mitochondrial metabolism in differentiated and undifferentiated neuroblastoma cells. *Journal of Bioenergetics and Biomembranes*, 46(1), 17–31.



# Comparative analysis of some aspects of mitochondrial metabolism in differentiated and undifferentiated neuroblastoma cells

Aleksandr Klepinin · Vladimir Chekulayev · Natalja Timohhina · Igor Shevchuk · Kersti Tepp · Andrus Kaldma · Andre Koit · Valdur Saks · Tuuli Kaambre

Received: 26 June 2013 / Accepted: 13 September 2013 / Published online: 27 September 2013  
© Springer Science+Business Media New York 2013

**Abstract** The aim of the present study is to clarify some aspects of the mechanisms of regulation of mitochondrial metabolism in neuroblastoma (NB) cells. Experiments were performed on murine Neuro-2a (N2a) cell line, and the same cells differentiated by all-trans-retinoic acid (dN2a) served as *in vitro* model of normal neurons. Oxygraphy and Metabolic Control Analysis (MCA) were applied to characterize the function of mitochondrial oxidative phosphorylation (OXPHOS) in NB cells. Flux control coefficients (FCCs) for components of the OXPHOS system were determined using titration studies with specific non-competitive inhibitors in the presence of exogenously added ADP. Respiration rates of undifferentiated Neuro-2a cells (uN2a) and the FCC of Complex-II in these cells were found to be considerably lower than those in dN2a cells. Our results show that NB is not an exclusively glycolytic tumor and could produce a considerable part of ATP via OXPHOS. Two important enzymes - hexokinase-2 and adenylate kinase-2 can play a role in the generation of ATP in NB cells. MCA has shown that in uN2a cells the key sites in the regulation of OXPHOS are complexes

I, II and IV, whereas in dN2a cells complexes II and IV. Results obtained for the phosphate and adenine nucleotide carriers showed that in dN2a cells these carriers exerted lower control over the OXPHOS than in undifferentiated cells. The sum of FCCs for both types of NB cells was found to exceed significantly that for normal cells suggesting that in these cells the respiratory chain was somehow reorganized or assembled into large supercomplexes.

**Keywords** Energy metabolism · Metabolic control analysis · Neuroblastoma · Adenylate kinase · Hexokinase · Warburg effect

## Abbreviations

AChE	Acetylcholinesterase
AK	Adenylate kinase
ANT	Adenine nucleotide translocator
CAT	Carboxyatractyloside
CM	Cardiomyocytes
$C_{vi}^J$ or FCC	Flux control coefficient
CK	Creatine kinase
ETC	Electron transport chain
G6PDH	Glucose-6-phosphate dehydrogenase
HK	Hexokinase
$K_m$	Michaelis-Menten constant
MTR-CMXRos	MitoTracker® Red CMXRos
uMitCK	Ubiquitous mitochondrial creatine kinase
MCA	Metabolic Control Analysis
3-NP	3-nitropropionic acid
NB	Neuroblastoma
N2a	Neuro-2a
uN2a	Undifferentiated N2a cells
dN2a	Differentiated N2a cells

A. Klepinin · V. Chekulayev · N. Timohhina · I. Shevchuk · K. Tepp · A. Kaldma · A. Koit · V. Saks · T. Kaambre (✉)  
Laboratory of Bioenergetics, National Institute of Chemical Physics and Biophysics, Akadeemia tee 23, 12618 Tallinn, Estonia  
e-mail: tuuli.kaambre@kbfi.ee

V. Saks  
Laboratory of Fundamental and Applied Bioenergetics, Joseph Fourier University, Grenoble, France

A. Kaldma · A. Koit  
Department of Gene Technology, Tallinn University of Technology, Tallinn, Estonia

T. Kaambre  
Institute of Mathematics and Natural Sciences, Tallinn University, Tallinn, Estonia

OXPPOS	Oxidative phosphorylation
MOM	Mitochondrial outer membrane
PCr	Phosphocreatine
Pi	Inorganic phosphate
PIC	Inorganic phosphate carrier
PEP	Phosphoenolpyruvate
PK	Pyruvate kinase
RA	All-trans-retinoic acid
SDH	Succinate dehydrogenase
SNS	Sympathetic nervous system
TMPD	N,N,N',N'-tetramethyl-p-phenylenediamine
VDAC	Voltage dependent anion channel

## Introduction

Undifferentiated and poorly differentiated neuroblastomas are very aggressive tumors, which are characterized by high growth rates and strong inclination to metastasis. Studies performed during the past decade suggest that targeting cancer cell energy metabolism may be a new and very effective therapeutic strategy for selective ablation of malignancies (Geschwind et al. 2004; Gogvadze et al. 2009). However, today little is known about the key processes involved in the maintenance of energy homeostasis in NB cells as well as the bioenergetic capacity of their mitochondria.

Documented interest in energy metabolism and mitochondrial function in carcinogenesis started as early as in the 1930s, when Otto Warburg demonstrated (Pedersen 2007a; Warburg 1956) that cancer cells had an increased dependence on glycolysis to meet their energy needs, regardless of whether they were well-oxygenated or not – a phenomenon termed subsequently “aerobic glycolysis” or “Warburg effect”. Although, the glycolytic phenotype of many cancer cells and tumors has been demonstrated at the biochemical and molecular levels (Atsumi et al. 2002; Marin-Hernandez et al. 2006; Pedersen 1978; Pedersen 2007b; Xu et al. 2005), the presumed impairment of mitochondrial function as the cause of malignant transformation has unambiguously never been proved in cancer biology (Pedersen 1978). Previous studies have shown that aerobic glycolysis could provide a growth advantage to tumor cells and mediate their increased resistance to apoptotic stimuli (Gatenby & Gillies 2004). A glycolytic phenotype was found in a high percentage of human cancers, and it was suggested that inhibition of glycolysis could be an effective approach for tumor ablation therapy (Ihrlund et al. 2008; Matsushita et al. 2012; Pedersen 2012). Recent studies have shown that the respiratory activity and significance of oxidative phosphorylation (OXPPOS) versus glycolysis in bioenergetics of malignancies vary greatly depending on their histological type, growth stage and vascularization (Apte & Sarangarajan 2008; Gatenby & Gillies 2004;

Moreno-Sánchez et al. 2009). Cancer cells can utilize lactate, free fatty acids, ketone bodies, butyrate and glutamine as key respiratory substrates and may cause reprogramming of normal surrounding cells towards aerobic glycolysis – “reverse Warburg” effect (Whitaker-Menezes et al. 2011). It has also been demonstrated that targeting mitochondria can be a very effective tool for tumor cell elimination (Gogvadze et al. 2009). Thus, heterogeneity of bioenergetics profiles of tumors requires personalized treatment strategies for choosing effective anticancer treatment, including high-risk NBs. Literature on bioenergetics of human NBs is on the other hand still very limited.

Neurons have a high metabolic rate and use more energy than other cells. They normally derive ATP exclusively through aerobic mechanisms (OXPPOS). Studies performed on post-operational material (Beemer et al. 1984) and data obtained on cultured cells and animal models (Krieger-Hinck et al. 2006) suggest that rapidly proliferating human NBs are highly-glycolytic tumors which display a Warburg phenotype. Even under aerobic conditions, human NB cells can convert remarkable amounts of glucose to lactate instead of using glucose oxidation (Deubzer et al. 2010) and that some inhibitors of glycolysis, such as 3-bromopyruvic acid and 2-deoxyglucose, can suppress NB cell growth *in vitro* (Chuang et al. 2013; Matsushita et al. 2012). Although, cancer cells can produce a significant (~ 50–70 %) part of their ATP via aerobic glycolysis (Pedersen 2007b), the exact molecular mechanisms underlying the Warburg effect are not completely understood. In accordance with the literature data, several aerobic glycolysis key mechanisms, mediating a Warburg phenotype were observed in NB cells, and these could be crucial targets for medical intervention.

Hexokinase (HK) 2 was found to be over-expressed in many human malignancies, including NBs (Beemer et al. 1984; Levy et al. 2012; Pedersen et al. 2002). In this relation, Pedersen and colleagues have formulated the existence of a supercomplex consisting of ATP synthasome, voltage dependent anion channel (VDAC) and HK-2 in cancer cells that helps in explanation of the Warburg effect (Pedersen 2008). It was demonstrated that binding of HK-2 with mitochondria increased almost 5-fold its affinity for ATP (Bustamante & Pedersen 1980). The complex of HK-2 with mitochondria not only decreases product inhibition initiated by glucose-6-phosphate (Bustamante & Pedersen 1977; Nakashima et al. 1988) but also provides rapid access to ATP required by HK-2 to phosphorylate glucose to glucose-6-phosphate and therefore “jump starts” the glycolytic pathway and produces the Warburg effect.

Our recent studies have demonstrated that variations in the expression of some tubulin isotypes in cancer cells could mediate their Warburg phenotype (Guzun et al. 2011; Rostovtseva et al. 2008). We found (Guzun et al. 2011) that the localization and function of  $\beta$ -tubulin isotypes varied in different muscle tissues and tumor cells: in adult rat cardiomyocytes  $\beta$ -tubulin class II is associated with mitochondria, but it is absent in cardiac HL-1



tumor cells having a glycolytic phenotype. The absence of  $\beta$ III-tubulin in cancer cells allows binding of HK-2 to VDAC mediating thereby the initiation of the Warburg effect. It was presumed that HK-2, if directly bound to mitochondria through VDAC and, according to the model proposed by Majewski and coauthors (Majewski et al. 2004), supported VDAC to leave an open state. As a consequence, HK-2 consumes practically all of the ATP produced via OXPHOS and thereby causes elevated glycolysis even in the presence of oxygen. This suggests that increased rates of aerobic glycolysis in cancer cells may occur even without any disturbances in the functional activity of mitochondria.

In NB cells, a metabolic shift from OXPHOS to aerobic glycolysis could be largely mediated by specific alterations in the function of their mitochondria. Defective OXPHOS complexes, linked with mutations of mitochondrial DNA, were found in many other human malignancies. Deficiency of the Complex-I of the mitochondrial respiratory chain, associated with enhanced production of reactive oxygen species (Sharma et al. 2011), has been observed in human gastric cancer tissue (Puurand et al. 2012), renal and thyroid oncocyctomas (Bonora et al. 2006; Simonnet et al. 2003). Some literature data suggests that NB cells are deficient in Complex-II activity, since mutations in genes encoding the subunits of the mitochondrial succinate dehydrogenase (SDH) complex have been shown in these malignancies (Cascon et al. 2008; Schimke et al. 2010).

The presented work was, therefore, aimed to clarify the bioenergetic function of mitochondria and main energy fluxes in NB cells. Our experiments were performed on murine NB cells of the Neuro-2a (N2a) line. These cells are well studied and present an excellent model system for clarifying the energetics of human NBs. N2a cells were shown to express mitochondria-bound HK (Krieglstein & Mwasekaga 1987; Krieglstein et al. 1981) and to display the Warburg phenotype (Kaambre et al. 2012a). In our study, the N2a cells differentiated by all-trans-retinoic acid (RA) served as an *in vitro* model of normal neurons. It was shown that RA acid-induced differentiation of human NB cells restored the respiratory activity of mitochondria (Xun et al. 2012).

Understanding the control and regulation of energy metabolism requires analytical tools, which relate the properties of metabolic systems to the kinetic characteristics of the component enzymes and their impact on network function. A powerful experimental approach for this purpose is Metabolic Control Analysis (MCA) (Fell 2005). MCA has been suggested to be beneficial for the description of enzymatic abnormalities in syndromes associated with mitochondrial dysfunction (Kuznetsov et al. 2008). Recently, Moreno-Sanchez and Westerhoff's groups have successfully applied MCA to investigate the control of glycolytic flux and mitochondrial respiration in different types of tumor cells growing in culture. Main conclusion of these studies was that the significance of OXPHOS in bioenergetics of cancer cells should be re-

evaluated and experimentally determined for each particular type of neoplasm (Marin-Hernandez et al. 2006; Moreno-Sanchez et al. 2007; Moreno-Sánchez et al. 2009; Moreno-Sanchez et al. 2010).

In the present work MCA along with oxygraphy was applied to characterize the function of OXPHOS in undifferentiated and RA-treated N2a cells. We quantified the control exerted by different components of the respiratory chain and the ATP synthasome complex in both of these cell types. To determine the flux control coefficients, the flux was measured as the rate of  $O_2$  consumption by permeabilized N2a cells when all components of the OXPHOS system were titrated with their specific inhibitors to stepwise decrease separate respiration complex activities. It is important to note that the using of MCA and the permeabilized techniques which enable to estimate OXPHOS function without isolation of mitochondria and thereby avoiding artifacts linked to their isolation procedure and the loss of components involving in the regulation. Furthermore, these methodological approaches preserve intimate interactions between mitochondria in the cell as well as the intactness of their cytoskeletal structures. Additional experiments were also performed in the present work to study the significance of creatine kinase (CK) and adenylate kinase (AK) reactions in the maintenance of energy homeostasis in NB cells.

## Materials and methods

### Chemicals

Antibodies, chemicals and enzymes were purchased from Abcam®, Sigma-Aldrich, Fluka or Roche, whereas growth media, heat-inactivated fetal bovine serum (FBS) and antibiotics were obtained from PAA Laboratories GmbH, Austria.

### Isolation of rat heart cardiomyocytes

Adult cardiomyocytes (CM) were isolated after perfusion of the rat heart with collagenase-A (1.0 mg/ml, Roche) exactly as described in our previous work (Saks et al. 1991). The cells sarcolemma was permeabilized by saponin treatment (25  $\mu$ g/ml, for 5 min at 25 °C) directly in oxygraphic chambers keeping the mitochondrial membranes intact (Tepp et al. 2011).

### Cultivation of N2a cells and their differentiation

Stock culture of N2a cells was obtained from the American Type Culture Collection, Cat. No. CCL-131. Unless otherwise specified, the murine NB cells were grown as a loosely adhering monolayer at 37 °C in 5 %  $CO_2$  in high glucose Dulbecco's modified Eagles medium supplemented with L-

glutamine, 10 % FBS, 100 U/ml penicillin and 100 µg/ml streptomycin (complete growth medium). N2a cells were maintained at 80–90 % confluence at the time of subculture.

Neural differentiation of N2a cells to cholinergic neurons was induced by their treatment with 7 µM all-trans-retinoic acid (RA) in complete growth medium for 5 days (Blanco et al. 2001).

The cells growing in Petri dishes were harvested by centrifugation washed twice with Mitomed-B solution (Kaambre et al. 2012a) supplemented with 10 µM leupeptin and were then resuspended in the medium at a cell density of  $\sim 1 \times 10^7$  cells/ml.

#### Determination of cell growth

The effect of RA on the rate of N2a cells growth (seeded in 96-well plates) was estimated by the use of MTT Cell Proliferation Assay Kit (ATCC® 30-1010 K) according to the manufacturer manual. The absorbance of samples at 570 nm (reference wavelength, 620 nm) was measured spectrophotometrically using a microplate reader (Multiscan Spectrum, Thermo Electron Corporation).

#### Cell permeabilization and oxygraphic measurements

Plasma membrane was permeabilized with saponin treatment (Kuznetsov et al. 2008). Saponin concentration of 40 µg/ml was used as it gave the maximal respiratory response for exogenously added ADP whereas the integrity of the mitochondrial membranes was preserved.

Rates of oxygen consumption by permeabilized N2a cells (at a concentration of  $\sim 5 \times 10^5$  cells/ml) were measured under magnetic stirring (300 rpm) at 25 °C in 2-ml glass chambers of a two-channel titration-injection respirometer (Oxygraph-2 K, OROBOROS Instruments, Austria) in medium-B supplemented with 5 mM glutamate, 2 mM malate and 10 mM succinate as respiratory substrates. The plasma membrane in the cells was permeabilized by saponin treatment by adding it directly into oxygraphic chambers (incubation time 5 min at 25 °C); solubility of oxygen was taken as 240 nmol/ml.

Effects of exogenously added succinate, creatine, glucose, ADP and Km for AMP were measured in medium-B supplemented with 5 mM glutamate and 2 mM malate and in the presence of pyruvate kinase (PK) –phosphoenolpyruvate (5 mM) ADP trapping system (Kaambre et al. 2012b; Guzun et al. 2009).

#### Enzymatic activities

HK activity was measured as the total glucose phosphorylating capacity of whole cell extracts, using a standard glucose-6-phosphate dehydrogenase (G6PDH)-coupled

spectrophotometric assay (Biswas et al. 1997). One milliunit (mU) of HK activity was calculated as the amount of enzyme activity required to phosphorylate 1 nmol of glucose in 1 min at 25 °C.

The CK activity was assessed spectrophotometrically at 25 °C in the direction of ATP formation in the presence of di(adenosine-5') pentaphosphate (an adenylate kinase inhibitor (Lienhard & Secemski 1973)), 20 mM phosphocreatine (PCr) and with 2 U/ml G6PDH and 2 U/ml HK as the coupled enzymes (Monge et al. 2009). One mU of CK activity represents the formation of 1 nmole of ATP per minute at 25 °C.

AK activity of whole-cell extracts was measured at 25 °C by a coupled enzyme assay (Dzeja et al. 1999). The reaction was initiated with 2 mM ADP, and the arising changes in absorbance at 340 nm were recorded using a Cary 100 Bio UV-visible spectrophotometer. One mU of AK activity represents the formation of 1 nmole of ATP per minute at 25 °C.

The activity of acetylcholinesterase (AChE) in N2a cells was measured spectrophotometrically applying the technique of Ellman et al. (Ellman et al. 1961). One unit of AChE activity (U) represents the hydrolysis of 1 µmol of the chosen substrate (acetylthiocholine) per minute at 37 °C.

#### Confocal microscopy imaging of N2a cells

MitoTracker® Red CMXRos (Molecular Probes) was used to label mitochondria in N2a cells. The labeling procedure was carried out according to the manufacturer instructions. MitoTracker Red stained N2a cells were placed over glass microscope slides with ProLong Gold antifade reagent supplemented with DAPI (Molecular Probes®) for visualizing cell nucleus. Cells were imaged by an Olympus FV10i-W inverted laser scanning confocal microscope equipped with a 60× water immersion objective, using 560 nm laser excitation for MTR-CMXRos and light excitation at 405 nm for DAPI.

#### Metabolic control analysis

MCA quantifies the degree of control exerted by an enzymatic or transport step through the flux control coefficient (FCC). FCC is defined as the ratio of the fractional change in the steady-state flux with respect to an infinitesimal variation in the biochemical activity which may cause the change in flux (Fell 1997). If a small change in an enzyme activity promotes a significant variation in pathway flux, then this enzyme exerts an elevated control over the regulation of pathway. In contrast, if a rather small or negligible change in flux is observed when a complex activity is greatly varied, the enzyme has low FCC and decreased ability to influence on overall flux (Fell 1997; Tepp et al. 2010).

The FCC or  $C_{vi}^J$  is defined according to the equation (Fell 1997; Moreno-Sanchez et al. 2008):

$$C_{vi}^J = \left( \frac{dJ}{dv_i} \right) / \left( \frac{J}{v_i} \right) = \frac{d \ln J}{d \ln v_i}$$

in which the expression  $dJ/dv_i$  describes the variation in flux ( $J$ ) when an infinitesimal change takes place in the enzyme  $i$  concentration or activity. Groen et al. (Groen et al. 1982) have derived a method to determine experimentally the  $C_{vi}^J$  using titration with specific enzyme inhibitors. The value of the  $C_{vi}^J$  coefficient is given by Groen (Groen et al. 1982) and Moreno-Sanchez (Moreno-Sanchez et al. 2008):

$$C_E^J = (\Delta J / \Delta I) * (I_{\max} / J_0)$$

where  $(\Delta J / \Delta I)$  is the initial slope of the flux/inhibition graph,  $I_{\max}$  is the inhibitor concentration giving complete inhibition, and  $J_0$  is the initial steady-state flux value.

Experimentally, the FCCs for permeabilized N2a cells were determined for all mitochondrial respiratory chain and ATP synthasome complexes after their stepwise titration with specific irreversible inhibitors upon direct activation of respiration by exogenously added ADP (at 2 mM).  $C_{vi}^J$  values were calculated by using graphical method described by Fell (Fell 1997). The following inhibitors were used: rotenone for Complex-I of the mitochondrial electron transport chain (ETC); 3-nitropropionic acid (3-NP) for Complex-II; antimycin for Complex-III; sodium cyanide for Complex-IV; oligomycin for complex-V (ATP synthase); carboxyatractyloside (CAT) for adenine nucleotide translocator (ANT); and mersalyl for inorganic phosphate carrier (PIC).

## Statistics

Data in the text, tables and figures are presented as mean  $\pm$  standard error of the mean (SEM). Results were analyzed by Student's  $t$ -test. Values of  $P < 0.05$  were considered statistically significant. To reduce the possibility of random errors, our experiments were repeated at least five times and the fitting technique was used to calculate the  $C_{vi}^J$  value. Apparent  $K_m$  values for ADP and AMP were estimated by fitting experimental data to a non-linear regression (according to a Michaelis-Menten model) equation.

## Results

Proliferative activity, the number of mitochondria, morphological and enzymatic changes in N2a cells treated with retinoic acid

Experiments showed that the described protocol for N2a cells differentiation enabled to obtain a practically pure culture of

neural cells with morphological and biochemical parameters typical for normal mature neurons; this is in a good agreement with the data from other laboratories (Blanco et al. 2001). We found that treatment of uN2a cells with RA resulted in strong neurite outgrowth that appeared on day 2 and extended on days 4 and 5 (Fig. 1). In addition, RA induced the formation of a population of neural cells with an increased number of mitochondria as illustrated by confocal microscopy (Fig. 1). In both cell types, mitochondria are predominantly localized around the cell nucleus; in dN2a cells a significant part of mitochondria are found to be localized in large neurites possibly attached to microtubule structures.

Moreover, it was established that RA-treated N2a cells lose their proliferative capacity (Fig. 2) and had an elevated AChE activity (Table 1). Similar effects of RA on the activity of AChE in N2a cells were also observed in other laboratories (Sato et al. 2002).

Activities of enzymes, which were involved in the maintenance of cellular energy homeostasis, were also measured in both uN2a and RA-treated cells. Table 1 shows that HK, AK and CK activities in dN2 cells exceed considerably those measured in immature N2a cells, suggesting that dN2a cells have increased metabolic rates and energy demand.

The influence of saponin treatment on the intactness of mitochondrial membranes in N2a cells

For comparison of respiratory activities of mitochondria in undifferentiated and dN2a cells, the technique of permeabilized cell, elaborated by Kuznetsov (Kuznetsov et al. 2008), was used. The technique gives an opportunity to study the mitochondrial function at nearly physiological conditions. The plasma membrane of the studied cells was permeabilized by saponin treatment directly in the oxygraph chamber as described previously (Kuznetsov et al. 2008). To evaluate the intactness of mitochondrial membranes, the cytochrome-c and CAT tests were applied for both undifferentiated N2a and dN2a cells (Saks et al. 1998). Respiration was activated with 2 mM ADP; addition of cytochrome-c (final concentration, 8  $\mu$ M) did not cause any marked increase in the rate of oxygen consumption, indicating the intactness of the outer mitochondrial membrane. Addition of carboxyatractyloside (1  $\mu$ M) decreased the respiration rate back to the basal rate ( $V_o$ ) level showing the intactness of the mitochondrial inner membrane (Fig. 3). Therefore the saponin concentration of 40  $\mu$ g/ml was considered suitable.

Function of respiratory chain complexes in undifferentiated and differentiated N2a cells

Activities of various segments of the respiratory chain were studied by using a specific step-by-step substrate inhibitor titration oxygraphic protocol. The ADP (at 2 mM) activated

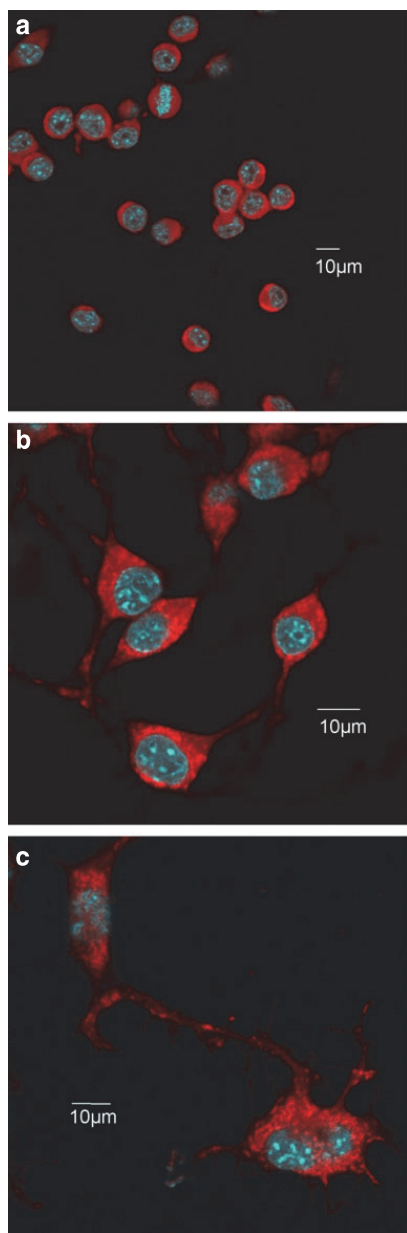


**Fig. 1** Confocal microscopy images of N2a cells with and without all-trans-retinoic acid (RA) treatment. **a** -control cells, whereas **(b)** and **(c)** are N2a cells treated with 7  $\mu$ M RA for 5 days. Mitochondria in the cells were stained with MitoTracker Red CMXRos (red fluorescence) and cell nuclei with DAPI (blue fluorescence). After 5 days of culture, N2a cells treated with RA (see photos **b** and **c**) are characterized by an increased number of mitochondria, display stronger substrate adherent and a flattened morphology, with an increase in cell body size and neurite extension occurring around the soma

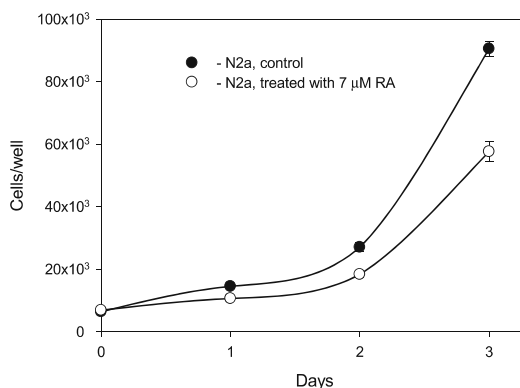


**Fig. 2** Effect of all-trans-retinoic acid (RA) on proliferation of N2a cells; cell count was performed by MTT assay at 1, 2 and 3 days of culture. RA-treated N2a cells show decay in their proliferative activity comparing to control N2a cells. Bars are SEM

respiration was found to be inhibited in undifferentiated and dN2a cells by addition of rotenone, this was a characteristic feature of cells with active Complex-I (Fig. 4). The next step was to measure the Complex-II dependent respiration which was achieved by addition of its substrate, succinate (final concentration, 10 mM). The obtained results showed that in normal neurons as well as in the NB cells, the Complex-I was suppressed in comparison with Complex-II. This finding is in good accordance with our previous data on HL-1 tumor cells where the mitochondrial Complex-II is more effective in comparison with Complex-I (Monge et al. 2009). Inhibition of Complex-III with antimycin A (it suppresses the electron flow from Complex-III to cytochrome-c) was followed by measurement of Complex-IV dependent respiration. Experiments with antimycin showed that Complex-III might be functionally active not only in normal neurons, but also in undifferentiated NB cells (Fig. 4). In order to activate Complex-IV, 1 mM TMPD with 5 mM ascorbate was added which resulted in an approximately 3-fold activation of respiration for both cell types (Fig. 4). The cytochrome-c (at 8  $\mu$ M) exerted only a minor effect on the TMPD-ascorbate activated respiration, suggesting thereby that the applied permeabilization procedure did not injure the intactness of the external mitochondrial membrane in these cells.

**Table 1** Enzymatic activities in undifferentiated (uN2a) and all-trans-retinoic acid differentiated (dN2a) N2a cells

Enzyme activities, mU per $1 \times 10^6$ cells	uN2a cells, mean $\pm$ SE, $n=5$	dN2a cells, mean $\pm$ SE, $n=5$	$P$ -values
Acetylcholinesterase	2.52 $\pm$ 0.52	4.62 $\pm$ 0.27	< 0.02
Hexokinase	19.57 $\pm$ 1.86	32.15 $\pm$ 3.73	< 0.05
Creatine kinase	7.59 $\pm$ 0.89	11.78 $\pm$ 0.59	< 0.001
Adenylate kinase	121.5 $\pm$ 9.4	151.1 $\pm$ 8.5	< 0.05

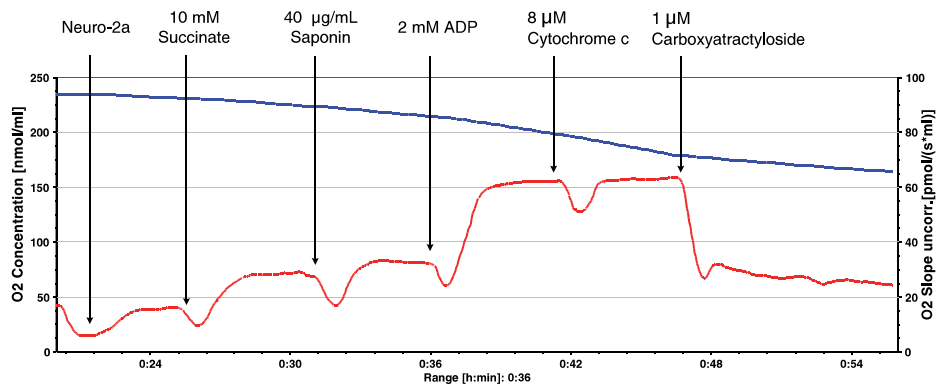


**Fig. 3** Quality test for intactness of mitochondrial membranes in permeabilized N2a cells. This experiment was performed in medium-B with 5 mM glutamate, 2 mM malate, and 10 mM succinate as respiratory substrates. Blue traces represent the O<sub>2</sub> concentration and red traces the respiration rates. Respiration was activated with 2 mM ADP; addition of

8 µM cytochrome-c did not cause any marked increase in the rate of oxygen consumption, indicating the intactness of outer mitochondrial membrane. Addition of 1 µM carboxyatractylsido decreased respiration rate back to the basal respiration rate (V<sub>o</sub>) level showing the intactness of mitochondrial inner membrane

### Coupling of OXPHOS with HK reactions

Our studies confirm, that NB cells have, in comparison with normal differentiated neural cells, decreased activity of OXPHOS. The maximal respiration rate (V<sub>max</sub>, in the presence of 2 mM ADP) of RA-treated N2a cells exceeds nearly 2 times that measured for undifferentiated cells (Fig. 6a). In cancer cells HK-2 locates predominantly on the outer mitochondrial membrane binding with VDAC. This binding increases HK affinity for ATP which generated via OXPHOS

(Pedersen 2008). In this work we investigated the interaction of mitochondrial-associated HK with OXPHOS in NB cells (ADP trapping PK/PEP system was used to exclude involvement of cytoplasmic HK isoforms). We measured the total HK activity in undifferentiated and dN2a cells and performed oxygraphic analysis of the coupling of mitochondria-associated HK with OXPHOS for both types of cells. The total HK activity of dN2a cells was assayed as 32.15 ± 3.73 nmol glucose/min/10<sup>6</sup> cells; in undifferentiated cells this value was approximately 40 % lower (19.57 ± 1.86 nmol glucose/min/10<sup>6</sup> cells, Table 1). The revealed stimulatory effects of 10 mM glucose on mitochondrial respiration in both undifferentiated and RA-treated N2a cells confirmed the considerable role of HK-2 in energy metabolism of NB cells (Fig. 5). Our results (Fig. 5) are in a good agreement with the previous work (Xun et al. 2012) which reports that RA improves the function of mitochondria in NB cells, but also increases glycolysis (raised HK activity was found in Table 1). In spite of the fact that the aerobic glycolysis in uN2a cells has an important role in the ATP production as compared to that of differentiated cells which have high activity of OXPHOS (Fig. 5).

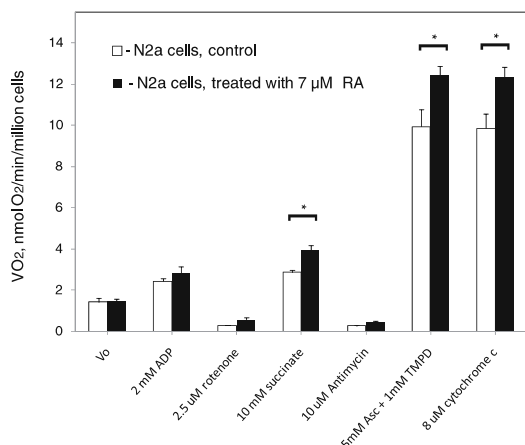


**Fig. 4** The activities of the respiratory chain complexes in undifferentiated and all-trans-retinoic acid (RA) differentiated N2a cells. The experiment was performed in medium-B with 5 mM glutamate and 2 mM malate as respiratory substrates. TMPD - N,N,N',N'-tetramethyl-p-phenylenediamine, Asc - ascorbic acid. Bars are SEM. \* indicates a statistical significant difference between the mean values; *p* < 0.05

Coupling of OXPHOS with creatine and adenylate kinase systems, K<sub>m</sub> values for exogenously added AMP and ADP

Precise coupling of spatially separated intracellular ATP-producing and ATP-consuming processes is fundamental to the bioenergetics of living organisms, ensuring a fail-safe operation of the energetic system over a broad range of cellular functional activities. For this purpose neural cells, like CM, skeletal muscles, and many other cells, exert AK and CK systems (Dzeja & Terzic 2009; Dzeja & Terzic 2003; Saks

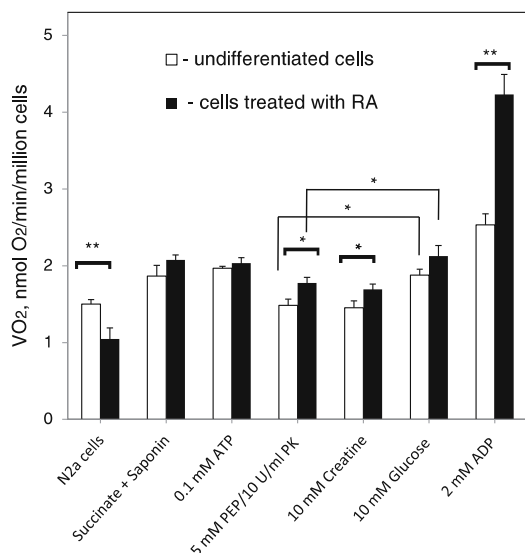


**Fig. 5** Effects of exogenously added creatine and glucose on the rate of oxygen consumption by permeabilized RA-treated N2a cells and undifferentiated N2a cells. The creatine (10 mM) and glucose (10 mM) influence on mitochondrial respiration were estimated in the presence of pyruvate kinase/phosphoenolpyruvate ADP trapping system and exogenously added 0.1 mM MgATP. Finally, 2 mM ADP was added for maximal activation of respiration. The used reagents were added to N2a cells successively as shown on the x-axis. Bars are SEM. \* and \*\* indicate a statistical significant difference between the mean values;  $p < 0.05$  and  $p < 0.01$ , respectively

et al. 2003). In cells with high and fluctuating energy requirements, like neurons and muscle cells, ubiquitous mitochondrial creatine kinase (uMtCK) plays a key role in the maintenance of energy homeostasis by coupling of cytoplasmic phosphotransfer reactions with OXPHOS (Dzeja & Terzic 2003; Saks et al. 2003). Recent studies have shown that uMtCK is downregulated in some human cancers (Kaambre et al. 2012a; Patra et al. 2012), but little is known about its expression and functioning in NBs.

Our experiments showed that addition of creatine (up to 10 mM, in the presence of a PK-PEP system and exogenously added 0.1 mM MgATP) had no effect on the rate of O<sub>2</sub> consumption by uN2a as well as RA-treated cells (Fig. 5). These findings indicate that uMtCK plays a minor role in the generation of PCr and energy transfer processes in NB cells. This finding is in a good accordance with our previous results obtained in HL-1 tumor cells (Monge et al. 2009; Seppet et al. 2006). Thus, the measured CK activity in N2a cells can be largely ascribed to CK-BB or perhaps even CK-MM isoform (Table 1).

We found that N2a cells possess AK activity. The total AK activity of uN2a cells is found to be 20 % lower in comparison with RA-treated cells (Table 1). Further studies showed that

AMP in the presence of a PK-PEP system could increase the rate of O<sub>2</sub> consumption in permeabilized N2a cells. We measured the apparent K<sub>m</sub> value for exogenously added AMP (K<sub>m</sub><sup>AMP</sup>) for both types of cells. The K<sub>m</sub><sup>AMP</sup> value for RA-treated N2a cells (175±30 μM) was practically equal to the value found for adult rat cardiomyocytes (175±31 μM) but almost two times less than that for uN2a cells (79±9 μM) (Fig. 6b). These findings confirmed that in undifferentiated NB cells the permeability of the mitochondrial outer membrane (MOM) for exogenously added AMP is increased. Additional studies are needed to uncover possible mechanisms of the phenomenon.

The kinetics of regulation of mitochondrial respiration by exogenously added ADP was also studied in undifferentiated and dN2a cells. Titration curves of the corresponding respiratory experiments are shown in Fig. 6a. In uN2a cells and dN2a cells, the apparent K<sub>m</sub> values for ADP were measured as 20.3±1.4 μM and 19.4±3.2 μM, respectively ( $n=5$ ). The obtained K<sub>m</sub> value for exogenously added ADP in uN2a cells was found to be close to the values observed for murine tumor cells of the line HL-1 (47±15 μM) and for isolated mitochondria (in the range of 10–20 μM) (Monge et al. 2008). For permeabilized rat brain synaptosomes the K<sub>m</sub> value was remarkably higher - 110±11 μM (Monge et al. 2008).

#### Metabolic control analysis of respiration regulation in malignant and differentiated N2a cells

The tool of MCA makes it possible to identify the key regulatory complexes of the energy metabolism pathways and to find the best targets for effective antineoplastic treatment (Moreno-Sanchez et al. 2010; Moreno-Sanchez et al. 2008). In undifferentiated and RA-treated N2a cells mitochondrial respiration was activated by exogenously added ADP (final concentration, 2 mM) due to the absence of uMtCK activity.

Figure 7 shows representative traces of O<sub>2</sub> consumption by permeabilized uN2a cells treated with increasing concentrations of 3-NP, an inhibitor of Complex-II (Huang et al. 2006). The measurements were carried out in a steady state conditions. Similar titration curves were obtained for other inhibitors of the mitochondrial ETC and ATP synthasome complexes. They were plotted as relative rates of O<sub>2</sub> consumption (VO<sub>2</sub>, J/J<sub>0</sub>) versus a concentration of used inhibitors (Fig. 8). From these plots, corresponding FCCs, also presented in Table 2, were calculated. The FCCs for undifferentiated and RA-treated N2a cells were determined by the graphical method by Fell (Fell 1997) as described in our previous work (Tepp et al. 2010).

MCA showed that in uN2a cells the key sites of OXPHOS were Complex-I (FCC=1.11), Complex-II (FCC=0.99) and IV (FCC=0.92), whereas FCCs for other mitochondrial complexes were found to be equally and significantly lower (Table 2). FCCs for Complex-I, II and IV have high and close

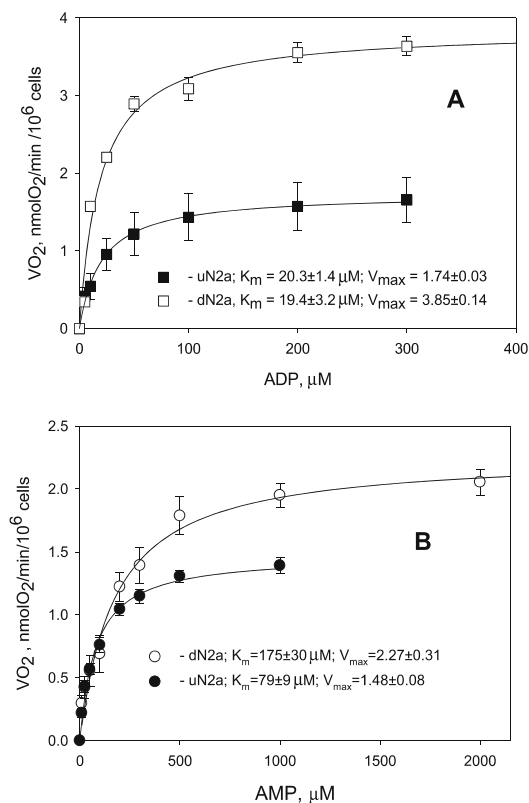


**Fig. 6** The dependence of the respiration rate of undifferentiated and RA-differentiated N2a cells (uN2a and dN2a, respectively) on the extracellular ADP (a) or AMP (b) concentrations. Respiratory substrates served: 5 mM glutamate, 2 mM malate and 10 mM succinate. In the case of AMP activated respiration, rates of O<sub>2</sub> consumption were measured in the presence of 2 mM ATP and pyruvate kinase/phosphoenolpyruvate system. From the presented plots corresponding apparent K<sub>m</sub> values for exogenously added ADP and AMP were calculated. Bars are SEM

values in uN2a cells, showing that these complexes may work as one unit in these cells. In dN2a cells, the key points for metabolic control were found to be Complex-II (FCC=1.34) and IV (FCC=0.99); at the same time, the FCC for Complex-I is significantly lower, 0.38 *versus* 1.11 in uN2a cells. Our data indicates that there are considerable differences between uN2a and dN2a cells in FCCs for Complex-II, PIC and ANT (Table 2). In dN2a cells, PIC and ATP/ADP carrier exert lower control over the OXPHOS than in undifferentiated NB cells. It was also shown that the FCC for PIC in uN2a cells exceeded 7 times that of what was measured in oxidative muscle cells (rat cardiomyocytes, FCC=0.064±0.04) (Table 2). Thus, our results confirm that in mitochondria of malignant NB cells these ATP synthasome complexes have more control in regulation of OXPHOS as compared to normal fully differentiated N2a cells or cardiomyocytes.

The sum of FCCs calculated for uN2a cells (5.06) was found to exceed significantly the theoretic value for linear systems (close to 1) (Kholodenko & Westerhoff 1993) and was higher than for RA-treated cells (Σ=3.93) and normal rat CMs (Σ=1.93) (Table 2). It can be concluded that the role of respiratory chain and ATP synthasome complexes in energy metabolism of NB cells may differ considerably from that in normal neuronal cells. The some explanation of MCA theory about the increased sum of the FCCs may be due to the existence of direct channeling of a substrates between the protein complexes or formation of supercomplexes (Kholodenko & Westerhoff 1993). Structurally tight alignment of the complexes of respiratory chain could be one of the ways for malignant cells to avoid apoptosis, as the cytochrome-c, which should be released during the apoptosis process, is tied in the supercomplex.

### Discussion

In order to quantitatively characterize some energy fluxes and the functional capacity of mitochondria in NB cells we applied the techniques of permeabilized cell and MCA. In our studies, RA-treated N2a cells served as an *in vitro* model of normal neural cells. A set of experiments demonstrated that the treatment of uN2a cells with 7 μM RA induced the formation of a cell population, where morphological (cell size, neurite organization, substrate attachment, number of mitochondria) and biochemical characteristics (AChE activity) as well as growth rates were very similar to mature fully-differentiated sympathetic neurons (see Figs. 1 and 2, Table 1).

According to established ideas, human high-risk NB is considered to be a highly-glycolytic tumor of the Warburg phenotype (Almeida et al. 2010; Beemer et al. 1984; Feichtinger et al. 2010; Krieger-Hinck et al. 2006; Levy et al. 2012). Our results suggest that in human NB cells high levels of HK-1 or HK-2 expression could be associated with binding either one or both isoforms to VDAC in the MOM. VDAC and ANT move the synthesized ATP to the active sites of HK-2. The interaction of ATP synthase, ANT, VDAC and HK results in a rapid and very efficient production of glucose-6-phosphate (Mathupala et al. 2006), a precursor for other glycolytic steps and key biosynthetic metabolites via the pentose phosphate pathway and Krebs acid cycle. The mechanism of the Warburg’s effect proposed by Pedersen and colleagues (Pedersen 2008) could partly explain high rates of aerobic glycolysis in human NBs. The mitochondrially-bound HK-2 can also provide the elevated resistance of NB cells to apoptotic stimuli. It was discovered that HK-2, a key glycolytic enzyme, played also a role in the regulation of the mitochondria-initiated apoptosis in cancer cells (Chen et al. 2009). Our results support the view (Levy et al. 2012; Matsushita et al. 2012) that in NB cells there are reprogramming of energy metabolism towards aerobic glycolysis.

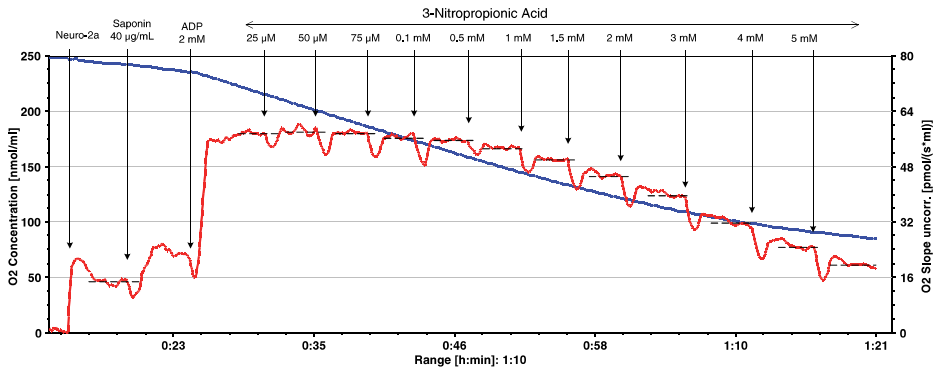


**Fig. 7** Representative trace of change in the rate of oxygen consumption by undifferentiated N2a cells during the titration of the reaction medium with increasing concentrations of 3-nitropropionic acid (an inhibitor of

complex-II) and in the presence of 10 mM succinate. Steady-state respiration rates are shown by dashed lines

We established that murine N2a cells (Table 1), like human NB cells (Ishiguro et al. 1990), had relatively low CK activity. Our data demonstrates that the MtCK-mediated energy transfer system is not functional in the N2a cells (Fig. 5). The

downregulation of uMtCK was also monitored in malignancies of another histological type, such as human breast cancer (Kaambre et al. 2012a), colon adenocarcinoma, and sarcoma cells (Patra et al. 2008; Patra et al. 2012). Since uMtCK is

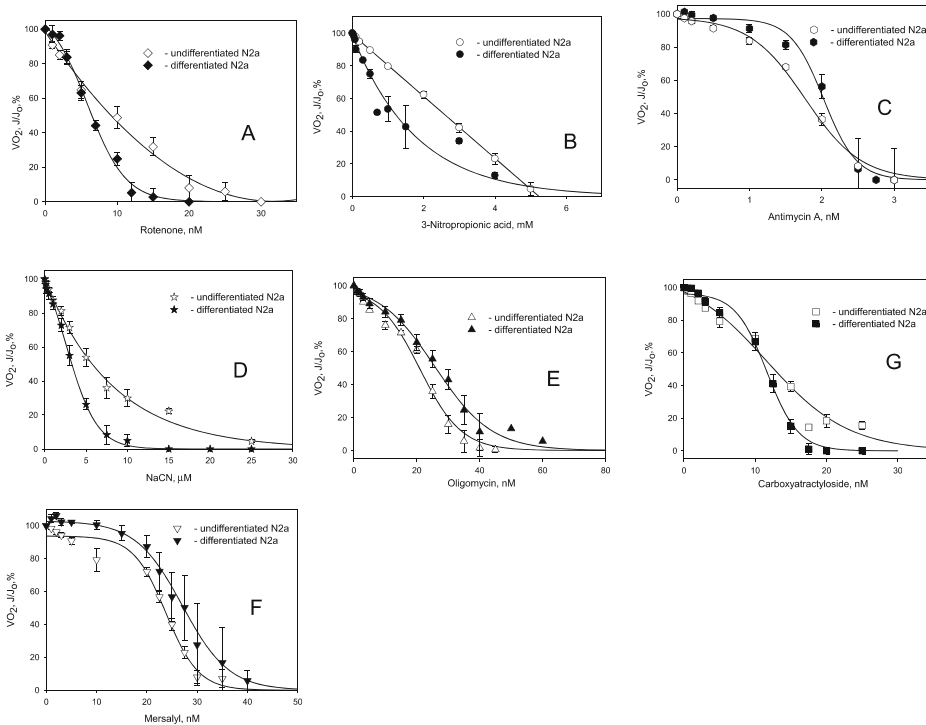


**Fig. 8** Titration curves of inhibition of respiratory complexes in permeabilized N2a cells (both undifferentiated and differentiated) with: **a** rotenone, in the absence of succinate; **b** 3-nitropropionic acid, in the presence of 10 mM succinate as a respiratory substrate (without malate

and glutamate; **c** antimycin-A; **d** NaCN; **e** oligomycin; **f** mersalyl; and **g** carboxyatractyloside (respiratory substrates 2 mM malate and 5 mM glutamate). Bars are SEM



**Table 2** Flux control coefficients (FCC) of respiratory chain complexes for undifferentiated (uN2a) and differentiated (dN2a) by retinoic acid N2a cells as well as isolated rat cardiomyocytes determined upon direct activation of respiration with 2 mM ADP

Complexes	Inhibitors used	uN2a cells, FCC±SEM	dN2a cells, FCC±SEM	Cardiomyocytes, FCC±SEM (Tepp et al. 2011)
Complex-I	Rotenone	1.11±0.32	0.38±0.21	0.20±0.04
Complex-II	3-nitropropionic acid	0.99±0.07	1.34±0.18	0.60±0.06
Complex-III	Antimycin	0.41±0.07	0.36±0.11	0.41±0.08
Complex-IV	NaCN	0.92±0.09	0.99±0.43	0.39±0.09
ATP/ADP carrier	Carboxyatractyloside	0.61±0.17	0.28±0.16	0.20±0.05
ATP synthase	Oligomycin	0.59±0.06	0.55±0.26	0.065±0.01
P <sub>i</sub> carrier	Mersalyl	0.44±0.08	0.03±0.08	0.064±0.04
Sum	–	5.06	3.93	1.93

downregulated in N2a cells, it could be assumed that the revealed CK activity in the cells can be mediated by CK-BB. Our data suggests (Table 1) that the CK-BB activity in undifferentiated NBs may be about 40 % lower as compared with normal differentiated neurons of the SNS with higher energy needs. Despite the contention that CK-MM is the muscle specific protein, a few research groups have reported that the human brain tissue contains significant amounts of the CK-MM isotype (Hamburg et al. 1990; Tsung 1976). The precise expression of CK isoforms and clarification of the mechanisms of their involvement in energy metabolism of neuronal tumor cells need definitely further clarification.

It is well-known that AK-catalyzed phosphotransfer plays one of the key roles in the maintenance of energy homeostasis in fully differentiated cells with a high-energy demand, particularly, in neural cells (Ames 2000). Currently there is only very limited information about the function of AK system in human NBs. There are some indications in literature that NB cells can express AK1 (de Bruin et al. 2004). In neurons, AK isozymes have a distinct intracellular distribution and preferred substrate. AK1 is a cytosolic enzyme for which ATP is the substrate. AK2 catalyzes the same reaction in the mitochondrial intermembrane space. AK3 is present in the mitochondrial matrix and prefers GTP over ATP as the substrate. Cytoplasmic AK1 participates in energy metabolism when local high energy phosphate levels are low, by sustaining ATP levels at the expense of ADP (Dzeja & Terzic 2003). Previous studies showed that NB cells could express, like normal neurons, the cytoplasmic AK1 and plasma membrane-bound AK1 $\beta$  (de Bruin et al. 2004; Neary et al. 1996). In our experiments, the addition of AMP to permeabilized N2a cells in the presence of a PEP-PK external ADP trapping system and 2 mM ATP led to a strong activation of mitochondrial respiration suggesting the presence of AK2 (Fig. 6b). These results indicate that in NB cells the mitochondrial isoform AK2 may be one of the main ATP producers. But more detailed studies with the use of human material are needed to confirm the assumption. The total AK activity of uN2a cells was slightly (~ 20 %) decreased in comparison with RA-treated cells. In parallel, the apparent  $K_m$  value for exogenous AMP in the regulation of respiration in uN2a was much lower (79±9  $\mu$ M)

than for RA treated N2a cells (175±30  $\mu$ M). These results are taken to show that in RA treated N2a cells the permeability of MOM for AMP is low and possibly controlled by some cytoplasmic proteins. The cellular mechanism of regulation of respiration seems to be similar to CK mediated processes.

In NB cells, the permeability of MOM for adenine nucleotides is significantly higher than in normal tissues of oxidative type. In contrast to  $K_m$  values for AMP, the  $K_m^{app}$  values of MgADP for undifferentiated and dN2a cells were determined as 20.3 and 19.4  $\mu$ M, i.e. nearly the same as that for isolated muscle mitochondria (in the range of 10–20  $\mu$ M) (Monge et al. 2008). In NB cells, the kinetics of regulation of respiration by ADP is changed substantially as compared to normal tissues of oxidative type; for rat cardiac and *m. soleus* the apparent  $K_m$  value was found to be in the range of 300–400  $\mu$ M (Anmann et al. 2006; Seppet et al. 2001). These striking differences in metabolic regulation of respiration could be mediated by a decreased expression of some cytoskeletal proteins. To find out the candidate protein(s) for this regulation in NB cells thorough proteomics studies are needed.

Our studies strongly suggest that NB is not an exclusively glycolytic tumor. Indeed, we found that uN2a cells contain a considerable number of mitochondria (Fig. 1) and displayed the ADP-stimulated respiration suggesting that the OXPHOS system played a notable role in the production of ATP in NB cells. However, we showed that all respiration rates of uN2a as well as the activity of Complex-II in the cells were significantly lower in comparison with RA-treated cells. This suggested that mitochondria in NB cells had a decreased bioenergetic capacity. It is in a good agreement with recent studies performed in other laboratories. Mutations in genes encoding the subunits of the mitochondrial SDH complex were shown in NBs (Cascon et al. 2008; Schimke et al. 2010) as well as in related tumors, such as pheochromocytomas (Astuti et al. 2003; Astuti et al. 2004; Bardella et al. 2011). Moreover, it was reported (Feichtinger et al. 2010) that in human NBs, in comparison with normal adjacent tissue, practically all components of the mitochondrial ETC and the activity of ATP synthase were downregulated; this was attributed to a strong decrease in the number of mitochondrial DNA copies in NB cells.

Our MCA studies were carried out on Complex I, II, III, IV, ATP synthase, ANT and PIC. In uN2a cells, all the flux control coefficients were found to have extremely high values. The reason for these high FCCs is clearly not diffusion restrictions, because the concentration ranges for inhibitors does not differ from those that are used for isolated cardiomyocytes (Table 2). MCA showed that in uN2a cells the key sites in the regulation of OXPHOS were Complex-I (FCC=1.11), Complex-II (FCC=0.99) and IV (FCC=0.92), whereas in dN2a cells these were Complex-II and IV (Table 2). Results obtained for the P<sub>i</sub> and adenine nucleotide carriers showed that there were fundamental differences in the control of OXPHOS in undifferentiated and dN2a cells. Indeed, in dN2a cells, these carriers exert much lower control than in undifferentiated cells (Table 2). Our MCA studies suggested that in NB cells the ANT could be up-regulated, as compared to normal cells with high OXPHOS rates; for uN2a, dN2a cells and rat CMs the corresponding FCC values were assayed as 0.61, 0.28 and 0.2, respectively (Table 2). One possible explanation for these differences may be the different profiles of ANT isoforms expressions (Dolce et al. 2005). Each ANT isoform possesses a specific expression depending on cell type, nature of tissue, developmental stage and status of cell proliferation. ANT1 is known to be highly expressed in differentiated tissues such as skeletal muscle, heart and brain (Stepien et al. 1992). Unlike the ANT1 and ANT3 isoforms, ANT2 was found to be strongly over-expressed in many types of human cancers (Chevrollier et al. 2005; Chevrollier et al. 2011; Le Bras et al. 2006). In hypoxic conditions, NB cells could maintain the integrity of their mitochondria and effective survival due to over-expression of ANT2. Unlike the ANT1 and ANT3 isoforms, ANT2 is not pro-apoptotic and may therefore contribute to carcinogenesis (Zamora et al. 2004). Since the expression of ANT2 is closely linked to the mitochondrial bioenergetics of tumors, it should be taken into account for individualizing cancer treatments and for the further development of anticancer strategies.

The sum of the FCCs over the entire ATP synthasome and ETC complexes for uN2a was found to be around 5, and this value exceeded remarkably that for RA treated cells (3.93) and some normal tissues of oxidative type – adult rat cardiomyocytes (1.93) (Table 2). Very high FCCs value (with  $\Sigma \approx 4$ ) was also showed in MCA studies performed on human breast cancer fibers (Kaambre et al. 2012a). According to Lenaz and Genova (Lenaz & Genova 2010) a sum of FCCs exceeding one may indicate the presence of supramolecular associations of the respiratory chain complexes that was confirmed by electron microscopy, native gel electrophoresis and single particle image processing (Lenaz & Genova 2009; Lenaz & Genova 2010). We assume that the theory of supercomplexes is one of the possible explanations for high sum of FCCs for NB cells, but more detailed studies are needed to support this hypothesis. It is possible that the presence of respirasomes is the common feature of malignant cells. Several functions for the formation of

respiratory supercomplexes have been suggested: channeling of ubiquinol and cytochrome c, avoiding competition from other enzymes; catalytic enhancement from reduced diffusion times of substrates and prevention of the generation of superoxide (Hoefs et al. 2012). The formation of supercomplexes can give an explanation for increased resistance of malignancies to apoptotic stimuli via suppressing the cytochrome-c, a pro-apoptotic factor, release into the cytosol.

## Conclusion

Our data supports the opinion that human NB is a tumor with downregulated OXPHOS. But, it should not be regarded as a neoplasm of purely glycolytic type; we found that uN2a cells displayed significant rates of O<sub>2</sub> uptake, and could produce a substantial part of their ATP via OXPHOS. The complex-II of the mitochondrial ETC was found to be downregulated in NB cells as compared to differentiated neural cells. This finding indicates that in NB cells silencing of Complex-II by appropriate agents could provide a selective tumoricidal effect. Our studies suggest that in NB cells, HK, AK, Pi carrier, ANT and Complex-I could play an important role in the regulation of mitochondrial respiration. In NB cells, some of them may be possible targets for chemotherapeutic treatment. Nevertheless, further study is needed to clarify the precise metabolic profile of human NB cells and the regulation of energy fluxes.

**Acknowledgements** This work was supported by grants: No. 8987 from the Estonian Science Foundation, SF0180114Bs08 from Estonian Ministry of Education, and by the project “Aid for research and development in health care technology” of Archimedes foundation No. 3.2.1001.11-0027. The authors sincerely thank Maire Peitel from Laboratory of Bioenergetics (National Institute of Chemical Physics and Biophysics, Tallinn) for everyday technical support.

**Interest conflicts** The authors declare no conflict of interest.

## References

- Almeida A, Bolaños JP, Moncada S (2010) E3 ubiquitin ligase APC/C-Cdh1 accounts for the Warburg effect by linking glycolysis to cell proliferation. *Proc Natl Acad Sci* 107(2):738–741. doi:10.1073/pnas.0913668107
- Ames A (2000) CNS energy metabolism as related to function. *Brain Res Rev* 34(1–2):42–68. doi:10.1016/S0165-0173(00)00038-2
- Annam T, Guzun R, Beraud N, Pelloux S, Kuznetsov AV, Kogerman L et al (2006) Different kinetics of the regulation of respiration in permeabilized cardiomyocytes and in HL-1 cardiac cells. Importance of cell structure/organization for respiration regulation. *Biochim Biophys Acta* 1757(12):1597–1606. doi:10.1016/j.bbapbio.2006.09.008
- Apte SP, Sarangarajan R (2008) Cellular respiration and carcinogenesis. Springer, New York
- Astuti D, Hart-Holden N, Latiff F, Lalloo F, Black GC, Lim C et al (2003) Genetic analysis of mitochondrial complex II subunits SDHD,

- SDHB and SDHC in paraganglioma and pheochromocytoma susceptibility. *Clinical Endocrinology* 59(6):728–733. doi:10.1046/j.1365-2265.2003.01914.x
- Asuti D, Morris M, Krona C, Abel F, Gentle D, Martinsson T et al (2004) Investigation of the role of SDHB inactivation in sporadic pheochromocytoma and neuroblastoma. *Br J Cancer* 91(10):1835–1841
- Atsumi T, Chesney J, Metz C, Leng L, Donnelly S, Makita Z et al (2002) High expression of inducible 6-phosphofructo-2-kinase/fructose-2,6-bisphosphatase (iPFK-2; PFKFB3) in human cancers. *Cancer Res* 62(20):5881–5887
- Bardella C, Pollard PJ, Tomlinson I (2011) SDH mutations in cancer. *Biochim Biophys Acta (BBA) Bioenerg* 1807(11):1432–1443. doi:10.1016/j.bbabi.2011.07.003
- Beemer FA, Vlug AM, Rousseau-Merck MF, van Veelen CW, Rijksen G, Staal GE (1984) Glycolytic enzymes from human neuroectodermal tumors of childhood. *Eur J Cancer Clin Oncol* 20(2):253–259
- Biswas S, Ray M, Misra S, Dutta DP, Ray S (1997) Selective inhibition of mitochondrial respiration and glycolysis in human leukaemic leucocytes by methylglyoxal. *Biochem J* 323(Pt 2):343–348
- Blanco V, Lopez Camelo J, Carri NG (2001) Growth inhibition, morphological differentiation and stimulation of survival in neuronal cell type (Neuro-2a) treated with trophic molecules. *Cell Biol Int* 25(9):909–917
- Bonora E, Porcelli AM, Gasparre G, Biondi A, Ghelli A, Carelli V et al (2006) Defective oxidative phosphorylation in thyroid oncogenic carcinoma is associated with pathogenic mitochondrial DNA mutations affecting complexes I and III. *Cancer Res* 66(12):6087–6096. doi:10.1158/0008-5472.CAN-06-0171
- Bustamante E, Pedersen PL (1977) High aerobic glycolysis of rat hepatoma cells in culture: Role of mitochondrial hexokinase. *Proc Natl Acad Sci* 74(9):3735–3739
- Bustamante E, Pedersen PL (1980) Mitochondrial hexokinase of rat hepatoma cells in culture: solubilization and kinetic properties. *Biochemistry* 19(22):4972–4977
- Cascon A, Landa I, Lopez-Jimenez E, Diez-Hernandez A, Buchta M, Montero-Conde C et al (2008) Molecular characterisation of a common SDHB deletion in paraganglioma patients. *J Med Genet* 45(4):233–238. doi:10.1136/jmg.2007.054965
- Chen Z, Zhang H, Lu W, Huang P (2009) Role of mitochondria-associated hexokinase II in cancer cell death induced by 3-bromopyruvate. *Biochim Biophys Acta (BBA) Bioenerg* 1787(5):553–560. doi:10.1016/j.bbabi.2009.03.003
- Chevrollier A, Loiseau D, Chabi B, Renier G, Douay O, Malthiery Y et al (2005) ANT2 isoform required for cancer cell glycolysis. *J Bioenerg Biomembr* 37(5):307–316. doi:10.1007/s10863-005-8642-5
- Chevrollier A, Loiseau D, Reynier P, Stepien G (2011) Adenine nucleotide translocase 2 is a key mitochondrial protein in cancer metabolism. *Biochim Biophys Acta (BBA) Bioenerg* 1807(6):562–567. doi:10.1016/j.bbabi.2010.10.008
- Chuang J-H, Chou M-H, Tai M-H, Lin T-K, Liou C-W, Chen T et al (2013) 2-Deoxyglucose treatment complements the cisplatin- or BH3-only mimetic-induced suppression of neuroblastoma cell growth. *Int J Biochem Cell Biol* 45(5):944–951. doi:10.1016/j.biocel.2013.01.019
- de Bruin W, Oerlemans F, Wieringa B (2004) Adenylate kinase I does not affect cellular growth characteristics under normal and metabolic stress conditions. *Experimental Cell Research* 297(1):97–107. doi:10.1016/j.yexcr.2004.02.025
- Deubzer B, Mayer F, Kuci Z, Niewisch M, Merkel G, Handgretinger R et al (2010) H(2)O(2)-mediated cytotoxicity of pharmacologic ascorbate concentrations to neuroblastoma cells: potential role of lactate and ferritin. *Cell Physiol Biochem* 25(6):767–774. doi:10.1159/000315098
- Dolce V, Scarcia P, Lacopetta D, Palmieri F (2005) A fourth ADP/ATP carrier isoform in man: identification, bacterial expression, functional characterization and tissue distribution. *FEBS Lett* 579(3):633–637. doi:10.1016/j.febslet.2004.12.034
- Dzeja PP, Terzic A (2003) Phosphotransfer networks and cellular energetics. *J Exp Biol* 206(Pt 12):2039–2047
- Dzeja P, Terzic A (2009) Adenylate kinase and AMP signaling networks: Metabolic monitoring, signal communication and body energy sensing. *Int J Mol Sci* 10(4):1729–1772. doi:10.3390/ijms10041729
- Dzeja PP, Vitkevicius KT, Redfield MM, Burnett JC, Terzic A (1999) Adenylate kinase-catalyzed phosphotransfer in the myocardium: increased contribution in heart failure. *Circ Res* 84(10):1137–1143
- Ellman GL, Courtney KD, Andres V Jr, Feather-Stone RM (1961) A new and rapid colorimetric determination of acetylcholinesterase activity. *Biochem Pharmacol* 7:88–95
- Feichtinger R, Zimmermann F, Mayr J, Neureiter D, Hauser-Kronberger C, Schilling F et al (2010) Low aerobic mitochondrial energy metabolism in poorly- or undifferentiated neuroblastoma. *BMC Cancer* 10(1):149
- Fell D (1997) Understanding the control of metabolism. Portland Press, London
- Fell D (2005) Metabolic Control Analysis. In (pp. 69–80).
- Gatenby RA, Gillies RJ (2004) Why do cancers have high aerobic glycolysis? *Nat Rev Cancer* 4(11):891–899. doi:10.1038/nrc1478
- Geschwind JF, Georgiades CS, Ko YH, Pedersen PL (2004) Recently elucidated energy catabolism pathways provide opportunities for novel treatments in hepatocellular carcinoma. *Expert Rev Anticancer Ther* 4(3):449–457. doi:10.1586/14737140.4.3.449
- Gogvadze V, Orrenius S, Zhivotovsky B (2009) Mitochondria as targets for cancer chemotherapy. *Seminars in Cancer Biology* 19(1):57–66. doi:10.1016/j.semcancer.2008.11.007
- Groen AK, Wanders RJ, Westerhoff HV, van der Meer R, Tager JM (1982) Quantification of the contribution of various steps to the control of mitochondrial respiration. *J Biol Chem* 257(6):2754–2757
- Guzun R, Timohhina N, Tepp K, Monge C, Kaambre T, Sikk P et al (2009) Regulation of respiration controlled by mitochondrial creatine kinase in permeabilized cardiac cells in situ. Importance of system level properties. *Biochim Biophys Acta* 1787(9):1089–1105. doi:10.1016/j.bbabi.2009.03.024
- Guzun R, Karu-Varikmaa M, Gonzalez-Granillo M, Kuznetsov AV, Michel L, Cottet-Rousselle C et al (2011) Mitochondria-cytoskeleton interaction: Distribution of beta-tubulins in cardiomyocytes and HL-1 cells. *Biochim Biophys Acta* 1807(4):458–469. doi:10.1016/j.bbabi.2011.01.010
- Hamburg RJ, Friedman DL, Olson EN, Ma TS, Cortez MD, Goodman C et al (1990) Muscle creatine kinase isoenzyme expression in adult human brain. *J Biol Chem* 265(11):6403–6409
- Hoefs SJG, Rodenburg RJ, Smeitink JAM, van den Heuvel LP (2012) Molecular base of biochemical complex I deficiency. *Mitochondrion* 12(5):520–532. doi:10.1016/j.mito.2012.07.106
- Huang LS, Sun G, Cobessi D, Wang AC, Shen JT, Tung EY et al (2006) 3-nitropropionic acid is a suicide inhibitor of mitochondrial respiration that, upon oxidation by complex II, forms a covalent adduct with a catalytic base arginine in the active site of the enzyme. *J Biol Chem* 281(9):5965–5972. doi:10.1074/jbc.M511270200
- Ihrlund LS, Herlund E, Khan O, Shoshan MC (2008) 3-Bromopyruvate as inhibitor of tumour cell energy metabolism and chemopotentiator of platinum drugs. *Mol Oncol* 2(1):94–101
- Ishiguro Y, Kato K, Akatsuka H, Ito T (1990) The diagnostic and prognostic value of pretreatment serum creatine kinase BB levels in patients with neuroblastoma. *Cancer* 65(9):2014–2019
- Kaambre T, Chekulayev V, Shevchuk I, Karu-Varikmaa M, Timohhina N, Tepp K et al (2012a) Metabolic control analysis of cellular respiration in situ in intraoperational samples of human breast cancer. *J Bioenerg Biomembr* 44(5):539–558. doi:10.1007/s10863-012-9457-9
- Kaambre T, Chekulayev V, Shevchuk I, Karu-Varikmaa M, Timohhina N, Tepp K et al (2012b) Metabolic control analysis of cellular

- respiration in situ in intraoperative samples of human breast cancer. *J Bioenerg Biomembr*. doi:10.1007/s10863-012-9457-9
- Kholodenko BN, Westerhoff HV (1993) Metabolic channelling and control of the flux. *FEBS Lett* 320(1):71–74
- Krieger-Hinck N, Gustke H, Valentiner U, Mikecz P, Buchert R, Mester J et al (2006) Visualisation of neuroblastoma growth in a Scid mouse model using [<sup>18</sup>F]FDG and [<sup>18</sup>F]FLT-PET. *Anticancer Res* 26(5A):3467–3472
- Kriegstein J, Mwasekaga S (1987) Effect of methohexital on the relationship between hexokinase distribution and energy metabolism in neuroblastoma cells. *Arzneimittelforschung* 37(3):291–295
- Kriegstein J, Schachtschabel DO, Wever K, Wickop G (1981) Influence of thiopental on intracellular distribution of hexokinase activity in various tumor cells. *Arzneimittelforschung* 31(1):121–123
- Kuznetsov AV, Veksler V, Gellerich FN, Saks V, Margreiter R, Kunz WS (2008) Analysis of mitochondrial function in situ in permeabilized muscle fibers, tissues and cells. *Nat Protoc* 3(6):965–976. doi:10.1038/nprot.2008.61
- Le Bras M, Borgne-Sanchez A, Touat Z, El Dein OS, Deniaud A, Maillier E et al (2006) Chemosensitization by knockdown of adenine nucleotide translocase-2. *Cancer Res* 66(18):9143–9152. doi:10.1158/0008-5472.CAN-05-4407
- Lenaz G, Genova ML (2009) Structural and functional organization of the mitochondrial respiratory chain: a dynamic super-assembly. *Int J Biochem Cell Biol* 41(10):1750–1772
- Lenaz G, Genova ML (2010) Structure and organization of mitochondrial respiratory complexes: a new understanding of an old subject. *Antioxid Redox Signal* 12(8):961–1008. doi:10.1089/ars.2009.2704
- Levy A, Zage P, Akers L, Ghisoli M, Chen Z, Fang W et al (2012) The combination of the novel glycolysis inhibitor 3-BrOP and rapamycin is effective against neuroblastoma. *Investigational New Drugs* 30(1):191–199. doi:10.1007/s10637-010-9551-y
- Lienhard GE, Secemski II (1973) P<sub>1</sub>, P<sub>5</sub>-Di(adenosine-5')pentaphosphate, a potent multisubstrate inhibitor of adenylate kinase. *J Biol Chem* 248(3):1121–1123
- Majewski N, Nogueira V, Bhaskar P, Coy PE, Skeen JE, Gottlob K et al (2004) Hexokinase-mitochondria interaction mediated by Akt is required to inhibit apoptosis in the presence or absence of Bax and Bak. *Mol Cell* 16(5):819–830. doi:10.1016/j.molcel.2004.11.014
- Marin-Hernandez A, Rodríguez-Enriquez S, Vital-Gonzalez PA, Flores-Rodríguez FL, Macias-Silva M, Sosa-Garrocho M et al (2006) Determining and understanding the control of glycolysis in fast-growth tumor cells. Flux control by an over-expressed but strongly product-inhibited hexokinase. *FEBS J* 273(9):1975–1988. doi:10.1111/j.1742-4658.2006.05214.x
- Mathupala SP, Ko YH, Pedersen PL (2006) Hexokinase II: cancer's double-edged sword acting as both facilitator and gatekeeper of malignancy when bound to mitochondria. *Oncogene* 25(34):4777–4786. doi:10.1038/sj.onc.1209603
- Matsushita K, Uchida K, Saigusa S, Ide S, Hashimoto K, Koike Y et al (2012) Glycolysis inhibitors as a potential therapeutic option to treat aggressive neuroblastoma expressing GLUT1. *Journal of Pediatric Surgery* 47(7):1323–1330. doi:10.1016/j.jpedsurg.2011.12.007
- Monge C, Beraud N, Kuznetsov A, Rostovtseva T, Sackett D, Schlattner U et al (2008) Regulation of respiration in brain mitochondria and synaptosomes: restrictions of ADP diffusion in situ, roles of tubulin, and mitochondrial creatine kinase. *Mol Cell Biochem* 318(1–2):147–165. doi:10.1007/s11010-008-9865-7
- Monge C, Beraud N, Tepp K, Pelloux S, Chahboun S, Kaambre T et al (2009) Comparative analysis of the bioenergetics of adult cardiomyocytes and nonbeating HL-1 cells: respiratory chain activities, glycolytic enzyme profiles, and metabolic fluxes. *Can J Physiol Pharmacol* 87(4):318–326. doi:10.1139/y09-018
- Moreno-Sanchez R, Rodríguez-Enriquez S, Marin-Hernandez A, Saavedra E (2007) Energy metabolism in tumor cells. *FEBS J* 274(6):1393–1418. doi:10.1111/j.1742-4658.2007.05686.x
- Moreno-Sanchez R, Saavedra E, Rodríguez-Enriquez S, Olin-Sandoval V (2008) Metabolic control analysis: a tool for designing strategies to manipulate metabolic pathways. *J Biomed Biotechnol* 2008:597913. doi:10.1155/2008/597913
- Moreno-Sánchez R, Rodríguez-Enriquez S, Saavedra E, Marin-Hernández A, Gallardo-Pérez JC (2009) The bioenergetics of cancer: Is glycolysis the main ATP supplier in all tumor cells? *BioFactors* 35(2):209–225. doi:10.1002/biof.31
- Moreno-Sanchez R, Saavedra E, Rodríguez-Enriquez S, Gallardo-Perez JC, Quezada H, Westerhoff HV (2010) Metabolic control analysis indicates a change of strategy in the treatment of cancer. *Mitochondrion* 10(6):626–639. doi:10.1016/j.mito.2010.06.002
- Nakashima RA, Paggi MG, Scott LJ, Pedersen PL (1988) Purification and characterization of a bindable form of mitochondrial bound hexokinase from the highly glycolytic AS-30D rat hepatoma cell line. *Cancer Res* 48(4):913–919
- Neary JT, Rathbone MP, Cattabeni F, Abbraccio MP, Burnstock G (1996) Trophic actions of extracellular nucleotides and nucleosides on glial and neuronal cells. *Trends Neurosci* 19(1):13–18
- Patra S, Bera S, SinhaRoy S, Ghoshal S, Ray S, Basu A et al (2008) Progressive decrease of phosphocreatine, creatine and creatine kinase in skeletal muscle upon transformation to sarcoma. *FEBS J* 275(12):3236–3247. doi:10.1111/j.1742-4658.2008.06475.x
- Patra S, Ghosh A, Roy SS, Bera S, Das M, Talukdar D et al (2012) A short review on creatine-creatine kinase system in relation to cancer and some experimental results on creatine as adjuvant in cancer therapy. *Amino Acids* 42(6):2319–2330. doi:10.1007/s00726-011-0974-3
- Pedersen PL (1978) Tumor mitochondria and the bioenergetics of cancer cells. *Prog Exp Tumor Res* 22:190–274
- Pedersen PL (2007a) The cancer cell's "power plants" as promising therapeutic targets: an overview. *J Bioenerg Biomembr* 39(1):1–12. doi:10.1007/s10863-007-9070-5
- Pedersen PL (2007b) Warburg, me and Hexokinase 2: Multiple discoveries of key molecular events underlying one of cancers' most common phenotypes, the "Warburg Effect", i.e., elevated glycolysis in the presence of oxygen. *J Bioenerg Biomembr* 39(3):211–222. doi:10.1007/s10863-007-9094-x
- Pedersen PL (2008) Voltage dependent anion channels (VDACs): a brief introduction with a focus on the outer mitochondrial compartment's roles together with hexokinase-2 in the "Warburg effect" in cancer. *J Bioenerg Biomembr* 40(3):123–126. doi:10.1007/s10863-008-9165-7
- Pedersen PL (2012) 3-bromopyruvate (3BP) a fast acting, promising, powerful, specific, and effective "small molecule" anti-cancer agent taken from labside to bedside: introduction to a special issue. *J Bioenerg Biomembr* 44(1):1–6. doi:10.1007/s10863-012-9425-4
- Pedersen PL, Mathupala S, Rempel A, Geschwind JF, Ko YH (2002) Mitochondrial bound type II hexokinase: a key player in the growth and survival of many cancers and an ideal prospect for therapeutic intervention. *Biochim Biophys Acta (BBA) Bioenerg* 1555(1–3):14–20. doi:10.1016/S0005-2728(02)00248-7
- Puurand M, Peet N, Piirsoo A, Peetsalu M, Soplepmann J, Sirotkina M et al (2012) Deficiency of the complex I of the mitochondrial respiratory chain but improved adenylate control over succinate-dependent respiration are human gastric cancer-specific phenomena. *Mol Cell Biochem* 370(1–2):69–78. doi:10.1007/s11010-012-1399-3
- Rostovtseva TK, Sheldon KL, Hassanzadeh E, Monge C, Saks V, Bezrukov SM et al (2008) Tubulin binding blocks mitochondrial voltage-dependent anion channel and regulates respiration. *Proc Natl Acad Sci USA* 105(48):18746–18751. doi:10.1073/pnas.0806303105
- Saks VA, Belikova YO, Kuznetsov AV (1991) In vivo regulation of mitochondrial respiration in cardiomyocytes: specific restrictions for intracellular diffusion of ADP. *Biochim Biophys Acta* 1074(2):302–311

- Saks VA, Veksler VI, Kuznetsov AV, Kay L, Sikk P, Tiivel T et al (1998) Permeabilized cell and skinned fiber techniques in studies of mitochondrial function in vivo. *Mol Cell Biochem* 184(1–2):81–100
- Saks V, Kuznetsov A, Andrienko T, Usson Y, Appaix F, Guerrero K et al (2003) Heterogeneity of ADP diffusion and regulation of respiration in cardiac cells. *Biophys J* 84(5):3436–3456. doi:10.1016/S0006-3495(03)70065-4
- Sato C, Matsuda T, Kitajima K (2002) Neuronal Differentiation-dependent Expression of the Disialic Acid Epitope on CD166 and Its Involvement in Neurite Formation in Neuro2A Cells. *J Biol Chem* 277(47):45299–45305. doi:10.1074/jbc.M206046200
- Schinke RN, Collins DL, Stolle CA (2010) Paraganglioma, neuroblastoma, and a SDHB mutation: Resolution of a 30-year-old mystery. *Am J Med Genet A* 152A(6):1531–1535. doi:10.1002/ajmg.a.33384
- Seppet EK, Kaambre T, Sikk P, Tiivel T, Vija H, Tonkonogi M et al (2001) Functional complexes of mitochondria with Ca, MgATPases of myofibrils and sarcoplasmic reticulum in muscle cells. *Biochim Biophys Acta* 1504(2–3):379–395
- Seppet EK, Eimre M, Anmann T, Seppet E, Piirsoo A, Peet N et al (2006) Structure-function relationships in the regulation of energy transfer between mitochondria and ATPases in cardiac cells. *Exp Clin Cardiol* 11(3):189–194
- Sharma LK, Fang H, Liu J, Vartak R, Deng J, Bai Y (2011) Mitochondrial respiratory complex I dysfunction promotes tumorigenesis through ROS alteration and AKT activation. *Hum Mol Genet* 20(23):4605–4616. doi:10.1093/hmg/ddr395
- Simonnet H, Demont J, Pfeiffer K, Guenaneche L, Bouvier R, Brandt U et al (2003) Mitochondrial complex I is deficient in renal oncocytomas. *Carcinogenesis* 24(9):1461–1466. doi:10.1093/carcin/bgg109
- Stepien G, Torroni A, Chung AB, Hodge JA, Wallace DC (1992) Differential expression of adenine nucleotide translocator isoforms in mammalian tissues and during muscle cell differentiation. *J Biol Chem* 267(21):14592–14597
- Tepp K, Timohhina N, Chekulayev V, Shevchuk I, Kaambre T, Saks V (2010) Metabolic control analysis of integrated energy metabolism in permeabilized cardiomyocytes - experimental study. *Acta Biochim Pol* 57(4):421–430
- Tepp K, Shevchuk I, Chekulayev V, Timohhina N, Kuznetsov AV, Guzun R et al (2011) High efficiency of energy flux controls within mitochondrial interactosome in cardiac intracellular energetic units. *Biochim Biophys Acta Bioenerg* 1807(12):1549–1561. doi:10.1016/j.bbabi.2011.08.005
- Tsung SH (1976) Creatine kinase isoenzyme patterns in human tissue obtained at surgery. *Clin Chem* 22(2):173–175
- Warburg O (1956) On respiratory impairment in cancer cells. *Science* 124(3215):269–270
- Whitaker-Menezes D, Martinez-Outschoom UE, Lin Z, Ertel A, Flomenberg N, Witkiewicz AK et al (2011) Evidence for a stromal-epithelial "lactate shuttle" in human tumors: MCT4 is a marker of oxidative stress in cancer-associated fibroblasts. *Cell Cycle* 10(11):1772–1783
- Xu R-h, Pelicano H, Zhou Y, Carew JS, Feng L, Bhalla KN et al (2005) Inhibition of Glycolysis in Cancer Cells: A Novel Strategy to Overcome Drug Resistance Associated with Mitochondrial Respiratory Defect and Hypoxia. *Cancer Res* 65(2):613–621
- Xun Z, Lee DY, Lim J, Canaria CA, Barnebey A, Yanonne SM et al (2012) Retinoic acid-induced differentiation increases the rate of oxygen consumption and enhances the spare respiratory capacity of mitochondria in SH-SY5Y cells. *Mech Ageing Dev* 133(4):176–185. doi:10.1016/j.mad.2012.01.008
- Zamora M, Granell M, Mampel T, Vinas O (2004) Adenine nucleotide translocase 3 (ANT3) overexpression induces apoptosis in cultured cells. *FEBS Lett* 563(1–3):155–160. doi:10.1016/S0014-5793(04)00293-5

## Curriculum Vitae

**Name:** Aleksandr Klepinin

**Date of birth** 07.02.1989

**Phone** +372 56678374

**E-mail** [aleksandr.klepinin@kbfi.ee](mailto:aleksandr.klepinin@kbfi.ee)

### Education:

2014-2018	Tallinn University of Technology, PhD, Gene Technology
2011-2014	Tallinn University of Technology, Master study, Gene Technology
2008-2011	Tallinn University of Technology, Bachelor study, Gene Technology
2005-2008	Tallinn Laagna Secondary School

### Supplement courses:

14.11.2016-31.07.2017	Mayo Clinic, Rochester Minnesota, USA, exchange student
01.02.2016-05.02.2016	Laboratory Animal Science II course at the Estonia University of Life Sciences
24.08.2016-03.09.2015	Laboratory Animal Science I course at the Estonia University of Life Sciences
26.08.2013-30.08.2013	MIP Summer 2013 "Mitochondria Physiology – Theory and Praxis"

### Professional Employment:

2014-2016	National Institute of Chemical Physics and Biophysics, Junior Researcher
2011-2014	National Institute of Chemical Physics and Biophysics, insener

### Honors and Awards:

2017	Graduate school of Biomedicine and Biotechnology scholarship
2016	Kristja Jaak scholarship fore to be exchange student in Mayo Clinic Rochester Minnesota USA
2015	Scholarship of Internationalisation Programme DoRa Activity 8 Participation on International research conferences
2012	Scholarship of Internationalisation Programme DoRa Activity 8 Participation on International research conferences

## Publications:

Tepp K., Puurand M., Timohhina N., Adamson J., **Klepinin A.**, Truu L., Shevchuk I., Chekulayev V., Kaambre T. (2017) Changes in the mitochondrial function and in the efficiency of energy transfer pathways during cardiomyocyte aging. *Mol Cell Biochem* 432(1-2):141-158.

Ounpuu L., **Klepinin A.**, Pook M., Teino I., Peet N., Paju K., Tepp K., Chekulayev V., Shevchuk I., Koks S., Maimets T., & Kaambre T. (2017) 2102Ep embryonal carcinoma cells have compromised respiration and shifted bioenergetic profile distinct from H9 human embryonic stem cells. *Biochim Biophys Acta* 1861(8):2146-2154.

Koit A., Shevchuk I., Ounpuu L., **Klepinin A.**, Chekulayev V., Timohhina N., Tepp K., Puurand M., Truu L., Heck K., Valvere V., Guzun R., & Kaambre T. (2017) Mitochondrial Respiration in Human Colorectal and Breast Cancer Clinical Material Is Regulated Differently. *Oxid Med Cell Longev* 2017:1372640.

**Aleksandr Klepinin**, Lyudmila Ounpuu, Rita Guzun, Vladimir Chekulayev, Natalja Timohhina, Kersti Tepp, Igor Shevchuk, Uwe Schlattner, Tuuli Kaambre. (2016) Simple oxygraphic analysis for the presence of adenylate kinase 1 and 2 in normal and tumor cells. *Journal of Bioenergetics and Biomembranes*, 48 (5), 531–548.

Chekulayev, Vladimir; Mado, Kati; Shevchuk, Igor; Koit, Andre; Kaldma, Andrus; **Klepinin, Aleksandr**; Timohhina, Natalja; Tepp, Kersti; Kandashvili, Manana; Ounpuu, Lyudmila; Heck, Karoliina; Truu, Laura; Planken, Anu; Valvere, Vahur; Kaambre, Tuuli (2015). Metabolic remodeling in human colorectal cancer and surrounding tissues: alterations in regulation of mitochondrial respiration and metabolic fluxes. *Biochemistry and Biophysics Reports*, 4, 111–125

Kaldma, Andrus; Klepinin, Aleksandr; Chekulayev, Vladimir; Mado, Kati; Shevchuk, Igor; Timohhina, Natalja; Tepp, Kersti; Kandashvili, Manana; Varikmaa, Minna; Koit, Andre; Planken, Margus; Heck, Karoliina; Truu, Laura; Planken, Anu; Valvere, Vahur; Rebane, Egle; Kaambre, Tuuli. (2014). An in situ study of bioenergetic properties of human colorectal cancer: The regulation of mitochondrial respiration and distribution of flux control among the components of ATP synthasome. *The International Journal of Biochemistry & Cell Biology*, 55C, 171 - 186.

**Klepinin, Aleksandr**; Chekulayev, Vladimir; Timohhina, Natalja; Shevchuk, Igor; Tepp, Kersti; Kaldma, Andrus; Koit, Andre; Saks, Valdur; Kaambre, Tuuli (2014). Comparative analysis of some aspects of mitochondrial metabolism in differentiated and undifferentiated neuroblastoma cells. *Journal of Bioenergetics and Biomembranes*, 46(1), 17 - 31.

## Elulookirjeldus

**Nimi:** Aleksandr Klepinin

**Sünniaeg ja -koht:** 07.02.1989, Tallinn

**Telefon:** +372 56678374

**E-mail:** [aleksandr.klepinin@kbfi.ee](mailto:aleksandr.klepinin@kbfi.ee)

### Haridustee:

2014-2018	Tallinna Tehnikaülikool, doktoriõpe, geenitehnoloogia
2011-2014	Tallinna Tehnikaülikool, magistriõpe geenitehnoloogia erialal
2008-2011	Tallinna Tehnikaülikool, bakalaureuseõpe geenitehnoloogia erialal
2005-2008	Tallinna Laagna Gümnaasium

### Täienduskoolitus

14.11.2016-31.07.2017	Mayo kliinik, Rochester Minnesota, USA, vahetusüliõpilane
01.02.2016-05.02.2016	Katselooma tehnika kursus II, Eesti Maaülikool
24.08.2016-03.09.2015	Katselooma tehnika kursus I, Eesti Maaülikool
26.08.2013-30.08.2013	Suvekool MIP Summer 2013 "Mitochondria Physiology – Theory and Praxis"

### Teenistuskäik:

2014-2016	Keemilise ja Bioloogilise Füüsika Instituut, Nooremteadur
2011-2014	Keemilise ja Bioloogilise Füüsika Instituut, insener

### Stipendiumid

2017	Biomeditsiini ja biotehnoloogia doktorikooli
2016	Kristja Jaagu Tasemeõppe stipendium osalemaks vahetusüliõpilasena Mayo kliinikumis Rochester Minnesota USA
2015	ESF DoRa programmi stipendium Tegevus 8 Noorteadlaste osalemine rahvusvahelises teadmisteringluses
2012	ESF DoRa programmi stipendium Tegevus 8 Noorteadlaste osalemine rahvusvahelises teadmisteringluses



## Publikatsioonid:

Tepp K., Puurand M., Timohhina N., Adamson J., **Klepinin A.**, Truu L., Shevchuk I., Chekulayev V., Kaambre T. (2017) Changes in the mitochondrial function and in the efficiency of energy transfer pathways during cardiomyocyte aging. *Mol Cell Biochem* 432(1-2):141-158.

Ounpuu L., **Klepinin A.**, Pook M., Teino I., Peet N., Paju K., Tepp K., Chekulayev V., Shevchuk I., Koks S., Maimets T., & Kaambre T. (2017) 2102Ep embryonal carcinoma cells have compromised respiration and shifted bioenergetic profile distinct from H9 human embryonic stem cells. *Biochim Biophys Acta* 1861(8):2146-2154.

Koit A., Shevchuk I., Ounpuu L., **Klepinin A.**, Chekulayev V., Timohhina N., Tepp K., Puurand M., Truu L., Heck K., Valvere V., Guzun R., & Kaambre T. (2017) Mitochondrial Respiration in Human Colorectal and Breast Cancer Clinical Material Is Regulated Differently. *Oxid Med Cell Longev* 2017:1372640.

**Aleksandr Klepinin**, Lyudmila Ounpuu, Rita Guzun, Vladimir Chekulayev, Natalja Timohhina, Kersti Tepp, Igor Shevchuk, Uwe Schlattner, Tuuli Kaambre. (2016) Simple oxygraphic analysis for the presence of adenylate kinase 1 and 2 in normal and tumor cells. *Journal of Bioenergetics and Biomembranes*, 48 (5), 531–548.

Chekulayev, Vladimir; Mado, Kati; Shevchuk, Igor; Koit, Andre; Kaldma, Andrus; **Klepinin, Aleksandr**; Timohhina, Natalja; Tepp, Kersti; Kandashvili, Manana; Ounpuu, Lyudmila; Heck, Karoliina; Truu, Laura; Planken, Anu; Valvere, Vahur; Kaambre, Tuuli (2015). Metabolic remodeling in human colorectal cancer and surrounding tissues: alterations in regulation of mitochondrial respiration and metabolic fluxes. *Biochemistry and Biophysics Reports*, 4, 111–125

Kaldma, Andrus; **Klepinin, Aleksandr**; Chekulayev, Vladimir; Mado, Kati; Shevchuk, Igor; Timohhina, Natalja; Tepp, Kersti; Kandashvili, Manana; Varikmaa, Minna; Koit, Andre; Planken, Margus; Heck, Karoliina; Truu, Laura; Planken, Anu; Valvere, Vahur; Rebane, Egle; Kaambre, Tuuli. (2014). An in situ study of bioenergetic properties of human colorectal cancer: The regulation of mitochondrial respiration and distribution of flux control among the components of ATP synthasome. *The International Journal of Biochemistry & Cell Biology*, 55C, 171 - 186.

**Klepinin, Aleksandr**; Chekulayev, Vladimir; Timohhina, Natalja; Shevchuk, Igor; Tepp, Kersti; Kaldma, Andrus; Koit, Andre; Saks, Valdur; Kaambre, Tuuli (2014). Comparative analysis of some aspects of mitochondrial metabolism in differentiated and undifferentiated neuroblastoma cells. *Journal of Bioenergetics and Biomembranes*, 46(1), 17 - 31.